CR 114371
AVAILABLE TO THE PUBLIC

SD 70-361-1

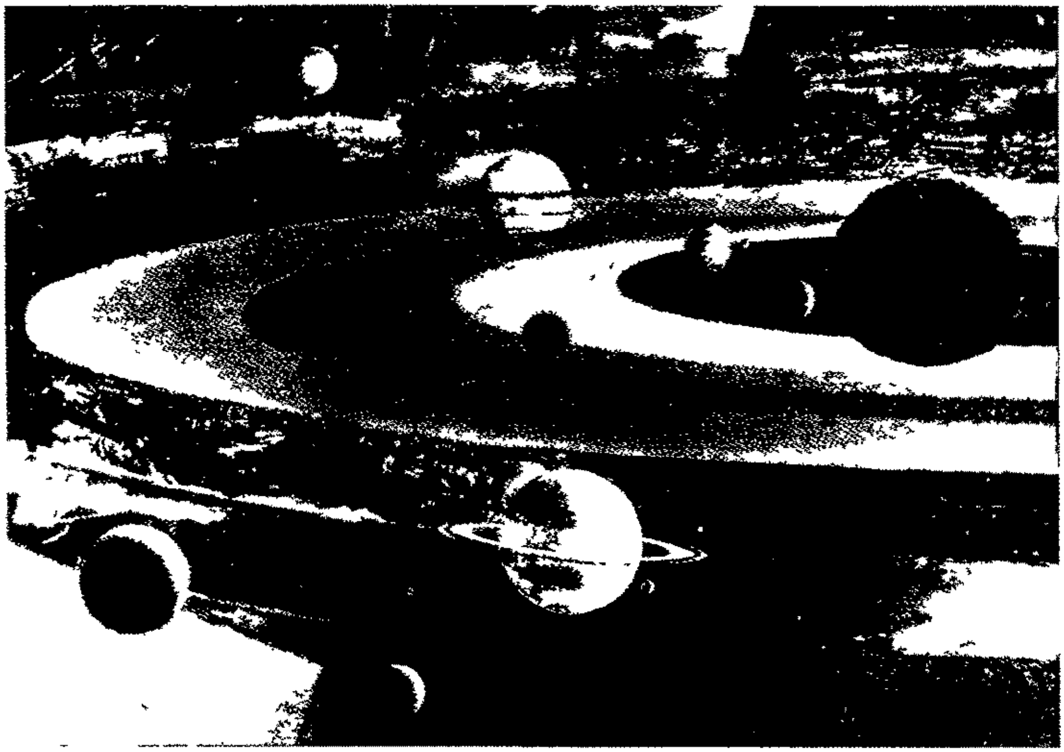

Remote Sensor Systems for Unmanned Planetary Missions

(NAS2-5647)

Space Division
North American Rockwell

SD 70-361-1

Remote Sensor Systems for Unmanned Planetary Missions

Phase II of Contract NAS2-5647

September 1970

Remote Sensor Support Requirements
for Planetary Missions
Prepared for Mission Analysis Division
National Aeronautics and Space Division

Space Division
North American Rockwell

PRECEDING PAGE BLANK NOT FILMED

FOREWORD

This report presents the results of a study to define candidate sensor types suitable for future planetary exploratory missions and to develop scaling laws depicting the relationships between the sensors, their support requirements and their measurement capabilities During the course of the program, flight trajectory data for selected missions were analyzed and plotted to provide a basis for determination of specific measurement and support requirements for these missions

This effort represents Phase II of a three-phase program being conducted by Space Division of North American Rockwell Corporation for the NASA, Office of Advanced Research and Technology, Mission Analysis Division under Contract NAS2-5647 Phase I of this program (covered in Report SD 70-24) established the scientific and engineering objectives and requirements for planetary exploration Phase III will establish families of remote sensors compatible with selected missions, and tabulate the support requirements for specific sensors and for selected missions

ACKNOWLEDGEMENTS

This study was conducted under the direction of A C Jones, Study Manager, who was assisted in the technical integration and coordination by A E. Wheeler The greater part of the study was performed by personnel drawn from the Space Division's Outer Planet Missions Group Specifically, the portion of the report dealing with sensor system descriptions and the development of scaling laws was prepared by W F McQuillan Dr J B. Weddell and D G. Brundige were responsible for the development and application of computer programs while the mission trajectory analysis portion was accomplished under the direction of R. P. Nagorski Support in the sensor analysis and scaling law portions was provided by personnel from the Autonetics Division and from the Science Center of North American Rockwell Corporation

CONTENTS

Section | Page

Section | Page

Section	Page

Section	Page

ILLUSTRATIONS

PRECEDING PAGE BLANK NOT FILMED

TABLES

1 0 INTRODUCTION

Unmanned missions utilizing remote sensing systems provide an effective means of exploring the planets One of the major tasks in planning planetary missions is the definition of experiment payloads and the determination of the support requirements for transport and operation of these payloads To determine the payloads and their support requirements, it is necessary to have (1) an understanding of the scientific and engineering objectives pertinent to a given target, (2) the measurement requirements associated with these objectives, (3) knowledge of the operational conditions for a particular encounter, and (4) flexible models of sensors capable of meeting all or part of the requirements under the operational conditions

The scientific and engineering knowledge and measurement requirements for planetary exploration in the 1975 to 1985 time period were determined and evaluated previously (Reference 1)

The specific objectives of the study covered in this report are to (1) define remote sensor types compatible with the observation objectives previously determined, (2) develop scaling laws depicting design and performance versus support requirements, (3) develop a computer program for application of these scaling laws, (4) develop trajectory parameters for selected outer planet missions, and (5) define future sensor development requirements to better fulfill the observation objectives as previously defined

The candidate remote sensor types identified for each of the previously identified objectives are discussed in Section 3 of the report, which also includes the development of a computer program for evaluation of sensor measurement requirements The development of the scaling laws for the various types of instruments considered and the methodology for application of these are considered in Section 4 In the Appendix, a computer program for application of the scaling laws is discussed, and an example presented

The scaling laws as presented represent sensor models which provide a basis upon which sensor systems may be developed to meet the specific requirements of a given mission, after the mission trajectory parameters and other physical constraints have been established In developing scaling laws for sensor systems, the primary goal has been to establish procedures which permit estimation of sensor support requirements to meet specific scientific objectives The scaling laws are then a means of establishing first-order characteristics of sensor systems and the associated support requirements In this sense, the scaling law approach is not intended to be a complete design procedure for each sensor type but rather a means of establishing essentially gross sensor system characteristics which have significant impact on support requirements Generally the scaling law procedure results in the establishment of overall sensor system operational characteristics and capabilities, as well as the gross physical properties

In order to keep the scaling law procedures within reasonable bounds, it is frequently necessary to use approximations and/or simplifying assumptions Where such procedures are used, they are indicated The simplifications and approximations do not invalidate the results of the scaling law procedure but rather tend to limit the results to the purpose of the study, that is support requirement estimation, rather than establishment of firm system specification requirements

An Appendix, Computer Program User's Manual, includes the listing, flow diagrams, array and module maps, definition of variables, data preparation instructions, and sample data and results, of the Space Experiment Requirements Analysis (SERA) program This program stores planetary observation requirements and trajectory data, determines sensor measurement requirements, calculates sensor support requirements from the scaling laws, and evaluates the work of a sensor in terms of its ability to satisfy the observation requirements when used on a given mission

The logical flow of the present study phase is depicted in Figure 1-1 The numbers shown in each box refer to the sections of this report where the indicated procedures or data are presented Figure 1-1 thus serves as a "road map" to guide the user of this report

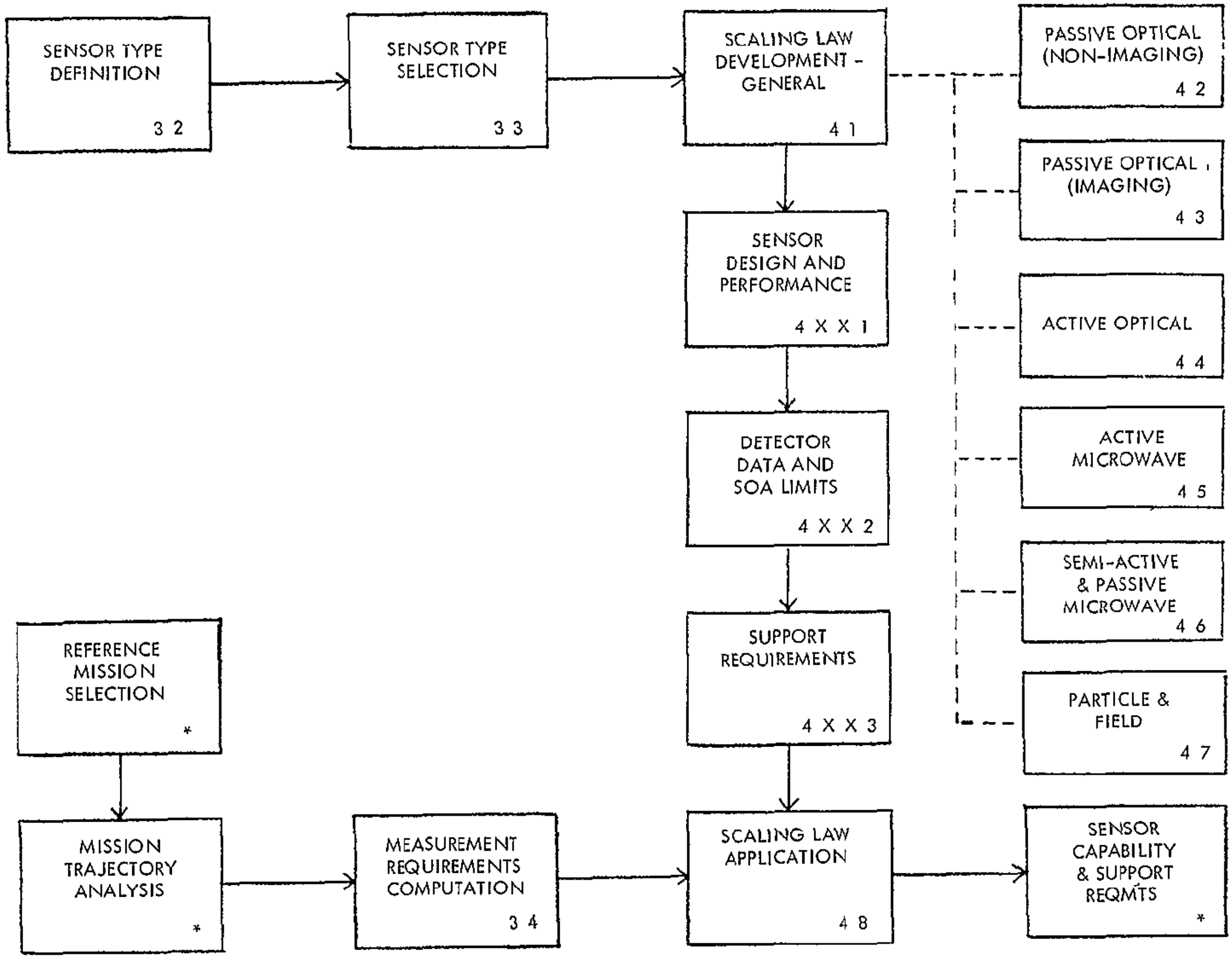

*TO BE DESCRIBED IN PHASE III REPORT

Figure 1-1 Study Phase II Logic

2 0 SUMMARY

Described in this report is a set of scaling laws for remote sensors that depict their relationship to operational and support requirements for specific planetary missions Each scaling law developed presents functionally or graphically the relationship among measurement capabilities and support requirements of one generic type of sensor The scaling laws take into consideration the limitations imposed by current state-of-the-art and fundamental physical limits of the sensing technique applied

Scaling laws are developed for the following instrument classes

Passive Optical Instruments

Active Optical Instruments

Active Microwave Instruments

Passive and Semi-active Microwave Instruments

Particles and Field Measuring Instruments

Sensor types are further differentiated into image forming and non-image forming, with secondary classifications according to spectral region and function Image forming systems include both fixed and scanning types, non-image forming systems include spectrometric and radiometric types

Each of the scaling laws is developed from the basic concept of signal-to-noise ratio, defined as the ratio of peak-to-peak signal voltage or current to rms noise in the detector The modulation transfer function concept is introduced where several external and internal factors contribute to sensor sensitivity and resolution

The bases for scaling laws for Passive Optical Instrument Systems include

1 The measurement requirements

2 The observation geometry and the time available for the measurement, as imposed by the trajectory of the spacecraft

3 The electromagnetic energy available for measurement

4 The thermal and other sources of background or noise

Many instrument types could be considered in the category of Active Optical Instruments but the state-of-the-art of coherent light generation restricts these to Laser Radar, or Lidar types The support requirements are extrapolated from known systems

Scaling laws for Active Microwave Systems provide a range of design alternatives to meet various kinds of measurement requirements Sensor types included are

1 Non-coherent Mapping Systems

2 Coherent Mapping Systems

3 High Resolution Ground Mapping Systems

Semi-active and Passive Microwave Systems all require an antenna and receiver on the spacecraft The design of subsystems is essentially deterministic once a set of measurement parameters has been defined Tradeoffs which are open to selection are readily summarized in the form of nomograms, which are established to cover the range of parameters most likely to be encountered in planetary exploration

The basis for scaling laws for Particles and Field Measuring Systems is to define point design on the basis of existing and developmental space instrumentation for each of the specific sensors considered The energy or field intensity range provides the basis for selection of the specific design

The measurement requirements for various points along the trajectory of a given mission depend upon the spacecraft position with reference to the target planet A computer program was developed to permit determination of these measurement requirements at selected trajectory points, based on the mission parameters Flyby missions to Mercury, Venus, Jupiter, Saturn, Uranus, and Neptune were selected for the computation of specific measurement requirements In addition, non-imaging sensor measurement and support requirements are to be determined later for orbiters at Mercury, Venus, Mars, and Jupiter

The Space Experiment Requirements Analysis (SERA) computer program, described in Appendix A to this report, includes the following

1 Module 1, which stores observation requirements for the selected target planets

2 Module 2, which calculated trajectory dependent measurement requirements for selected missions

3 Module 3, which calculates the support requirements and the worth of a sensor in terms of its capability to perform the required observations from a given trajectory

4 A scaling law subroutine for each sensor type

5 An executive program which calls into execution the three modules and approximate scaling law subroutines, by means of overlay techniques

3 0 REMOTE SENSOR SELECTION

3 1 GENERAL

The identification of sensor types capable (at least in principle) of meeting planetary observation requirements is a critical part of this study By a sensor types is meant a kind of measurement capability or an operational principle common to all sensors of this type For example, vidicon camera telescopes constitute a sensor type, while the Mariner 6 narrow-angle camera is a particular sensor Hence, there should be a one-to-one correspondence of scaling laws and sensor types

In this section, candidate sensor types are identified and then associated with the observation objectives and requirements previously identified (References 1 and 2) A given sensor type may, of course, support several observation objectives Conversely, some observation objectives may require several sensor types, e g , atmospheric spectrometry requires instruments operating in the infrared, visible, and ultraviolet regions Sensor types that contribute little to the planetary exploration goals are of less importance than those that contribute much Development of scaling laws for the former can be omitted without serious loss to the usefulness of the study results Also, some sensor types are so simple, or allow a single design capable of meeting all observation requirements, that their scaling laws can be replaced by fixed design data These cases are identified and used to limit the scope of scaling law development

The observation requirements have been defined in terms of intrinsic planetary properties It is first necessary to express these requirements in terms commensurate with quantitative measures of sensor capability That is, measurement requirements must be commensurable with the ability of a sensor to perform the measurements on a given mission When such measurement requirements are known, preliminary selection of candidate sensor types can be made on the basis of performance data for particular instruments Also, cases where the measurement requirements far exceed present or projected capabilities can be recognized and such sensor types removed from consideration The mathematical problem of converting observation requirements to measurement requirements is discussed in Section 3 4

3 2 SENSOR SYSTEM DEFINITIONS

3 2 1 Candidate Sensor Types

Requirements for remote observations of planetary properties have been defined in detail, and the techniques for effecting each of the observations have been tentatively identified (References 1 and 2) One of the initial steps in the present study phase was the identification of candidate sensor types for each technique-property combination The observable properties are listed in Table 3-1, and observation techniques in Table 3-2 It should be noted that several of the properties are identified as outside the scope of the study, as they involve in situ observation or non-planetary observations, these remain in the listings as indications that omissions were not unintentional They are identified as "outside scope"

The identification of candidate sensor types for each property/technique combination has been made carefully, and only after evaluation of the suitability of various methods for making the measurement, and selection of the most important in those cases offering several possibilities The candidate sensor types identified for possible application and for detailed evaluation are shown in Table 3-3, they are also identified as being imaging or non-imaging types This listing serves as the basis for developing the scope of the scaling law derivation program

The selection of candidate sensor types is based upon several factors, including potential capabilities for making the required measurements, commonality of usages for more than one measurement, physical limitations of the technique and/or sensor system, and state of development for spacecraft use within the prescribed time period In each instance, the identification of candidate types and the selection of those to be considered further were accomplished by a specialist in the field having knowledge both of the theoretical aspects and the state-of-the-art of sensor development Whenever possible, the state-of-the-art is based on operational data for existing or developmental sensors, which are presented in tabular format in Table 3-3

During the course of the investigation it was ascertained that candidate sensors for a few of the properties and techniques specified were not actually within the state-of-the-art for the projected time period, and this is noted in the right-hand column of Table 3-3 Also, for a few sensors the data which could be derived were of a relatively low priority (as discussed in paragraph 3 2 2), and as such did not warrant full development and application of the scaling laws This condition is also noted in Table 3-3

Table 3-1 Observable Properties

No.	Description
1	Optical images of surface and/or atmosphere
2	Radar images of surface and/or atmosphere
3	Satellite orbital parameters*
4	Chemical/nuclear assay (direct)*
5	Spacecraft trajectory parameters*
6	Active seismic detection*
7	Passive seismic detection*
8	Temperature vs depth below surface
9	Magnetic field near surface*
10	Magnetic field above atmosphere
11	Mineralographic, petrographic, crystallographic assay (direct)*
12	Gamma ray flux and spectrum
13	Charged particle flux, spectrum, angular distribution
14	Electric field, currents, conductivity at and below surface*
15	Microwave radiation flux, emissivity, absorptivity
16	Microwave spectrum
17	Infrared radiation flux, emissivity, absorptivity
18	Infrared spectrum
19	Visible/ultraviolet radiation flux, emissivity, absorptivity
20	Visible/ultraviolet spectrum
21	Radio flux and spectrum
22	Biological assay and activity
23	Surface temperature (direct)*
24	Laser beam reflectivity/absorptivity of atmosphere
25	Atmospheric temperature (direct)*
26	Atmospheric pressure (direct)*
27	Radio reflectivity/transmissivity of atmosphere
28	Entry probe trajectory parameters*
29	Electric field and currents in atmosphere*
30	Surface mechanical properties (direct)*
31	Gravitometric data
32	Electromagnetic signal time and ray deflection
33	Wind velocity and direction (direct)*
34	Dust storm intensity and movement (direct)*
35	Radio-frequency permittivity, resistivity, susceptibility
36	Optical permittivity, resistivity, susceptibility
37	Acceleration and deceleration of vehicle*
38	Distance, altitude of spacecraft from topographic features, etc

Table 3-1. Observable Properties (Cont)

No	Description
39	Electromagnetic phase shift
40	Polarization (amount, type, rotation, etc)
41	Stellar occultation (photometric)
42	X-ray absorption and emission
43	X-ray spectrum induced by solar electrons
44	Fast/slow albedo neutron flux ratio

*Outside scope of study (*in situ* observation or nonplanetary observation)

Table 3-2. Observation Techniques

No	Description
1	Radio flux measurement (nonimaging) (wavelengths longer than 1 cm)
2	Microwave radiometry (1 cm to 100 micron)
3	Infrared radiometry (100 to 0.7 micron)
4	Visible photometry (0.7 to 0 4 micron)
5	Ultraviolet photometry (0.4 micron to 100 A)
6	X-ray photometry (100 A to 0 1 A)
7	γ-ray flux measurement (<0 1 A, or photon energies >120 kev)
8	Multiband flux measurement
11	Radio-wave spectrometry
12	Microwave spectrometry
13	Infrared spectrometry
14	Visible spectrometry
15	Ultraviolet spectrometry
16	X-ray spectrometry
17	γ-ray spectrometry
18	Multiband spectrometry
21	Passive radio-wave imagery
22	Passive microwave imagery
23	Passive infrared imagery
24	Passive visible imagery
25	Passive ultraviolet imagery
26	Passive X-ray imagery
27	Passive γ-ray imagery
28	Passive multiband imagery
31	Monostatic radar (nonimaging)
32	Monostatic radar imagery
33	Bistatic radar (nonimaging)
34	Bistatic radar imagery
35	Laser transmission/reflection/scattering
36	Earth occultation (radio)
38	Other observations involving active artificial sources of electromagnetic radiation (e g , another spacecraft)
39	Occultation of natural sources of electromagnetic radiation (e.g., stars)
41	Radio-wave polarimetry
42	Microwave polarimetry
43	Infrared polarimetry
44	Visible polarimetry
45	Ultraviolet polarimetry

Table 3-2 Observation Techniques (Cont)

No	Description
46	X-ray polarimetry
47	γ-ray polarimetry
48	Multiband polarimetry
51	Magnetic field measurement
52	Electric field measurement
53	Charged particle (electrons, protons, and heavy nuclei) flux or dose measurement
54	Charged particle spectrometry
55	Neutral particle (neutrons) flux or dose measurement
56	Neutral particle spectrometry
57	Auroral and airglow emission spectrometry*
58	Microwave tracking
99	Other observation types

*Special case of types 14 and 15.

Table 3-3 Candidate Sensor Types

Item	Observable Property	Observation Technique	Sensor Type	Remarks
1	Optical Images	Passive Visible Imagery	Television Camera	Same law as (1)
2	Optical Images	Passive Multiband Imagery	Multispectral TV Camera	
3	Radar Images	Microwave Radiometry	Scanning (mapping) Radiometer	
4	Radar Images	Monostatic Radar Imagery	High Resolution Radar	
5	Radar Images	Passive Microwave Imagery	Scanning Radiometer	Same type as (3)
6	Magnetic Field Near Surface	Magnetic Field Measurement	Flux Gate Magnetometer	
7	Magnetic Field Above Atmosphere	Magnetic Field Measurement	Helium Magnetometer	
8	Gamma Ray Emission	Gamma Ray Spectrometry	Gamma Ray Spectrometer	
9	Charged Particle Spectrum	Charged Particle Spectrometry	Charged Particle Spectrometer	
10	Charged Particle Spectrum	Charged Particle Spectrometry	Corpuscular Spectrometer	Same type as (9)
11	Charged Particle Spectrum	Charged Particle Spectrometry	Electrostatic Plasma Spectrometer	
12	Charged Particle Spectrum	Charged Particle Flux Measurement	Geiger Mueller Counter Array	
13	Charged Particle Spectrum	Charged Particle Flux Measurement	Ion Chamber	
14	Charged Particle Spectrum	Charged Particle Flux Measurement	Proportional Counter Array	
15	Electric Field Near Surface	Electric Field Measurement	Langmuir Probe	No feasible experiment
16	Electric Field Near Surface	Electric Field Measurement	Ion Density Probe	No feasible experiment
17	Electric Field Near Surface	Electric Field Measurement	Electric Field Mill	No feasible experiment
18	Microwave Flux	Microwave Polarimetry	Radiometric Polarimeter	
19	Microwave Flux	Microwave Radiometry	Temperature Measuring Radiometer	
20	Microwave Spectrum	Microwave Spectrometry	Radio Spectrometer	(Bandwidth Requirements e ceeds State of the Art)
21	Microwave Spectrum	Microwave Radiometry	Mic owave Spectrometer	
22	Infrared Flux	Infrared Radiometry	IR Radiometer	
23	Infrared Flux	Passive Infrared Imagery	IR Thermal Mapper (imaging)	State of Art questionable
24	Infrared Flux	Solar Occulation Spectrometry	IR Spectrometer	Law is a variant of (22)
25	Infrared Spectrum	Infrared Radiometry	IR Spectrometer	Law is a variant of (22)
26	Infrared Spectrum	Infrared Spectrometry	IR Grating Spectrometer	Law is a variant of (22)
27	Infrared Spectrum	Infrared Spectrometry	IR Michelson Spectrometer	Law is a variant of (22)
28	Infrared Spectrum	Infrared Spectrometry	Filter Spectrometer	Law is a variant of (22)
29	Visible Ultraviolet Flux	Visible Photometry	Visible UV Photoelectric Photometer Array	
30	Visible Ultraviolet Flux	Occultation of Natural Sources of Electromagnetic Radiation	Filter Radiometer	Law is a variant of (22)
31	Visible-Ultraviolet Flux	Ultraviolet Photometry	Telescope With Visible UL Photoelectric Photometers	Same type as (29)
32	Visible-Ultraviolet Spectrum	Ultraviolet Spectrometry	Normal Incidence Grating Spectrometer	Law is a variant of (22)
33	Visible Ultraviolet Spectrum	Ultraviolet Spectrometry	Grazing Incidence Grating Spectrometer	Same type as (32)
34	Visible Ultraviolet Spectrum	Visible Spectrometry	Visible UV Scanning Spectrometer	
35	Visible Ultraviolet Spectrum	Multi Band Spectrometry	Ebert Spectrometer	
36	Visible Ultraviolet Spectrum	Multi Band Spectrometry	Michelson Interferometer	Law is a variant of (22)
37	Visible Ultraviolet Spectrum	Ultraviolet Photometry	Visible-UV Photoelectric Photometer Array	Same type as (29)
38	Visible Ultraviolet Spectrum	Ultraviolet Spectral Mapping	UV Scanning Spectrometer	Law is a variant of (29)
39	Radio Flux and Spectrum	Occultation of Natural Sources of Electromagnetic Radiation	Microwave Spectrometer	Same type as (20)
40	Radio Flux and Spectrum	Radio Flux Measurement (Non Imaging)	Microwave Spectrometer	Same type as (20)
41	Coherent Light Reflectivity	Laser Transmission/Reflection/ Scattering	Laser Radar (lidar)	
42	Radio Reflectivity	Radio Wave Polarimetry	Bistatic Radar	No feasible experiment
43	Radio Reflectivity	Microwave Polarimetry	Radiometric Polarimeter	Same type as (18)
44	Radio Reflectivity	Bistatic Radar Imagery	Bistatic Radar	Same type as (42)
45	Radio Reflectivity	Monostatic Radar Imagery	Pulsed Microwave Radar	
46	Radio Reflectivity	Passive Microwave Imagery	Imaging (mapping) Radiometer	Law is a variant of (18)
47	Radio Reflectivity	Monostatic Radar (Non Imaging)	Pulsed Microwave Radar	Same type as (45)
48	Electromagnetic Signal Propagation Time	Earth Occultation (Radio)	Coherent Transponder	Beyond state of art
49	Electromagnetic Signal Propagation Time	Monostatic Radar (Non Imaging)	Pulsed Microwave Radar	Same type as (45)
50	Electromagnetic Phase Shift	Earth Occultation (Radio)	Two Frequency Radio Occultation Receiver	
51	Polarization	Visible Polarimetry	Optical Analyzer and Polarimeter	Same law as (29)
52	Polarization	Microwave Polarimetry	Radiometric Polarimeter	Same type as (18)
53	Stellar Occultation	Visible Photometry	Telescope With Visible UV Photoelectric Photometers	Same type as (29)
54	X-Ray Spectrum	X Ray Spectrometry	X-Ray Spectrometer	
55	Albedo Neutron Flux	Neutral Particle Flux Measurement	LiI Scintillation Spectrometer	

3 2 2 Sensor System Performance Requirements

The determination of some measurement requirements has been shown to depend on mission data or on assumptions concerning sensor design and operation Such determination could not proceed until specified trajectories had been calculated and the sensor assumptions had been made It was necessary to identify candidate sensor types at an early stage of this study phase, both to provide a background for these assumptions and to assure timely completion of study objectives This identification was made possible, on a tentative basis, by examination of these measurement requirement parameters that are identical to the observation requirement parameters defined in Reference 1 These identical parameters are listed in Table 3-4

The parameters most important to the identification of candidate sensor types are maximum wavelength, minimum wavelength, spectral resolution, phase shift resolution, and amount of polarization The wavelength data govern the spectral range of the sensor (infrared, ultraviolet, etc) The required spectral resolution may indicate the selection of either a radiometer or a spectrometer If phase shift or polarization requirements are stated, instruments to measure these quantities are required

In addition to the mission-independent measurement requirements, both horizontal and vertical spatial resolution requirements govern sensor type selection If an extensive area is to be covered at a high horizontal resolution, a map of the area is produced and an imaging sensor is required Non-imaging sensors either have poor angular resolution (limited by the sensor aperture angle) or sample widely separated spots in a given region A vertical resolution requirement dictates use of a radar system unless observations of phenomena near the planetary limb are feasible with passive sensors Passive stereo sensors to provide vertical resolution are considered beyond the state-of-the-art for the missions considered in this study Experiments requiring simultaneous use of two spacecraft are not considered

Table 3-4 summarizes the mission-independent measurement requirements considered in preliminary selection of candidate sensors These requirements represent the extremes of the optimal observation requirements presented in Reference 1 An example of individual measurement requirement values, including those dependent on sensor location or design assumptions, is presented in Section 6 Particle and field measurement requirements not included in Table 3-4 cover charged and neutral particle energies from 0 02 eV to 300 MeV and magnetic field strengths from 1×10^{-5} to 10 gauss

No conclusion is made here whether a sensor of the candidate type can actually support the measurement requirements Such conclusions depend on quantitative evaluation of scaling laws, and are reached in Section 6 in a

Table 3-4 Summary of Mission-Independent Measurement Requirements

Spectral region (nominal)	Radio	Microwave	Infrared	Visible	Ultraviolet	X-ray, γ-ray
Maximum wavelength (micron)	-	$1\ 0 \times 10^{4}$	100	0 7	0 4	0 01
Minimum wavelength (micron)	1×10^{4}	100	0 7	0 4	0 01	-
Spectral resolution (micron)						
Maximum (finest)	10	100	1×10^{-5}	1×10^{-5}	1×10^{-5}	5×10^{-5}
Minimum (coarsest)	1×10^{5}	1000	10	0 3	0 1	5×10^{-5}
Imaging required	No	Yes	Yes	Yes	No	No
Non-imaging required	Yes	Yes	Yes	Yes	Yes	Yes
Phase shift measurement	Yes	No	No	No	No	No
Polarization measurement	Yes	Yes	No	Yes	No	No
Vertical resolution required	Yes	No	Yes	No	No	No

sample case The candidate types selected are those viewed as most likely of feasible application The selections made here determine which scaling laws require development and application

3 3 SENSOR TYPES VERSUS OBSERVATION REQUIREMENTS

3 3 1 Sensor Types Evaluation

The selected candidate sensor types are associated with observable properties and general observation techniques in Table 3-3 This table indicated redundancies of the sensor types themselves or of the scaling laws of sensor types that differ in only a few details In a few instances discussed in Section 4, state-of-the-art considerations showed immediately that no sensor of the candidate type could achieve even the marginal measurement requirements No scaling law development was undertaken in these cases

To focus attention on the most significant sensor types and their scaling laws, a priority rating system was applied to the candidate types First, the worth of the observation objectives supported by each type was determined from the worth data presented in References 1 and 2 The cumulative worth

$$W = \sum_i \sum_j w_{ji} \quad (1)$$

where w_{ji} is the worth of fully attaining the j^{th} observation objective at the i^{th} planet If the objective is irrelevant to a given planet (e g , cloud imagery at Mercury) or is outside the scope of the study, $w_{ji} = 0$ A priority number Q_W was assigned as indicated in Table 3-5

Table 3-5 Observation Priority Numbers

Cumulative Worth (W)	Priority Number (Q_W)
$W > 20$	1
$10 \leq W \leq 20$	2
$W < 10$	3

The more complicated a scaling law, the more important are its formulation and application Very simple scaling laws, or ones that degenerate to single sensor designs which satisfy all measurement requirements (e g , a magnetometer), can be applied manually to evaluate sensor support requirements Therefore, a preliminary assessment of the probable complexity of each set of scaling laws was made A scaling law complexity priority number Q_S was then assigned as follows high complexity, $Q_S = 1$, moderate complexity, $Q_S = 2$, low complexity, $Q_S = 3$ The overall priority

$$Q = Q_W Q_S \quad (2)$$

was evaluated In some cases where Q = 6 or 9, the sensor scaling laws were not formulated beyond degenerate point designs, and will not be incorporated in the SERA computer program (Section 4 8) Values of W, Q_W, Q_S, and Q are presented in Table 3-6

3 4 OBSERVATION/MEASUREMENT REQUIREMENTS CONVERSION

3 4 1 Conversion Methodology

Planetary observation requirements appropriate conceptually to remote sensing have been defined in References 1 and 2 The requirements stated in Reference 1 were expressed in terms of observation parameters that characterize the required range, precision, and quantity of observations as well as the location and extent of the observable phenomena The observations were formulated with reference to the planet, independently of the sensors that might make the observations or the trajectory of the spacecraft carrying these sensors For example, a spatial resolution requirement was expressed in meters along the surface of the planet, without regard to the the angular resolution of an instrument or the range and direction from a spacecraft to the region to be viewed From the list of I=40 observation parameters in Table 3-7, I_j parameters were selected to define the jth observation requirement The following information was supplied for the i th parameter a_i $(1 \leq i \leq I_j)$

a_i' = optimal value of a_i (i e , the value that fully satisfies the scientific and technological objectives corresponding to the given observation requirement)

a_i'' = marginal value of a_i (i e., the value that barely provides useful information)

Table 3-6 Sensor Type Priority Numbers

Sensor Type	Cumulative Worth (W)	Worth Priority (Q_W)	Complexity Priority (Q_s)	Overall Priority (Q)	Scaling Law Developed	Scaling Law Computer Subroutine
Television camera	12 90	2	1	2	Yes*	Yes
Multispectral TV camera	2 80	3	1	3	Yes	Yes
Scanning radiometer	9 60	3	2	6	Yes	Yes
High-resolution radar	4 80	3	2	6	Yes	Yes
Flux gate magnetometer	18 00	2	3	6	Yes	No
Helium magnetometer	24 00	1	3	3	Yes	No
Gamma-ray spectrometer	1 40	3	2	6	No	No
Charged particle spectrometer	0 80	3	2	6	Yes	No
Geiger-Mueller counter array	0 50	3	3	9	No	No
Proportional counter array	0 50	3	3	9	No	No
Ion chamber	0 50	3	3	9	Yes	No
Electrostatic plasma spectrometer	0 50	3	2	6	Yes	No
Radiometric polarimeter	14 16	2	2	4	Yes	Yes
Temperature-measuring radiometer	63 60	1	2	2	Yes	Yes
Radio spectrometer	33 40	1	2	2	No**	No
Microwave spectrometer	17 58	2	2	4	No**	No
IR radiometer	45 60	1	2	2	Yes	Yes
IR thermal mapper (imaging)	38 80	1	1	1	Yes*	
IR spectrometer (any variant)	44 77	1	1	1	Yes	Yes
Telescope with visible-UV Photoelectric photometers	49 50	1	2	2	Yes	Yes
Filter radiometer	1 75	3	3	9	Yes	Yes
Grating spectrometer (visible UV)	9 20	3	1	3	Yes	Yes
Visible - UV scanning spectrometer	4 20	3	2	6	Yes*	Yes
Ebert spectrometer	12 00	2	1	3	Yes	
Michelson interferometer	15 80	2	1	3	Yes	Yes
Lasar radar (lidar)	8 40	3	2	6	Yes	Yes
Pulsed microwave radar	32 30	1	1	1	Yes	Yes
Two-frequency radio occultation receiver	26 10	1	3	3	Yes	No
Optical analyzer and polarimeter	14 00	2	2	4	Yes	Yes
X-ray spectrometer	0 50	3	2	6	No	No
LiI scintillation spectrometer	0 40	3	2	6	No	No

* Developed under Contract NAS2-4494 (Reference 2)
** Beyond foreseeable state-of-art

Table 3-7. Observation Parameters

No	Definition	Unit
1	Longest wavelength of spectral region	Micron
2	Shortest wavelength of spectral region	Micron
3	Spectral resolution, at wavelength requiring highest resolution	Micron
4	Spatial resolution at target	Meter
5	Fraction of surface area of planet covered	Percent
6	Northernmost latitude of area covered (negative if in northerm hemisphere)	Degree
7	Southernmost latitude of area covered (negative if in northern hemisphere)	Degree
8	Maximum Sun elevation angle above horizon at target	Degree
9	Minimum Sun elevation angle above horizon	Degree
10	Vertical resolution	Meter
11	Maximum altitude of observed property (above surface at Mercury and Mars, above visible cloud tops at other planets)	Meter
12	Minimum altitude of observed property	Meter
13	Number of observations or samples	---
14	Time elapsed during one observation	Second
15	Interval between commencement of two successive observations	Second
16	Intensity resolution (gray scale, spectral line strength, field strength, and particle flux)	Percent of maximum intensity
17	Planetocentric angle from planet center-to-spacecraft line	Degree
18	Angle at planet surface from surface element-to-spacecraft line	Degree
19	Angular resolution	Degree
20	Phase shift precision	Degree
21	Polarization (amount)	Percent
22	Rotation angle of plane of polarization (positive counter-clockwise)	Degree
23	Albedo	Percent
24	Magnetic field strength	Oersted
25	Electric field strength	Volt m^{-1}
26	Gravitational acceleration	m sec^{-2}
27	Particle flux	m^{-2} sec^{-1}
28	Particle or photon energy	Electron volt
29	Electromagnetic energy flux	Watt m^{-2}
30	Maximum temperature	°K
31	Minimum temperature	°K
32	Temperature resolution	°K
33	Maximum pressure	Bar
34	Minimum pressure	Bar
35	Pressure resolution	Bar
36	Velocity	m sec^{-1}
37	Longitude	Degree
38	Latitude interval	Degree
39	Longitude interval	Degree
40	Other than above	Degree

w_o = worth of achieving a_1'

F = index number indicating the form of the worth function $w(a_1)$ for values of a_1 between a_1'' and a_1'. By definition $w(a_1'') = 0$

The capabilities of candidate sensors are expressed in terms of their intrinsic resolution, discrimination, dynamic range, field-of-view angle, etc. To compare these capabilities to the observation requirements, the latter must be transformed to measurement requirements commensurable with the sensor measurement capabilities. Some of these transformations depend on the relative locations or velocity of the sensor and the sensed region. Planetary environmental conditions such as illumination and temperature also affect the capability of certain sensors.

The evaluation of measurement requirements involves three kinds of transformation of the observation requirements data.

1. The measurement parameter is identical to an observation parameter.

2. The measurement requirement is a unique function of the instantaneous position and velocity of the sensor relative to the viewed region, certain sensor design parameters and the observation parameters.

3. The measurement requirement applies to a planetary encounter as a whole, and is calculable only by means of some integration along the flight path.

Measurement parameters identical to observation parameters are listed in Table 3-8.

Some measurement parameters are determinable directly from the observation parameters at any sensor location and velocity. The more common transformations are described here, others appear as part of certain sensor scaling laws in Section 4. The geometry of the spacecraft and field of view is illustrated in Figure 3-1. The angular resolution of the sensor

$$\Delta\alpha = \frac{\text{projection of spatial resolution normal to viewing direction}}{\text{slant range to field of view}}$$

Table 3-8 Measurement Parameters Identical to Observation Parameters

Maximum wavelength
Minimum wavelength
Spectral resolution
Number of samples *
Sampling collection duration *
Sampling interval *
Intensity **
Intensity resolution ***
Phase shift resolution
Polarization (amount)
Angle of rotation of polarization plane
Time resolution

*If specified as an observation parameter Otherwise these may be varied as sensor design parameters.
**(Flux, field strength, etc)
***Resolution of any measure of the observed property (field strength, energy, temperature, etc)

$$\Delta\alpha = \frac{\Delta r \sin\xi}{R_F} \qquad (3)$$

where the slant range

$$R_F = (R_p - H) \cos\alpha - \left[(R_p + H)^2 \cos^2\alpha - H\,(2R_p + H)\right]^2 \qquad (4)$$

and

R_p = planetary radius (oblateness is ignored)

Δr = spatial resolution at surface of planet

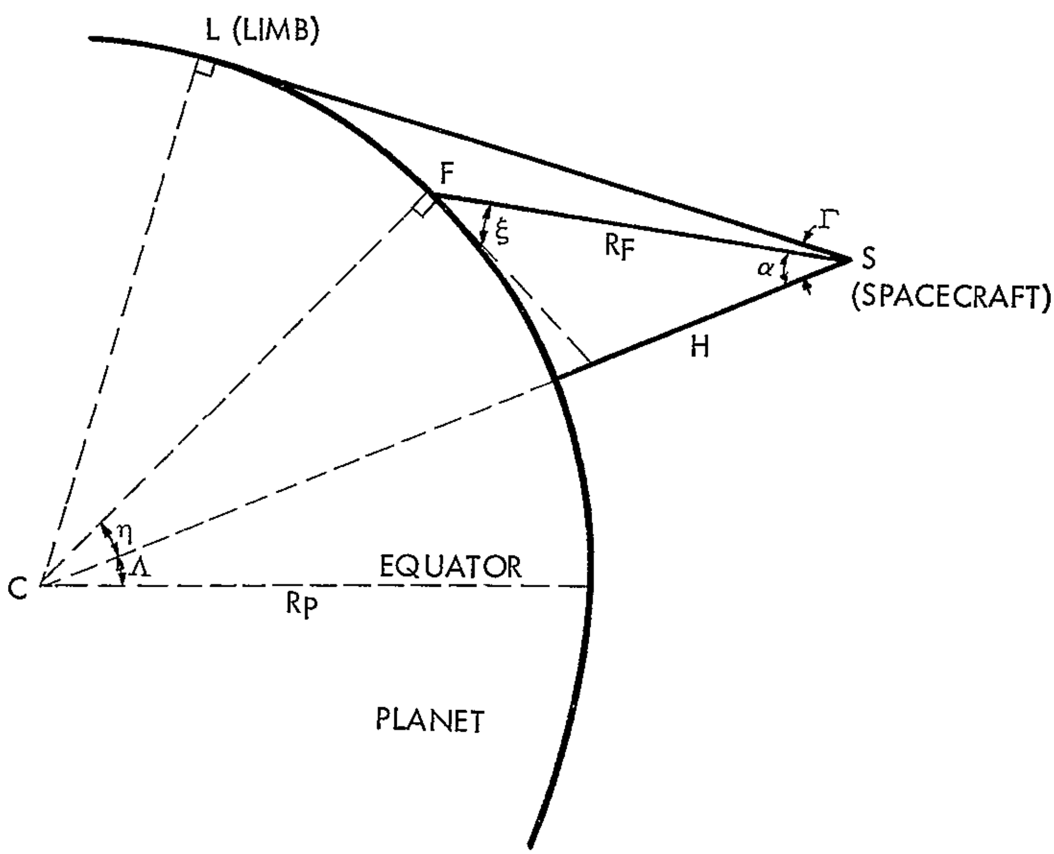

Figure 3-1 Spacecraft Planet Geometry

H = spacecraft surface altitude

α = viewing direction angle to vertical at spacecraft

ξ = viewing axis angle to tangent plane at center of viewed area

For greater accuracy, replace α by $(\alpha + r)$ in Equation (3-2) where 2r is the field-of-view angle The swath width (i e , the width of the field of view parallel to the direction in which the sensor is scanned) is

$$Y = R_F \gamma \qquad (5)$$

The field-of-view length in the direction of scan

$$X = R_F \gamma_F / \sin \xi \qquad (6)$$

The aperture half-angle is a variable design parameter of the sensor, selected during application of the scaling law (Section 6)

The overlap of successive fields of view or swaths, and the fraction of the planetary surface covered, are usually complicated functions of the spacecraft trajectory and sensor operating schedule Certain scaling laws incorporate requirements on field overlap Swath overlap and surface coverage are not evaluated in this study phase

To solve Equations (3) through (6) and to evaluate certain scaling law relationships presented in Sections 4 and 6, various trajectory parameters must be specified A trajectory parameter defines the location of a spacecraft relative to a given planet, as a function of time measured from periapsis passage The trajectory parameters involved in this study are listed in Table 3-9 Symbols shown in parenthesis are in common use elsewhere

In addition, it is useful to specify the inclination launch date (constrains sensor selection), solar distance (affects planetary illumination), and earth distance (affects bifrequency radio occultation responder requirements) The calculation of trajectory parameters is described, and results for a selected mission are presented in Section 5

The worth of a measurement capability parameter value is equal to that of the corresponding observation parameter The identity transformations of Equations (3) through (6) are linear, so the form F of the functional dependence of the worth is preserved Evaluation of the worth of a sensor in terms of its measurement and observation capabilities was discussed in Section 3 4 1

Table 3-9 Trajectory Parameters

Parameter	Unit	Symbol
Central distance	km	R
Surface altitude	km	H
Latitude	deg	$\Lambda(\lambda)$
Longitude (0 at periapsis)	deg	$\Phi(\phi)$
Ground speed	km s^{-1}	v_h (v_g)
Spacecraft velocity	km s^{-1}	V (v)
Radius rate	km s^{-1}	R (v_r)
Sun-planet spacecraft angle	deg	η_s
Earth-planet spacecraft angle	deg	η_e
Nadir angle rate	deg s^{-1}	Ξ
Time after periapsis passage	s	t
True anomaly	deg	θ

3 4 2 Measurement Requirements Computer Program

The processing of information relating to observation requirements, measurement requirements, sensor measurement capabilities, and sensor support requirements is accomplished in this study by means of a Space Experiment Requirements Analysis computer program (SERA) Since the entire SERA program requires the use of core storage exceeding that available, SERA is structured as three modules called into execution by an executive program with the use of overlay techniques Briefly, the three modules perform the following operations

1 Module 1 (SERA-1) stores and prints the observation requirements, stated in terms of intrinsic properties of the observed planets

2 Module 2 (SERA-2) converts the observation requirements to measurement requirements, stated in terms of intrinsic properties of generic sensor types, at selected points on a specified planetary encounter trajectory or orbit

3 Module 3 (SERA-3) uses sensor scaling laws to design a sensor of a given type to satisfy a set of measurement requirements, subject to state-of-the-art limitations, and then calculates the sensor support requirements

Module 1 and its results are described in Reference 1 Module 3 is discussed in Section 4 8 of this report The present section gives a general description of Module 2 A program user s manual (Appendix) contains a detailed description of the entire SERA program

In SERA-2, we have the option to evaluate measurement requirement parameters (MRP) based on a single set or on several sets of observation requirement parameter (ORP) values A single set of ORP is defined as corresponding to one observation objective However, several sets of ORP may, at least in principle, be satisfiable by a single sensor If more than one set of ORP is chosen, the optimal value of any measurement parameter corresponds to the most stringent value of the corresponding ORP That is, suppose a'_{i1}, a'_{i2}, , a'_{iJ} are the optimal values of ORP a_i corresponding to observation objectives 1, 2, , J Then the optimal MRP value

$$b'_m = f_{im}(a'_i, p_k) \tag{7}$$

where a'_{ij} is the most stringent of the set $(a'_{i1}, a'_{i2}, \ , a'_{iJ})$ f_{im} is the operator that transforms the i<u>th</u> ORP to the m<u>th</u> MRP, and p_k represents the I_J different trajectory parameters in the transformation Attainment of $a_i = a'_{ij}$ implies attainment of all other a'_i in the set A relationship similar to Equation (3-4) holds for the marginal MRP

$$b''_m = f_{im}(a''_{ij}, p_k) \tag{8}$$

where a''_{ij} represents attainment of only the least stringent a''_i in the set (The term "most stringent" means most difficult to attain, or most valuable if attained)

To transform one or more sets of ORP to a set of MRP, one to twenty points P_n (p_k) on each given encounter trajectory are selected. The first point (P_1) will often be an approximation to the first point on the trajectory from which a sensor of this type can satisfy the MRP The other points will usually be of special interest (e g , terminator crossing, periapsis passage, sun occultation entrance, last useful point, etc)

Several options are available for computation of optimal and marginal MRP and support requirements These options are illustrated by the logic diagram of Figure 3-2

1 The MRP are the optimal values, calculated by using the optimal ORP values a_1' in Equation 3-5, OR, the marginal ORP values a_1'' are used in Equation 3-6

2 The optimal and marginal values of the MRP are based on the optimal ORP values a_1' at points in the set (P_n), OR, the optimal MRP are based on the a_1', and the marginal MRP are based on the marginal ORP a_1'' (Other branches of this option, to use the a_1'' to calculate the optimal MRP, are of no interest)

3 The optimal and marginal sensor support requirements are based on the optimal and marginal MRP values, respectively OR, the optimal sensor support requirements are based on the sensor capability limits (The latter branch is taken if the optimal MRP values represent more stringent requirements than the capability limits) Table 3-10 indicates the most frequently chosen options, also shown by double lines in Figure 3-2

Table 3-10 Option Selection in SERA-2

Option	Branch
1	Use a_1' in Equation (6)
2	Base optimal MRP on optimal ORP, base marginal MRP on marginal ORP
3	Base optimal sensor requirements on optimal MRP or on sensor limitations, whichever represent less capability

The input to SERA-2 consists of

1 Program control parameters which determine SERA-2 input data requirements and output data format, and which identify transformations to be used in determining sensor measurement capabilities

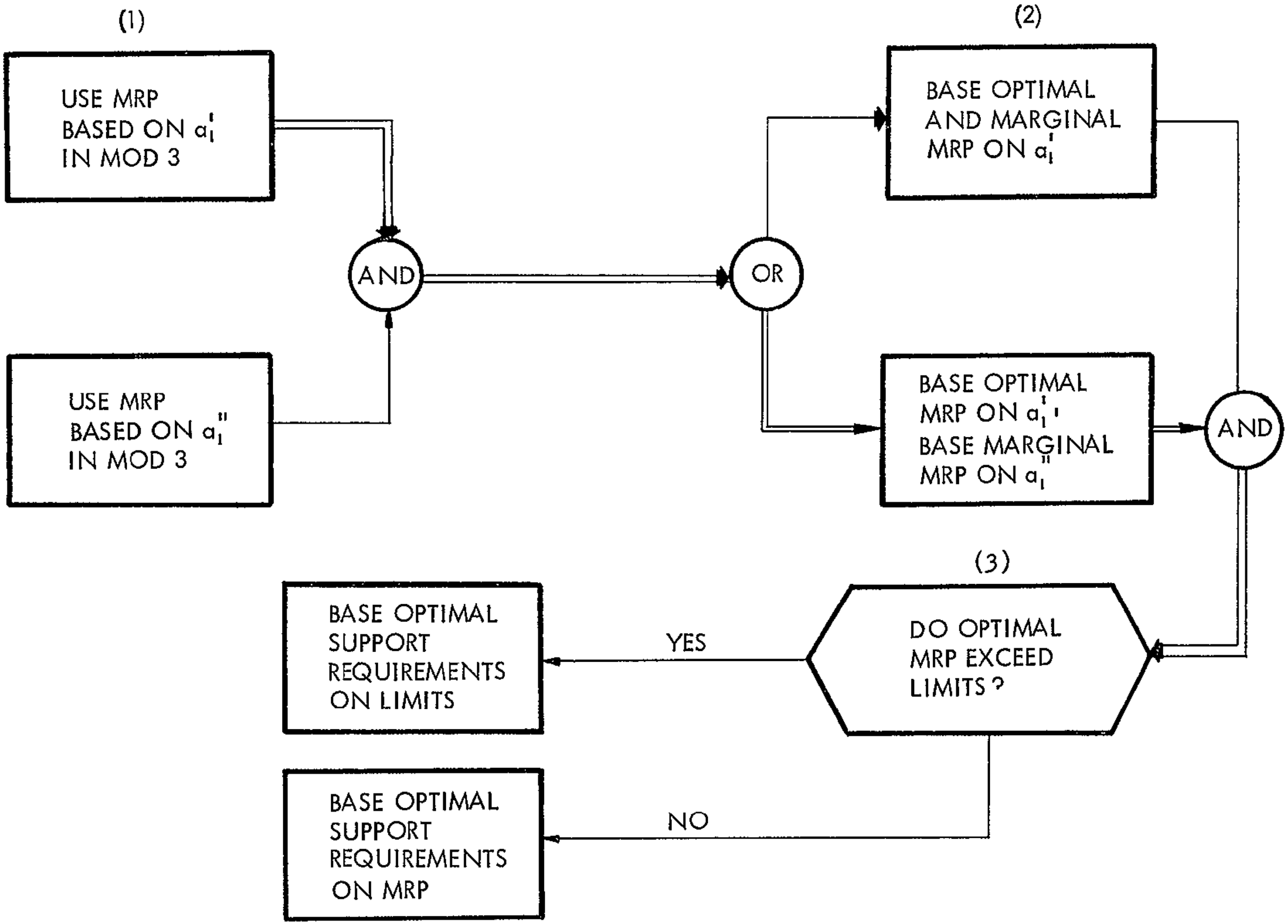

Figure 3-2 Measurement Requirements Computation Chart

2 Libraries of identification numbers and descriptive titles of mission parameters and measurement capability parameters

3 Numeric observation requirements data and selected descriptive or library data (transferred automatically) from SERA-1

4 Numeric measurement requirements and associated worth data where the requirements generated are of independent origin (i e , resulting from design criteria, externally calculated, etc)

The output data provided by SERA-2 is of two basic types, either or both of which can be selected for printout

1 Printout A - the optimal and marginal measurement capabilities for all observation objectives taken together are printed, together with the total worth corresponding to all the optional measurement capabilities taken together One basic set of data per case is provided

2 Printout B - the optimal and marginal measurement capabilities for each objective taken separately are printed, together with the total worth corresponding to all the optimal measurement capabilities (in support of that objective) taken together One basic set of data per objective is provided for the case

4 0 SCALING LAW DEVELOPMENT AND APPLICATION

4 1 INTRODUCTION

4 1 1 General

Scaling laws are developed by instrument class For descriptive purposes, the following classification is used

- Passive Optical Instruments
- Active Optical Instruments
- Active Microwave Instruments
- Passive and Semi-active Microwave Instruments
- Particles and Field Measurement Instruments

This grouping serves two purposes First and foremost it permits general discussion of design features which are common to all instruments in a classification Secondly, it puts emphasis on those areas which are significant for each classification while reducing the amount of repetition of the same material for each scaling law Thus in the discussion of Active Optical Instruments emphasis is placed on the unique feature of optical energy generation and transmission while the Passive Optical Instrument discussion serves the purpose of optical receiver design

Scaling laws may be used for many purposes but the most common use is to establish trade-off data for a sensor system or a subsystem of a sensor in terms of the interacting design variables The trade-off data are then used to define a preliminary engineering design model or models which serve as guidelines for detailed subsystem design In addition, the preliminary design serves as a guide in "sizing" the sensor It is used to estimate such physical properties as size and weight, viewing aperture requirements, power consumption, pointing accuracy requirements, etc In common engineering practice, preliminary design procedures result in one or more "point" designs to meet a given set of measurement objectives The usual procedure is to establish firm functional requirements for the sensor such as "Design a search radar capable of detecting a

10 square meter target at a range of 200 nmi over a hemi-spherical search volume The radar shall detect the target with a 90 percent probability The radar shall be capable of detecting all targets of appropriate size in the search volume which have equivalent ground speeds in the range of 500 to 2000 nmi " Based on the stated requirements, one or more search radar system designs are established with suitable trade-offs between such factors as transmitted power and antenna gain, target location accuracy versus system parameters, etc The net result is that a preliminary radar system description can be evolved from the definition of the requirements and available radar scaling techniques with suitable application of state-of-the-art limitations on generation of microwave power, antenna gain, receiver sensitivity, etc

In the case of remote sensing of planetary surfaces and environments such a relatively straightforward procedure is usually not meaningful since sensor measurement requirements are not limited to specific values but rather are constrained to a range of values over a wide variety of viewing conditions A point design would not serve the purpose of estimating sensor system characteristics which are sufficient to meet measurement requirements over a fairly broad range of measurement variables and conditions It is necessary, therefore, to maintain a somewhat more general approach in the scaling law procedure Many variables which would ordinarily be computed once and then fixed in a point design must be carried as design variables in the scaling law approach to preclude the generation of point design trade-off data

The very fact that the scaling law must be maintained as a general statement is an inherent limitation The limitation results from the fact that in order to make the scaling law computations tractable, it is frequently necessary to make approximations or to use average values This does not materially affect the outcome of the scaled values of system characteristics but it does result in a procedure which is not necessarily amenable to refinement into a detailed design procedure Therefore, in using the scaling laws and in interpreting the results, caution must be exercised, since the purpose of the scaling laws is not to permit detailed sensor system design but rather to estimate sensor system characteristics which impact spacecraft design The scaling laws are not intended as a design tool for establishing system specifications

4 1 2 Scaling Law Development

The scaling laws developed in this study are concerned principally with sensor systems for the electromagnetic spectrum The performance of electromagnetic sensors can generally be descirbed in terms of a signal-to-noise ratio The signal-to-noise ratio statement contains all of the significant parameters which establish sensor system performance System parameters are than established based on the requirement of achieving a given signal-to-noise ratio either for detection or recognition This approach underlies all of the scaling law developments although in certain cases, such as in television systems, the explicit statement of a signal-to-noise ratio is suppressed in the development of a statement of the attainable resolution of the sensor

With few exceptions, therefore, the scaling development consists of two essential steps (1) The derivation of an expression for signal-to-noise ratio for each sensor type of class, and (2) the imposition of a signal-to-noise ratio requirement to meet a given criterion of sensor system performance

The results are ordinarily an unbounded algebraic statement particularized to a given region of the spectrum and/or a given sensor type Bounds are than placed on the significant design parameters The bounds result from state-of-the-art limits as they are known to exist for current technology This is not the only form possible for presenting the results of a scaling law Frequently such devices as slide rules are used to scale such systems as radars and IR mappers The difficulty with mechanizing a scaling law in a fixed form such as a slide rule is that insight into the meaning of various system parameters is frequently lost and the devices are misused Another approach is to summarize the scaling law in the form of a nomogram or series of nomograms to permit rapid variation in system parameters without the tedium of multiple calculations However, nomographic procedures are most useful when system design requirements can be expressed in deterministic form with a minimum number of variables This procedure has been used in the description of the scaling law for passive microwave systems but experience indicates that even in this relatively straightforward case the results are subject to misinterpretation when applied indiscriminately

There are scaling procedures which are only incorporated in the overall procedure by implication The technique is commonly referred to as ratioing and consists essentially of establishing a new set of system characteristics from a computed set by a suitable adjustment of one or more parameters A typical case might be in the form of the increase in optical aperture required to maintain the performance of a radiometer if the viewing distance is doubled All else being equal, the aperture required can be scaled directly as a function of range by a simple ratio This type of scaling is most frequently useful for design equations which are deterministic, as in antenna size scaling as a function of wavelength It may be misleading when used to scale complete systems since more than one variable may be a function of such parameters as viewing distance However, ratioing is extremely useful under many circumstances and may be used to reduce the tedium of multiple detailed calculations of system characteristics

4 1 3 Scaling Law Application

In applying the scaling laws to specific missions, a stepwise procedure can usually be applied although there are a few notable exceptions where an interative procedure is required The general approach to the application of the scaling laws can be summarized in three essential steps as follows

1 Assemble all known requirements and limitations for accomplishing a given scientific objective This step amounts to a definition of sensor measurement requirements, the selection of a reasonable model under which measurements are to be accomplished such as illumination levels (photometric or radiometric model, reflectivity, etc) and the geometric constraints imposed by mission trajectories and dynamics This step defines measurement requirements and limitations in quantitative terms and imposes bounds on sensor system performance

2 The second step involves the selection of sensor type and the definition of sensor characteristics to meet the measurement requirements In order to bound the problem, the limits imposed by the state-of-the-art are imposed on the system parameters at this point Likewise the detection criterion which the sensor must meet is established and imposed at this point

It is frequently convenient to isolate one or more sensor system parameters which have major impact on sensor system support requirements For example, in optical sensors, it is frequently convenient to calculate the aperture diameter based on known or assumed characteristics of the other components of the sensor This approach is not always sufficient, however, since it may be necessary to match the primary optics with other system components Under these circumstances an iterative procedures is necessary to obtain a consistent system design

This step must be carried out in sufficient detail to obtain sensor system physical and operational characteristics as inputs to step 3

3 Once an adequate sensor system description is obtained from step 2, the support requirements are calculated from the relatively simple algebraic expressions or from scaling factors

4 2 PASSIVE OPTICAL INSTRUMENTS

4 2 1 Introduction

An important means of obtaining scientific information remotely is the detection and quantification of electromagnetic radiation in the optical portion of the electromagnetic spectrum For classification purposes the optical portion of the spectrum is considered to extend from the long wavelength far infrared (λ = 100 microns) to the so-called vacuum ultraviolet (λ = 0 2 microns) The bounds on the optical portion of the spectrum are not precise since they are established primarily for the purpose of indicating the applicability of so-called optical tehniques to sensor system design Alternatively, the optical spectrum can be considered to be that portion of the spectrum in which the approximations of geometric optics are applicable

In spite of the sub-division of the optical spectrum into regions such as the infrared, visible and ultraviolet, instrumentation design techniques are similar over the entire optical spectrum, with perhaps the most notable exception being detection techniques which are specifically selected to match the spectral region Other variations may also be significant since it would be fortuitous to find materials which have wavelength-independent characteristics over a range of approximately 1000 to one Materials are selected by spectral characteristics to obtain required index of refraction, transmission, and reflectivity, for specific regions

With these exceptions in mind, scientific instrumentation for the remote sensing of radiation in the optical spectrum can be classified into generic types in several ways For the purpose of developing scaling laws, sensor types are differentiated primarily into non-image forming and image forming sensors with secondary classifications by spectral region and function The classes of instrumentation considered are of the following types

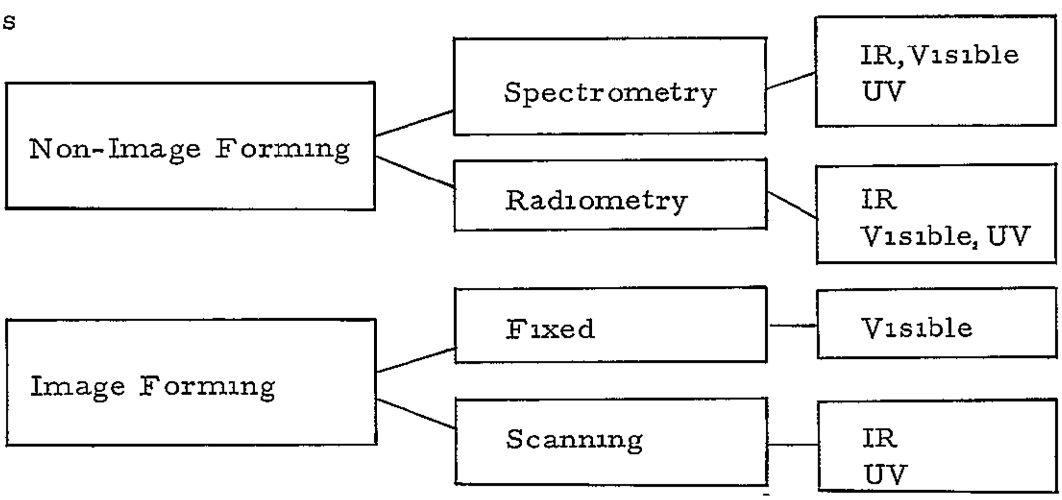

The classes indicated are not all-inclusive since image forming systems may also include such functions as relatively coarse spectrometry in the form of multispectral imagery and a non-image forming radiometer may include an optical analyzer to function as a polarimeter The general classifications given above are intended to indicate the types of scaling laws which are significant but are in no way intended to preclude multi-functional use by adding on relatively straightforward refinements which expand their function

4 2 2 Scaling Law Basis

Passive optical instrumentation for outer planet remote sensing is designed primarily to measure solar energy interaction with the planet and its atmosphere or the self-emission from the planet due to its thermodynamic temperature To a lesser extent stellar radiation which is encountered during star occultation by the planet with a spacecraft may be useful but no specific instrumentation is designed for this purpose From the point of view of measurement instrumentation it is then necessary to establish the levels of the radiation which are available for measurement over the spectral ranges of interest and to establish design requirements for one or more instrument types to meet observation requirements

The procedure, while straightforward in concept, may be difficult to apply because of obvious uncertainties in the levels of radiation at the several planets and limitations in the state-of-the-art of instrument design This leads to conflicts in attaining all measurement objectives The scaling laws developed are not intended to reconcile the conflicts but rather to establish design procedures which are sufficiently flexible to permit a wide range of choices to be made in trading off observation capabilities with support requirements in the form of size, weight, power consumption, data rate and sensor platform stability

The bases for developing a scaling law are the following

1 The measurement requirements

2 The observation geometry and time available for measurement imposed by the trajectory of the spacecraft

3 The electromagnetic energy available for measurement

The measurement requirements and trajectory dynamics are developed separately It is necessary to establish a means for predicting radiant energy levels as the primary input to sensor system design This is developed first

The scaling laws are then developed by instrument type according to their primary function Two general classes are considered, the non-imaging and image forming types As appropriate, further classification is established by spectral class and primary function In this way, all optical instruments are grouped together by function such as spectrometer, radiometer, etc

The scaling laws for non-image forming systems are grouped according to spectral band by function In each spectral band a natural grouping is by function although the separation into functional groups is partly artificial since there may be little or no difference between a polarimeter and a radiometer Furthermore a basic telescopic sensing system may be adapted to many functions by the addition of relatively lightweight optical components in the focal plane of the sensor Thus a radiometer may be used as a polarimeter by the addition of relatively simple optical components Such cases are not treated as separate scaling laws but rather as minor variations to basic scaling laws

Each of the scaling laws is developed from the statement of a signal-to-noise ratio which, according to custom, is the ratio of peak-to-peak signal voltage or current to rms noise under the assumption that the target fills the instantaneous field of view of the optics

Each instrument type considered has common features such as an optical aperture for radiant energy collection and one or more detectors to convert the collected energy into a form which can be analyzed and processed for interpretation In addition, many optical instruments process the collected energy prior to detection to effect a channeling of information or to facilitate post detection processing Both collecting optics and pre-detection optical processing techniques are, to a first approximation, wavelength independent over the optical spectrum They are considered sufficiently general that a single discussion for all of the instrument types described above is adequate

While a general requirement for one or more detectors exists, there is such a large variety of detector types applicable to the full range of the optical spectrum that a general discussion is inappropriate Detectors are discussed with reference to spectral regions under the sensor type where they are first used

Scaling laws for passive optical instruments are developed using the approach most commonly used in the technical literature for specific wavelength regions or according to practices which have evolved either by custom or convenience This approach is a practical necessity, since much of the available information on which scaling law development is based is particularized either to a wavelength region or to specific instrument design procedures It is not the only approach which could be used since, at least in theory, an all-encompassing scaling law for all optical instruments could be developed but attempts at developing such an approach to optical instrument performance have not, as yet, proved useful The difficulty with a general approach is that it is based on a detection criterion incorporating the signal-to-noise ratio of the instrument This approach requires a definition of the signal output of the detector and the overall description of the noise, irrespective of the source The many types of detectors used and the associated noise generating mechanisms tend to make a general description of the noise both tenuous and cumbersome The problem of noise in detection systems for the optical spectrum has been given wide consideration in technical literature Excellent discussions of the general problem as well as specific cases can be found in References 3 through 10 Reference 3 covers the problem in broad scope while Reference 4 through 10 discuss specific detection mechanisms and their associated noise problems The references should be consulted for detailed background information on the development of signal-to-noise ratios and their application to specific instrument designs

4 2 3 Photometric and Radiometric Models of the Planets

4 2 3 1 Photometric Models

In a formal sense, photometric modeling of the planets can be established in multimaterial form based on the input power to the planet, generally from the sun, the spectral reflectance-absorptance characteristics of the planet and its atmosphere and the viewing geometry As discussed in Reference 2, the amount of solar energy per unit time reflected in a given direction at a given wavelength is

$$W(i, \epsilon, \alpha, \lambda) = \frac{H\lambda}{\pi} a(\lambda) f(i, \epsilon, \alpha)(\cos)\epsilon \qquad (1)$$

where

W is the spectral radiance

H is the solar spectral irradiance

$a(\lambda)$ is the surface normal albedo

f is the planetary photometric function

The photometric function depends on the angle of incidence i measured from the surface normal, the angle of relection and the luminance longitude measured from the plane containing the sun surface line An approach using the complete photometric function presents many difficulties since much of the necessary information required to establish a useful model is lacking Much of the spectrally dependent reflectance data has not been established In addition, the practical difficulties of estimating reflection mechanisms are likely to be unrewarding since even today a definitive photometric model of the Earth is not available

For these reasons two separate simplified approaches are used depending upon whether or not the planet has an atmosphere In all cases the solar irradiance is based on the assumption that the spectral variation is equivalent to the sun as a blackbody radiator at a temperature of 5000 deg K The power spectral density function at one AU for solar irradiance is shown in Figure 4-1 in radiometric units For other planets the spectral distribution is assumed to be identical but the power density is scaled as an inverse square law of distance relative to the Earth at one AU For photometric units the solar constant at the Earth is taken as 1 3 x 10^5 meter-candles and scaled to other planet distances by the same inverse square propagation law

For planets with relatively dense gaseous atmospheres such as Saturn a reflection moded in the form

$$W = H\rho \cos^2\theta \qquad (2)$$

is used where

W is the radiance of the scene

H is the solar constant at the planet

ρ is the albedo

θ is the sun-planet-observation point angle as shown in Figure 4-2

The variation with observation angle is assumed to be $\cos^2\theta$ to account for limb darkening One of the most difficult problems is to estimate values of albedo variation with spectral band Based on available though incomplete information the values of spectral band albedos for planets with gaseous atmospheres shown in Table 4-1 will be used

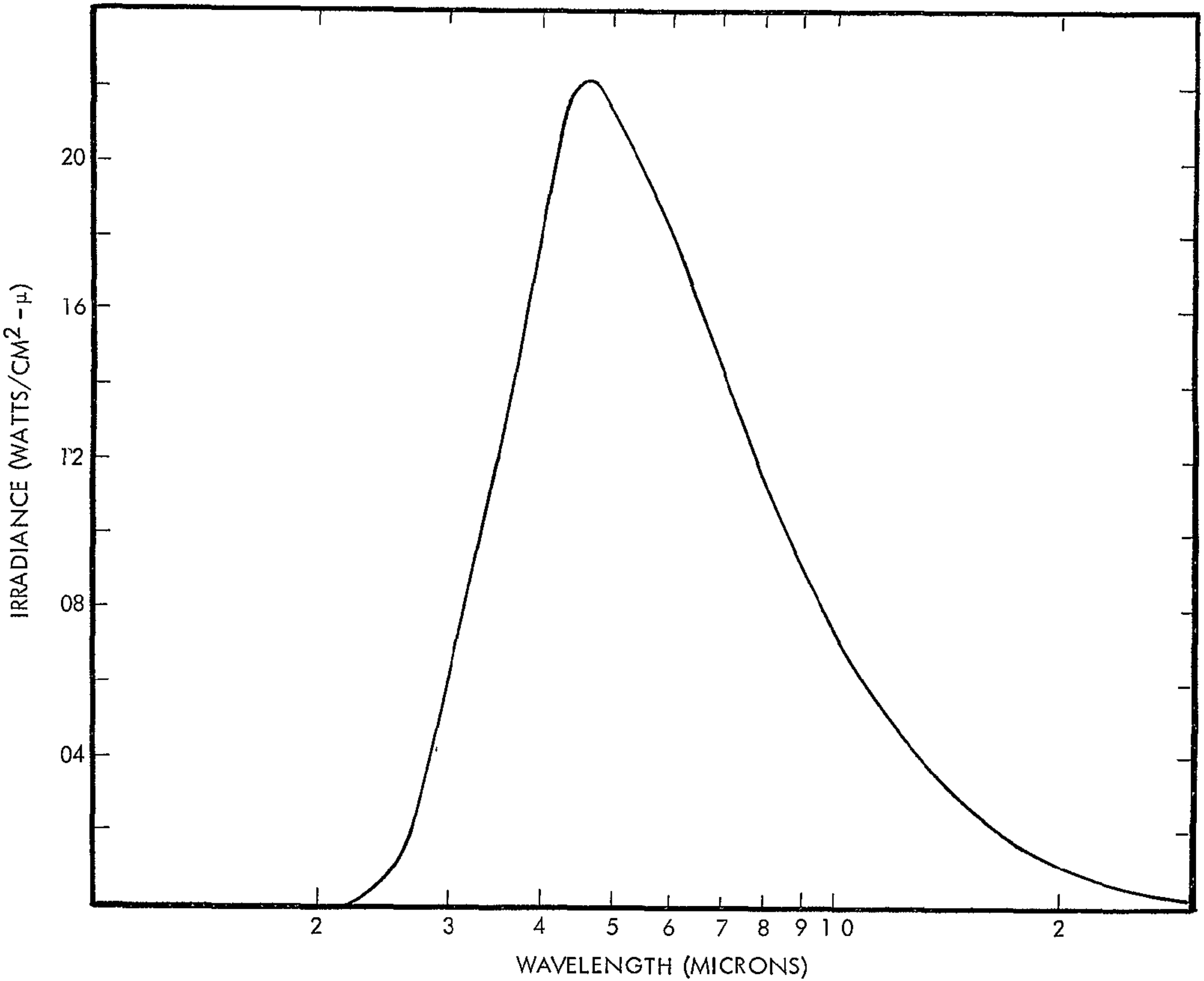

Figure 4-1. Solar Spectral Irradiance at 1 AU

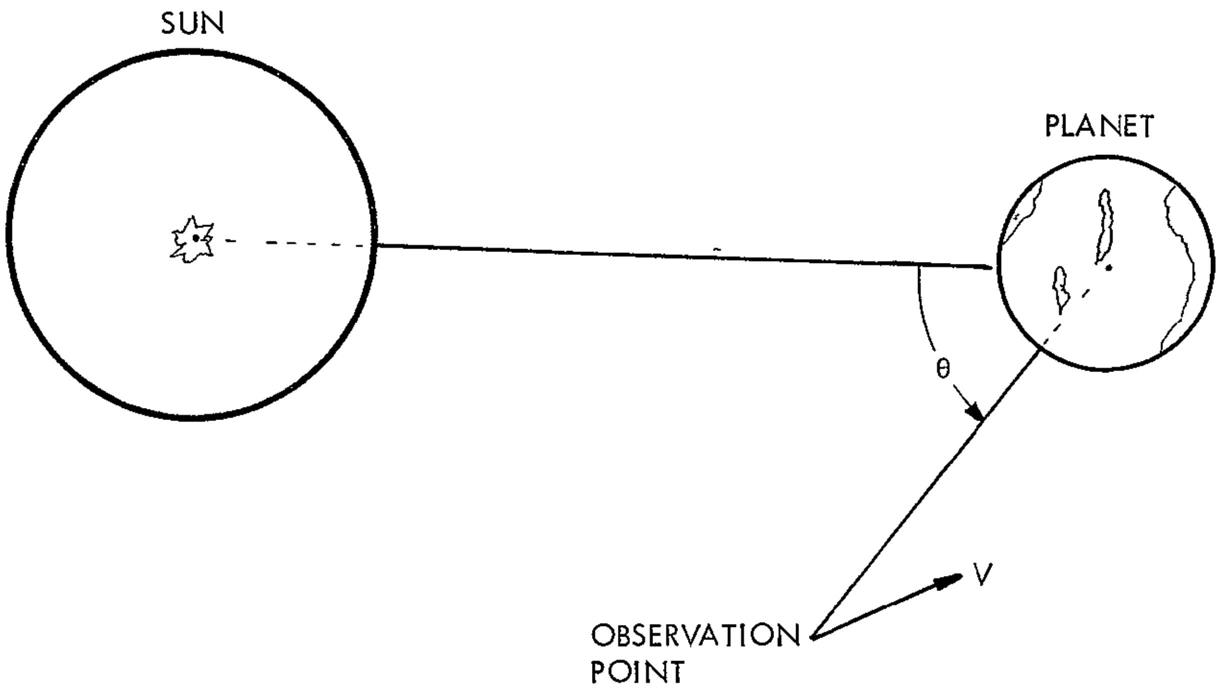

Figure 4-2 Observation Geometry

For planets which do not have an observable atmosphere or have only a tenuous atmosphere a Lambertian reflecting surface is assumed In this case the scene radiance is given by

$$W = H \rho \cos \theta \tag{3}$$

where the quantities are as described previously The values of planetary albedo to be used in computing W are given in Table 4-2

Values of $H(\lambda)$ can be computed by numerical integration of the spectral power density of the blackbody radiation curve of the sun for an assumed temperature of 5000 deg K While the procedure is tedious it can be simplified if a narrow spectral band is assumed and the albedo is assumed independent of wavelength In a strict sense the appropriate value for W is of the form

$$W = \int_{\lambda 1}^{\lambda 2} W(\lambda)\, d\lambda \tag{4}$$

Table 4-1 Characteristics of Planets with Dense Atmospheres

	Solar Constant (W/m^{2})				Average Albedo				Distance Average From Sun
	Total	UV	Visible	IR	UV	Vis	IR	Total Bond	
Venus	2 676x10^{3}	2 42x10^{2}	1 08x10^{2}	6 62x10^{2}	0 35	0 76	0 42	0 85	1 08x10^{8}km
Jupiter	5 2x10^{1}	4 7	20 3	12 9	0 3	0 45	0 15	0 58	7 8x10^{8}km
Saturn	1 5x10^{1}	1 36	5 85	3 71	0 35	0 76	0 42[illegible]	0 57	14 3x10^{8}km
Uranus	4	0 36	1 56	0 99	0 3[illegible]	0 93	0 3[illegible]	0 80	28 7x10^{8}km
Neptune	2	0 18	1 17	0 49	0 3[illegible]	0 84	0 25	0 71	45x10^{8}km

Table 4-2 Characteristics of Planets with Tenuous Atmospheres

	Solar Constant (W/m^2)				Average Albedo				Distance Average From Sun
	Total	UV	Vis	IR	UV	Vis	IR	Total Bond	
Mercury	$9\ 343 \times 10^3$	$8\ 45 \times 10^2$	$3\ 64 \times 10^3$	$2\ 31 \times 10^3$	0 07	0 11	0 30	0 059	$5\ 8 \times 10^7$ km
Mars	$6\ 03 \times 10^2$	54 6	$2\ 35 \times 10^2$	$1\ 46 \times 10^2$	0 05	015	0 35	0 15	$2\ 3 \times 10^8$ km
Pluto	1	0 09	0 39	0 25	0 07	0 14	0 30'	0 15	59×10^8 km

(*Estimated from similar planet type)

However, if spectral independence is assumed over narrow spectral bands then to a first approximation

$$W = \bar{\rho} \cos \bar{\theta} \; H\lambda \tag{5}$$

where the bar indicates averages at the wavelength of interest

4 2 3 2 Radiometric Models

Thermal or self-emission of planetary surfaces can be characterized by the blackbody radiation curves of measured or estimated planetary surface temperatures shown in Table 4-3 Under the assumption of an emissivity of one, the spectral radiance can be estimated directly However, the sensitivity of a thermal mapper to an incremental temperature or emissivity difference is dependent upon the slope of the radiant emittance with respect to temperature For the range of significant planetary surfaces shown in Table 4-3 the following function has been evaluated

$$\frac{\partial W}{\partial T} = \int_{o}^{\lambda} \frac{\partial W_{\lambda}(T)}{\partial T} d\lambda \tag{6}$$

and plotted in Figure 4-3 As an example of the use of the curves, assume that the value of the integral is required between 10 and 12 microns for a temperature of 300°K, from Figure 4-3 the following values are found

$$\frac{\partial W}{\partial T} = \int_{0}^{12} \frac{\partial W_{\lambda}(300)}{\partial T} d\lambda - \int_{0}^{10} \frac{\partial W_{\lambda}(300)}{\partial T} d\lambda \tag{7}$$

$$= 3\ 5\text{x}10^{4} - 2\ 65\text{x}10^{-4}$$

$$\frac{\partial W}{\partial T} = 8\ 5\text{x}10^{-5} \frac{\text{watts}}{\text{cm}^2 \text{ deg K}} \tag{8}$$

4 2 4 Optical System Design Considerations

4 2.4 1 Design Procedures

In contrast with the great diversity of detection mechanisms which are employed in the optical portion of the electromagnetic spectrum, the

Table 4-3 Planetary Temperature Characteristics

Planet	Atmospheric Temperature (deg K)	Surface Temperature (deg K)
Mercury	—	100*
Venus	200	750
Mars	150	200
Jupiter	100	150'
Saturn	100	100**
Uranus	100**	90**
Neptune	95**	70*
Pluto	—	63 **

* dark side minimum

** estimated

design of optical systems is highly unified for the spectral region from the far infrared to the vacuum ultraviolet Both the art and the science of optical system design are highly developed and generally applicable over the full range of the optical spectrum so that a single optical design procedure is generally sufficient This is not meant to indicate that an optical system which is useful in the IR portion of the spectrum would be satisfactory at UV since material characteristics, required tolerances, etc , are generally wavelength dependent The materials used are selected to optimize performance in a particular spectral region Exclusive of this type of limitation, the procedures used in establishing optical system characteristics are essentially the same throughout the optical spectrum

4 2 4 2 Modulation Transfer Functions

The design of an optical system to meet required performance specifications has in the past been based on the tedious process of ray tracing (geometric optics) and the skill of the designer in selecting combinations of materials of varying index of refraction and geometry to meet requirements While the procedure has been adequate it has proved to be inflexible since it has not always been possible to predict variations in

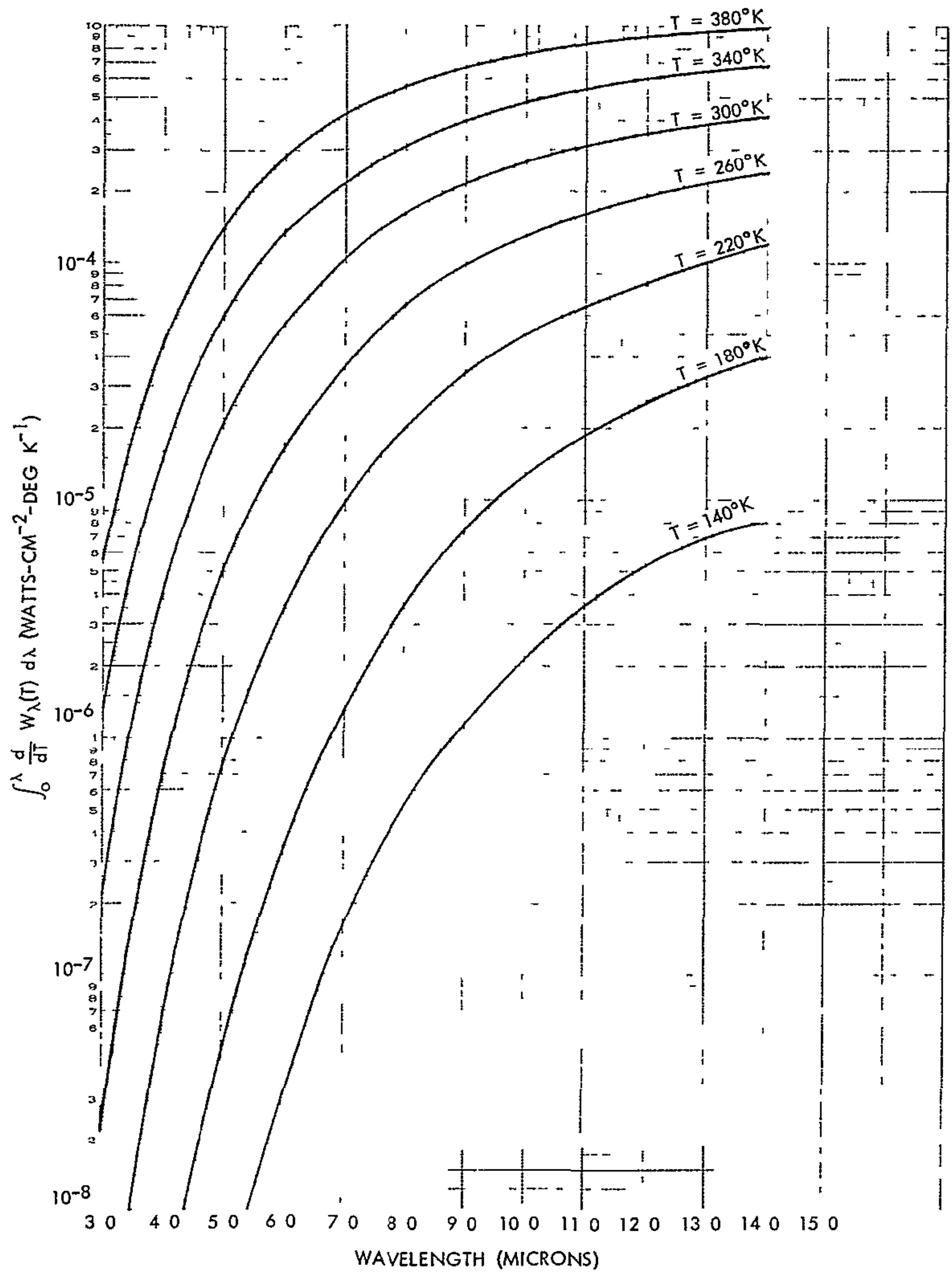

Figure 4-3 Temperature Sensitivity

performance of an overall optical instrument resulting from variations in optical system characteristics or operating conditions

Modern optical design technology has generally circumvented the more cumbersome procedures used in detailed design with the application of the optical transfer function approach to optical design In essence the optical transfer function is not new since it is a consequence of diffraction of a point source of illumination by a finite aperture The application of the approach to complete instrument design however is of fairly recent origin and as insight into the power of the method has increased it has become more widely applied

With a few notable exceptions the optical transfer function per se has not been widely used but rather a quantity associated with it has had wider application This quantity is defined as the modulation transfer function (MTF) which is the absolute value of the optical transfer function with all phase information surpressed For non-coherent sources of illumination the MTF is generally adequate and it is only when coherent sources are used as in holography that the optical transfer function is required

It is a consequence of diffraction that a point source of illumination focused by an optical system onto an image plane results in the spreading of the illumination in the image plane over a finite area In a purely mathematical sense, the MTF is the Fourier transform of the point spread function of the optical system Furthermore the point source of illumination is mathematically equivalent to an impulse function in electrical networks In a formal sense the MTF is the equivalent of the impulse response of an electrical network The transition from electrical network theory to optical theory requires only the proper definition of such terms as frequency in the optical sense before the technology of network theory is applicable to optical design The optical analogy of electrical frequency is spatial frequency where for normalization purposes spatial frequency is described as variation in contrast in the image plane of the optical system Standard practice is to describe the variation in terms of optical line pairs per millimeter of distance in the image plane abbreviated to lines per millimeter In this sense each element of an optical instrument can be considered as a low pass filter of spatial frequency The overall spatial frequency response can be obtained by cascading the MTF's of each element of the optical system, considered as a low pass filter, to obtain overall system response Overall system response is therefore the product of the response of each element which has a definable MTF A detailed procedure for applying the methodology is given in Reference 11 as well as the procedures necessary to develop MTF"s for all of the elements of an optical instrument

In addition to system performance prediction, it has become common practice to describe optical system design in terms of one or more MTF's Typical of this is the description of diffraction limited optical systems in terms of the ideal performance and the resulting degradation resulting from aberrations A typical set of generalized MTF's for an optical system is shown in Figure 4-4 for the diffraction limited performance of a circular aperture A range of levels of aberration is indicated Much useful information is contained in the figure since it demonstrates the best possible performance that can be obtained with a given optical system, the diffraction limited performance, and the tolerance which must be maintained as a function of aperture ratio ("f" number) and wavelength

The information contained in Figure 4-4 is based on the assumption of an optimized optical design with maximum angular resolution at the longest wavelength for a given aperture diameter This type of optics is referred to as diffraction limited It is based on the Rayleigh resolution criterion for a circular aperture in the form

$$\alpha = 1.22\frac{\lambda}{D} \qquad (9)$$

where

α is the angular resolution in radians

λ is the wavelength of the radiation

D is the aperture diameter in the same units as λ

In the image plane, it follows from the geometry, that the minimum size of a point source in object space is approximately

$$a = N\lambda \qquad (10)$$

where

a is the dimension of a point source in the image plane

N is the focal ratio or f number $= \frac{f}{D}$,

f is the focal length of the optical system,

D is the aperture diameter,

λ is the wavelength of the light

2 ⊕

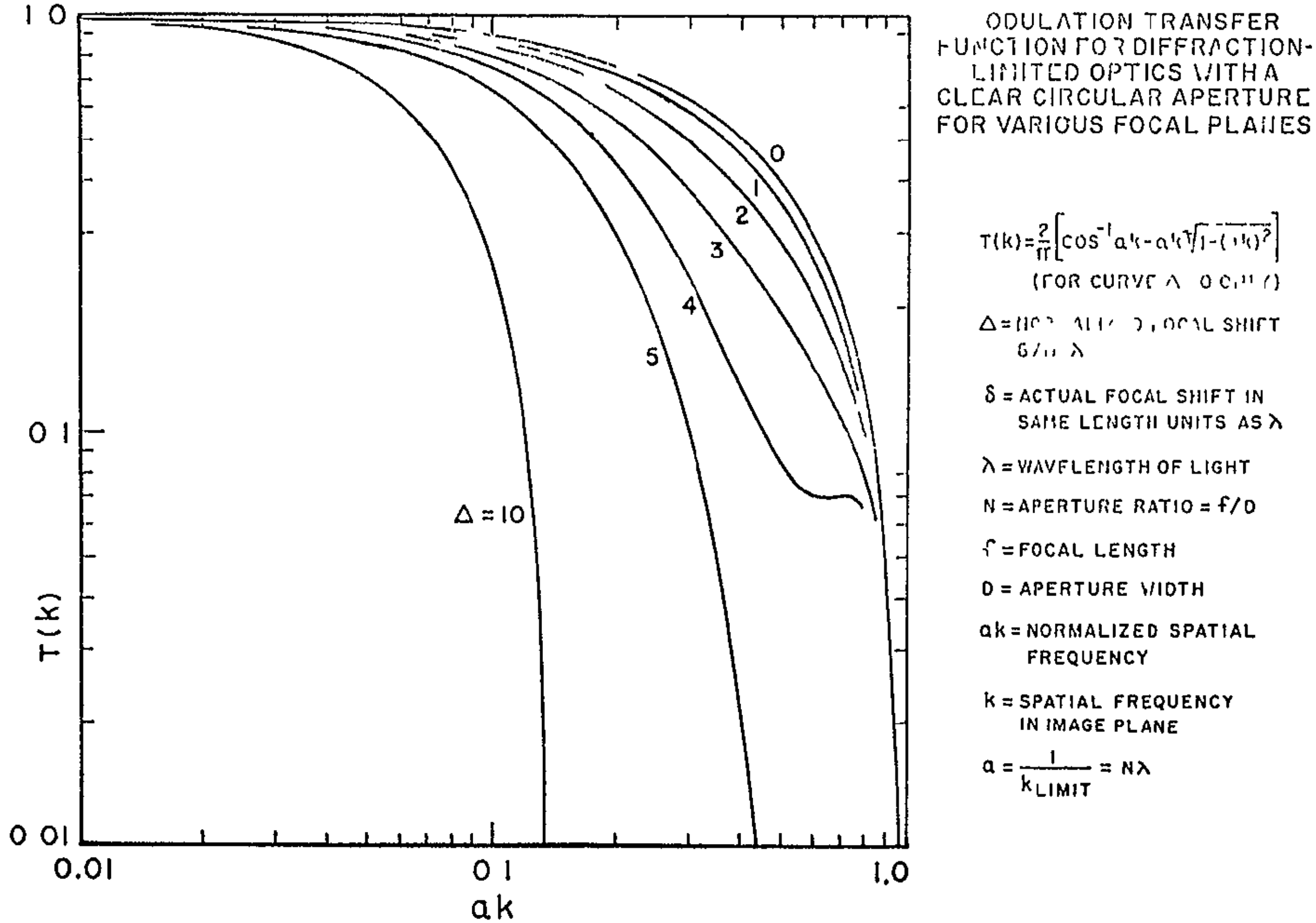

Figure 4-4 Generalized MTF Optical System

In terms of spatial frequency in the image plane it follows that the maximum spatial frequency for a diffraction limited optical system is

$$K_{max} = \frac{1}{a} \text{ lines per millimeter} \tag{11}$$

if "a" is in millimeters The limiting resolution as a function of focal ratio over the wavelength region of optical instruments is shown in Figure 4-5 However, diffraction limited optics do have a limitation on attainable aperture ratios (f number) resulting from aberrations A common criterion for aberration limits is the Rayleigh tolerance on focal shift in the form

$$\delta = \lambda N^2 \tag{12}$$

where δ is the amount of shift of "best" focus in the image plane in the same units as λ For an aberration-free system δ is zero but as tolerances are relaxed to obtain wide spectral response there is an accompanying loss in resolution This effect is also indicated in Figure 4-4 Since the Rayleigh tolerance is a measure of how much focal shift can be tolerated, it follows that large aperture ratios permit lower quality optics It also leads to a limitation on state-of-the-art capabilities in large aperture, diffraction limited optics Thus in the visual and UV portion of the spectrum, a state-of-the-art limit of aperture ratios in the range of 3 to 4 is imposed by optical quality On the other hand, intermediate to long wavelength IR optical systems can be designed with very small aperture ratios in the range of 0 5 to 1

4 2 4 3 Optical Aperture Size

The requirement for high angular resolution, where it exists, imposes the requirement for large aperture diameter It is possible to conceive of a space rated optical system design which is equivalent to the largest Earth-based telescopes This would lead to the conclusion that a reflective system with an aperture as large as 200 inches could be designed for space use As a matter of economic feasibility however it is doubtful that the investment would be made since there does not appear to be an overriding requirement to warrant the investment Several research and development programs have been conducted to design diffraction limited 100 inch aperture systems for space applications but the overall optical quality of such systems is difficult to demonstrate for long term unattended operation so that the application of large diameter optics has been confined to manned space missions where realignment and refocusing can be accomplished While improvements can be expected in this area it appears that a realistic limit on optical apertures for unmanned systems is of the order of 100 inches

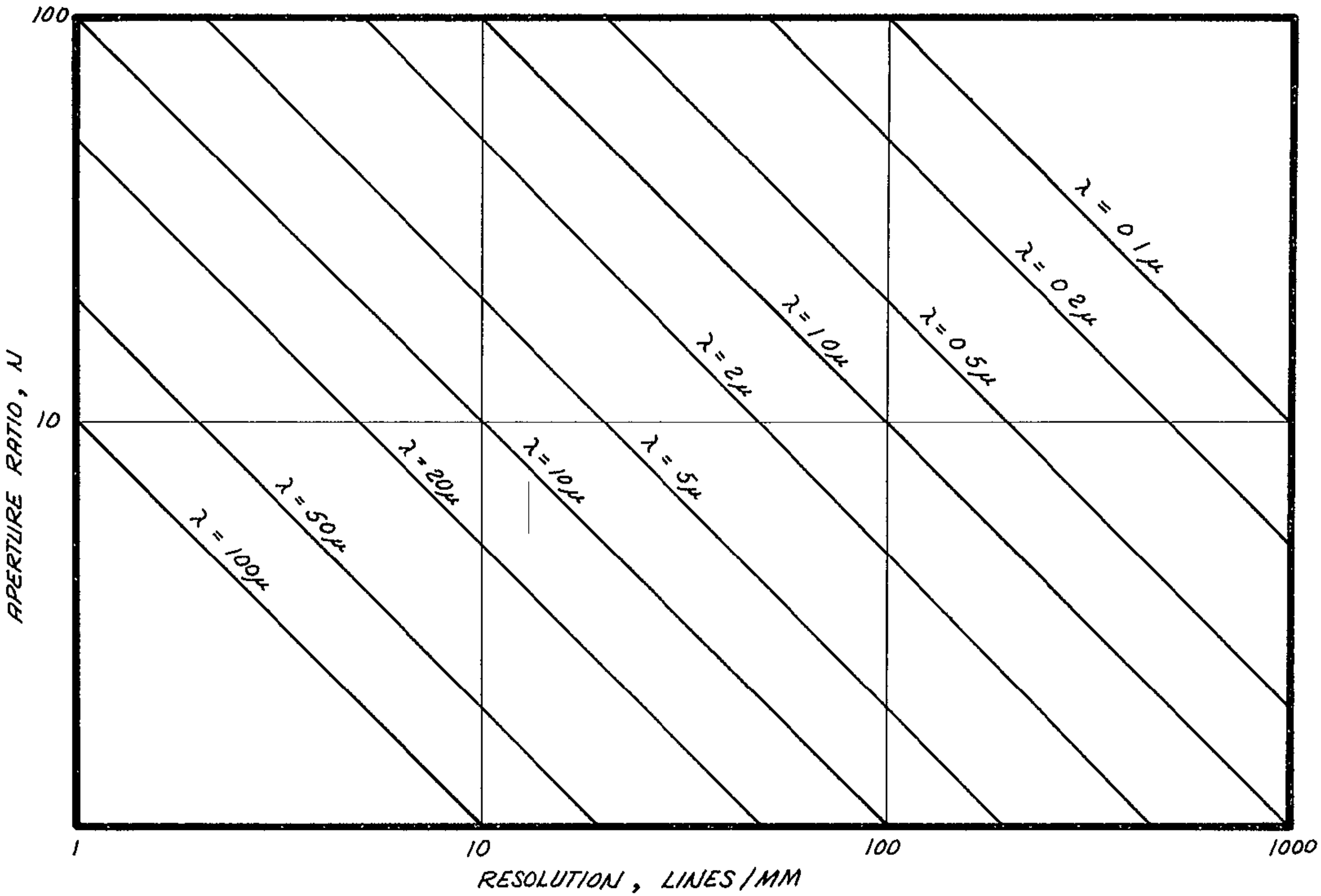

Figure 4-5 Diffraction Limited Resolution as a Function of Aperture Ratio

The 100 inch limitation applies basically to either purely reflective or catadioptric configurations since purely refractive systems become extremely difficult to design and handle for diameters greater than 36 inches even in a ground environment The state-of-the-art limit for refractive systems for unattended space operation is of the order of 16 inches although slightly larger diameters could be accommodated if a firm requirement for a refractive system is established The choice between a reflective or refractive system is generally based on field of view requirement Wide fields of view generally dictate refractive optics but the weight advantage of reflective or catadioptric systems is such that it is frequently more advantageous to sacrifice field of view and use a reflective system In a typical comparison of moderately large apertures, a 16 inch refractive system would have a weight five times as large as a 16 inch catadioptric system

In estimating support requirements of optical sensors, it is obvious that one of the heaviest, most dense systems to be put on a spacecraft is a large aperture optical system For image forming systems with discrete detector arrays such as IR and UV mappers, the difficulty is increased by the addition of a scanning mechanism which usually consists of a driven mirror system to change the direction of look of a fixed optical aperture In Reference 12, data were presented on optical system weights which while adequate were applicable to high speed scan systems The basic weight estimate for an optical aperture was estimated empirically to be in the form

$$M_c = 168\ D_c^{\ 2} \tag{13}$$

where

M_c is the mass of the collector optics in kilograms
D_c is the diameter of the collector optics in meters

The expression was obtained from survey data for actual systems as shown in Figure 4-6 The expression for estimating mass given above is shown by the solid curve in the figure It can be seen that for large diameter optics the mass increases faster than the square of the diameter The dashed line in the figure shows a cubic power dependence which would be obtained without any optimized design approach to reduce excess weight A better fit to the available data appears to be a 5/2 power law which is shown by the heavy dotted line in the figure

The 5/2 power law can be rationalized according to the following reasoning based on a reflective optical system Small pyrex glass mirrors for telescopes have a thickness of 1/6th of the diameter from which a cubic weight law would follow As the mirror diameter is increased and significant weight reductions can be obtained by optimizing the structural design of the mirror, such procedures are generally followed Thus it is common practice

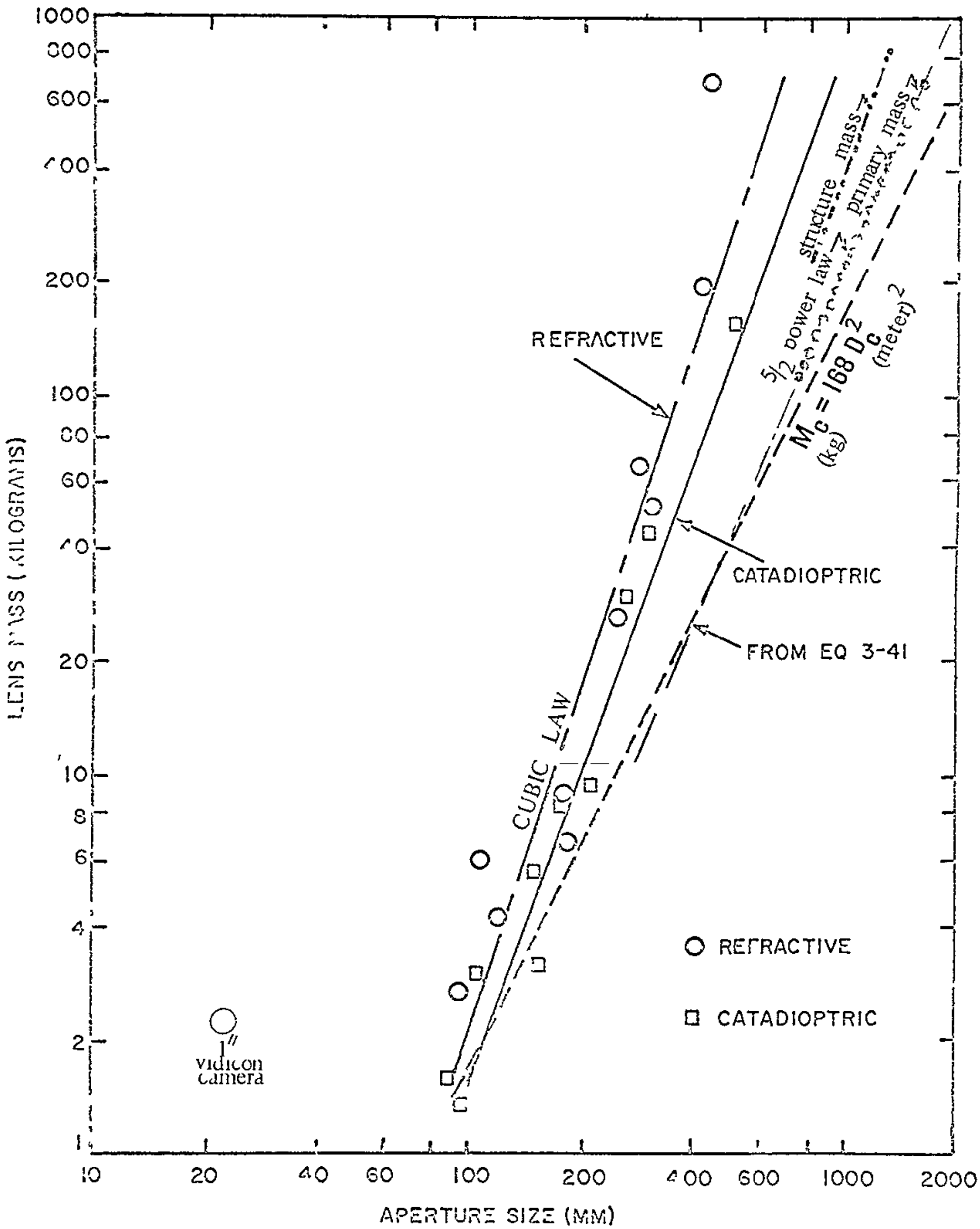

Figure 4-6 Estimated Weight of Large Diameter Optics

to cast large glass mirror blanks using a cellular structure and to form metal mirrors on a metal webbing or ribs   The break in the design procedure is not firm but generally results in significant weight reduction when the mirror diameter is greater than 10 inches   Thus the 5/2 power low appears to give better agreement with experience   It is also substantiated by optical design practice wherein mirror blank thickness before polishing is generally one sixth of the diameter (Ref 13)

A commonly used configuration for large diameter optics in spacecraft is shown in Figure 4-7, such that the optical path to the detector or image plane is folded in either the Cassegranian or Newtonian configuration as indicated   The primary optical assembly thus consists of a secondary mirror to fold the optical path and an external mirror which can be driven to rotate the field of view about the primary optical axis   For image forming systems which employ discrete detectors the external mirror may be used to scan the object plane in the cross track direction to spacecraft motion

In addition to the primary mirror it is also necessary to estimate the weight of the secondary mirror as well as the external mirror, to obtain a realistic estimate of total optical system weight   Since the secondary for a Cassegranian configuration requires the removal of some of the center portion of the primary it follows that the primary weight is reduced as a function of the diameter of the secondary, D_s In estimating the primary weight of a Cassegranian telescope the following expression is used

$$M_c = K \left[D_c^{5/2} - D_s^{5/2} \right] \tag{14}$$

where K is a scaling constant depending upon the material used   From the design equations of a Cassegranian telescope it can be estimated that the diameter of the secondary is given by

$$D_s = 0\ 5 \frac{D_c}{N} \tag{15}$$

where N is the telescope focal ratio   For a Newtonian system a slightly smaller secondary can be used resulting in

$$D_s = 0\ 42 \frac{D_c}{N} \tag{16}$$

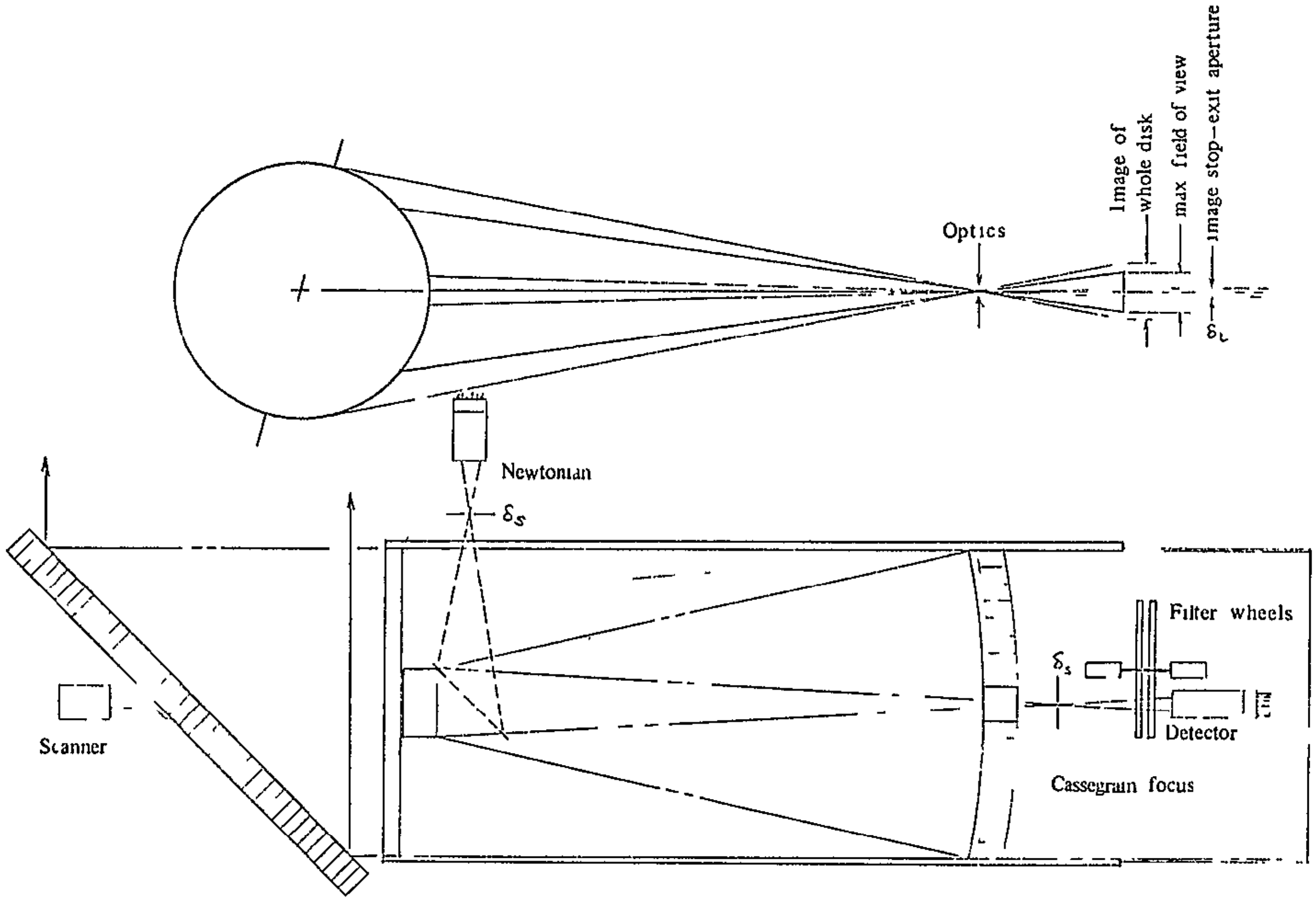

Figure 4-7 Optical Layout for Large Diameter Optics

It follows that the mass of the secondary reflector is given by

$$M_s = K\left(\frac{0.5 D_c}{N}\right)^{5/2} \quad \text{Cassegranian} \qquad (17)$$

$$M_s = K\left(\frac{0.42 D_c}{N}\right)^{5/2} \quad \text{Newtonian} \qquad (18)$$

The weight of the associated scan mirror is difficult to estimate because it is highly dependent on overall system requirements and spacecraft limitations For example in the configuration shown in Figure 4-7 there may be no overriding requirement for an external mirror for planetary missions so that the primary aperture is pointed at the planet of interest On the other hand, the conical scan mirror configuration described in Reference 12 may be required to obtain high speed scan of the object plane High speed scan is generally not required for mapping especially for flyby missions of the outer planets, so that only the single mirror case has general application This point is exemplified by such current mapping missions as the Multispectral Point Scanner (MSPS) for the Earth Resources Technology Satellite (ERTS) The MSPS uses an oscillating mirror to obtain transverse scan Using the 1/6 thickness criterion and an assumed optimum structural design of the scan mirror it follows that

$$M_m = \frac{\pi}{24} \quad \rho D_c^{5/2} \qquad (19)$$

where

M_m is the mass of the scan mirror

ρ is the material density

D_c is the diameter of the primary

It is common practice to incorporate large diameter optics into a spacecraft such that the spacecraft structure is the telescope housing It is then problematical whether the weight penalty of the telescope housing is properly apportioned to the telescope or the spacecraft For planning purposes it will be assumed that an additional weight penalty is incurred since special provisions may be necessary to obtain a sufficiently rigid spacecraft structure to accommodate the telescope

It is common practice in the design of large telescopes to design the primary mirror and associated prime aperture with an aperture ratio of 1 to 1 5 Assuming an aperture ratio of one, it follows that the length of the telescope is approximately equal to the aperture diameter To a first approximation, optimized space structure techniques would permit a structural design which has 80 percent of the primary mirror thickness The structure considered as applicable is basically thin and rigid truss members with stretched panel cladding The shell structural volume would then be

$$V_{ss} = \frac{\pi}{15} D^{5/2} \tag{20}$$

and the structural mass would be

$$M_{ss} = \frac{\pi}{15} \rho D^{5/2} \tag{21}$$

where ρ is the structural material density which is probably aluminum with a density of $2\ 7 \times 10^3$ kg/m^3

For reference purposes the weight estimating approximations are summarized in Table 4-4 The values in the table are based on a density of $1\ 85 \times 10^3$ kg/m^3 for beryllium, $2\ 7 \times 10^3$ kg/m^3 for aluminum and $7\ 9 \times 10^3$ kg/m^3 for glass For the primary mirror system beryllium is generally optimum on a weight, strength and temperature coefficient basis Aluminum structure is assumed

4 2 4 4 Auxiliary Optical Components

One of the principal functions of non-image forming optical systems is the resolution of radiant energy into spectral components or bands Spectral resolution may be accomplished in a large variety of ways depending upon the spectral resolution required and the available electromagnetic energy With the exception of such techniques as haze reduction by filtering in photographic systems, any optical instrument which employs bandpass spectral filters can be considered a spectrometer Depending upon the filtering technique used, the resulting spectral resolution may range from crude to high The scientific purpose to which the spectroscopy will be applied generally determines the type of filtering employed

Table 4-4 Mass Relationships for Estimating Primary Optical System Weight Penalties

	Cassegranian	Newtonian
1 Primary Mirror Mass M_c		
Glass	$300 (D_c^{5/2} - D_s^{5/2})$	$305 D_c^{5/2}$
Beryllium	$230 (D_c^{5/2} - D_s^{5/2})$	$235 D_c^{5/2}$
2 Secondary Diameter, D_s	$\frac{0.5 D_c}{N}$	$0.42 \frac{D_c}{N}$
3 Secondary Mirror Mass, Ms		
Glass	$195 (D_c/N)^{5/2}$	$170(D_c/N)^{5/2}$
Beryllium	$150 (D_c/N)^{5/2}$	$130(D_c/N)^{5/2}$
4 Scan Mirror Mass		
Glass	$300 D_c^{5/2}$	$300 D_c^{5/2}$
Beryllium	$230 D_c^{5/2}$	$230 D_c^{5/2}$
5 Telescope Structure	$567 D_c^{5/2}$	$567 D_c^{5/2}$

Mass in Kg
Dimensions in meters

There are a large variety of spectral filtering techniques available for scientific instrumentation They are generally classified, according to the filtering mechanism employed, into the following classes

1 absorption

2 interference

3 dispersive

Dispersive filters are further categorized according to the dispersion technique into prismatic and diffraction grating

One of the most common filter techniques used is absorption filtering Colored glass and gelatin emulsions in a glass sandwich act as absorbers of radiant energy to isolate a portion of the optical spectum Absorption filters can be obtained in a large variety of combinations ranging from high pass to low pass and bandpass to band stop spectral configurations The spectral resolution of absorption filters is limited by the filtering mechanism to values of the order of 500 A° (50 mμ) so that they are most frequently used when crude spectral data is of interest The primary limitation on absorption filters is poor optical transmission especially in narrow band applications, where several filterlayers are used in cascade Thus a 500 A° absorption filter may have an optical transmission as low as 0 30 The advantage of absorption filters is that they are relatively inexpensive and function over relatively large fields of view

A principal type of filter is the dielectric sandwich interference filter based on the principle of constructive and destructive interference of electromagnetic radiation By proper selection of materials and control of material thickness an optical sandwich can be constructed such that the transmission is high over a finite wavelength interval Outside of the passband of the filter, destructive interference occurs resulting in a narrow bandpass spectral filter The basic assumption of an interference filter is that the sandwich in combination with a suitable reflector is one half wavelength, thus double passage through the filter results in constructive propagation However, a limitation of interference filters is that any wavelength for which the filter is an integral number of wavelengths are also passed This may result in multiple spectral response regions The unwanted spectral regions can be removed by suitable absorption filters The advantage of sandwich interference filters is the flexibility of the design approach available and the improved spectral resolution Current technology in dielectric sandwich filters results in filters of approximately 25A° bandwidth and optical transmission of 0 75

The limitation of interference filters, in addition to the multiple spectral response, is imposed by the assumption that the illumination of the filters is collimated For non-parallel incident radiation the bandpass characteristics of the filter shift so that the total field of view of the filter is limited, especially for high spectral resolution For good spectral resolution over a narrow spectral range it is generally necessary to incorporate an optical collimator with attendant penalty of increased weight and complexity If dielectric interference filters are used in place of absorption filters over wider spectral ranges then the field of view of the optical system must be limited to less than 30 degrees to obtain controlled spectral resolution

Somewhat higher spectral resolution with interference filters can be obtained by the use of birefringent crystals, that is crystals which exhibit anisotropic transmission properties By a careful selection of optical components, birefringent crystals can be used to obtain constructive interference over a narrow spectral region Birefringent filters as narrow as 6 Å have been used in astronomical work but they are both complex and of limited flexibility They have found principal application in isolating specific spectral lines and would have only limited application in planetary spectroscopic investigations

Recent developments in spectroscopy are based on the principle of temporal scanning of a Michelson interferometer as discussed in paragraph 4 2 5 1

The technique most frequently used to obtain high resolution spectral separation is dispersion of the received electromagnetic energy into spectral regions which are uniquely related to an angular position of viewing The two most commonly used dispersion techniques are prisms and diffraction gratings The figure of merit of dispersive separation filters is the resolving power which is defined as

$$Rs = \frac{\lambda}{\Delta \lambda} \qquad (22)$$

where Rs is the spectroscopic resolving power

λ is the wavelength of the radiation

which is just resolved from a wavelength of λ' such that
$$\Delta \lambda = \lambda - \lambda' \qquad (23)$$

It can be shown from geometric reasoning that the resolving power of a prism is given by

$$Rs = t_p \frac{d\mu}{d\lambda} \qquad (24)$$

where

t_p is the width of the prism base illuminated by the optical aperture

$\frac{d\mu}{d\lambda}$ is the rate of change of index of refraction of the prism material with wavelength (25)

Prism spectrometers are therefore limited by both the size of the prism which can be illuminated and the material from which the prism is built Typical values of resolution for a flint glass prism of 5 cm base are 5000 at a wavelength of 600 mμ and 12, 000 at 450 mμ A quartz prism of the same base has a resolving power of 2000 at 600 mμ but increases to 75, 000 at 200 mμ The increased resolving power of quartz in the ultraviolet frequently permits relatively good spectral resolutions in the 180 to 250 mμ region of the ultraviolet The lack of high dispersion materials in the infrared generally precludes the use of prismatic spectrometers in the IR portion of the spectrum

To obtain high spectral resolution in the visible and IR portions of the spectrum the most generally applicable technique is the diffraction grating A large variety of grating structures have been built for spectroscopic investigations in both transmission and reflecting forms The resolving power of a diffraction grating is determined by the size of the grating and the fineness of the spacing of the lines which can be ruled on the grating This results in the resolution being determined by the total number of grating lines However, the spacing of the lines in the grating is generally several wavelengths so that the resulting diffraction pattern may have several secondary maxima The secondary maxima are classified by order number into socalled secondary spectra Thus the resolving power of a diffraction grating is of the form

$$Rs = \frac{\lambda}{\Delta\lambda} = mN \tag{26}$$

where

N is the total number of lines in the grating and

m is the order of the spectrum or the number of the subsidiary maximum

For the primary grating lobe the value of m is one whereas for extremely high spectral resolution orders as high as 10 may be used For space applications the third order spectrum appears to be a practical limit Gratings up to 10 inches wide with as many as 15, 000 lines per inch have been built A grating this large would then have a resolution of 150, 000 in the first order Thus at 500 mμ, a ten inch grating is capable of producing a spectral resolution of 0 001 mμ in the third order

4 2 4 5 Optical System Power Requirements

The power required for optical sensor systems is of three basic types

1 Operational power for electronic functions

2 Scan mechanism operation and precision pointing

3 Auxiliary functions such as closed cycle cryogenic cooling for IR detectors and radiant energy source operation for calibration

The requirements imposed by the first and third types are particularized to the type of detectors used and the spectral region of operation Scan mechanism operating power requirements are, with few exceptions, equivalent for all spectral bands where scanning, whether spatial or spectral, is employed Therefore, scanning mechanism power requirements are established under a single set of assumptions and can be used whenever scanning is indicated Operational power requirements, other than scanning, are discussed in the appropriate sections either by detector or sensor type

Two requirements for power in the mechanization of scanning optical systems can be differentiated depending upon whether a continuous or an oscillatory scan mechanism is employed If a segmented scan mirror with n faces is used to obtain high speed scan then the power required to maintain a constant rotation speed is relatively small since only the loss in the bearings must be supplied to maintain the rotational speed To estimate the power required, consider the scanning portion of the system to be a segmented conical mirror, rotating about the axis of the cone For a rotational speed of ω radians per second, the kinetic energy of the rotating mirror is

$$E = I\omega^2 \tag{27}$$

where I is the moment of inertia of the assumed right circular cone Assuming that the base of the cone is equal to the diameter of the primary optics, D_o, then the moment of inertia of the cone about its altitude as axis is given approximately by

$$I = \frac{0\ 3\ M_M D_o^2}{4}\ \text{kg - m}^2 \tag{28}$$

and the kinetic energy is

$$E = 0\ 075\ M_M D_o^2 \omega^2 \text{ joules} \tag{29}$$

where

M_M is the total mirror mass in kg

D_o is the diameter of the primary optics in meters

ω is the rotational speed in radians per second

The power required to bring the mirror up to speed can be approximated from

$$P = \frac{E}{t} \text{ watts} \approx E\,\omega \text{ watts} \tag{30}$$

so that

$$P = 0.075\, M_M D_o^2 \omega^3 \text{ watts} \tag{31}$$

For high quality bearings, the total requirement for maintaining speed including drive motor inefficiency is estimated to be 10 percent of the initial power so that a constant speed drive would require

$$P = 7.5 \times 10^{-3}\, D_o^2\, M_M\, \omega^3 \text{ watts} \tag{32}$$

for continuous rotation of a segmented mirror

If a single scanning mirror is used in an oscillatory search mode, then under the assumption of a linear acceleration - deceleration operation, a scan half angle ϕ is covered in time $t_{f/2}$ under an angular acceleration α then the scan half angle is given by

$$\phi = \frac{1}{8}\,\alpha\, t_f^2 \tag{33}$$

Likewise, during the second half of the scan the mirror is decelerated by the same amount so that

$$-\phi = -\frac{1}{8}\,\alpha\, t_f^2 \tag{34}$$

The torque applied is given by

$$T = I_M \alpha \tag{35}$$

where

I_M is the moment of inertia of the mirror

α is the angular acceleration (or deceleration)

Substituting for α gives

$$T = \frac{8 \phi I_M}{t_f^2} \tag{36}$$

If the mirror is assumed to be a thin disc of diameter D_M and mass M_M rotated about an axis through the center of mass and lying in the plane of the disc, the moment of inertia is

$$I_M = \frac{M_M D_M^2}{16} \tag{37}$$

and the torque is

$$T = \frac{M_M D_M^2 \phi}{2t_f^2} \tag{38}$$

during acceleration

The work done on the mirror is then

$$W = T\phi = \frac{M_M D_M^2 \phi^2}{2t_f^2} \tag{39}$$

and the power required to rotate the mirror through the angle ϕ in time $t_{f/2}$ is

$$P = \frac{2W}{t_f} = \frac{M_M D_M^{2} \phi^{2}}{t_f^{3}} \text{ watts} \tag{40}$$

Since the same amount of power is required to decelerate the mirror, the total power required at the mirror is

$$P_T = \frac{2M_M D_M^{2} \phi^{2}}{t_f^{3}} \tag{41}$$

Assuming an electric drive, a high quality electric motor may have an efficiency of 25 percent so that

$$P_{in} = 4P_T = \frac{8M_M D_M^{2} \phi^{2}}{t_f^{3}} \text{ watts} \tag{42}$$

The same approach can be used for any rotational optical component such as reticles and filters, but because they are generally of low mass (less than 100 grams) and low moment of inertia the power required can be approximated as a fixed small amount for each function For estimating purposes, a power requirement for rotation or movement of lightweight optical components of 0 1 watt per function is realistic

In the event that the optical sensor is mounted on a gimbal for image motion compensation purposes, then the power required to operate the gimbal control is a function of the sensor mass For estimating purposes, the gimbal control power can be obtained from Figure 4-8 as a function of the optical parameters of the sensor The data in the figure were obtained from Ref 12

The power requirements for optical system scanning and pointing are summarized in Table 4-5

Table 4-5 Power Required For Scanning And Pointing

Function		Power Required (Watts)
1	Scan Mirror Rotation	$7\ 5 \times 10^{-3} D_o^2 M_M \omega^3$
2	Oscillating Mirror	$8 D_M^2 M_M \phi^2 / t_f^3$
3	Reticles, Rotating Filters, etc	0 1 Watt per function
4	Gimballed Structure for Pointing	Figure 4-8

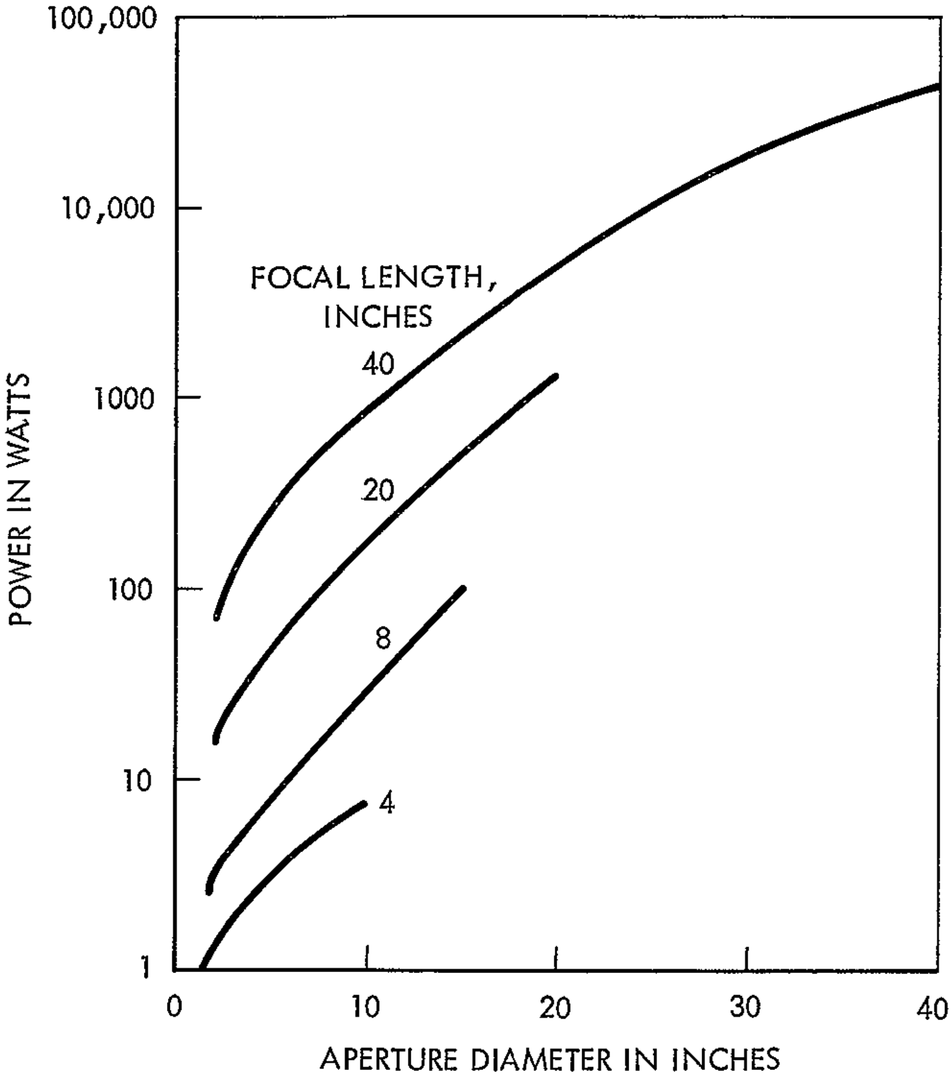

Figure 4-8 Gimbal Power Required for Large Aperture Optics

4 2 5 Infrared Spectrometer and Radiometer

An infrared spectrometer or radiometer consists of a collecting lens, frequency selective elements (either an appropriate set of filters or a dispersive element), and an intensity modulating element such as a chopping reticle, a detector and an electronic system to amplify and code the signal Requirements regarding the necessary spectral interval, spectral resolution, and instrument sensitivity, have led to the development of several prototype configurations, many of which have been flown in satellites and balloons

4 2 5 1 Design and Performance

Four basic instrument types of spectrometers are considered as candidates Their characteristics are discussed briefly

Filter Radiometer This is the simplest configuration with reasonable sensitivity but with low spectral resolution It is the best instrument in terms of weight, volume and power consumption but the information content is limited since it is not a scanning device An optical schematic for this instrument is shown in Figure 4-9 The incoming radiation is focused onto a detector A set of transmission filters are rotated in turn into the incoming beam and the transmitted signal is detected The number of filters employed determines the number of spectral intervals, and the transmission band pass of each of the filters determines the spectral resolution of the instrument !

NOTE Spectroscopists usually deal in wave numbers and frequency rather than wavelength and wavelength interval This results in no basic difficulty provided that caution is exercised By definition the wave number is

$$n = \frac{1}{\lambda} \tag{43}$$

where λ is the wavelength of the radiation in centimeters By definition it follows that

$$\Delta n = - \frac{1}{\lambda^2} \Delta \lambda \tag{44}$$

or

$$|\Delta \lambda| = \lambda^2 \Delta n \tag{45}$$

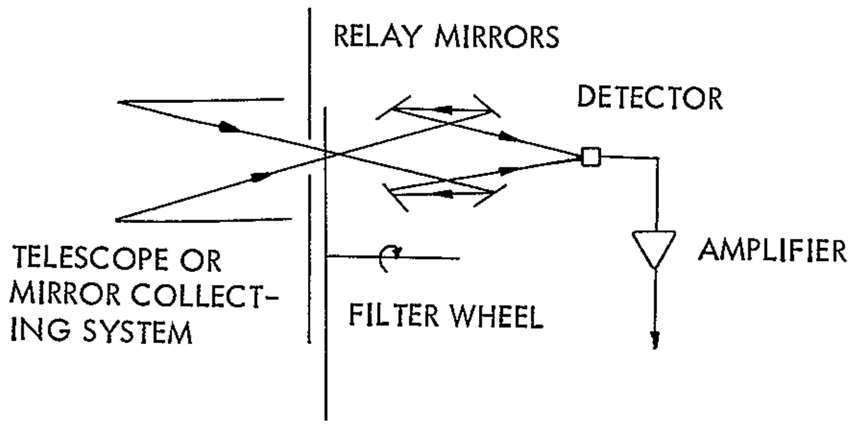

Figure 4-9 Optical Schematic - Filter Spectrometer

If

$$\lambda = 10\mu \text{ and } \Delta n = 3 \text{ cm}^{-1} = 3 \times 10^{-4} \ \mu^{-1}$$

then

$$|\Delta \lambda| = 10^2 \times 3 \times 10^{-4} = 3 \times 10^{-2} \ \mu$$

The same procedure is followed in converting frequency ν and frequency interval $\Delta \nu$ into equivalent wavelengths quantities Thus since

$$\nu\lambda = C \tag{46}$$

$$\Delta\nu = - \frac{C}{\lambda^2} \Delta\lambda \tag{47}$$

where C is the velocity of light in vacuum It should be noted however that

$$\Delta\nu = - \frac{C}{\lambda} \frac{\Delta\lambda}{\lambda} \tag{48}$$

so that

$$\frac{\Delta\nu}{\nu} = \frac{\Delta\lambda}{\lambda} \tag{49}$$

In specifying the resolution of a spectrometer it is immaterial whether frequency or wavelength is used

The state-of-the-art for the maximum spectral resolution in IR interference filters is about 3 cm^{-1} ($3x10^{-2}$ μ) but a resolution of 10 cm^{-1} (0 1μ) is more reasonable over the infrared spectrum This instrument is ideally suited to making average atmospheric emissivity measurements, since for these measurements high resolution is not required and broadband filters may be used to obtain a suitable average of the detected radiation The instrument is, in summary, a low resolution, reasonably sensitive radiometer

Polychromator Radiometer The instrument uses a dispersing element such as a grating and a bank of detectors each located at the desired sampling frequency at the exit plane of the spectrometer A schematic for the system is shown in Figure 4-10 Up to 10 detectors may be used to obtain a ten channel spectrometer

The advantage of this system over a filter spectrometer is that all channels, and therefore all spectral intervals, are observed simultaneously, so that the integration time for each spectral band is increased over that for sequential observation for a given observation time The improvement in integration time for each sampling frequency, or in the required observation time if the integration time is fixed, is by the square root of the number of sampling channels In addition, each detector may be chosen such that its response is maximized for the particular wavelength interval whereas in the previous case, the detector must be broadband to encompass the range of the observed spectrum This results in an improvement of about an order of magnitude in sensitivity However, it is not possible for this system to utilize the very fast optical system at the detector as was the case for the filter spectrometer For a given resolution, the detector size is limited by the dispersive properties of the grating and overall improvement in signal to noise at comparable resolution is consequently only about a factor of 4 to 5 This modest improvement in sensitivity is offset by the complexity of

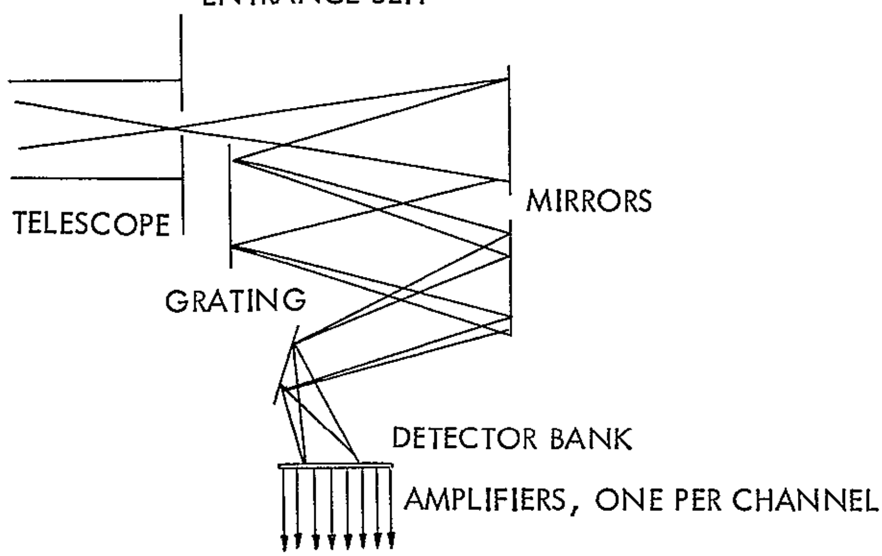

Figure 4-10 Optical Schematic - Polychromator Spectrometer

the system as well as by the heavier weight and larger volume requirement The operational spectrometer systems of this type utilized in TIROS and NIMBUS satellites weigh in the order of 90 pounds whereas a filter system should weigh only 10 pounds It is, however, capable of high resolution at a sacrifice of observation time required (better than 1 cm^{-1})

Scanning Spectrometer A spectrally scanning spectrometer is in principle identical to conventional laboratory instruments A typical configuration is shown in Figure 4-11

The usual spectral range of the grating is about three to one ($f_{max} = 3 f_{min}$) and the instrument can, in principle, be scanned continuously over this frequency range with very high resolution Practical considerations such as observation time and intensity of signal available, however, limits the usefulness of such a device The resolution is proportional to the slit width whereas the intensity at the detector is falling off as the square of the slit width Therefore, the high resolution capability is achieved only at a great sacrifice in integration time This drawback limits the usefulness of such as system to applications where relatively long observation times are available (on the order of minutes)

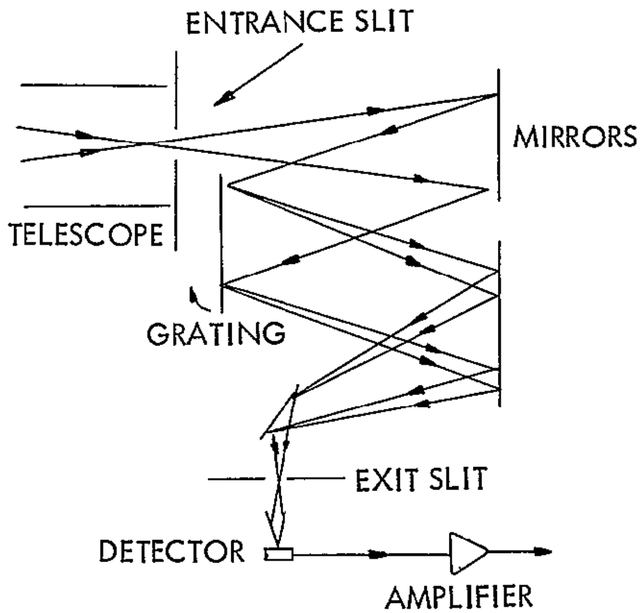

Figure 4-11 Optical Schematic - Scanning Spectrometer

Michelson-Type Interferometer The interferometer offers the best characteristics as a candidate spectrometer in terms of resolution and sensitivity, as well as information content of the measured observables Prototypes developed in the past for balloon and satellite applications have achieved resolutions much better than 1 cm^{-1} and over an order of magnitude in spectral range Advanced developments in this area are being actively pursued which will enable this type of instrument to be used for a wide variety of remote sensing applications Its primary disadvantages are that the system is necessarily complicated and the analysis of the interferogram obtained requires somewhat complicated mathematical analysis of the recovered data A basic Michelson interferometer is shown in Figure 4-12

The incident radiation from the source is collected by a telescope system The beam is then split into two equal-intensity parts by a beam splitter Thin films of Ge or Si on BaF or GaF_2 are generally used for the near infrared region whereas for the longer wavelength region (far-infrared), metallic mesh and mylar films have been used with success The two beams are then recombined at the detector via the two reflecting mirrors and a lens system As the movable mirror's position is changed, a phase difference is introduced between the optical pathlength of the two beams and an interferogram results at the detector The output F(x) at the detector as a function of the displacement x is then given by,

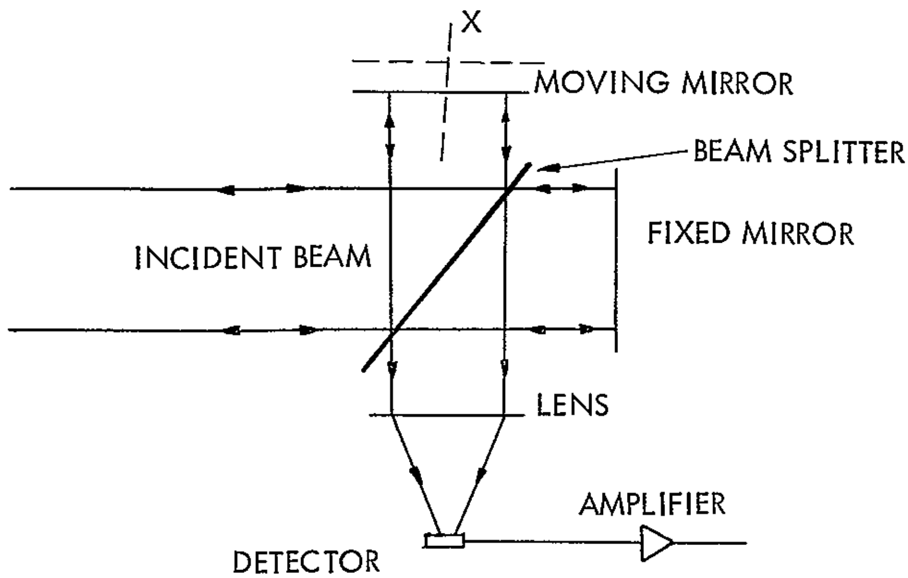

Figure 4-12 Optical Schematic - Michelson Interferometer Spectrometer

$$F(x) = \int_{\nu_1}^{\nu_2} B(\nu)(\cos 2\pi x \nu) d\nu \tag{50}$$

where ν is the frequency in wavenumbers (cm^{-1}), $B(\nu)$ is the desired spectrum extending over the frequency interval from ν_1 to ν_2 $B(\nu)$ is then recovered from the interferogram by taking the inverse transform, (usually through a computer),

$$B(\nu) = \int_{-\infty}^{\infty} F(x) \cos (2\pi \nu x) dx \tag{51}$$

In reality, however, the computation represented by the above equation which is necessary for the faithful recovery of the spectral distribution of $B(\nu)$, cannot be realized, since the maximum path difference, x_{max}, is necessarily finite The sampling of F(x) is by discrete intervals rather than as an analytic expression These conditions essentially define the resolution and the maximum frequency coverage of the instrument The resolution of the instrument is given by

$$\Delta \nu = 1/2x_{max} \tag{52}$$

and the maximum frequency, ν_{max}, is given by

$$\nu_{max} = 1/2\Delta x \tag{53}$$

where Δx is the sampling interval

The minimum number of sampling points required is then $(x_{max}/\Delta x)$ or $(\nu_{max}/\Delta \nu)$ The actual number of samples is usually taken to be twice the minimum or $2\nu_{max}/\Delta \nu$ Practical limitations on the accuracy with which the mirror movement can be measured usually limits the resolution to about 0 1 cm^{-1} whereas the sampling points required impose an observation time for a complete interferogram of about 10 sec

4 2 5 2 Infrared Detectors

Infrared detectors are available in many forms but the most frequently used, in other than laboratory environments, are the solid state and bolometric types Solid state detectors, frequently called photon detectors, are classified according to the detection mechanism used as photoconductive (PC), photovoltaic (PV), and photoelectromagnetic (PEM) Most IR detector cells are of the photoconductive and photovoltaic type although some developmental detectors are operated in the PEM mode The great preponderance of detectors are photoconductive which undergo changes in resistance when they absorb photons of suitable wavelength Because the change in resistance is the measured quantity, photoconductors are most frequency operated with an external bias source Photovoltaic detectors find wide application in power conversion systems for spacecraft and the photovoltaic effect in semiconductors can be exploited for radiant energy detection They are generally not competitive with photoconductive detectors at long wavelength but find application in the near IR and in the transition region between IR and the visible spectrum

Bolometric detectors are basically of the energy absorption type and are frequently referred to as heat sensors Bolometers are of several types but the principle ones are the radiation thermocouple or thermopile, thermistors, and superconducting doped semiconductors

The sensitivity of IR detectors can be described in many ways but it has become standard practice to describe the performance in terms of specific detectivity, D For photovoltaic and photoconductive detectors D* may be a gross over simplification because the detectivity is a function of many parameters which are suppressed in order to establish a simple quality factor for comparing performance Thus it can be shown that detector response is characterized not only by a variation in radiation wavelength but by a long wavelength threshold such that at wavelengths longer than the threshold the response is essentially zero Because of the energy relations involved in raising an electron from the valence to the conduction band in the detector material, it follows that the detectivity is highest at the long wavelength cutoff This is frequently approximated by

$$D^*_\lambda = \frac{\lambda}{\lambda p} D^*_p \ (\lambda \leq \lambda p) \tag{54}$$

where

D^*_p is the peak value of the specific detectivity

λ_p is the wavelength of peak response

In addition to the long wavelength cutoff, the temperature at which the detectivity is measured, the temperature of the source, and the field of view of background ambient radiation to which the detector is exposed may have a marked effect on its detectivity Many radiation detectors exhibit so called 1/f noise where f is the modulation frequency of the incident radiation The requirement for modulating solid state detectors arises from the difficulty of building stable d-c amplifiers To reduce the 1/f noise to insignificant levels it is common practice to chop the incident radiation at as high an audio frequency as possible consistent with the response time of the detector From these considerations it follows that a statement of the specific detectivity should be in the form

$$D^* (T, \theta , f) = \frac{\lambda}{\lambda p} D^*_p (T, \theta , f) \tag{55}$$

where

T is the operating temperature of the source

θ is the field of view to which the detector is exposed (Common values of θ are 60 degrees and 180 degrees)

f is the modulation frequency which for most detectors is taken as 1 kHz resulting in negligible contribution of 1/f noise

For computation purposes many of the factors which affect D^* are either implicit, such as f and θ, or are stated separately so that a simple expression is used

The characteristics of some typical IR detectors are discussed below to indicate the current state of detector technology. In addition, a wider range of detector types with typical characteristics is given in Table 4-6. While the data is specifically for point detectors, some of the limitations imposed by current technology on the construction of detector arrays for image formation are also included.

The sensitivity of radiation detectors is limited by noise generated by the detector itself since the signal level must be greater than this if it is to be detected. Detector noise is often expressed as noise equivalent power (NEP), the input power level required to give a signal to rms noise ratio of one. The noise is usually generated evenly across the surface of the detector, and is uncorrelated from point to point. In such cases, the NEP will increase with the square root of the area of the detector. Further, if the noise spectrum is constant, or "white," the NEP will be proportional to the square root of the measuring bandwidth. These considerations have led to the simplified definition of D* (D-star),

$$D^* = \frac{\sqrt{A_D \; \Delta f}}{NEP} \tag{56}$$

where Δf is the measuring bandwidth, A_D is the area of the detector in cm^2, and NEP is the noise equivalent power in watts. The NEP is relatively independent of the shape of the detector and measuring bandwidth for most types of detectors.

The ultimate sensitivity of a radiation detector is limited by the total incident radiation, or background level. This radiation is quantized into discrete energy units, photons, which arrive randomly, causing shot noise. If the NEP of a detector is no larger than the photon shot noise level, the detector is said to be background limited. The background limited D* of a detector producing a signal proportional to the incident photon flux is

$$D^* = \frac{\lambda}{hc} \sqrt{\frac{\eta}{2 \, Q_B}} \tag{57}$$

where λ is the wavelength of the signal radiation, c is the velocity of light, h is Planck's constant, Q_B is the background photon flux level on the detector (photons/cm^2-sec), and η is the quantum efficiency, i.e., the fraction of incident photons which are converted.

As discussed previously there are three types of detectors useful in the infrared regions Bolometers, photoconductive detectors, and photovoltaic detectors They are discussed below

Bolometers Bolometers offer the advantage of ambient temperature operation, and uniform spectral response independent of wavelength Their sensitivity is usually lower than other types of detectors and their response time is generally longer The response time of a bolometer is determined by conduction to a heat sink, and is thus controllable to a certain extent The D* of a bolometer, however, is usually proportional to the square root of the response time, which thus should be made as long as possible for the given application If the bolometer were so well isolated from the heat sink that heat in the bolometer would be dissipated by radiation rather than by conduction, the bolometer would be background limited It is theoretically possible to have an ambient temperature bolometer with a D* of 10^{10} For this degree of performance, a heat sensing material with very low specific heat would be required

Thermistor Bolometers The most commonly used bolometer is probably the thermistor It is rugged and gives a signal level large enough to be used with most high impedance amplifiers It is basically a resistor whose resistance is a decreasing function of temperature These detectors are available as small as about 5 mils in size, have a D* of 10^8 and a 1 millisecond time constant

Radiation Thermocouple The radiation thermocouple is used extensively in spectrophotometers Because of its low impedance it requires a rather bulky output coupling transformer, although radiation thermopiles of equal or better sensitivity, and requiring no transformer, have appeared recently A D* of 2×10^9 is possible with a 50 millisecond time constant These devices have a better D* at a given time constant than thermistor bolometers, and may, upon further development, replace them

Ferroelectric Bolometers A relatively new detector is the ferroelectric bolometer It contains a small piece of ferroelectric ceramic whose Curie temperature is ten or twenty degrees below room temperature The capacitance of such material is a rapidly decreasing function of temperature, this provides the heat sensing mechanism This detector type can provide a D* of 3×10^8 over a 500 cycle bandwidth Unfortunately, a good detector cannot be made smaller than about 020 in , and D* cannot be traded for bandwidth because of the inherent large 1/f noise These difficulties will probably be reduced or eliminated after further development

Cooled Germanium Bolometer The bolometer with the highest performance is the cooled germanium bolometer This is a flake of germanium doped with an impurity such as gallium so that its resistance near absolute zero is a rapidly varying function of temperature This bolometer is operated at liquid helium temperature or lower, and is background limited Since other detectors generally perform better with less cooling, this bolometer is used only when its flat response over virtually unlimited spectral range is desired,

Photovoltaic and Photoconductive Detectors Photovoltaic and photoconductive detectors produce a signal roughly proportional to the incident photon flux for all wavelengths shorter than some cut-off wavelength, and have zero response to longer wavelengths Both types of detectors are made from semiconductor material, and they often can both be made from the same material The cut-off wavelength of photovoltaic detectors is determined by the energy band gap of the intrinsic detector, while the cut-off wavelength for the photoconductive detectors is determined either by the band gap, if the material is sufficiently pure, or the doping level, if the material is doped Thus, while photodiodes are at present limited to wavelengths shorter than about 15 μ photoconductors have been built which operate down to microwave frequencies

A common characteristic of these detectors is their temperature sensitivity Above some maximum operating temperature, their sensitivity degrades exponentially with temperature, while below this temperature they are often background limited

Lead Sulfide This detector is prepared as a photoconductive thin film and is useful in the medium infrared region When cooled to liquid nitrogen temperature, the detector is sensitive to wavelengths out to about 4 μ, and yields a D* of about 10^{11} The low temperature is required primarily to shift the long wave response, not to increase sensitivity These detectors are available in single form or arrays of elements 001" x 001" each They are one of the oldest infrared detectors still being used, and their technology is the most advanced Their characteristics tend to drift with time, however, and they should be aged several months before use Variation from element to element in large arrays would cause streaking in thermal images sensed by such arrays This might make them unsuitable for use in equipment that had to operate for long unattended periods Unfortunately, precise data on aging characteristics are unobtainable

Lead Selenide This material is also prepared as a thin film photoconductor and is available in several modified forms The most useful form for the systems considered is optimized for use at -80°C, at which temperature it produces a D* of about 2×10^{10} and cuts off just beyond 5 μ Large arrays are available with detectors as small as 002" x 002", they suffer from the same instability problems as lead sulfide The principal supplier of lead selenide, Santa Barbara Research Center, claims that the stability of both of these detectors has been improved recently so that they are useful for infrared imaging

Indium Antimonide This material is available as both photodiodes, and photoconductors The photodiode is the best choice for imaging applications, however, because of its stability The detector is operated at liquid nitrogen temperature, and yields a D of about 8 x 10^{10} with a cut-off wavelength of 5 5 μ Large arrays of elements as small as 004" x 004" are available

HgCdTe and PbSnTe These semiconductors are mixed crystals (HgTe with CdTe, and PbTe with SnTe) whose band gap, and thus cut-off wavelength, can be adjusted over a wide range The goal of the development of these detectors is to produce a fast, sensitive detector for the 10 μ region, which will operate at liquid nitrogen temperature Although this appears possible theoretically, it has proved difficult to achieve The detectors are in the development stage, and both photoconductors and photodiodes have been built D* values as high as 8 x 10^9 have been reported for HgCdTe, which has a time constant of 20 nanoseconds

Mercury Doped Germanium This material is photoconductive as a result of the photoionization of the mercury which is added to the germanium crystal The detector must be cooled to about 30°K, at which temperature it is background limited for all practical background levels Its radiation absorption is rather low, however, and thus the detectors must be made thick, at least one millimeter This has made it difficult to produce large arrays, or small detectors The background limited behavior of the detector makes it possible, however, to mask a large detector, the sensitivity will then be the background limited sensitivity associated with the open areas of the mask The cut-off wavelength of mercury doped germanium is 13 5 μ, and its quantum efficiency is about 30 percent It is readily available in hand-assembled arrays with elements as small as 020"

Mercury doped germanium has high responsivity in addition to high sensitivity The conductivity of the material is directly proportional to the infrared radiation entering the sensor This high responsivity makes it possible for a thermal mapper using these detectors to measure absolute temperature, rather than temperature differences, without using an internal standard This is extremely difficult to do with other detectors These advantages are so great that once the problems associated with building large arrays and long term cooling are solved, this type of detector will probably replace others for thermal mapping

Detector Cooling The salient feature of the response of photovoltaic and photoconductive detectors is the dependence of the spectral response on the operating temperature of the detector Long wavelength and high D* are obtained at the expense of low temperature operation For laboratory operation, temperatures in the range of liquid helium may be obtained but it is difficult to postulate such a cooling system for a detector which would meet reliability requirements for planetary missions Much research has been done on cooling systems for radiation detectors but practical, long life cooling systems of the closed cycle type are not available except as postulated developments If a firm requirement for long wavelength IR detectors can be established then it does not appear to be beyond the state-of-the-art to develop a closed cycle cryogenic cooling system to operate at 77°K This would permit detection in the 15 to 20 micron region of the IR spectrum using discrete detectors This conclusion is based on the following

Arthur D Little Corporation, Cambridge, Massachusetts, and Airesearch Corporation of Los Angeles, California have both built working prototypes of 77°K coolers that exhibit long life potential They use closed gas bearings and appear capable of running indefinitely A space-rated model based on the Airesearch design could be built in one year, and one designed to cool to a temperature of 30°K could be available in two years The major limitation is large power consumption The 77°K cooler requires about 500 watts and the 30°K cooler would require about one kilowatt Both would provide two watts of detector cooling

The Arthur D Little design is more efficient, but development is not as advanced A 30°K cooler could be developed by Arthur D Little in three to five years It would require less than 200 watts power per watt of cooling A more efficient design has been proposed by Hughes Aircraft Co for a long wavelength detector for the ERTS Multispectral Point Scanner (MSPS) Hughes Aircraft Co has built and flight tested a closed cycle cooler for detector operation in the 80°K range It is capable of cooling a 600 milliwatt heat load which is the approximate heat generated by the ERTS IR detector to 80°K The current device is being built for a lifetime of 3000 hours but it is claimed that only minor modification would be required to extend the life to 10,000 hours The cooler in the ERTS application would consume approximately 40 watts of electrical power and weigh 3 pounds It would therefore be a high efficiency, lightweight device It should be noted however, that in spite of the apparent availability of a closed cycle cryostat, the long wave IR channel has been eliminated from the multispectral point scanner (MSPS) for the Earth Resources Technology Satellites A and B

A more efficient approach to the problem of detector cooling, especially for outer planet missions, would be radiative cooling to deep space which is essentially passive In Reference (12) a single stage radiant cooler based on a NIMBUS design uses a one-half pound radiative horn capable of dissipating 20 milliwatts is discussed The resulting detector operating temperature is approximately 135°K While passive cooling is obviously advantageous, it does not appear that any reasonable system can be designed to obtain temperatures in the range of 30 to 77°K The thermal design of radiative coolers, while attractive, appears to be at least partly conjecture so that a design based on a radiative aperture is not believed to be within the state-of-the-art Even if a radiative system were used, the support requirements are nominal since the primary requirement is to furnish sufficient radiating aperture to remove the heat load from the detector

For support requirements estimating the Hughes Aircraft design is assumed as a useful guide The scaling coefficients given in Table 4-7 can then be used to estimate the support requirements for an 80°K detector operations temperature

4 2 5 3 IR Spectrometer Scaling Law

The necessary instrument criteria in order to satisfy a given set of observation requirements are described below We shall first consider the constraint on the optical system of the instrument imposed by the ground resolution This, together with the satellite velocity, bounds the total observation time available The sensitivity of the available detectors, together with the characteristics of each of the previously described instrument types will then enable the evaluation of the maximum obtainable spectral resolution and intensity resolution

Consider a satellite moving at a velocity v_s at an altitude H from the surface of a planet of radius R Then from Figure 4-13, the plane to centric half angle θ, defined by the desired resolution length W, is given by

$$\theta = \frac{W}{2R} \text{ (radians)} \tag{58}$$

W is constrained by the geometry to be

$$W \leq 2R\cos^{-1}\left[\frac{R}{R+H}\right] \tag{59}$$

Table 4-7 IR Detector Cooling Scaling Coefficients

Detector head load	= 300 milliwatts per detector
Cooler electrical power consumption	= 20 watts per detector
Cooler weight	= 1 5 lbs per detector
Cooler volume	= 0 25 ft^3/detector

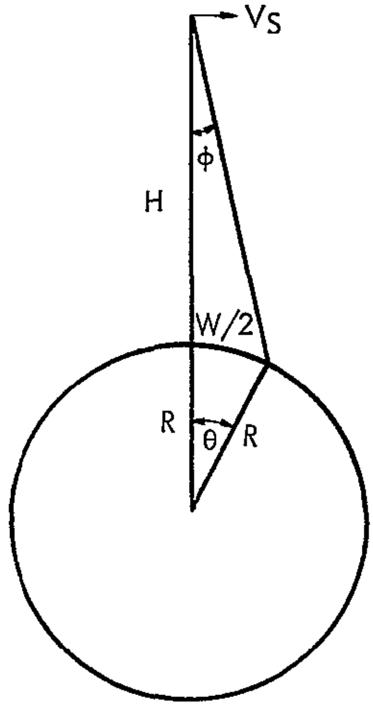

Figure 4-13 Planetary Viewing

The half angle field of view of the instrument is then given by,

$$\phi = \cot^{-1}\left[\frac{R+H}{R\sin\,(W/2R)} - \cot\frac{W}{2R}\right] \tag{60}$$

For small θ, i e , for $W << R$, the expression reduces to the planar case,

$$\phi = \tan^{-1}\left[\frac{W}{2H}\right]$$

The solid angle Ω , subtended by the surface is then

$$\Omega = \pi \sin^2 \phi = \pi \sin^2\left[\cot^{-1}\left\{\frac{R+H}{R\sin(W/2R)} - \cot\left[\frac{W}{2R}\right]\right\}\right] \tag{61}$$

The total observation time available, t, without image motion compensation, is taken to be the time in which the field of view of the instrument will have traversed a complete sampling grid (or linear dimension W) on the ground Therefore

$$t = \frac{W}{v_g} \tag{62}$$

where v_g is the apparent ground velocity For slowly rotating planets (Venus, Mercury, Mars), $v_s = v_g$ whereas for rapidly rotating planets, the angular velocity of the planet becomes non-negligible and v_g becomes the vector sum of the satellite velocity v_s and the velocity of the observation point due to planetary motion

Again for the case of $W << R$,

$$W = 2H \tan \phi = 2H\sqrt{\frac{\Omega}{\pi}} \tag{63}$$

Therefore, the available observation time t is given by

$$t = \frac{2H\sqrt{\frac{\Omega}{\pi}}}{v_g} \tag{64}$$

For the general case, W must be solved in terms of Ω via Eq (61) and then substituted into Eq (62) to obtain the time t

A slightly more accurate expression assuming $W << R$, and retaining the next higher-ordered term in W/R gives,

$$t \approx \frac{2H\sqrt{\frac{\Omega}{\pi}}}{v_g} \left[1 + \frac{\Omega}{2\pi} \left(\frac{H}{R}\right)\right] \tag{65}$$

Detection Sensitivity The ability of an instrument to perform satisfactorily in a particular application is determined by the sensitivity of the instrument to the measured signal with the required spectral resolution within the specified observation time This criterion can be expressed in terms of the signal-to-noise ratio (S/N) of the system over the frequency interval $\Delta \nu$, which is given by

$$S/N = \int_{\Delta\nu} D_{sys}(\nu) P(\nu) d\nu \qquad (66)$$

where

$D_{sys}(\nu)$ is the system detectivity

$P(\nu)$ is the available radiant power

If the instrument resolution $\Delta\nu$ is small, then $D_{sys}(\nu)$ and $P(\nu)$ can be replaced by the average value over ν and

$$S/N = D_{sys}(\nu) P_\nu \Delta\nu \qquad (67)$$

The detectivity is determined by the noise of the system and the characteristics of the detector used,

$$D_{sys} = \frac{1}{NEP} = \frac{D^*_\nu}{\left[A_d \Delta f\right]^{1/2}} \qquad (68)$$

where

(NEP) is the noise equivalent power of the system

A_d is the detector area

Δf is the noise equivalent bandwidth

D^*_ν is the specific detectivity of the detector

For photon detectors (photovoltaic and photoconductive cells, etc), which exhibit a long wave cut-off threshold, D^* is independent of the value of the detector time constant but is inversely proportional to the frequency,

$$D^*_\nu = \frac{\nu_o}{\nu} D^*_o \qquad (69)$$

where

ν_o is the frequency of peak response

D_o^* is the measured detectivity at ν_o

For thermal detectors (thermocouples, bolometers, etc), the detectivity is independent of frequency but is proportional to the square root of the detector time constant τ_D

$$D' = D_o^* \sqrt{\tau_D} \tag{70}$$

Typical values for various detectors are shown in Table 4-6

The available spectral radiant power, $P_\nu \Delta\nu$, at the detector is proportional to the aperture area, A_o, the solid angle Ω and the efficiency η of the system, and the spectral radiance I_ν (watts-cm^{-2} - steradian^{-1} - cm^{-1}) seen by the detector Therefore,

$$P_\nu \; \Delta\nu = \eta \; A_o \; \Omega \; I_\nu \; \Delta\nu \tag{71}$$

The detector area A_d and the solid angle Ω_d under which the detector is illuminated is related to the aperture via,

$$A_o \, \Omega = A_d \, \Omega_d \tag{72}$$

and Ω_d is expressible in terms of the focal length f, and the aperture ratio, N, of the system by

$$\Omega_d = \frac{A_o}{f^2} = \frac{C}{N^2} \tag{73}$$

where

C is a constant relating area to the effective diameter of the collector

Substituting Eqs (68), (71), (72) and (73) into Eq (67),

$$S/N = \eta \; (CA_o \, \Omega/\Delta f)^{1/2} \, D^* \, I_\nu \, \Delta\nu/(N) \tag{74}$$

If the requirement is not to measure the total radiance but to measure an absorption or emission feature of intensity ΔI_ν superimposed upon a background, I_ν, then

$$\Delta S/N = \eta \; (CA_o \, \Omega/\Delta f)^{1/2} \, D^*_\nu \, \Delta I_\nu \, \Delta\nu/(N) \tag{75}$$

Substituting for Ω from Eq (64) then gives,

$$S/N = \eta \; (CA_o \, \pi/\Delta f)^{1/2} \, D^*_\nu \, t v_g \, I_\nu \, \Delta\nu/2H(N), \tag{76}$$

and

$$\Delta S/N = \eta \; (CA_o \, \pi/\Delta f)^{1/2} \, D^*_\nu \, t v_g \, \Delta I_\nu \, \Delta\nu/2H(N) \tag{77}$$

We shall now specialize the above general expressions for the case of the four instruments previously described

To indicate the variation in performance which can be expected for the various types of spectrometer-radiometers a typical set of design parameters is selected for discussion purposes The values are selected to show performance variations and are used to demonstrate overall performance for a constant aperture design For illustrative purposes an optical aperture area of 100 cm^2 is assumed

<u>Filter Radiometer</u> For an aperture of 100 cm^2 and focal length of 10 cm, the aperture ratio, N, is unity, and C can be taken as one The noise bandwidth of the system is taken as 1/2t The efficiency of the system is given by the transmission losses in the optical system and the filter, the detector time constant, and noise factors of the detector bias and amplifier A reasonable figure is $\eta = 0\ 05$ Therefore, substituting into Eq (77), assuming a typical D^* of 10^9 $Hz^{1/2}$ cm/watt,

$$S/N = 0\ 6 \times 10^9 \, t^{3/2} (v_g/H) \, I_\nu \, (\Delta\nu) \tag{78}$$

<u>Polychromator Radiometer</u> The improvement in the S/N of this system over the previous one is mainly due to the longer integrating time available (by the square root of the number of channels) and that higher

specific detectivities can be achieved since each channel can be optimized However, the achievable aperture ratio of the optical system is only about 5 In addition, the solid angle is now limited by the spectral resolution rather than by the observation time t For a grating spectrometer, $\Omega \leq 0\ 17\ \Delta\nu/\nu$ which imposes an upper limit criterion on the maximum value of Ω

The resolution of a grating instrument can be written as

$$\frac{\Delta\nu}{\nu} = \frac{sn}{f \sin\theta} \qquad (79)$$

where

s is the slit width

f is the focal length

θ is the incident angle on the grating

n is the order of the spectrum

The solid angle, Ω, for a conventional spectrometer is given by the area of the slit divided by the square of the focal length f, i e ,

$$\Omega = s\ell/f^2 \qquad (80)$$

where

ℓ is the slit height

Combining the two expressions, then

$$\Omega = \left(\frac{\Delta\nu}{\nu}\right)\left(\frac{\ell}{f}\right) \frac{\sin\theta}{n} \qquad (81)$$

where

ℓ/f is then the angular height of the slit

For the case of n=1, the values of $(\ell/f)\sin\theta$ for various grating instruments has a range typically from about 0 02 to a maximum value of 0 17 Therefore, for the optimal case,

$$\Omega \leq 0.17 \frac{\Delta\nu}{\nu} \tag{82}$$

For a D^*_ν of 10^{10} $Hz^{1/2}$-cm/watt, and assuming $\pi v_g^2 t^2/4H^2 \leq 0.17\ \Delta\nu/\nu$, an n channel system would have a S/N of

$$S/N = 1.2 \times 10^9\ t^{3/2} (v_g/H)\ I_\nu (\Delta\nu)\ \sqrt{n} \tag{83}$$

If the required spectral resolution is such that it becomes the determining factor in the maximum allowable value of Ω, then

$$S/N = 3 \times 10^8\ t^{1/2}\ (\Delta\nu)^{3/2}\ I_\nu\ \nu^{-1/2}\ \sqrt{n} \tag{84}$$

Scanning Spectrometer The analysis for this instrument is similar to that of the filter radiometer The same criterion on Ω, due to the resolution requirement, exists as in the case of the polychromator radiometer, i e , $\Omega \leq 0.17\ \Delta\nu/\nu$ Provided that this condition is not exceeded, then

$$S/N = 0.6 \times 10^9\ t^{3/2} (v_g/H)\ I_\nu\ \Delta\nu \tag{85}$$

Otherwise a degradation in S/N occurs due to the fact that Ω must be kept small to be consistent with the required resolution For this case then, as before,

$$S/N = 1.5 \times 10^8\ t^{1/2}\ (\Delta\nu)^{3/2}\ I_\nu\ \nu^{-1/2} \tag{86}$$

Michelson-Type Interferometer Since the beam splitter reflects 1/2 the incident radiation back towards the source, Eq (71) is modified to become

$$P_\nu\ \Delta\nu = \frac{1}{2} \eta\ A_o\ \Omega\ I_\nu\ \Delta\nu \tag{87}$$

The noise equivalent power in an interferometer is given by

$$NEP = (1/D_\nu)(2A_d\ \Delta f/n)^{1/2} \tag{88}$$

where

n is the number of sample points taken per interferogram

The $n^{1/2}$ relationship results from the fact that the signal is self-coherent and is multiplied by n, the number of sample points, but the noise is incoherent so that it is multiplied by $n^{1/2}$. The signal required to give a signal to noise ratio of one, that is NEP, is then divided by $n^{1/2}$.

Therefore the system detectivity is given by

$$D_{sys,\,\nu} = D_\nu /(2A_d \Delta f/n)^{1/2}. \tag{89}$$

The noise equivalent bandpass and the number of sample points taken to obtain the interferogram is related to the total observation time t by

$$t = n/2\,\Delta f \tag{90}$$

Therefore, substituting Eq. (90) into Eq. (89) for Δf yields

$$D_{sys,\,\nu} = D_\nu^* \,(t/A_d)^{1/2} \tag{91}$$

Using Eq. (72) and (73) to relate A_d in terms of the aperture ratio, N, of the system and setting C=1, we obtain

$$D_{sys,\,\nu} = D_\nu^*/(N) \left[t/A_o\,\Omega\right]^{1/2} \tag{92}$$

Finally, combining Eq. (90) and Eq. (85)

$$S/N = D_{sys,\,\nu}\, P_\nu\, \Delta\nu = (\eta\, D_\nu^*/2N) \left[A_o\,\Omega\, t\right]^{1/2} I_\nu\, \Delta^\nu \tag{93}$$

For an interferometer, the solid angle Ω is related to the resolution of the instrument by

$$\Omega = 2\pi\,\Delta^\nu/\nu \tag{94}$$

Therefore, for the case of $\Omega = v_g^2 t^2/4H \leq 2\pi \Delta\nu/\nu$, then the S/N is given by

$$S/N = (\eta D_\nu^*/4f N)(A_o \pi)^{1/2} t^{3/2} (v_g/H) I_\nu \Delta \nu \tag{95}$$

Taking typical values of $A_o = 100 \text{ cm}^2$, $N = 1$, $D^* = 10^{10} \text{Hz}^{1/2}$-cm/watt, $\eta = 0.05$, then

$$S/N = 2 \times 10^9 t^{3/2} (v_g/H) I_\nu \Delta \nu \tag{96}$$

On the other hand, if the criterion on Ω is limited by the required spectral resolution rather than by the geometry involved for the necessary ground resolution, then $\Omega = 2\pi \Delta\nu/\nu$, and

$$S/N = (\eta D_\nu^*/2N)(2\pi A_o t)^{1/2} I_\nu (\Delta\nu)^{3/2} \nu^{-1/2} \tag{97}$$

Evaluating as before gives

$$S/N = 6 \times 10^9 t^{1/2} (\Delta\nu)^{3/2} I_\nu \nu^{-1/2} \tag{98}$$

and with equation (62)

$$S/N = 6 \times 10^9 \left(\frac{W}{v_g}\right)^{1/2} \nu^{1/2} (\Delta\nu)^{3/2} I_\nu \tag{99}$$

The advantage of this instrument over that previously described is two-fold First, the spectral coverage is continuous and therefore the information return is much higher for the same S/N. Secondly, as can be seen from comparing Eq (98) to the corresponding case of Eq (84) and Eq (86), for high resolution requirement the S/N is well over an order of magnitude higher In general, then, the interferometer is the most desirable instrument in terms of high resolution, spectral range, and information content of the measured data Penalties, however, have to be paid in terms of weight, complexity of system, and power requirement

The trade-off analysis and general characteristics of the competing instrument designs are summarized in Figure 4-14 The trade-off analysis is only the first step however since once an instrument type is selected it will then be necessary to establish the support requirements associated with a range of system parameters The scaling to establish support requirements is based on an interferometer design since it represents a generally difficult case exclusive of estimating the requirements of the primary optics which are similar for all the cases considered Spectrometer design flow logic is summarized in Figure 4-15

For instrument scaling law purposes and support requirement development the following guidelines will be used

1. A signal-to-noise ratio of 20 dB is the minimum acceptable on a single look basis If, with vehicle steering or image motion compensation, more than one look is available then it can be assumed that by post processing of the data the overall measurement signal-to-noise ratio may be improved as the square root of the number of looks The post-processing would be accomplished after return of the data to Earth

2 The instrument stability, principally from drift of analog electronic circuits, detector heating, etc , limits any single look to a maximum of 20 seconds without recalibration For an interferometer the calibration time is equal to the observation time so that the time between measurements is equal to the measurement time The value of 20 seconds for instrument stability is based on the best narrow band amplifier design available

3 Even for uncalibrated, relative spectrometry, a reference source is required if the observation time exceeds 20 seconds For radiometry a reference source is always assumed either for gain control referencing or for absolute reference calibration

4 Where appropriate, detector cooling will be used but because of limitations in cooling technology the maximum long wave cut-off of photo detectors is taken as 20 μ

   Detection beyond 20 μ is assumed to be beyond the state-of-the-art in realistic spacecraft systems because of the difficulty in reducing background thermal emission Such devices as cooled optical systems, and cooled filters are required to suppress ambient radiation below object field radiation beyond the stated long wave cut-off Since they are not available except as proposed

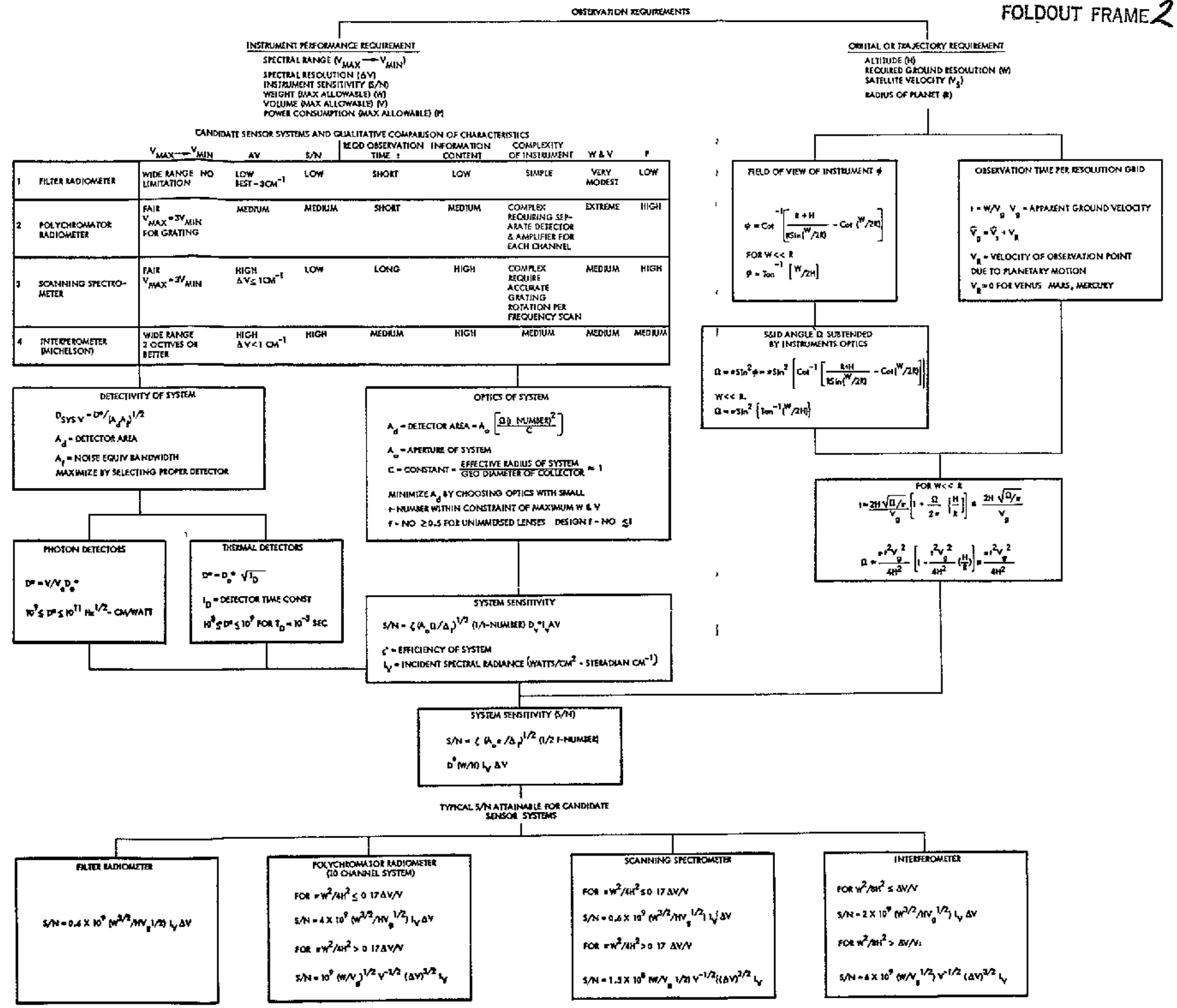

		$V_{MAX} \rightarrow V_{MIN}$	ΔV	S/N	REQD OBSERVATION TIME t	INFORMATION CONTENT	COMPLEXITY OF INSTRUMENT	W & V	P
1	FILTER RADIOMETER	WIDE RANGE NO LIMITATION	LOW BEST - 3CM^{-1}	LOW	SHORT	LOW	SIMPLE	VERY MODEST	LOW
2	POLYCHROMATOR RADIOMETER	FAIR $V_{MAX} = 3V_{MIN}$ FOR GRATING	MEDIUM	MEDIUM	SHORT	MEDIUM	COMPLEX REQUIRING SEPARATE DETECTOR & AMPLIFIER FOR EACH CHANNEL	EXTREME	HIGH
3	SCANNING SPECTROMETER	FAIR $V_{MAX} \approx 3V_{MIN}$	HIGH $\Delta V \leq 1CM^{-1}$	LOW	LONG	HIGH	COMPLEX REQUIRE ACCURATE GRATING ROTATION PER FREQUENCY SCAN	MEDIUM	HIGH
4	INTERFEROMETER (MICHELSON)	WIDE RANGE 2 OCTIVES OR BETTER	HIGH $\Delta V < 1\ CM^{-1}$	HIGH	MEDIUM	HIGH	MEDIUM	MEDIUM	MEDIUM

Figure 4-14 Scaling Laws for Infrared Radiometers and Spectrometers

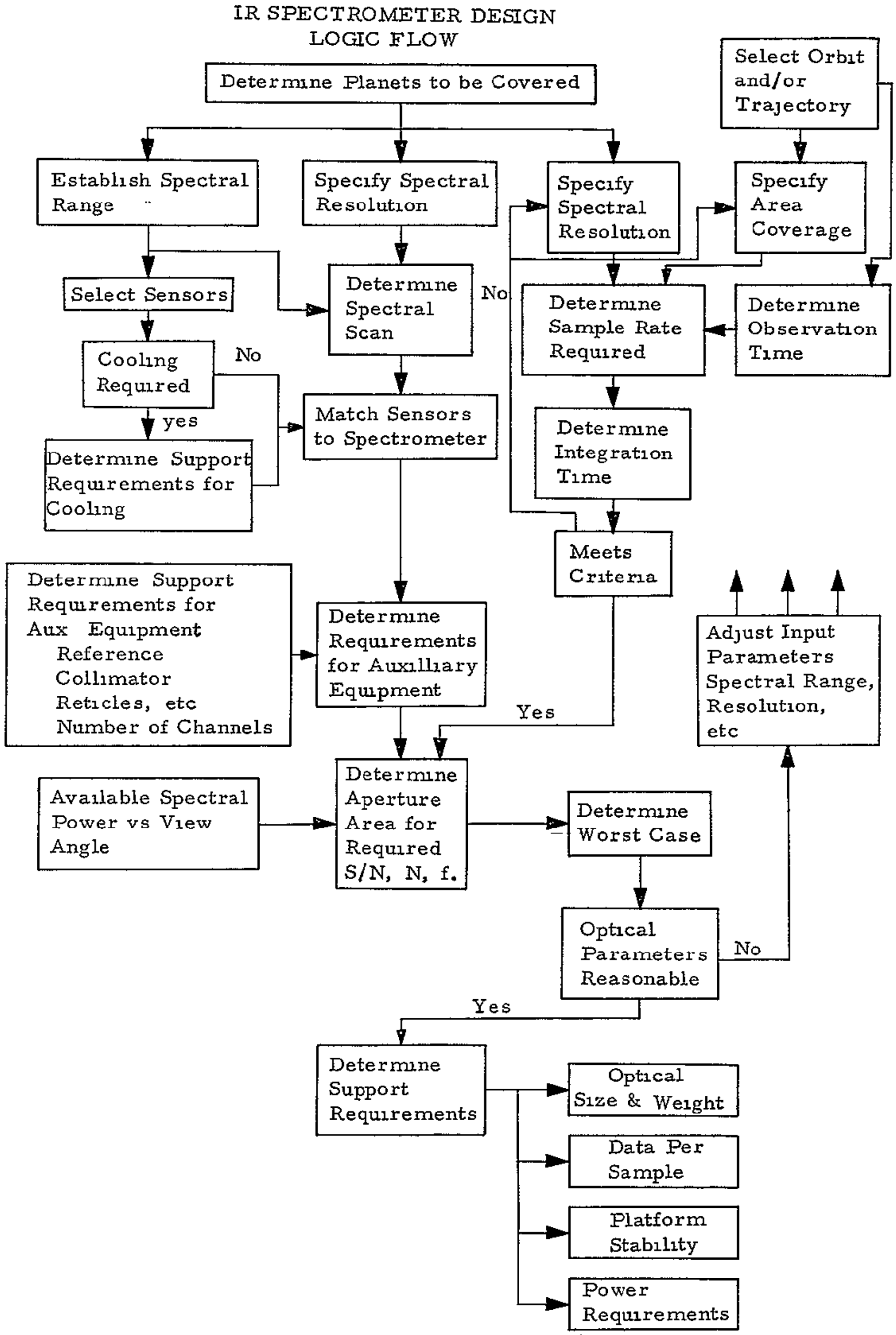

Figure 4-15 IR Spectrometer Design Logic Flow

development items they do not appear realistic in the time frame of the planetary missions

Basic optical system scaling laws for weights, volume and power are given in Paragraph 4 2 Certain general scaling laws for the electronics associated with non-image forming IR systems can be established for weight and volume estimating purposes The following general considerations apply

1 Infrared detectors are generally lightweight, pre-packaged devices of small size Depending upon the output coupling auxiliary optical components and the integration of the preamplifier into the detector package, they may range from a few grams to 0 1 kilogram Assuming that integrated circuit packaging techniques are used, a conservative estimate of 0 05 kg per detector can be used

2 Reference sources are frequently used with spectrometers as gain control devices and are a necessity for absolute radiometers The source may be external with the sun being the most frequently used reference For absolute radiometry an internal, calibrated reference source is used The two types of sources are not essentially different from the point of view of weight scaling so that a weight penalty 0 5 kg is used

3 Auxiliary components such as choppers or reticles, beamsplitters, filter wheels, drive motors, etc , are generally lightweight devices The design of auxiliary components is usually optimized after basic design of the instrument is established with such factors as duty cycle, aging characteristics, etc , having an effect on overall system weight or volume For estimating purposes, the weights given in Table 4-8 are assumed although many of the estimates may be in error by as much as 50 percent This is not a severe shortcoming, however, since with few exceptions the components are lightweight

4 The electronics at the output of the instrument depend upon the function performed and the detector type used Modern microcircuit technology permits functional packaging of the order of 0 005 kg per function and resulting packing densities of the order of 370 kg per cubic meter Thus an electronic package which performs ten functions such as amplification in five stages, automatic gain control, detection and conversion, would weigh approximately 0 05 kg and occupy a volume of 1 4 x 10^{-4} m^3

Table 4-8 Weight Estimation for Auxiliary Components of IR Optical Instruments

Function	Weight	Volume
IR Detector	0 05 kg/detector	1 3 x 10^{-4} m^3 *
Reference Source	0 5 kg	7 6 x 10^{-4} m^3 **
Gratings, Mirrors, Field Lenses, etc	4 x 10^2 ℓ^3 kg *****	$\frac{\ell^3}{6}$
Filter	0 25 kg/channel	***
Beamsplitter	0 05 kg/channel	***
Rotary Filter Drives and Auxiliary Motors	0 2 kg/channel	***
Mirror Scan Drive Motor (for scanning mirror)	0 2 (0 1 + D_p) ****	***
Electronics	0 05 kg/channel	1 4 x 10^{-4} m^3 *

* Microminiature Circuit Package 3 7 x 10^2 kg/m^3 (25 lbs/ft^3)

** Solid State Distributed Circuit Package 7 4 x 10^2 kg/m^3 (50 lbs/ft^3)

*** Included in Volume of Primary Telescope

**** D_p is the Primary Optical Aperture Diameter in Meters

***** ℓ is the Diameter or Width in Meters

4 2 5 4 Spectrometer Support Requirements

System Weight The weight of the spectroscopic instrument is contributed principally by two major subsystems - the primary telescope and the spectrometer The primary telescope weight can be established from the data given in Table 4-8, once the telescope parameters have been defined

The scanning mirror and detector of the Michelson Interferometer consists of the following basic components

1 A rigid optical bench

2 Input optics for collimation

3 A beam-splitter

4 A fixed mirror

5 A scanning mirror

6 Condensing optics

7 A detector assembly

Using a typical laboratory instrument as a prototype, the interferometer weight results primarily from the optical bench on which the optical components are mounted The diameter of the collimated input radiation is taken as two inches although it can range from one-half inch to several inches depending upon the sensitivity requirements and the angular resolution of the instrument An input diameter of two inches requires an optical bench surface of ten inches by ten inches For proper rigidity, the thickness of the bench is one fifth the surface dimension so that the volume of the bench is 200 in^3 ($3\ 13 \times 10^{-3}\ m^3$) At the density of steel of $7\ 83 \times 10^3$ kg per m^3, the weight of the bench alone is 24 5 kg

For an input diameter of 2 in (5×10^{-2} meters) the weights for the optical components can be determined from Table 4-8 The beamsplitter used in the interferometer must be at least $\sqrt{2}$ times the input diameter In addition, the weight of a reference source must be included for calibration purposes

The scan mechanism weight is included in the basic weight of the optical bench so that no additional weight penalty is associated with it

System Volume The volume of the primary telescope is established from the data given in Table 4-8

The volume of the spectrometer is determined by the surface area of the optical bench times the height consisting of the thickness of the bench, the diameter of the input collimated beam, and optical mounting mechanisms, for a total height of 0 75 of the base For a base dimension of 0 25 meters, the volume of the spectrometer package is $1\ 2 \times 10^{-2}\ m^3$

System Power The power for the spectroscopic instrument is of four types

1 The power to operate an external scan mirror if one is used

2 The power to operate the spectrometer mirror linear drive

3 Detector cooling power

4 The power to operate the detector electronics

Power requirements for types 1 and 2 can be obtained from Table 4-5, while detector electronics power can be obtained as indicated below

The power requirements for IR detector electronic circuits is quite modest Even for circuits with discrete components the power consumption per detector and associated electronics is less than 0 5 watt If integrated circuits are used the power consumption per detector is approximately 0 1 watt per detector.

In addition to the basic electronics of the detector, there is usually a requirement for a reference source for calibration The power required to operate the source is of the order of 5 watts If an array of detectors is used the requirements for the source should be increased to 10 watts

Data Rate The data rate for the Michelson interferometer is determined by the necessity of reconstructing the time modulated output signal To prevent signal frequency suppression the minimum number of samples to reconstruct the highest frequency with a given resolution is

$$n = \frac{2V}{\Delta V} \max \tag{100}$$

where ΔV is the resolution The best resolution is established by the accuracy of the mirror drive to approximately 0 1 cm^{-1} To scan a spectrum from V max to V min with a resolution of ΔV will then give a data rate of

$$\text{Data Rate} = \frac{n}{t} = \frac{2V}{t\Delta V} \text{ samples/sec} \tag{101}$$

Stabilization If the angular resolution of the instantaneous field of view of the optics is given by

$$\phi = \tan^{-1} \left[\frac{W}{2\ H}\right] \tag{102}$$

which is approximately

$$\phi \approx \frac{W}{2H} \tag{103}$$

for small angles and the time available for sampling is taken as the time in which the field of view traverses a resolution interval, W, then

$$\phi = \frac{t\ Vg}{2\ H} \tag{104}$$

since

$$W = tV_g \tag{105}$$

The stabilization of the optical axis in terms of field of view rate is

$$\phi = \frac{\phi}{t} = \frac{V_g}{2H} \text{ radians/sec} \tag{106}$$

For small fields of view at long ranges this requirement could pose stringent penalties since observation times may be long

4 2 6 Visible and UV Spectrometer and Radiometer

4 2 6 1 Design and Performance

The scaling laws for visible and UV spectrometers are not essentially different from the scaling laws for IR spectrometers In general the design procedures are identical with the principal difference being in the components used such as detectors and the attainable spectral resolution Typical spectral ranges of seven spectrometer types are shown in Figure 4-16 Of the types indicated in the figure the most commonly used laboratory instruments are the prism spectrometer and one of the several grating spectrometer indicated

Prism spectrometers, although relatively straightforward, have not found wide application in space because of the generally large attenuation through the prism material and the difficulty of obtaining good spectral resolution with a movable detector-prism combination The primary emphasis is on grating spectrometer although background information on prism spectrometers is included for reference purposes

Prism Spectrometers Basically, a prism spectrometer disperses light according to wavelength by employing a material which has a variation in refractive index as a function of wavelength The geometry of the prism produces an angular dispersion proportional to the dispersion in the index of refraction The geometry of a ray passing through a prism is shown in Figure 4-17 If there are two such rays of wavelength λ_1 and λ_2 and the respective indices of refraction for the two rays are n_1 and n_2 then

$$\Delta\theta = (n_1 - n_2) \frac{2 a \sin\frac{\alpha}{2}}{\sqrt{1-\bar{n}^{-2} \sin^2 \frac{\alpha}{2}}} \qquad (107)$$

where

$$\bar{n} = \frac{n_1 + n_2}{2} \qquad (108)$$

The system is defined to be at minimum deviation when $i_1 = i_2$ and $r_1 = r_2$ At minimum deviation, the theoretical ultimate resolving power

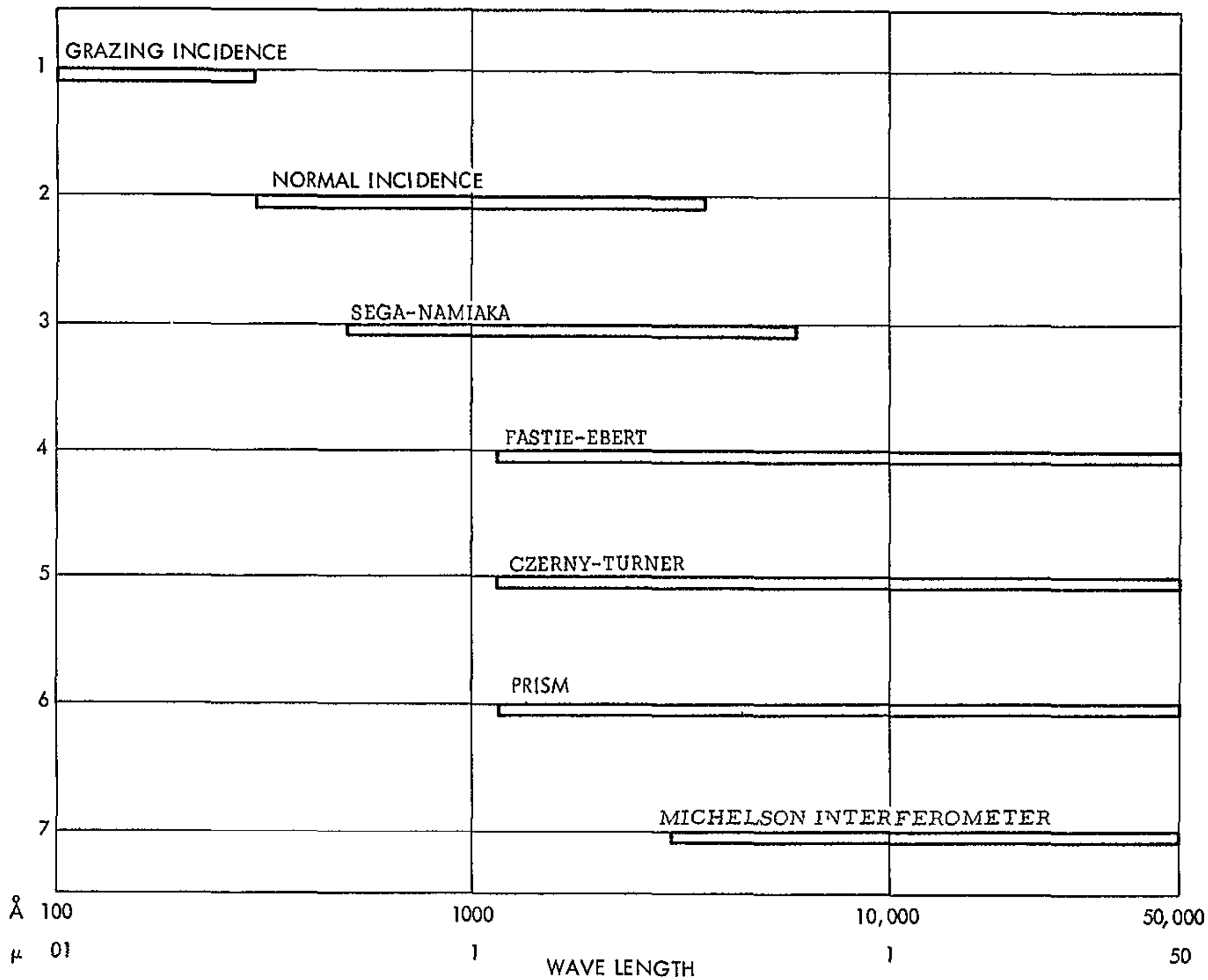

Figure 4-16 Spectral Range of Spectrometer Types

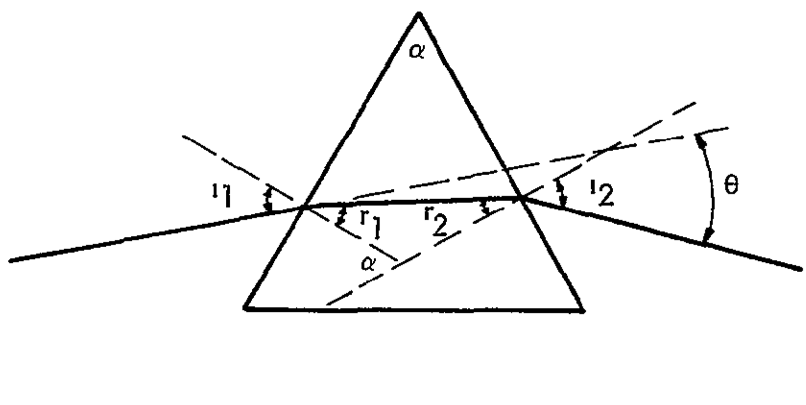

Figure 4-17 Path of a Ray Through a Prism

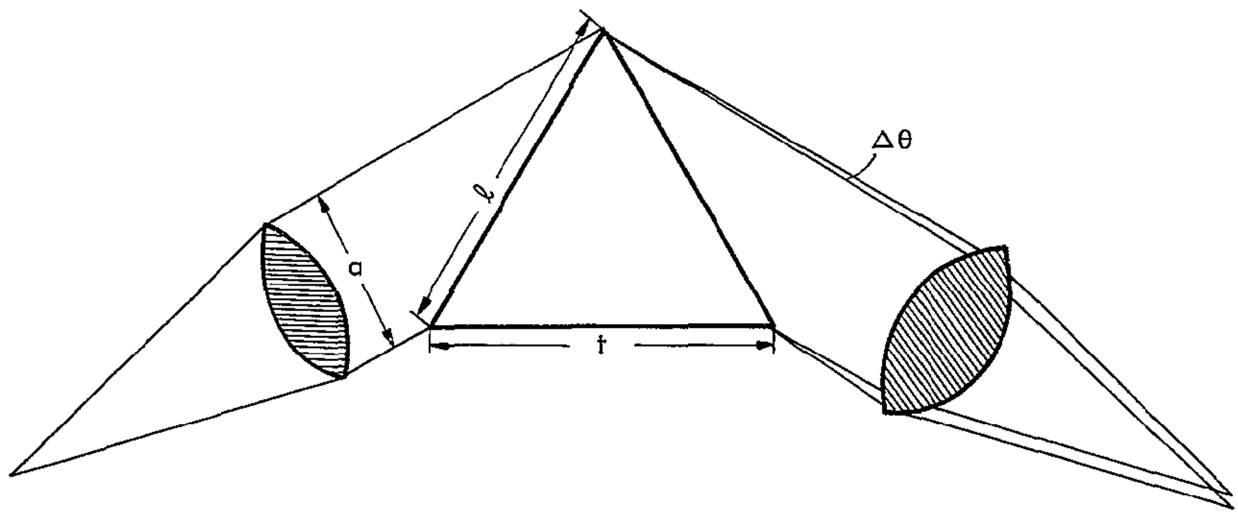

Figure 4-18 Just-Resolved Wavelengths at Minimum Deviation

for an infinitely narrow slit can be found Referring to the geometry in Figure 4-18, $\Delta\theta$ represents the minimum separation of outgoing rays which may be observed at the diffraction limit Then the resolving power is given by

$$R = \frac{\lambda}{\Delta\lambda} = t\frac{dn}{d\lambda} \tag{109}$$

where $dn/d\lambda$ is the rate of change of index of refraction with wavelength One may also express the dispersion in terms of angles, so that

$$\frac{d\theta}{d\lambda} = \frac{d\theta}{dn} \quad \frac{dn}{d\lambda} \tag{110}$$

where

$$\frac{d\theta}{dn} = \frac{2\sin\frac{\alpha}{2}}{\sqrt{1 - n^{-2}\sin^2\frac{\alpha}{2}}} \tag{111}$$

Table 4-9 shows n, $d\theta/d\lambda$ at the wavelength of the sodium D line and for a 60^o prism as well as region of transmission and region of best usefulness for several common prism materials

The resolution discussed above is for infinitely narrow non-diffracting slits The effects of a real input slit on a prism spectrometer is shown in Figure 4-19 where I_c is the peak intensity of a line, H_{NC} is the line width and $\psi_o d = \pi Bd/\lambda f$ where B is the slit width, λ is the wavelength used, f the focal length and d the semi-diameter of the collimator lens

The scaling for effective spectral width for a Littrow mount prism monochromator may be expressed by

$$\Delta\lambda_{(cm)} = \frac{\left[1 + n^2\sin^2\frac{\alpha}{2}\right]^{1/2}}{4\sin\alpha/2\,\frac{dn}{d\lambda}} \quad \frac{s}{f} + F(s)\frac{\lambda}{2b\frac{dn}{d\lambda}} \tag{112}$$

TABLE 4-9

DISPERSING PRISM CHARACTERISTICS

Formula	Material	n_D	$(d\theta/d\lambda)_D$	Region of Transmission	Region of Best Suitability
$Si0_2$	Quartz (Fused)	1 45848	517×10^{-5}	1850Å-3 5μ	1850Å-2 7μ
LiF	Lithium Fluoride	1 39177	286×10^{-5}	1200Å-6μ	2 7μ-5 5μ
CaF_2	Fluorite	1 43385	333×10^{-5}	1200Å-9μ	5μ-9μ
NaCl	Rock Salt	1 54431	938×10^{-5}	2000Å-17μ	8μ-16μ
KBr	Potassium Bromide	1 5581	$1\ 449 \times 10^{-5}$	2100Å-28μ	15μ-28μ

The resolution discussed above is for infinitely narrow non-diffracting slits The effects of a real input slit on a prism spectrometer are shown in Figure 4-19, where I_c is the peak intensity of a line, H_{NC} is the line width and $\psi_o d = \pi Bd/\lambda f$ where B is the slit width, λ is the wavelength used, f the focal length and d the semi-diameter of the collimator lens

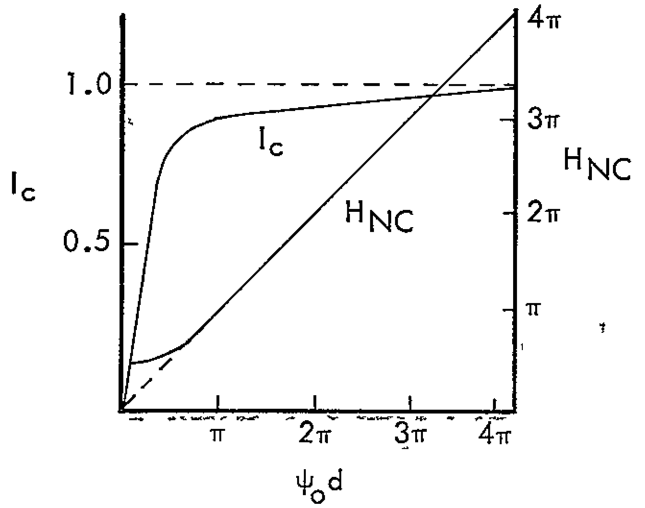

Figure 4-19 Intensity I_c and Line Width H_{NC} as a Function of Reduced Slit Width $\psi_o d$

where

λ	=	radiation wavelength in cm
n	=	index of refraction of the prism at wavelength
α	=	prism apex angle
$dn/d\lambda$	=	dispersion of prism at wavelength λ
s	=	mechanical slit width in cm
f	=	focal length in cm
b	=	effective prism base in cm

30

and

F(s) is a function running from approximately 0 9 for s = 0 to about 0 5 when first term above equals coefficient of F(s)

Grating Spectrometer Grating spectrometers for the visible and UV portions of the spectrum are not essentially different from the polychromator radiometer and scanning spectrometer discussed under IR spectrometers above However, because of the difference in specifying photomultiplier performance it is necessary to compute the signal-to-noise ratio in terms of responsivity rather than detectivity In terms of responsivity, R, the signal-to-noise ratio for a photomultiplier is

$$\frac{S}{N} = \frac{I_s}{2e\Delta f} \tag{113}$$

where

I_s is the output signal current

Δf is the noise equivalent bandwidth

e is the charge on the electron = 1 6 x 10^{-19} coulombs

The output signal current is determined by the overall responsivity of the photomultiplier and the available radiant power over the wavelength region of interest in the form

$$I_s = \int_{\lambda_1}^{\lambda_2} R(\lambda)\ P(\lambda)\ d\lambda \tag{114}$$

where

$R(\lambda)$ is the spectral responsivity in amperes per watt

$P(\lambda)$ is the spectral radiant power

$\lambda_2 - \lambda_1 = \Delta\lambda$ is the spectral passband of the detector

If the spectral resolution is small then $R(\lambda)$ and $P(\lambda)$ may be replaced by average values at the wavelength region of interest Therefore

$$I_s = \overline{R}_\lambda\ \overline{P}_\lambda\ \Delta\lambda \tag{115}$$

and the signal to noise ratio is

$$\frac{S}{N} = \frac{\overline{R_\lambda}\ \overline{P_\lambda}\ \Delta\lambda}{2e\Delta f} \tag{116}$$

Equation (116) is actually the power signal-to-noise ratio so that in terms of peak to peak signal to rms noise the signal-to-noise ratio is

$$\frac{S}{N} = \left[\frac{R_\lambda\ P_\lambda\ \Delta\lambda}{2e\Delta f}\right]^{1/2} \tag{117}$$

The available radiant power at the detector is of course determined by the spectral radiance, I_λ and the optical parameters in the form

$$P_\lambda\ \Delta\lambda = \eta\, A_o\, \Omega\, I_\lambda\, \Delta\lambda \tag{118}$$

where

η is the overall efficiency of the optical and detection process

A_o is the area of the collection optics

Ω is the instantaneous solid angular field of view of the optical system

I_λ is the spectral radiance

$\Delta\lambda$ is the spectral bandwidth

The primary design equation thus becomes

$$\frac{S}{N} = \left[\frac{\eta\ R_\lambda\ A_o\ \Omega\ I_\lambda\ \Delta\lambda}{2\epsilon\,\Delta f}\right]^{1/2} \tag{119}$$

as with any system which is limited by detector size, A_d, we have

$$A_d = A_o\, \Omega\, N^2 \tag{120}$$

where N is the aperture ratio or f/number of the complete optical system from entrance aperture to the detector including field lenses, collimator and, as appropriate, aperture stops or slits Since

$$\Omega \approx (1\ 22\frac{\lambda}{D})^2 \tag{121}$$

for a diffraction limited system and $\Omega << 1$, it follows that

$$A_d = K\lambda^2\ N^2 \tag{122}$$

or the linear dimension of the detector, ℓ, determines the best spatial resolution attainable with an instrument without loss of signal It also indicates a primary limitation at short wavelengths since

$$\ell = N\lambda \tag{123}$$

and as λ decreases the attainable value of N must increase to maintain instrument performance

In terms of the available observation time, t, from equation (64) of the IR spectrometer section

$$t = \frac{2H\sqrt{\frac{\Omega}{\pi}}}{V_g} \tag{124}$$

where

H is the altitude

V_g is the effective surface velocity

the value of the instantaneous field of view is

$$\Omega = \frac{\pi t^2\ V_g^{\ 2}}{4H^2}$$

Sustituting in equation (119) gives

$$\frac{S}{N} = \left[\frac{\eta \pi R_\lambda A_o I_\lambda \Delta\lambda}{2e\Delta f}\right] \frac{t V_g}{2H} \tag{125}$$

This is the primary design equation for the optical system of the spectrometer The values of R_λ are obtained from Figure 4-28 and I_λ is determined for the wavelength region of interest from Tables 4-1 and 4-2 in combination with the viewing geometry for specific planets

It would appear from all of the signal-to-noise ratio expressions for discrete detectors, that as large a signal-to-noise as is required could be obtained by making the bandwidth Δf decreasingly small The minimum bandwidth however is basic to the instrument stability criterion discussed in the spectrometer section Narrower and narrower bandwidths imply band-pass characteristics of increasing Q The minimum resistance losses of real components tend to limit attainable Q even with feedback so that overall instrument stability of approximately 20 seconds is an upper limit on the state-of-the-art

<u>Spectrometer Gratings</u> Diffraction gratings produce dispersion as the result of interference of light passing through many parallel slits The fundamental grating equation is

$$n\lambda = d(\sin\alpha + \sin\beta) \tag{126}$$

where λ is the wavelength, n is an integer, d is the grating width and angles α and β are shown in Figure 4-20

The resolving power of the plane diffraction grating is given by

$$\frac{\lambda}{\Delta\lambda} = \frac{\omega}{\lambda}(\sin\alpha + \sin\beta) \tag{127}$$

where ω is the electrical width of the grating in wavelengths and the other factors are as before It follows that

$$\frac{\lambda}{\Delta\lambda} = nN \tag{128}$$

where again n is an integer and N is the number of lines in the grating

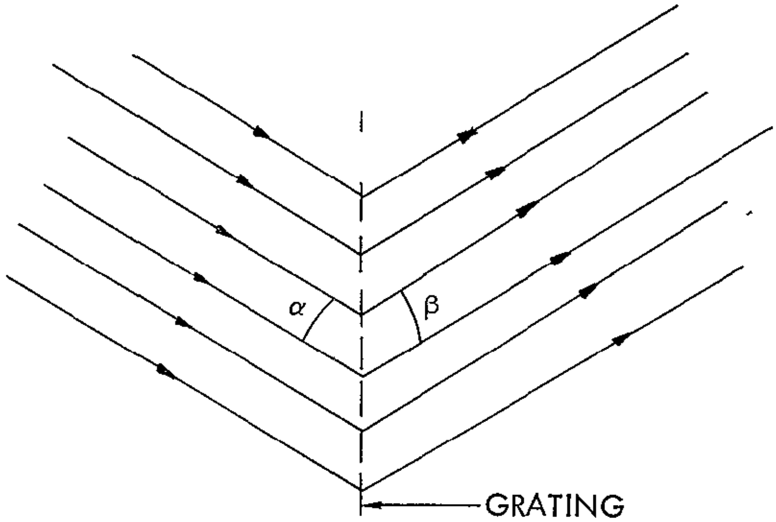

Figure 4-20 Diffraction Angles of a Plane Transmission Grating

Grating instruments in the visible and ultraviolet are reflective with grooves instead of slits, for which the above description holds exactly

Almost all reflection gratings are blazed That is the grooves are shaped so that the light is reflected most strongly for some $n\lambda$ of interest An unblazed grating has the highest intensity for $n = 0$ where there is no dispersion In selecting a blaze angle for a grating one must take the relative efficiency of the grating over a range of wavelengths into account Although grating design is at best an inexact science, it requires a high level of skill in manufacture since overall parameter adjustment to obtain an optimum grating is a cut and try process

The total flux transmitting power of a spectroscopic instrument may be scaled by the following relationship

$$F = kT \frac{\ell}{f} A \frac{d\theta}{d\lambda} \tag{129}$$

where

F = flux transmitted

k = a scaling constant independent of grating parameters

ℓ = slit height (maximum without changing resolution)

f = focal length

T = the optical transmission

A = hw cos i (the effective area of the grating)

where

h is height of the grating

w is width of the grating

i is the angle of incidence on grating

$\frac{d\theta}{d\lambda}$ is the angular dispersion of the grating

This relationship is for constant resolution and is employed to scale parameters as follows if two instruments are to be compared with flux transmission F_1 and F_2 then,

$$\frac{F_1}{F_2} = \frac{T_1 \; \ell_1 \; f_2 \; A_1 \left(\frac{\partial \theta}{\partial \lambda}\right)_1}{T_2 \; \ell_2 \; f_1 \; A_2 \left(\frac{\partial \theta}{\partial \lambda}\right)_2} \tag{130}$$

It is important to note that for such instruments the so-called f/number is not a good measure of flux transmission

The resolution as a function of f varies linearly down to a critical slit width w_c below which the resolution does not improve but the intensity drops rapidly

$$w_c = \frac{f}{D} \tag{131}$$

where

λ is the wavelength

f is the focal length

and D is the diameter of the collimator

<u>Collimating Optics</u> The basic assumption in grating design is that the grating is illuminated by plane waves, that is a parallel beam of radiation This requirement imposes an optical transformation between the primary focus of the collecting optics where the beam of radiation is convergent and the grating which requires a parallel beam of radiation The diameter of the collimated radiation is generally slightly larger than the dimension of the grating to permit motion of the grating in the collimated beam

A large variety of collimators have been used in grating spectrometers but two classes are the most common They are classified as straight through or dioptric and reflective The dioptric types are generally complex and heavy since they require a combination of field lens and negative lens to collimate the beam, and collecting optics to focus the output of the grating on a slit to illuminate the detector Since grating sizes up to 10 inches in width are feasible, the refractive components of the collimator would be in the size range of 12 to 15 inches in diameter Their weight and mechanical alignment problems would be generally large

A somewhat simpler configuration is obtained with reflective components In place of the field lens and negative lens at the focal plane, a slightly convex mirror is used to reform the convergent beam into an essentially collimated beam After illuminating the grating the radiation is refocused with a second concave mirror to illuminate the exit slit The result of this approach is the so-called Ebert spectrometer which uses a single mirror The diameter of the mirror is essentially twice the grating width In combination with a reflective grating the inner portion of the mirror surface serves as the collimating element and the outer portion is the condensing optics The advantages of such an approach are a folding of the optical path and a reduction in the number of optical components to be kept in mechanical alignment

There is a wide variety of possible optical arrangements for a grating spectrometer Schematic diagrams for spectrometers using a plane transmission and a reflection grating are shown in Figures 4-21 and 4-22

By using a curved reflection grating, a reduced weight system can be achieved with the same performance, but with increased complexity as indicated in Figure 4-23

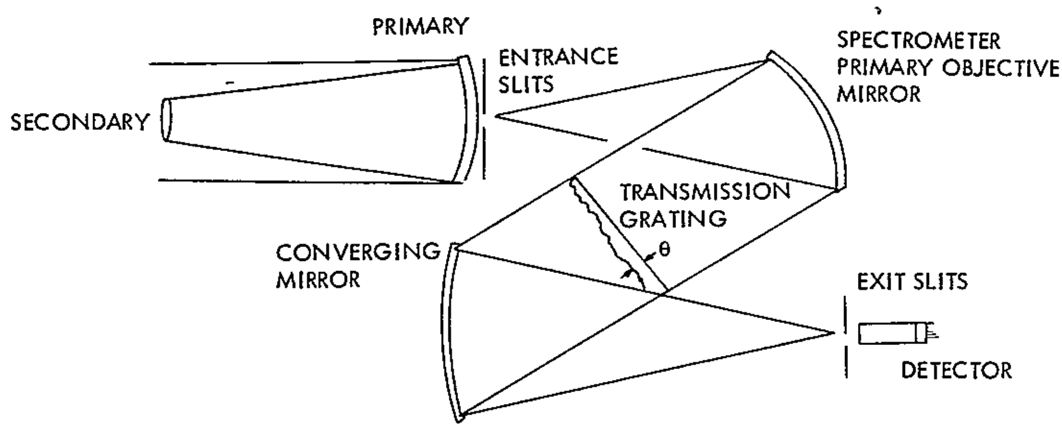

Figure 4-21 Transmission Grating UV Spectrometer

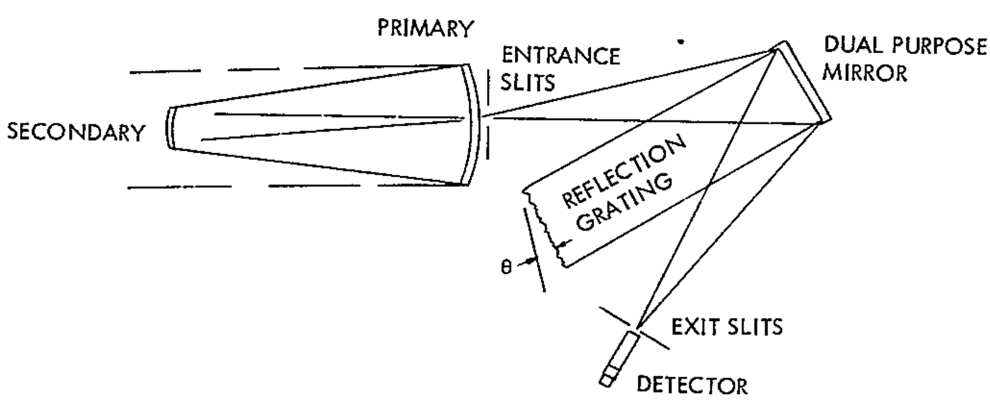

Figure 4-22 Reflection - Grating UV Spectrometer

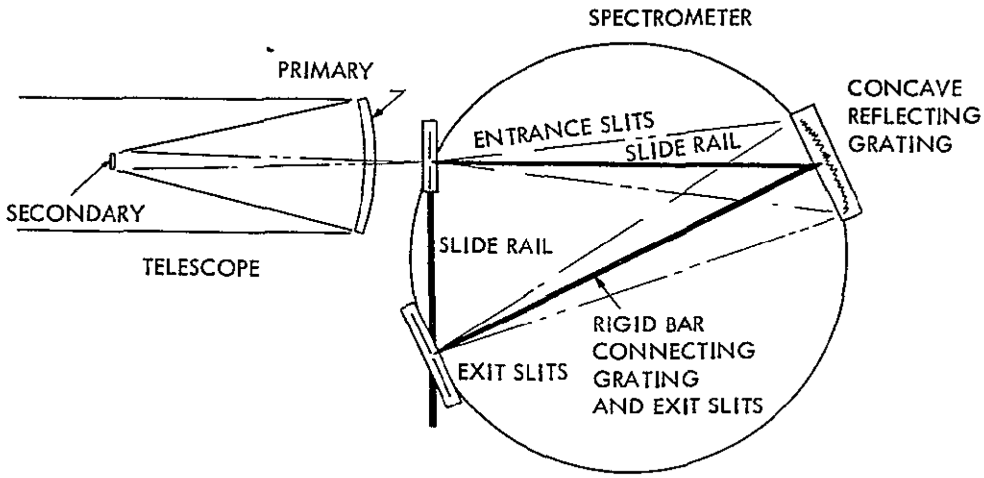

Figure 4-23 Rowland Mounting of a Curved Grating UV Spectrometer

The Paschen mounting on a Rowland circle, the Rowland mounting, or the more compact Eagle mounting could be considered in a spectrometer for planetary atmospheric study The Eagle mounting, as shown in Figure 4-24 is also based on the Rowland circle but on only a short, lower chord of it The entrance and exit slits are placed as close as possible to each other in the Eagle mounting This means that the detector must be placed just behind the primary mirror The focal point of the telescope should be placed about 6 inches behind the rear surface of the primary

The choice of mounting is dictated by the required spectral range of the instrument and the resolution requirements in addition to packaging limitations The Eagle mounting will be assumed for the following discussion of UV and visible spectrometers for the 0 2 and 0 8 micron range

Part of the problem of mounting stems from the requirements of the photodetectors needed to cover the spectral range of interest For wide spectral range an array of phototubes would be required

Each sensor is placed behind its own slit, and they would be operated in parallel It is assumed that all of the required photosensors needed to cover the wavelengths of interest could be housed in the same instrument and the entire spectral region from 0 2 to 0 8 microns could be covered by the same optics and diffraction grating

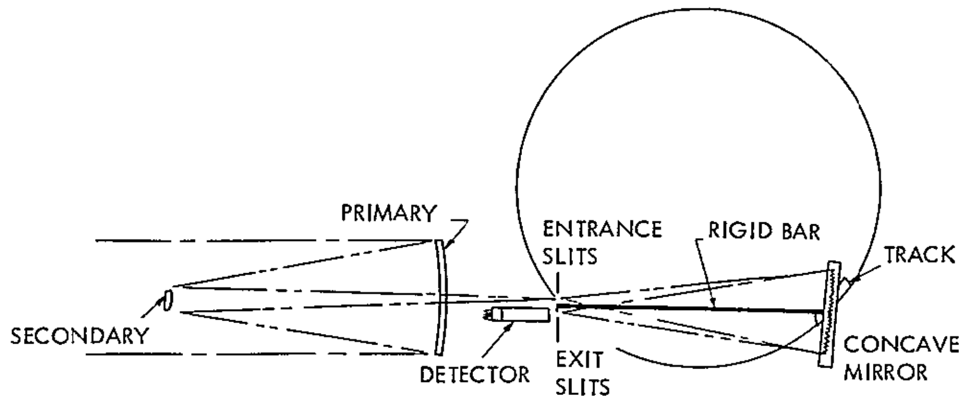

Figure 4-24 Eagle Mounting of a Curved Crystal Spectrometer

An example of a combined range type instrument is the Princeton OAO telescope and spectrograph package shown in Figure 4-25 This package consists of a Cassegrain telescope and fused-silica 2400 ℓ/mm curved grating on a Rowland circle Two sets of photodetectors are used covering the 750 to 1500 A^0 and the 1500 to 3000 A^0 region with a 0 $1A^0$ resolution

An earlier OAO package, shown in Figure 4-26, used six photodetectors with a combined spectrometer mirror (Ebert type reflection mount) as discussed above

An early rocket-borne ultraviolet spectrometer of the Ebert type by Perkin-Elmer is shown in Figure 4-27 The instrument did not use a telescope to provide a narrow view angle It covered the region between 875 to 1600 A^0 and the 1750 to 3000 A^0 region with separate photosensors A 6" Ebert mirror was used The total package weighed 46 kg

4 2 6 2 Visible and Ultraviolet Detectors

Discrete detectors for the visible and ultraviolet portions of the optical spectrum are almost universally of the photoemissive type However, the data presented in Table 4-6 indicate that silicon photodiodes can probably be used in the longwave visible portion of the spectrum in place of the more

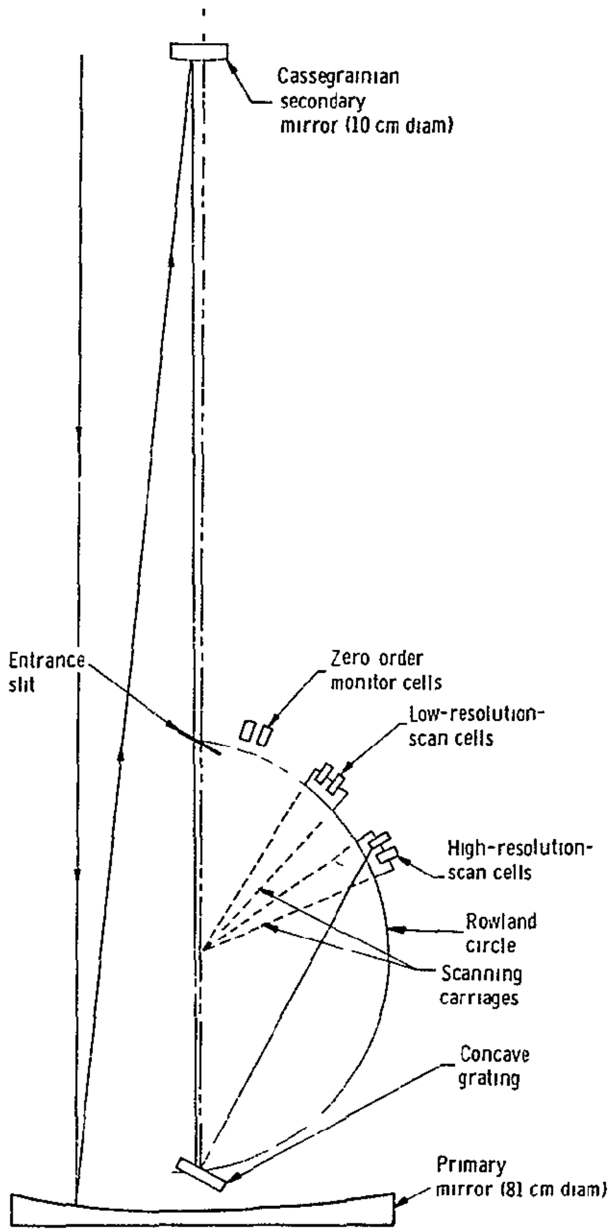

Optical layout of the telescope and spectrograph in the Princeton OAO Experiment

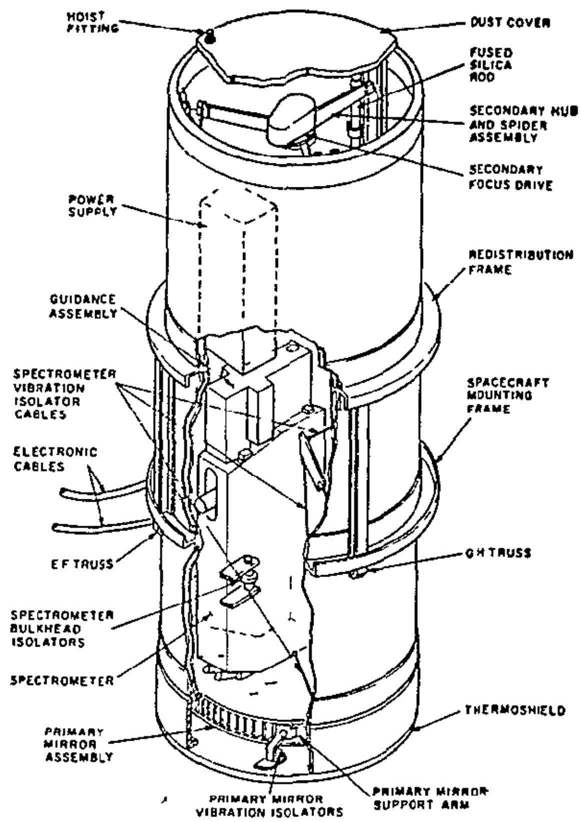

Mechanical arrangement of components in the Princeton Experiment Package The whole assembly fits into the central well of the OAO

Figure 4-25. Princeton OAO Experiment

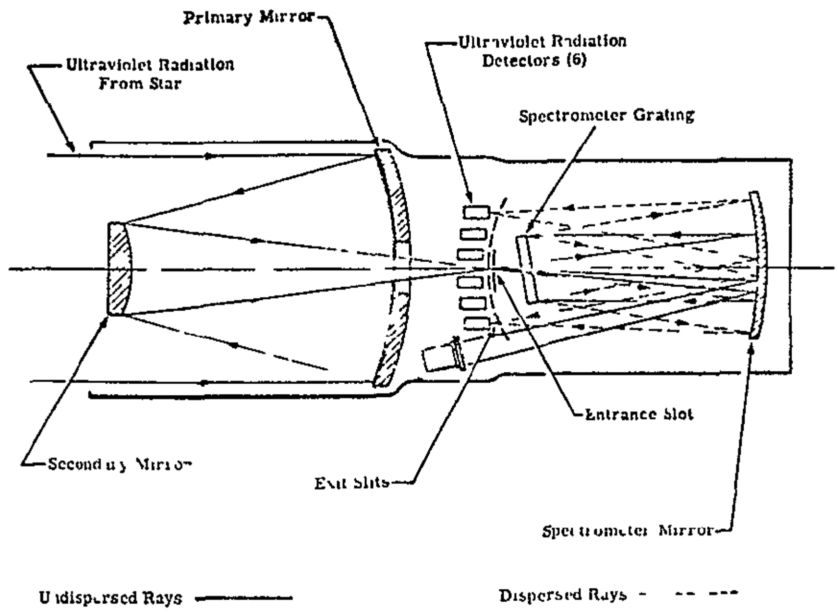

Optical diagram for the OAO Goddard Experiment Package In this Cassegrainian configuration the distance between the primary and secondary mirrors, is roughly 107 centimeters

Figure 4-26 Goddard OAO Experiment

complex photoemissive detectors The performance of photodiodes is significant not only for their competition with photoemissive detectors in the long wavelength visible spectrum but also because under certain conditions they can be shown to exceed the theoretical performance limits of discrete detectors shown in Table 4-6 The effect which produces the improved performance is commonly referred to as avalanche multiplication such that a single photon event produces a multitude or avalanche of output electrons rather than a single electron or none at all When operated in an avalanche mode, photodiodes have been reported with a D^* as high as 3×10^{13} which is several orders of magnitude above the performance obtainable with the best IR detectors This type of performance probably represents the near term maximum attainable D^* for solid state detectors since the reported performance is only on a laboratory basis It does not represent attainable performance of deliverable detectors

Aside from photovoltaic detectors, the most sensitive and commonly used discrete detector in the visible and ultraviolet is the photoemissive detector with gain which is commonly referred to as a photomultiplier In a sense it is quite similar to an avalanche photodiode since a single photon event may produce as many as 10^6 output electrons In operation however,

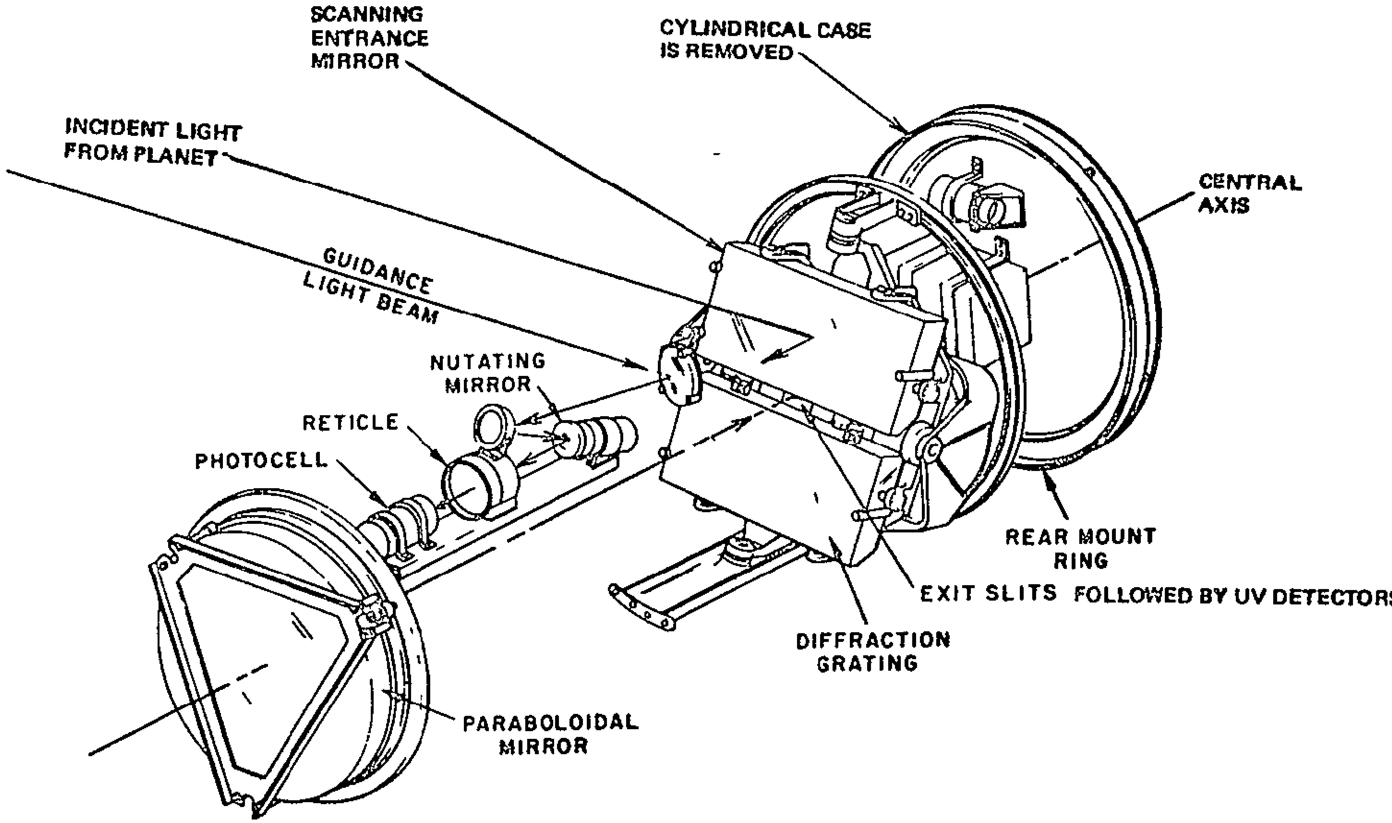

Figure 4-27. Rocket-Borne Ultraviolet Spectrometer

it is substantially different from an avalanche photodiode in that it can be shown that the signal-to-noise ratio at the output of a photomultiplier is always less than the signal-to-noise ratio at the detector cathode The difference is a function of the photomultiplier multiplication ratio

The performance of photomultipliers is described in a variety of ways In principle, performance canbe described in much the same way as photoconductive and photovoltaic devices, that is in terms of specific detectivity, D , in the form

$$D' = \frac{\sqrt{A_D \Delta f}}{NEP} \qquad (132)$$

where

A_D is the photocathode sensitive area

Δf is the equivalent noise bandwidth

NEP is the input power required to produce an output signal-to-noise ratio of one in a unit bandwidth

However, photomultiplier tube performance is not generally specified in terms of the cathode area so that D* is not used as a figure-of-merit for photomultipliers However, when it is computed it generally results in values of D* of the order of 5×10^{14} at wavelengths near peak response The improved performance of photomultipliers over IR detectors is indicative of the fact that they are generally background or photon shot noise limited

The noise equivalent input power is sometimes used as a figure-of-merit for photomultipliers For background noise-limited operation the minimum monochromatic power which a photocathode can detect is that which produces a signal current equal to the photon noise shot current which is assumed to have a Poisson probability density function For background limited operation the photon noise current can be shown to be given by

$$I_{RMS} = 2eI_{dc} \Delta f \qquad (133)$$

where

I_{dc} is the steady component of the signal resulting from photon conversion

e is the charge of the electron

Δf is the equivalent noise bandwidth

The signal current is generated by the arrival of photons and is defined as

$$I_{dc} = \bar{n} Q_e e \tag{134}$$

where

$\bar{n}$ is the average rate of photon arrival

Q_e is the quantum efficiency of the photocathode

Therefore

$$I_{RMS} = \sqrt{2e^2 Q_e \bar{n} \Delta f} \tag{135}$$

the product $\frac{Q_e e}{h\nu}$ has the units of amperes per watt where

h is Planck's constant

ν is the frequency of the radiation

Therefore P watts of signal can be converted into a signal current

$$I_{dc} = P \frac{Q_e e}{h\nu} \text{ amperes} \tag{136}$$

The same result can be obtained from the product of the average photon rate and the energy of a photon in the form

$$P = \bar{n} h\nu \text{ watts} \tag{137}$$

and substituting for $\bar{n}$

Equating the signal current to the shot noise current gives

$$P = h\nu \sqrt{\frac{2 n \Delta f}{Q_e}} \tag{138}$$

and the noise equivalent power, defined in terms of a unit bandwidth is

$$NEP = \frac{P}{\sqrt{\Delta f}} = h\nu \sqrt{\frac{2\pi}{Q_e}} \frac{\text{watts}}{\sqrt{\text{cps}}} \tag{139}$$

This expression is sometimes convenient if the only data available on the photocathode is the quantum efficiency as a function of spectral wavelength

The most common method of describing photomultiplier performance is in terms of the responsivity The responsivity of a detector with a current output is by definition the current output in terms of the signal power input, that is

$$R = \frac{I_{dc}}{P_{in}} \frac{\text{amps}}{\text{watt}} \tag{140}$$

or in photometric units in amperes per lumen While the responsivity is meaningful, some caution must be exercised in its use since the responsivity may be in terms of the cathode responsivity or the anode responsivity, output measured The two quantities are related by the current gain of the multiplier chain but are modified by internal noise contributions of the multiplier By definition of a photon noise limited photocathode the signal to noise ratio at the output of the cathode is

$$\left(\frac{S}{N}\right)_K = \frac{I_s^{\,2}}{I_N^{\,2}} \tag{141}$$

where

I_s is the signal current

I_N is the noise current

But for photon noise limited operation

$$I_N = \sqrt{2e\, I_s\, \Delta f} \tag{142}$$

so that

$$\left(\frac{S}{N}\right)_K = \frac{I_s}{2e\, \Delta f} \tag{143}$$

For a cathode responsivity of R amperes per watt and a signal of P watts, the cathode signal-to-noise ratio is

$$\left(\frac{S}{N}\right)_K = \frac{P(R)_K}{2e\Delta f} \tag{144}$$

However, in going through the dynode multiplication structure, a decrease in signal-to-noise ratio results. Thus not all of the electrons which leave the cathode are captured by the first dynode so that the signal-to-noise ratio at the input to the first dynode is reduced by the capture efficiency, ϵ, to

$$\left(\frac{S}{N}\right)_1 = \epsilon \left(\frac{S}{N}\right)_K \quad \epsilon \leq 1 \tag{145}$$

At the first dynode, a secondary emission process occurs such that each incident electron liberates an average of σ electrons. The secondary emission process is assumed to be a Poisson process so that the signal and noise components are similar to the cathode emission. The noise component of the dynode is assumed independent of the cathode noise so that the two noise components can be added

$$I_N^{\,2} = (I_{N1})^2 + (I_{N2})^2 \tag{146}$$

which upon substitution and reduction becomes

$$(I_N)^2 = 2e\Delta f I_2 (1 + \sigma) \tag{147}$$

and the signal-to-noise ratio out of the first dynode becomes

$$\left(\frac{S}{N}\right)_{01} = \left(\frac{\sigma}{1 + \sigma}\right) \left(\frac{S}{N}\right)_1 = \epsilon \left(\frac{\sigma}{1 + \sigma}\right) \left(\frac{S}{N}\right)_K \tag{148}$$

If the process is repeated for each of the dynodes and the electron multiplication σ, is assumed equal for all stages it can be shown that the anode signal-to-noise ratio approaches

$$\left(\frac{S}{N}\right)_a = \epsilon \frac{(\sigma - 1)}{\sigma} \left(\frac{S}{N}\right)_K \tag{149}$$

for a large number of dynodes. Typical values for the design parameters are $\sigma = 4$ and $\epsilon = 0.9$ so that the multiplication process does reduce the output signal-to-noise ratio by approximately 30 percent. In applying measured data to the computation of signal-to-noise ratio, care should be taken to distinguish between cathode and output responsivities

The photosensitive materials used in photocathodes exhibit broad but finite spectral response characteristics For photoemission to occur, the incident photons must provide enough energy to raise the energy level above the conduction level and the surface barrier potential before the electrons are ejected Photocathodes therefore exhibit a long wavelength threshold

At wavelengths shorter than the threshold, the quantum efficiency rises to a maximum until the optical absorption of the photo surface and any window material causes the available energy to decrease

The limits on spectral bandwidth have resulted in a large variety of photomultiplier tube types Typical spectral response characteristics are shown in Figure 4-28 The basic differences among tubes are in the photocathode type and the window material used The long wavelength cutoff for photoemitters is approximately 1 2 μ although high responsivity is generally limited to approximately 0 7μ In the ultraviolet region, normal glass envelopes cause a radiation cutoff at approximately 0 35μ Thin, special purpose windows cutoff at approximately 0 22μ while fused-silica glass extends the cutoff to approximately 0 165μ Special purpose UV tubes are available with lithium fluoride windows which extend the cutoff to as low as 0 1μ

4 2 6 3 Visible and Ultraviolet Spectrometer Scaling Law

Basic optical system scaling laws for weight, volume and power are given in Paragraph 4 2 4 3 Where appropriate, the weights and volumes of additional optical components are given for specific scaling laws Certain general scaling laws for the electronics associated with non-image forming visible and UV systems can be established for weight and volume estimating purposes The following general considerations apply

1 Visible and UV detectors are usually of the photomultiplier tube type If photovoltaic detectors are used in the visible, then they would have the same characteristics as IR detectors Since photomultipliers have internal gain and require a high voltage power supply for operation they are generally somewhat heavier For estimating purposes the photomultiplier is assumed equivalent to commercially available tubes which weigh approximately 0 1 kg Some difficulties usually arise in obtaining high level packaging density of photomultipliers in the image plane It is common practice to use transfer optics from the image plane to a convenient detector location Fiber optics are frequently used and add approximately 30 percent to the detector system weight A realistic estimate for a photomultiplier with transfer optics is therefore 0 13 kg per detector

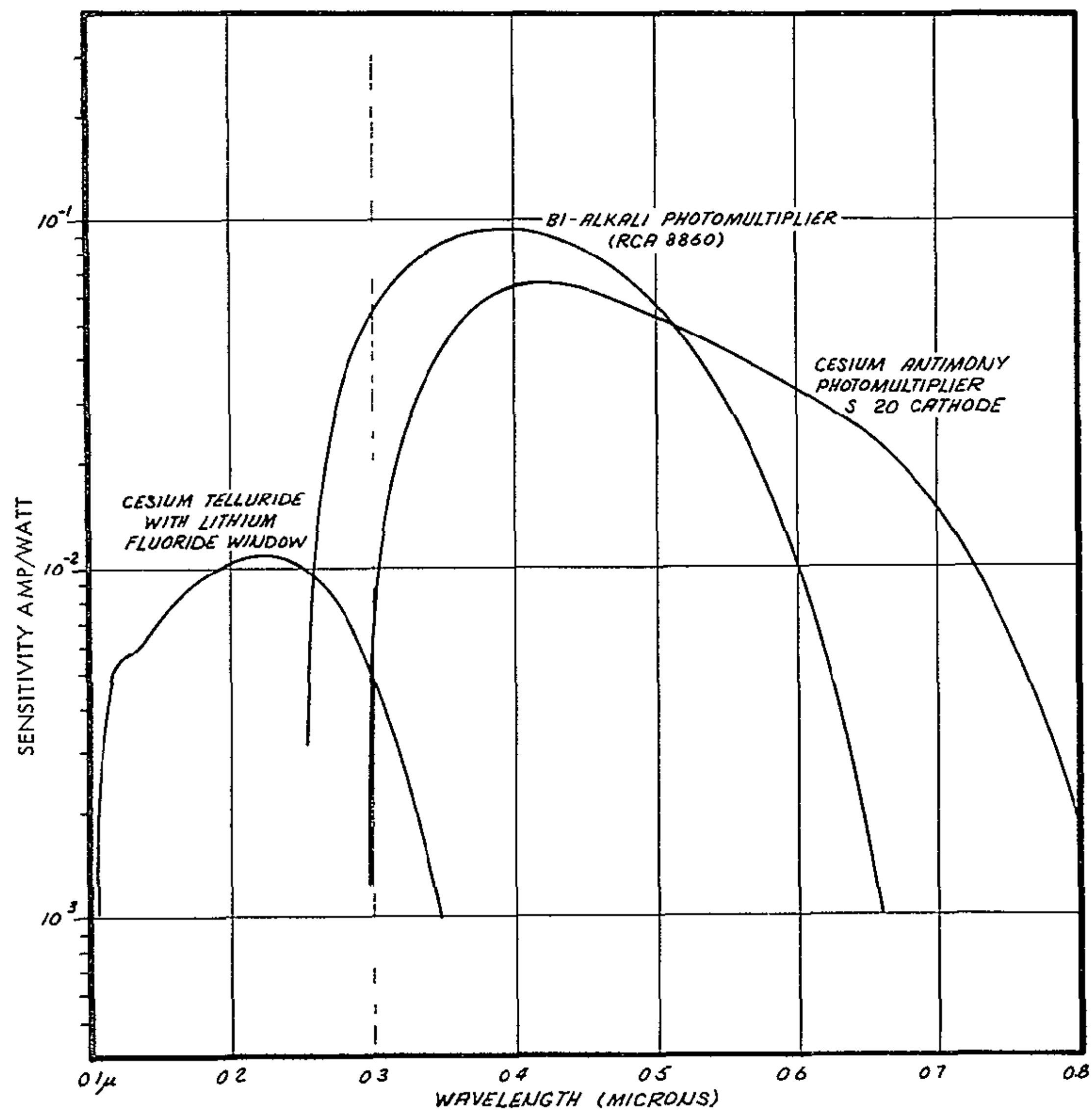

Figure 4-28 Spectral Response of Photomultipliers

2 Reference sources are frequently used with spectrometers as gain control devices and are a necessity for absolute radiometers The source may be external, with the sun being the most frequently used reference For absolute radiometry an internal, calibrated reference source is used The two types of sources are not essentially different from the point of view of weight scaling so that a weight penalty 0 5 kg is used

3 Auxiliary components such as field lenses, beamsplitters, filter wheels, drive motors, etc , are generally lightweight devices The design of auxiliary components is usually optimized after basic design of the instrument is established with such factors as duty cycle, aging characteristics, etc , having an effect on overall system weight or volume For estimating purposes the weights given in Table 4 8 are assumed although many of the estimates may be in error by as much as 50 percent This is not a severe shortcoming, however, since with few exceptions the components are lightweight

4 The electronics at the output of the instrument depend upon the function performed and the detector type used Modern microcircuit technology permits functional packaging of the order of 005 kg per function and resulting packing densities of the order of 370 kg per cubic meter Thus an electronic package which performs ten functions such as amplification in five stages, automatic gain control, detection and conversions, would weigh approximately 05 kg and occupy a volume of 1 4 x 10^{-4} m^3

5 Solid state high voltage power supplies weigh approximately 10 times as much as microminiature circuits but have packing densities which are approximately twice as high A typical high voltage power supply with rectifiers, inverters and regulators would then be sized by power drain and the degree of regulation A typical 100 milliampere high voltage supply for a photomultiplier would have 15 functions at 05 kg per function or a weight of 0 75 kg The volume would then be $10^{-3}m^3$

The first step in the scaling law is to determine the telescope parameters to meet the required signal-to-noise ratio and the spectral resolution requirements

Table 4-10 Weight Estimation for Auxiliary Components of Visible and UV Optical Instruments

Function	Weight	Volume
Photomultiplier (with fiber optics transfer)	0 13 kg/detector	$2 \times 10^{-4} m^3$ **
Reference Source	0 5 kg	$7\ 6 \times 10^{-4} m^3$ **
Gratings, Mirrors, Field Lenses, etc	$4 \times 10^2\ \ell^3$kg *****	$\frac{\ell^3}{6}$
Filter	0 25 kg/channel	***
Beamsplitter	0 05 kg/channel	***
Rotary Filter Drives and Auxiliary Motors	0 2 kg/channel	***
Mirror Scan Drive Motor (for scanning mirror)	$0\ 2\ (0\ 1 + D_p)$ ****	***
Electronics	0 05 kg/channel	$1\ 4 \times 10^{-4} m^3$ *
H V Power Supply	0 75 kg/10 channels	$1 \times 10^{-3} m^3$ **

* Microminiature Circuit Package — $3\ 7 \times 10^2$ kg/m^3 (25 lbs/ft^3)

** Solid State Distributed Circuit Package — $7\ 4 \times 10^2$ kg/m^3 (50 lb/ft^3)

*** Included in Volume of Primary Telescope

**** D_p is the Primary Optical Aperture Diameter in Meters

***** ℓ is the Diameter or Width in Meters

In terms of the input power, the signal-to-noise ratio is

$$\frac{S}{N} = \int_{\Delta\lambda} \frac{R(\lambda)\, P(\lambda)\, d\lambda}{2e\Delta f} \qquad (150)$$

and for narrow spectral bandwidth, this is given approximately by

$$\frac{S}{N} = \frac{\overline{R}(\lambda)\, \overline{P}(\lambda)\Delta\lambda}{2e\Delta f} \qquad (151)$$

where

$\overline{R}(\lambda)$ is the responsivity in amperes per watt

$\overline{P}(\lambda)\Delta\lambda$ is the available radiant power at the detector in wavelength interval $\Delta\lambda$

e is the charge on the electron $= 1.6 \times 10^{-19}$ coulomb

Δf is the electrical bandwidth

In terms of the aperture diameter, D_c, angular resolution ϕ and integration time, t, this can be expressed as

$$\frac{S}{N} = \eta D_c \Delta\phi \quad \frac{R\lambda \Delta\phi\, I\lambda \Delta\lambda\, t}{2e} \qquad (152)$$

where $I_\lambda \Delta_\lambda$ is the available spectral radiance determined from

$$I_\lambda \; \Delta_\lambda = H(\lambda)\; \rho\,(\lambda) \cos\,\theta\, \Delta\lambda \qquad (153)$$

where

$H(\lambda)$ is the solar constant at the planet of interest in the wavelength region of measurement

$\rho(\lambda)$ is the albedo from Tables 4-1 and 4-2

θ is the observation angle shown in Figure 4-37 a is the exponent determined by planet type

a = 1 for planets without atmospheres

a = 2 for planets with atmospheres.

The value of the efficiency, η, which accounts for all losses from input to signal output is taken as 0 25

An alternative expression given in Reference 2, is useful when the quantum efficiency of the photomultiplier is given rather than the responsivity In terms of the quantum efficiency, the signal-to-noise ratio is

$$\frac{S}{N} = 3\ 3 \times 10^{11} D_c \, \Delta\phi \left[\frac{Q_e\ (C_p f)\ \Delta\phi}{\omega}\right]^{1/2} \tag{154}$$

where

$\frac{1}{\omega}$ is the dwell time and is equivalent to the integration time

$(C_p f)$ is the available spectral radiance and is computed for narrow spectral bandwidth as indicated above That is, $(C_p f)$ can be replaced by $(C_p f) = I_\lambda \, \Delta\lambda$

The second step is to determine the spectrometer parameters based on the spectral resolution required and the spectral range The Eagle mount is assumed The mirrors and grating are sized and the weight estimated assuming that each is a mirror with scale weight given in Table 4-12 The volume required for the spectrometer is generally high because the aperture ratio of spectrometers is generally high The high aperture ratio results from the minimum spatial requirements for the collimation of the incident flux, the formation of the far field pattern of the diffraction grating, and the focal ratio of the collecting optics True aperture ratios for collimators are highly dependent upon the size of the grating but are generally in the range of 4 to 15 With folding and optimum design, the overall length can generally be reduced to one third of the equivalent focal length This results in a length approximately equivalent to

$$L = \frac{1}{3} f = \frac{ND}{3} \tag{155}$$

where

N is the aperture ratio of the spectrometer

D is the width of the grating

The spectrometer is assumed to be packaged in a cylindrical structure The diameter of the spectrometer housing is in the range of 1 5D to 2 5D depending upon the type For an Ebert mirror the diameter would be 2 5D but for a dioptric spectrometer it would be 1 5D For estimating purposes a value of 2D is a useful average value

The structure weight to hold the spectrometer can be estimated as a shell structure using the same procedure for telescope structures given in Table 4-4

4 2 6 4 Support Requirements

The procedure for estimating spectrometer support requirements is summarized in Figure 4-29

Data Rate In a photomultiplier, each photoelectron emitted from the photocathode undergoes cascade multiplication inside the tube and comes out of the tube as a pulse of many electrons If the photoelectrons were multiplied by this process to form pulses of exactly equal sizes, they would contribute equally to the signal current, but in actual photomultipliers the amount of multiplication is very different from one photoelectron to another Consequently, the stream of pulses coming out of a photomultiplier tube has a very broad range of amplitudes, some of the pulses contributing ten times as much to the photocurrent as others Since the pulses are not of equal size, it is evident that the signal-to-noise performance of a photomultiplier will be lower when used in combination with an ordinary current measuring or charge collecting (condenser-integrator) system than when used in a system that counts the pulses with equal weight regardless of these sizes However, the current measuring method is simpler to implement Because of the variation in emission rate with source intensity, a pulse counting technique would require a system of high capacity, high speed counters which become somewhat impractical for spacecraft applications So far as is known, a pulse counting system has not yet been implemented in a space system For this reason an analog integrator is assumed The data rate is then inversely proportional to the integration time and directly proportional to the number of channels and the dynamic range of the instrument

$$DR = \frac{nL}{t} \tag{156}$$

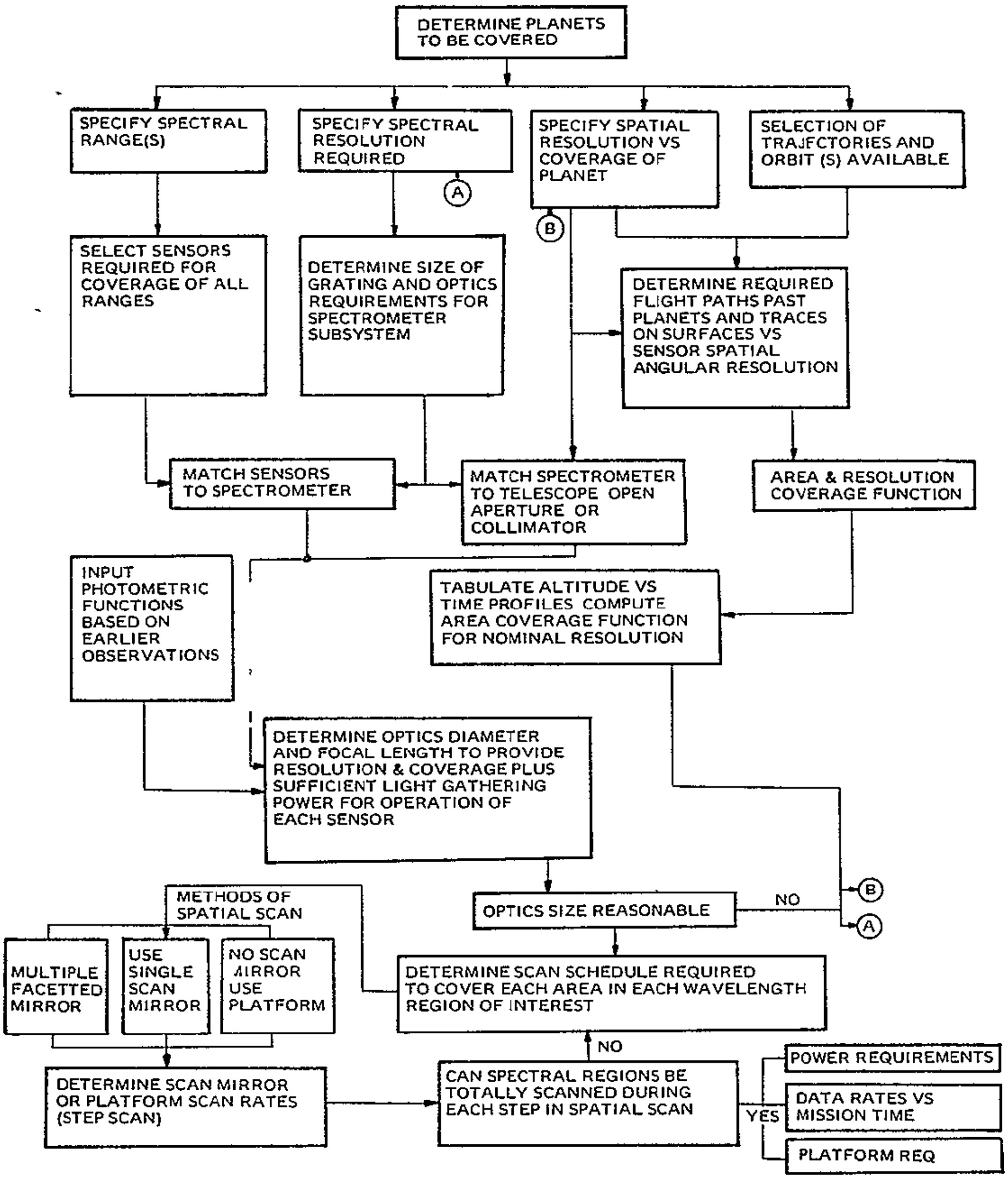

Figure 4-29 UV Spectrometer Design Logic Flow Diagram

where

n is the number of channels

L is the dynamic range

t is the integration time

The dynamic range requirements are highly dependent upon the function of the instrument but for estimating purposes a value of 100 to one is reasonable so that a maximum of seven bits per sample is assumed

If dynamic variations in the spectrum are of interest then a sampling rate to meet dynamic measurements must be established The data rate is then the product of the number of channels, the dynamic range and the sampling rate

Power Requirements The power for the spectroscopic instrument is of three types

1 The power to operate an external scan mirror if one is used

2 The power to operate the spectrometer scan drive if one is used

3 The power to operate the detector electronics

Power requirements for Types 1 and 2 can be obtained from Table 4-5

The power required to operate a photomultiplier is relatively modest For estimating purposes a value of 1 0 watt per detector is useful The estimate includes the high voltage power supply so that it would tend to be low for a single detector Therefore if an array of up to five photomultipliers is used, an additional power allowance of 2 watts should be made for the high voltage power supply

Stabilization If the angular resolution of the instantaneous field of view of the optics is given by

$$\phi = \tan^{-1}\left[\frac{W}{2H}\right] \tag{157}$$

which is approximately

$$\phi \approx \frac{W}{2H} \tag{158}$$

for small angles, and the time available for sampling is taken as the time in which the field of view traverses a resolution interval, W, then

$$\phi = \frac{t\ V_g}{2H} \tag{159}$$

since

$$W = tV_g \tag{160}$$

The stabilization of the optical axis in terms of field of view rate is

$$\phi' = \frac{\phi}{t} = \frac{V_g}{2H} \text{ radians/sec} \tag{161}$$

For small fields of view at long ranges this requirement could pose stringent penalties since observation times may be long

4 2 7 Polarimeter

A polarimeter is basically a telescope, an optical analyzer and one or more detectors The scaling law for this type of instrumentation is identical to that for a spectrometer with the optical analyzer package replacing the spectrometer at the output of the telescope Depending upon the spectral region, the detector would be photoconductive, photovoltaic, or a photomultiplier

The analyzer may be made in a variety of forms depending upon the application The most common forms of analyzers are based on birefringent crystals cut into various prismatic shapes The illumination of the prism must be collimated and the polarized light is focused on an exit slit to the detector To measure the polarization of the input illumination it is simple to rotate the prism to change the plane of polarization For scaling purposes the analyzer can be considered equivalent to the mirror assemblies of approximately 10 cm diameter The weight can then be established from Table 4-8. The scan motor is a low power device of the type used to drive a filter wheel The other scaling parameters are identical to a spectrometer with an equivalent aperture ratio of 5

The logic diagram for a spectrometer shown in Figure 4-29 can be used for a polarimeter

4 3 IMAGE FORMING OPTICAL SENSORS

4 3 1 Introduction

Any radiant energy detection system which results in a two dimensional geometric array of variation in radiant intensity can be considered as an image forming system For descriptive purposes, however, it is common practice to distinguish among the many possible types of image forming systems according to the spatial resolution and the method of illuminating the image plane Thus high resolution systems with large fields of view require detection mechanisms which are continuously distributed over the image plane as in a photographic emulsion or television pickup tube Low resolution systems with large fields of view have an array of individual detectors in the image plane Each detector has an output Image forming sensors with narrow fields of view generate an image by scanning the narrow field over a wide angular field with one or at most a limited number of individual detectors in the image plane The latter two types have resolutions which are limited by the smallest discrete detector which can be built The detector technology is identical to discrete detectors discussed previously so that only the limitations imposed by detector array size and/or mechanical scanning are considered

There is relatively little difference between the theoretical performance of photographic and television image forming sensor systems An adequate description of photographic systems is contained in Reference 2 so that only television systems are discussed here

Scanning systems are of many types depending upon their function They may be scanning radiometers, thermal mappers, scanning spectrometers and photometers and multispectral mapping systems However, all of the multispectral point detector scanning systems can be described by a single general scaling law with minor variations imposed by spectral band or function

4 3 2 Television Systems

4 3 2 1 Design and Performance

In describing the performance of television systems, it would be desirable to isolate the performance of the detection mechanism, as with discrete detectors, and establish a figure of merit to describe performance But in much the same way that the performance of a photographic emulsion cannot be separated from the method of developing the latent image, so the performance of a television cannot be specified separately from the method of reading the image information from the photosensitive surface Consideration of the detection mechanism used in wideangle image forming systems indicates the reason for this With discrete detectors such as IR cell detectors the output is in the form of an electrical signal produced with negligible delay at the output of the sensor With wide angle image forming systems the detected information is stored at the detection surface and is only available as an output after suitable processing Overall performance of image forming systems can therefore not be described accurately except as a complete system

Image forming sensors, whether photographic or photoelectric can all be specified on a common basis provided that specific definitions are established for the detection process Once a common method of specifying detection is established the highly developed techniques for photographic system design are applicable, at least in principle, to any image forming system but are particularly useful in television design The reduction of image forming design to a common set of parameters and techniques has been accomplished by O H Schade and described in detail in References 8 and 9 Schade had developed a unified approach to imaging system evaluation The overall system performance, defined in terms of a resolving power function is based on modulation transfer functions and is determined by the granularity of the image forming stage and the transfer functions which are required to convert image forming light into either an electrical signal or a permanent record

The crux of the approach is the definition of a sampling area, $\bar{a}$, in the image plane and a statistical description of the variation of particle density in the sampling area as a function of image coordinates In a television camera the input radiant energy is directed by a lens to an imaging surface The radiant energy excites electrons in the photosensitive surface and the array of stored charges in the surface is the latent image of the camera The latent image is extracted by an unmodulated electron stream, suitably focused, which "reads" the stored charge level by absorption of electrons as it neutralizes the stored charges The modulation of the reading beam is extracted, amplified and transferred out of the camera as an electronic signal for subsequent display. The conversion of the input radiant energy to equivalent charge in the storage surface is subject to statistical variations so that signal amplitude is subject to statistical fluctuations which is noise

A photographic emulsion functions in essentially the same manner since the input radiant energy releases electrons in the emulsion which are converted and stored as a silver atom image. In a subsequent development process the silver atoms are amplified to much larger grain, forming a visible image Again the conversion process is subject to statistical variations resulting in granularity noise

On this basis the problem of image formation is reduced in fundamental terms to a decision process based on the number of signal units produced in the sampling area compared to the number of noise units in the same area This is commonly referred to as the absolute signal-to-noise ratio in the sampling area In the conversion or detection process the number of signal units is given by

$$\bar{n}_s = \bar{n}_{s(1)} \bar{a} \qquad (1)$$

where $\bar{n}_{s(1)}$ is the signal density per unit area caused by exposure to the radiant energy and $\bar{a}$ is the sampling area The quantities $\bar{n}_{s(1)}$ and $\bar{a}$ are the essential parameters common to both photographic and television systems since it is precisely variations in these quantities which result in apparent differences in the resolution performance of the two processes Likewise, they account in large measure for the variations of performance among the several types of TV pickup or camera tubes

The statistics of the conversion process are generally difficult to describe in simple terms but for a random particle source it can be shown that the rms deviation in the signal unit count, that is the noise density, is never less than

$$n_{n(1)} = \sqrt{n_{s(1)}} \tag{2}$$

so that the absolute signal-to-noise ratio in unit area is

$$R_1 = \frac{n_{s(1)}}{n_{n(1)}} = \left(n_{s(1)}\right)^{1/2} \tag{3}$$

which is characteristic of Poisson shot noise If excess noise is present such as "fog" density in a photographic emulsion or dark currents in a TV system the absolute signal-to-noise ratio is given by

$$R_{(1)} = \frac{n_{s(1)}}{\left(n_{s(1)} + n_{d(1)}\right)^{1/2}} \tag{4}$$

where $n_{d(1)}$ is the excess particle density which is independent of signal density

These fundamentals can be extended directly to the concept of a difference signal-to-noise ratio which is generally more meaningful in describing resolution performance for a given contrast or modulation level, m_o in the object plane It can be shown that the difference signal, the mean signal and the modulation are related by

$$\Delta n_{s(1)} = m n_{s(1)} \tag{5}$$

where m is the modulation

Based on these fundamental concepts Schade develops a general method of comparison for photographic emulsions and TV photosensitive surfaces In order to use the approach it is necessary to review the meaningful parameters of the charge storage surfaces of the detection process Under the assumption of constant current charge and discharge of the storage surface the charge per unit area $q_{(1)}$ is given by

$$q_{(1)} = C_{(1)} V = \bar{\imath}_{s(1)} t \tag{6}$$

and the electron density is given by

$$n_{(1)} = q_{(1)}/q_e$$

where

$q_{(1)}$ = charge/mm^2 (coulombs)

$C_{(1)}$ = storage capacitance/mm^2 (farads)

V = potential at the storage surface

$\bar{i}_{s(1)}$ = mean current density per mm^2 during time t

q_e = charge of the electron = 1 6 x 10^{-19} coulombs

The electron or charge density, $n_{(1)}$, is built up during an exposure time t = t_e The charge potential is read out in a time, t_f, which may be larger, equal to, or smaller than t_e but is a characteristic system parameter since maximum signal extraction is determined by the level to which the stored change is neutralized Basic limitations are imposed by the readout process since the following two effects are inherent

1 The maximum charge potential which can be read out by a low velocity electron beam is limited to Vmax = 6 volts due to secondary emission and electron reflection

2 The value of the read-out beam current is limited to values less than 200 nanoamperes because of the increasing spread of electron velocities with beam current density

Therefore, for high definition storage surfaces where a high level of electron density is required, the only free parameters are the unit capacitance and the readout time The combination of large unit capacitance and large surface area leads naturally to read-out times which are of the order of several seconds Based on these considerations and the definition of an equivalent noise particle density of Kodak type 4404 high definition emulsion, Schade has developed the data given in Table 4-11

The noise equivalent sampling area of the 4404 emulsion has a diameter of 2 microns Because the equivalent potential spread of a point charge

Table 4-11 Approximate Characteristics and Minimum Readout Times of Charge Storage Surfaces ($V = V_{max}$, 90% Discharge)

Type of Surface	Equiv Thickness (microns)	C (pF)	$n_{s(1)}$/volt	Charge Potential Vmax	Readout Time* (Sec) ($A = 1\ cm^2$)	($A = 25\ cm^2$)
4404 Film	2	8	$5X10^7$	4 25	0 0345	0 86
ASOS photoconductor (Vidicon)	1	160	$1X10^9$	6	0 385	9 60
		80	$5X10^8$	6	0 192	4 8
Porous photo-conductor (Vidicon)	4	10	$6\ 25X10^7$	6	0. 024	0 60
Plumbicon	14 3	3 7	$2\ 3X10^7$	6	0 0089	Insuff. storage
S E C (Westinghouse)	12	0 8	$5X10^6$	6	0. 0019	0 0475
Glass Target Image Orthicon	25	0 35	$2\ 2X10^6$	4	0 00158	0 0395

*$t/C = 24$ for $V_{max} = 6V$

$t/C = 45$ for $V_{max} = 4V$

on an electrical storage surface is approximately equal to its thickness, d, an electrical storage surface having a thickness of 2 microns has the same sampling area as the 4404 emulsion (The beam senses the potential and not the charge itself)

Table 4-11 compares the constants of various charge storage surfaces with these reference values

The small thickness (d) of ASOS (antimony sulfide — antimony oxi-sulfide) and porous photoconductors used in vidicons indicates equivalent sampling areas comparable to or smaller than the 4404 emulsion and high resolving powers (for the surface itself) because the electron densities $\left(n_{s(1)} V_{max}\right)$ exceed that of the highest definition aerial film

The minimum read-out time (t_f) computed for a 90% discharge is given for a 1 cm^2 area (one-inch vidicons and similar television camera tubes) and for the 25-cm^2 area of developmental high-definition vidicons

The last three surfaces listed in Table 4-11 have small capacitances and are thus particularly suited for live pickup in standard television systems because an adequate discharge can be obtained in 1/30 second Their resolving power is lower, however, because of the greatest thickness and lower electron density

It is necessary to develop a methodology of describing the performance of an imaging system using specific parameters This can be accomplished in two essential steps which Schade has followed in defining a resolving power function in terms of state-of-the-art in photosensitive detectors, available image forming light and the modulation transfer functions of the components of the camera system Before applying the method developed by Schade there is one basic difficulty which must be reconciled As indicated previously, the principle of signal unit counting in a unit area is the foundation of the approach This leads naturally to the process by which radiant energy is converted to an equivalent charge density at the detector The common unit of intensity is the exposure, E, in meter-candle seconds, a photometric quantity which involves the response of the human eye through the so-called standard observer curve for photopic vision The candle and lumen are sufficiently imprecise that they are difficult to work with when attempting to define charge density at the detector

A natural unit of energy absorption at the detector is the photon which is a true radiometric quantity The difficulty arises in converting the known photometric values of a planet in the form of broad spectral band luminous intensity to an equivalent photon arrival rate at the detector surface which has a sensitivity which is also dependent on the spectral content of the illumination This follows from the fact that the energy of a photon is spectrally dependent since

$$E_{(\lambda)} = h\nu = \frac{1\ 964 \times 10^{-12}}{\lambda} \text{ ergs} \tag{7}$$

where λ is the wavelength in microns

h is Planck's constant

ν is the frequency

To at least partially reconcile the conflict between photometric and radiometric units, it is common practice to relate the exposure in meter-candle seconds to an incident monochromatic energy, U_{λ}, producing the same effect at a particular wavelength λ This involves rather tedious numerical integration of the products of the normalized standard observer curve and the relative energy distribution of the illuminant as well as the product of the relative spectral sensitivity of the detector and the spectral distribution of the illuminant Under very restricted and partially artificial conditions, this has been accomplished under the assumption of a daylight illuminant equivalent to a 5000 deg K black body and a detector spectral sensitivity equivalent to the standard response curve of the eye (standard observer or standard luminosity function) Under these assumptions the conversion equation is

$$\bar{E} = \frac{n_{s(1)1}}{7\ 5 \times 10^{9}} \text{ meter candle seconds} \tag{8}$$

where

$\bar{E}$ is the average exposure

$n_{s(1)1}$ is the average incident radiation or photon density per mm^2

This is a useful approximation for planning purposes but it may require adjustment under conditions of changing detector sensitivity or a more precise photometric model of the reflected sunlight The assumption of a spectral response which is equivalent to the standard observer curve is not arbitrary It closely approximates the normalized spectral response of the ASOS photosensitive detector used in high definition return beam vidicons (RBV) which are the most likely tubes for use in high definition TV

It is not within the scope of this study to establish a definitive photometric or radiometric model for the planets It is however, necessary to understand the basic limitation of the approach described here since ultimate system resolution may be limited by exposure or alternatively major changes in system parameters may result from large changes in any assumed simplified photometric model

The absolute limit of the resolution of an imaging sensor is shown by Schade to be established by the photon limit of the incident radiation, that is, the exposure, and the threshold of detection signal to noise ratio of the detection process, under the assumption that the incident photons are converted 100 percent by the photoelectric detection process In terms of exposure or incident energy in the image plane of the sensor, the resolution or resolving power, f_r expressed in standardized units of cycles per millimeter is given by

$$f_r = \frac{1\ 94 \times 10^5\ \overline{E}^{1/2} m_o}{K} \tag{9}$$

where

f_r = resolving power in cycles per mm

$\overline{E}$ = mean level exposure in meter-candle-seconds

m_o = the object modulation determined by the object plane contrast ratio C in the form m_o = C-1/C+1

K = the threshold signal-to-noise ratio

It is understood that the detector is not saturated although it will of necessity have a limited dynamic range

Extensive theoretical and experimental investigations have established the value of the threshold signal-to-noise ratio for visual imagery as

K = 3 6 for a single image

K = 2 for a moving image

Since live pickup of imagery is generally not meaningful for planetary sensing a value of K = 3 6 will be used throughout

The scaling factor 1 94 x 10^5 is not unique It contains all of the spectral variations of the radiant energy and the spectral sensitivity of the detector As a first approximation, it is constant for television camera pick-up tubes using solar illumination For first order design purposes, the value given is adequate

No system can approach the resolution given above since any real system has several sources of degradation A more realistic upper bound on absolute resolution must include the photoelectric quantum efficiency, ϵ, which is generally less than one The quantum efficiency reduces the inherent resolution as follows

$$f_r = \frac{1\ 94 \times 10^5 (\bar{E})^{1/2}\ m_o\ \epsilon^{1/2}}{K} \tag{10}$$

The quantum efficiency of photoconductors is generally in the range $0\ 1 \leq \epsilon < 1$ whereas the fastest photographic emulsions have quantum efficiencies $\epsilon < 0\ 01$ To a large extent this explains the superior performance of television image forming systems over photographic emulsions under low light level operating conditions

The quantum efficiency limited resolution of an imaging system is a highly simplified concept since it does not take account of the two principal causes of degradation in an imaging system These limiations are the insertion of noise in the image conversion process and the limited information bandwidth of any real system The combined effect of these two factors in resolution degradation is extremely complex but because of the assumed linear nature of the system, can be treated separately and the results combined in an overall statement of realizable system resolution These two factors are discussed below

Television camera system noise, exclusive of the thermal noise introduced by the output video amplifier, is highly dependent upon the type of photosensitive surface used and the number and type of conversion processes employed Thus image orthicons do not have all of the same noise generating process as return beam vidicons so that noise levels of the two sensing processes cannot be expected to be similar To establish the effects of system noise on resolving power, however, it can be shown that the overall effects of noise are identical This follows from the way in which resolving power is defined in terms of the threshold signal-to-noise ratio and exposure If the overall system signal to noise ratio is degraded by noise, the photon or quantum limited resolving power of the system can be restored by increasing the exposure, within limits, to a value which restores the threshold signal-to-noise ratio Since system noise is the result of the internal conversion processes only, it follows that the increased exposure results in a restoration of the resolving power The amount by which the exposure must be increased, called the exposure factor, F_n, is highly dependent upon sensor design factors over which the system engineer has no control Typical effects included in the exposure factor are quantum efficiencies, photon gain of image intensified stages, if used, the readout efficiency of the scanning electron beam, dark currents and residual charge effects in the storage surface Typically, values of the exposure factor are in the range of 10 to 4000 or more depending upon the type of sensor configuration Futhermore, the factors which determine F_n are functions of the exposure so that a straightforward calculation of resolving power is not feasible and graphical solution methods are indicated An example of the type of effects of F_n on the theoretical resolving power of a 3-inch image orthicon is shown in Figure 4-30 Conversion noise has its largest effect in the low exposure region The data presented in Figure 4-30 are for illustration only but are generally representative of the effects of conversion noise on the theoretical resolution of an image forming system which is extracted electronically

The types of results shown in Figure 4-30 are representative of the physics of the conversion process Improvement over the results indicated will only be obtained by basic research in materials and energy conversion processes Improvements of this type are extremely difficult to predict so that for planning purposes detection technology is based on essentially current state-of-the-art or modest predicted improvements in technology

Once having established the basic performance of a detection process, it is logical to inquire why practical systems appear to be so far from attaining predicted detection performance The answer lies in the fact that the information bandwidth of the information gathering and read-out portions of a television camera introduce major degradation in system performance especially in the high exposure-high resolving power region of the camera system The system information bandwidth is represented by the modulation transfer function (MTF) of the camera Degradation results from the limitations on attainable MTF's of both the visible light optics of the information gathering portion of the system and the electron optics of the information read-out mechanism The combined results of the MTF's represents an overall decrease in information bandwidth such that the resolving power of the camera is one or more orders of magnitude lower than the quantum limited performance The degradation may be worse than indicated, especially in the high exposure region of operation unless care is taken to select design parameters of the imaging and read-out portions of the camera which represent minimum degradation

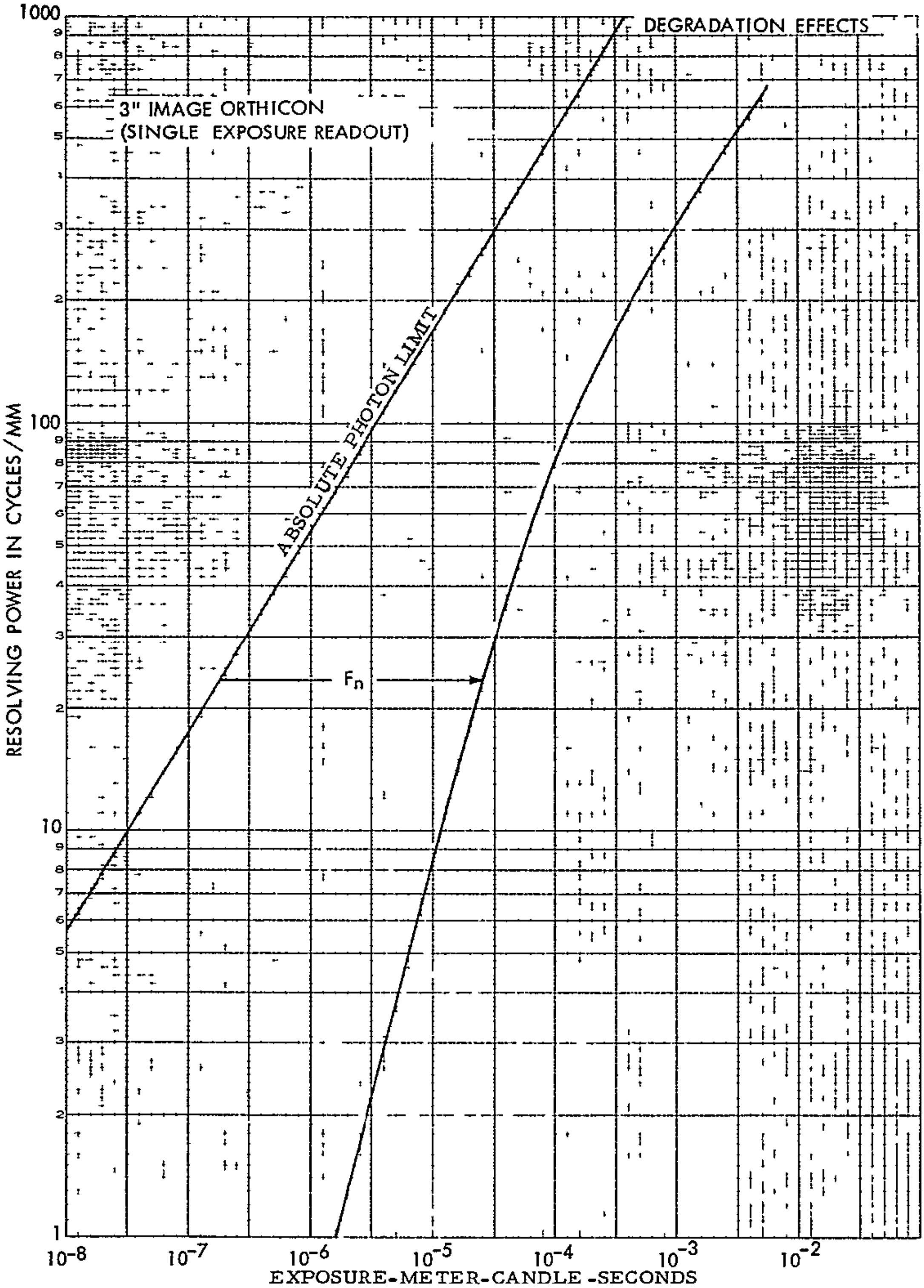

Figure 4-30 Conversion Noise Degradation Effects

Typical state-of-the-art MTF's for high quality television components are shown in Figure 4-31 Various combinations of the MTF's shown in the figure represent either existing camera systems or current experimental designs To determine the effect of system MTF on overall resolution it is generally necessary to use graphical procedures since the expression for the exposure $\bar{E}$ containing the effects of system MTF is of the form

$$\bar{E} = \frac{\bar{E}_o(f_r)}{r\,(f_r)^2} \quad \frac{F_n}{m_o^2} \tag{11}$$

where r (f_r) is the system MTF The difficulty in solving for $\bar{E}$ results from the fact that r (f_r) is a function of the resolving power which in turn is a function of $\bar{E}_o$ since

$$\bar{E}_o = 0\ 267K^2\ f_r^{\ 2} \times 10^{-10} \tag{12}$$

The difficulty is further compounded by the fact that F_n may also be dependent on $\bar{E}$ as shown in Figure 4-30 The procedure for obtaining overall camera system resolution is tedious but not difficult once the camera system definition is established The results of the reduction in resolution because of the MTF's however serve to indicate both areas where improvement can be made and an insight into apparent component improvements which do not result in overall camera system resolution improvements

To illustrate the effects of the MTF refer to Figure 4-32 reproduced from Schade The case shown in the figure is for illustration only It represents a quantum limited resolution of 300 lines per mm for an image orthicon at peak white exposure and high contrast The MTF of an excellent lens reduces the resolution to 100 lines per mm (MTF #1 in Figure 4-31) The combination of the lens, image section and reading beam (MTF's 1 x 4 x 5) reduce the resolution to 32 lines per mm at peak highlight exposure For low contrast (M_o = 0 1) targets, the maximum resolution attainable for the same MTF combination is reduced to approximately 15 lines per mm It should also be borne in mind that the values given in the figure are static resolution obtained with a continuous exposure and 1/30 sec frame time, that is "live" television pickup, so that further degradation can result either from single exposure operation or dynamic operation For the condition shown in the figure, the MTF combination 1 x 3 x 4 can be taken as an upper limit of improvement in image orthicon cameras A maximum resolution of approximately 60 lines per mm at high contrast and peak highlight exposure is the upper limit

1. 6.3 mm FAX ELNIKOR lens at f/5.6
2. Intensifier (p-20 or 6m fiber optic plate)
3. "Super" (40 gauss field,).7 mil aperture
4. High resolution beam, 70 gauss, 1.0 mil aperture
5. Standard beam, 70 gauss, 1.5 to 2 mil aperture

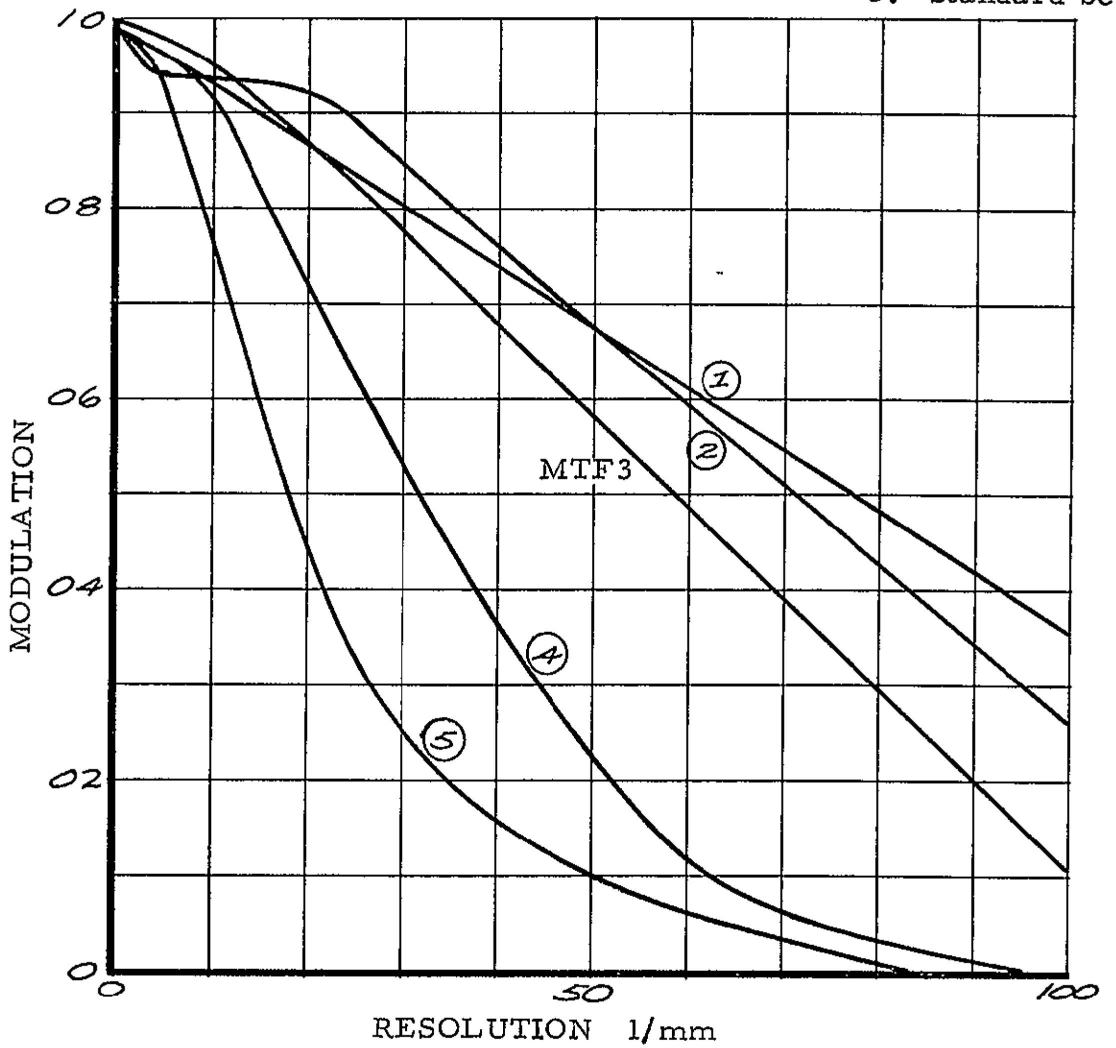

Figure 4-31 Sine Wave Modulation Transfer Functions (MTF's) of Television Camera

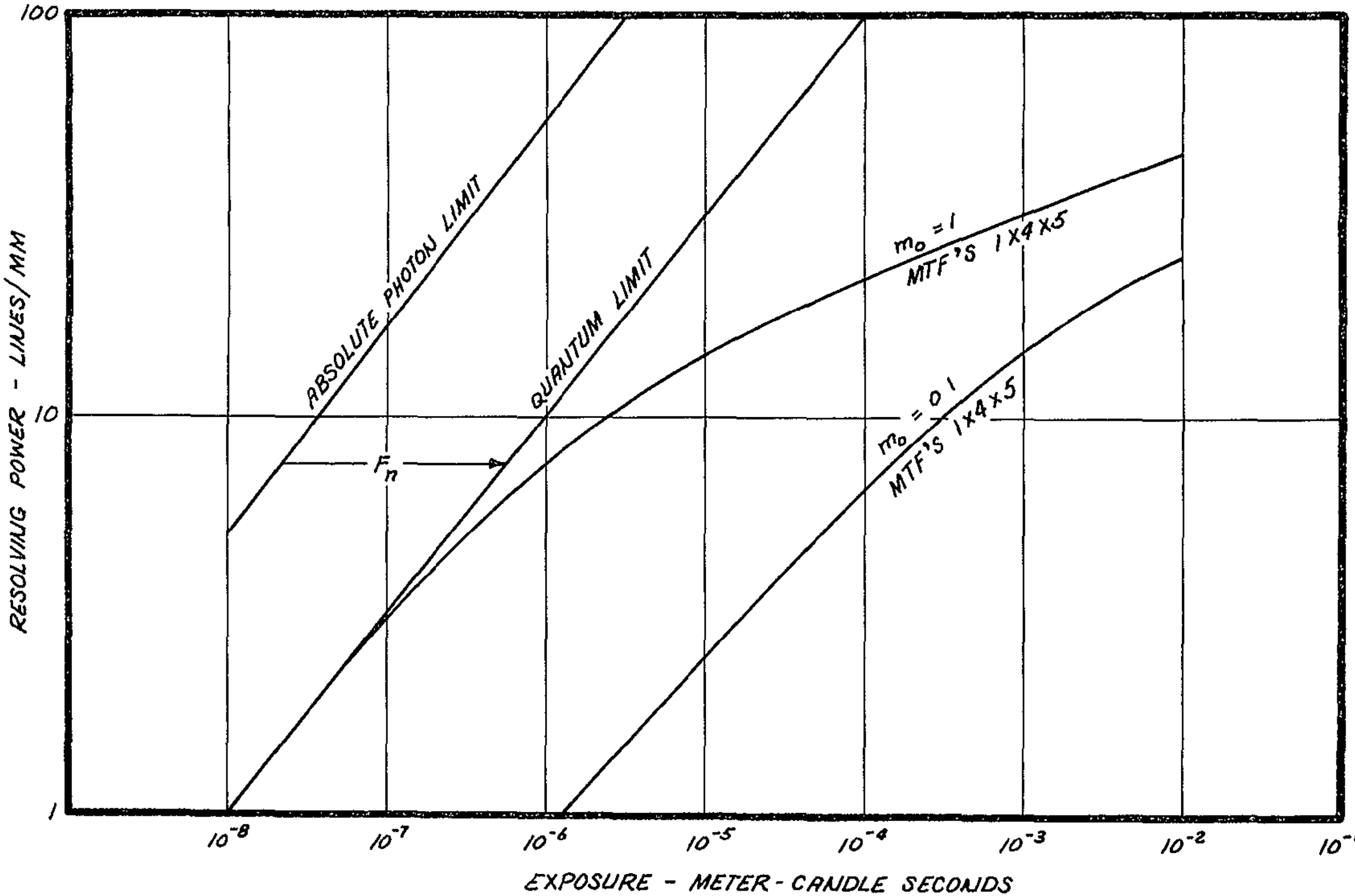

Figure 4-32 Quantum and Resolving Power of Image Orthicon

The use of an image intensifier stage in an orthicon may be useful in increasing low light level sensitivity but results in a basic reduction of maximum resolving power Three effects can be noted from the use of an image intensifier stage as follows

1 The exposure factor, F_n, is decreased by an amount proportional to the photon gain of the intensifier resulting in operation nearer the ultimate photon limited performance

2 The maximum exposure decreases by the amount which is inversely proportional to the photon gain so that the maximum resolving power is reduced

3 The introduction of the MTF of the intensifier stage further reduces the resolving power

The overall result of the intensifier is the improvement of low light level sensitivity at the expense of reduced resolving power in the high exposure region of the resolving power function

The level of resolution attainable with a television imaging system is determined in a gross sense by the resolving power function discussed above There are other factors which can either improve or degrade the predicted theoretical resolution depending upon overall imaging system design Typical of these are the following

1 High resolving power optimization with so-called aperture correction (MTF correction)

2 Scanning (raster) line density adjustment to take account of the self-sharpening effect of the scanning electron beam equivalent aperture which gives rise to the so-called Kell Factor

3 Dynamic operation which results in image smear unless image motion during exposure is insignificant A correlary to this is image blur resulting from overexposure or excess time between successive read-outs of imagery in the storage medium when continuous exposure is used

From a practical point of view these effects may or may not be significant depending upon the application of the TV system They are discussed briefly for the sake of completeness

<u>Aperture Correction</u> It has been demonstrated that the principal cause of difference between theoretical and practical resolution in a TV camera results from the decrease in system response at high spatial

frequency as described by the system MTF However, from the point of view of filter theory it can be shown that spatial frequency filtering can be used to improve overall system response with a properly designed filter such that the filter response to signal increases linearly while its response to noise increases only as a half power The same result may be obtained either optically or electrically but in TV systems is most frequently accomplished electrically by adjusting the response of the video amplifier at the output Typical results of electrical aperture correction are shown in Figure 4-33 Two types of correction are indicated for a typical response of an uncorrected MTF, curve 1 and an optimum high frequency correction function curve 2, the combination results in the response shown in curve 3 Alternatively, the curves shown dashed represent corrections (curve 4) for improved low frequency response of curve 1 The result, shown by curve 5, results in an image of improved sharpness

The results of aperture correction are not without drawbacks since under certain circumstances they may make the image difficult to interpret For this reason it is common practice to make aperture correction a selectable feature which can be switched out However, advanced television transmission systems are now being proposed in which a combination of pre-emphasis, or aperture correction, and noise weight filtering are used to obtain an improvement in effective transmission signal-to-noise ratio of as much as 15 db The aperture correction improvement cannot be applied twice so that its applicability is problematic

It is commonly assumed that there is a direct proportionality between raster line density or read-out beam scanning rate and the resolution of the TV as an imaging system This is generally not the case unless the reading beam is completely absorbed by the image target In most practical TV designs, only a portion of the beam is absorbed so that there is little direct correlation between the scan line number and the attainable resolution The raster pitch or line density is selected to give equal resolution in both scan directions, that is X and Y, such that the reading beam is advanced one beamwidth in the Y direction for each 5 scan lines The net result of this scheme is that maximum resolution is in the diagonal directional with the X and Y resolutions being equal to 707 of the maximum resolution This is the so-called Kell factor which is used to reduce the maximum attainable resolution under the assumption that a potential step in the charged target is completely discharged However, in the development of the resolving power function and the MTF of the reading beam of the camera, the loss in resolution is already accounted for The beam is self sharpening for a high density raster pitch so that the results of the Kell factor are insignificant and a Kell factor of one is used

<u>Image Motion Compensation</u> In the event that exposure times are long or the operating environment is turbulent, the attainable system MTF is

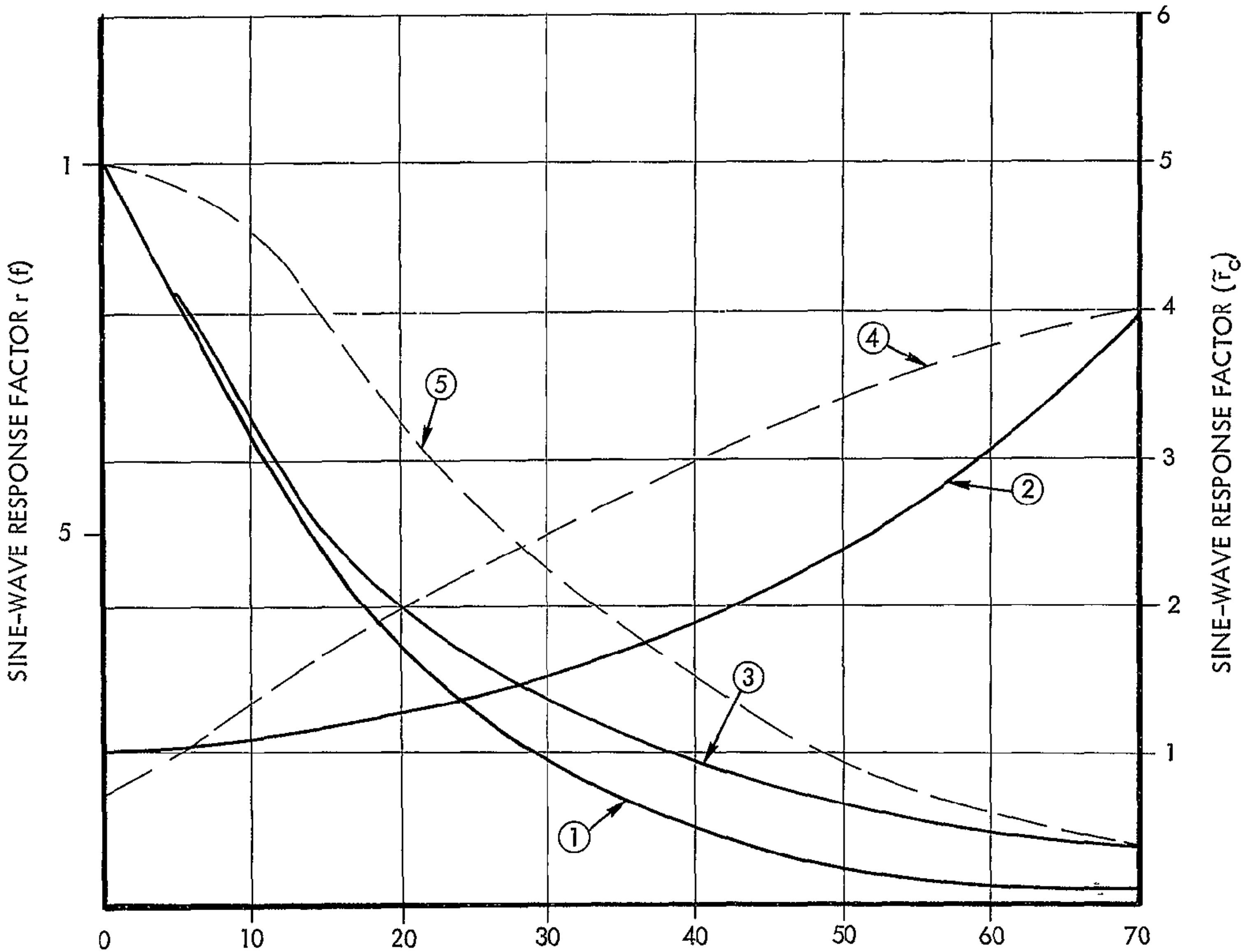

Figure 4-33. Aperture Correction

limited by the uncompensated portion of the motion of the image plane during exposure The MTF of equivalent image motion is given in Figures 4-34 and 4-35 for the most frequently encountered types of motion linear motion resulting from translation and camera mount random vibration For long range operation linear motion is generally small since it is determined by the ratio of velocity to height Camera mount steadiness however, may be the limiting factor since it may be made up of both periodic and random vibration imposed by both spacecraft design and servo control limitations

The MTF of uncompensated motion given in the figures must first be scaled to the operating parameters and then combined with other MTF's of the TV system to establish an overall MTF which is then combined with the quantum limited performance of the system to establish resolving power as a function of exposure In the event that the MTF of the uncompensated motion results in unsatisfactory performance, a specification of required IMC may be developed to establish satisfactory resolving power

Resolving Power The resolving power of a TV system has two basic limitations They are not completely independent so that several iterations of design parameters may be necessary to arrive at a satisfactory system description The first limitation, discussed above, is basically imposed by the requirement for suitable exposure to obtain a given resolving power The second limitation is imposed by electrical parameters of the output electronics These limitations are discussed briefly below

Exposure

The exposure of an image forming system is determined by

$$E = \frac{B \tau t_e}{4 (N)^2 F} \tag{13}$$

where

B is the object brightness

τ is the optical transmission

t_e is the exposure time

N is the optical speed or focal ratio

F is the filter factor which accounts for the percentage of available illumination which reaches the image plane

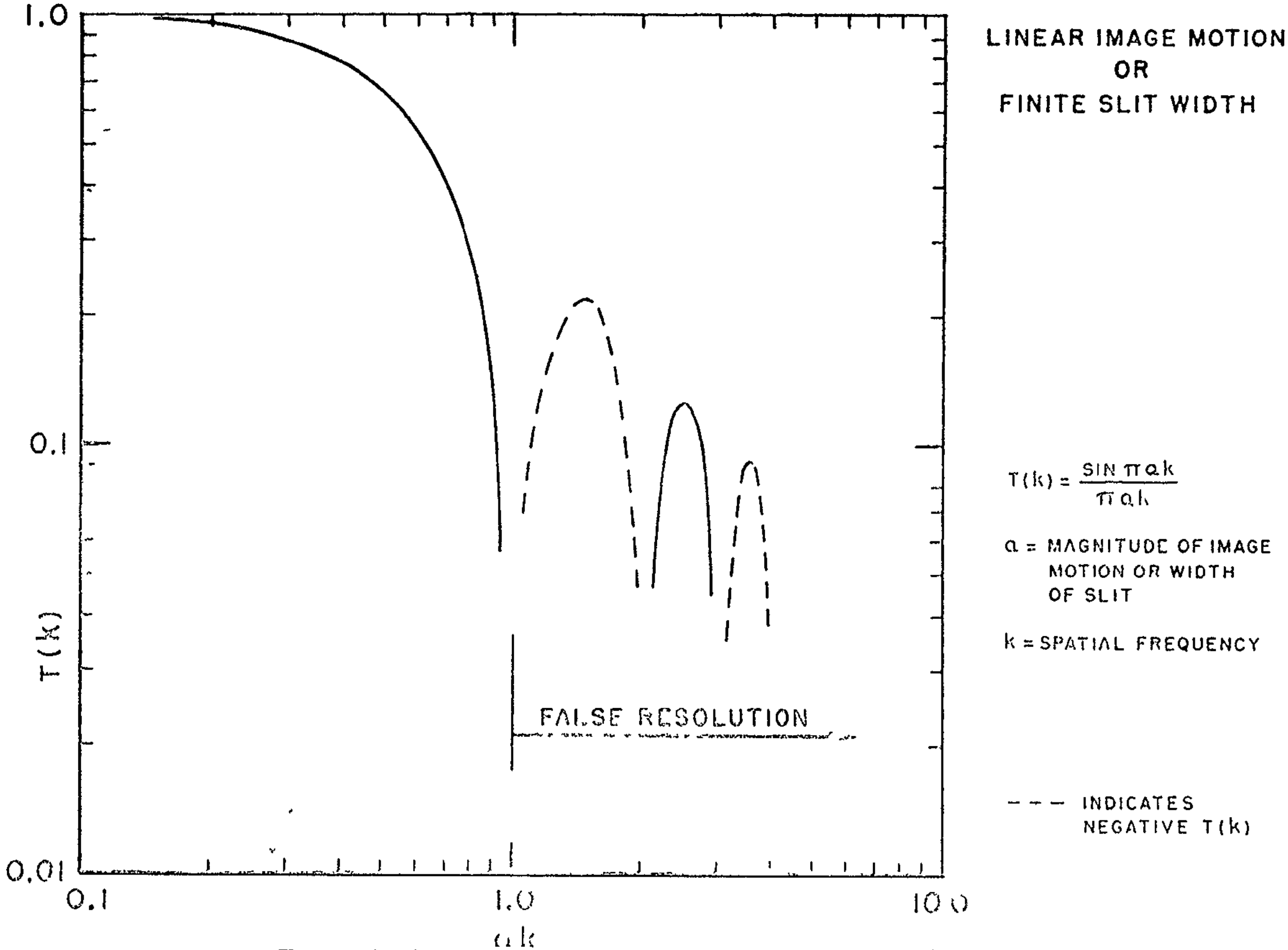

Figure 4-34. Linear Image Motion or Finite Slit Width

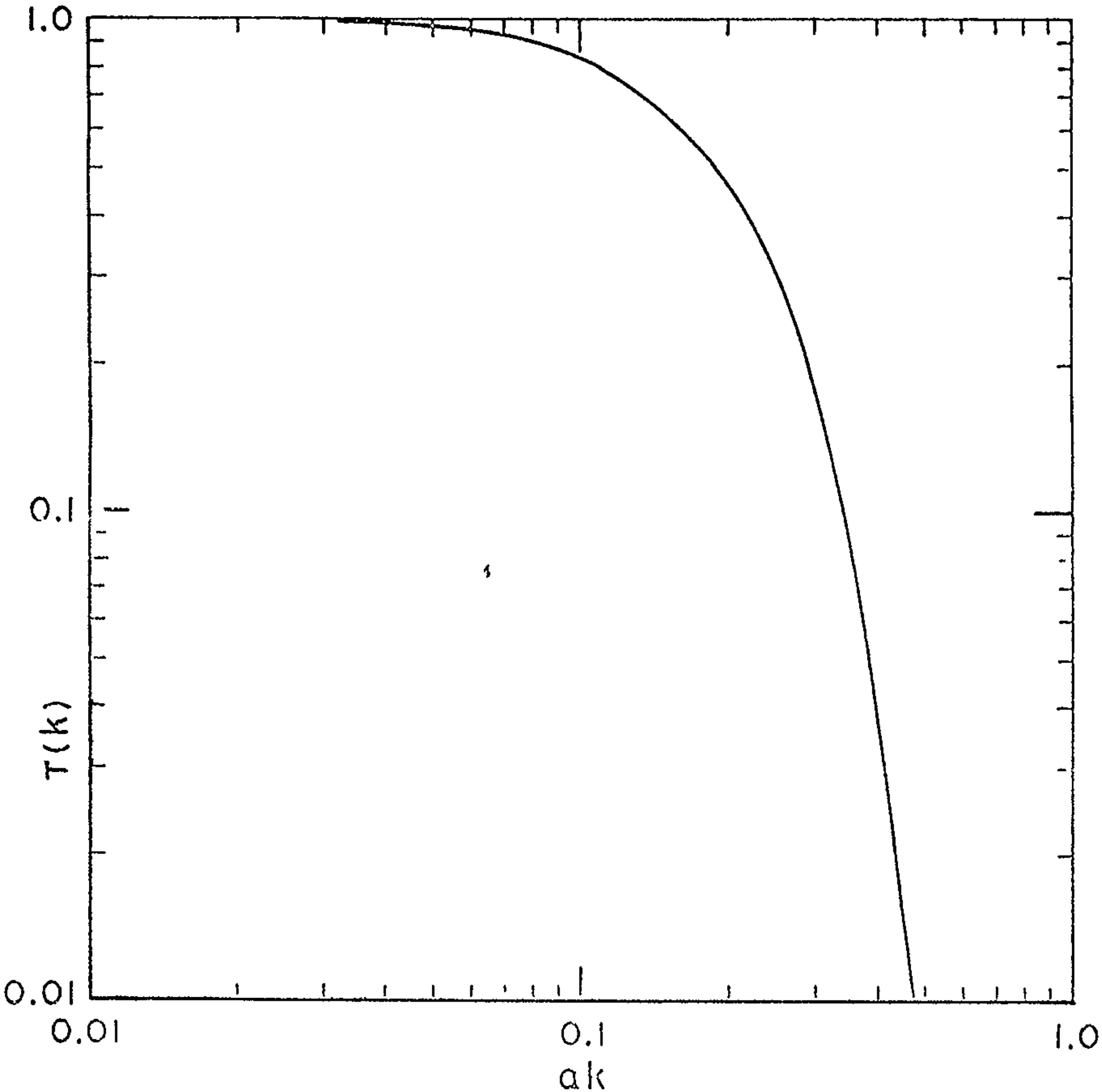

Figure 4-35. Random Image Motion

RANDOM IMAGE MOTION

$T(k) = e^{-2\pi^2 a^2 k^2}$

a = RMS VALUE OF IMAGE MOTION IN IMAGE PLANE

OR

$a = f\omega$

k = SPATIAL FREQUENCY IN IMAGE PLANE

Each of the factors has a significant effect in outer planet exploration since a system capable of a reasonable level of spectral resolution is required

In general, illumination levels are intermediate Typically, the solar constant at Saturn is only 1 percent of the solar constant at Earth If the solar constant is taken as 1 3 x 10^5 meter-candles at the Earth then it will be of the order of 1 3 x 10^3 meter-candle at Saturn If this value is used in combination with accepted values of albedo, then approximately 60 percent of the incident parallel illumination is reflected into space Accepting available evidence of limb darkening to indicate Lambertian scattering which follows a $\cos^2$ law, then the light available for image formation can be estimated as

$$I = 1\ 3 \times 10^3\ \rho \cos 2\ \theta \text{ meter candles} \tag{14}$$

where

ρ is the albedo assumed equal to 0 6

θ is the Sun-Saturn observation point angle

Figure 4-36 is a plot of this function for the assumed conditions It can be seen that, in general, light is available for image formation if a high quality optical system in combination with long exposure times are used Optical quality is generally expressed in terms of the lowest f numbers which result in near diffraction limited performance over the spectral range of interest and the optical transmission factor, τ State-of-the-art in optical design is always debatable but diffraction limited performance at aperture ratios smaller than three, over the visible spectrum, are very unlikely on a near term basis For planning purposes an aperture ratio range is therefore assumed from three to six for scaling purposes Likewise high quality optics for image forming sensors may have transmission factors approaching 0 9 Within these values, the image plane illumination or exposure may be established parametrically for Saturn, based on the available illumination given in Figure 4-36 The range of values of the exposure are given in Figure 4-37 for a range of exposure times For low observation angles, relatively short exposure times can be used to obtain near optimum resolution which occurs at exposure levels near one meter-candle-second However

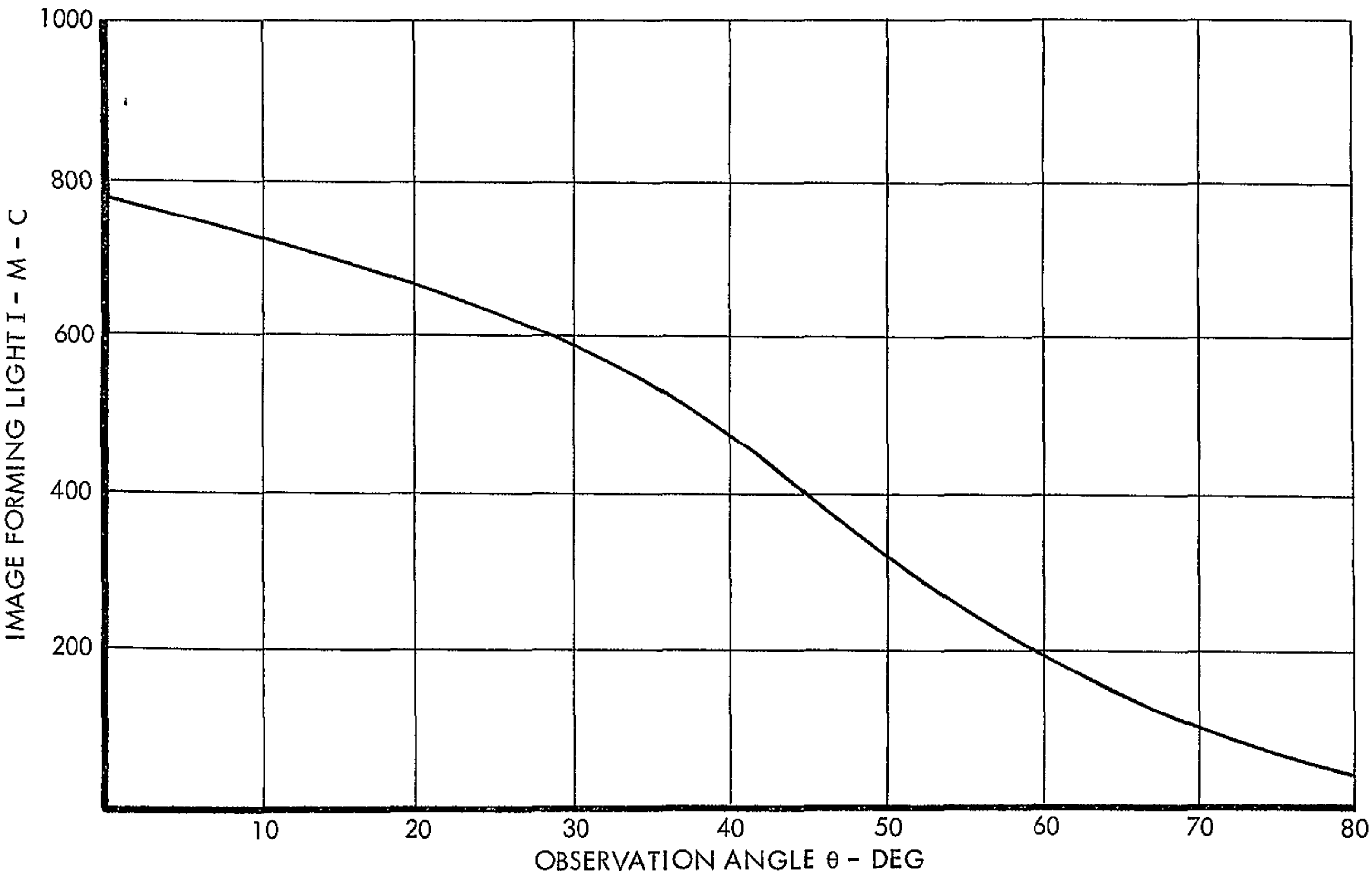

Figure 4-36 Available Image Forming Light at Saturn

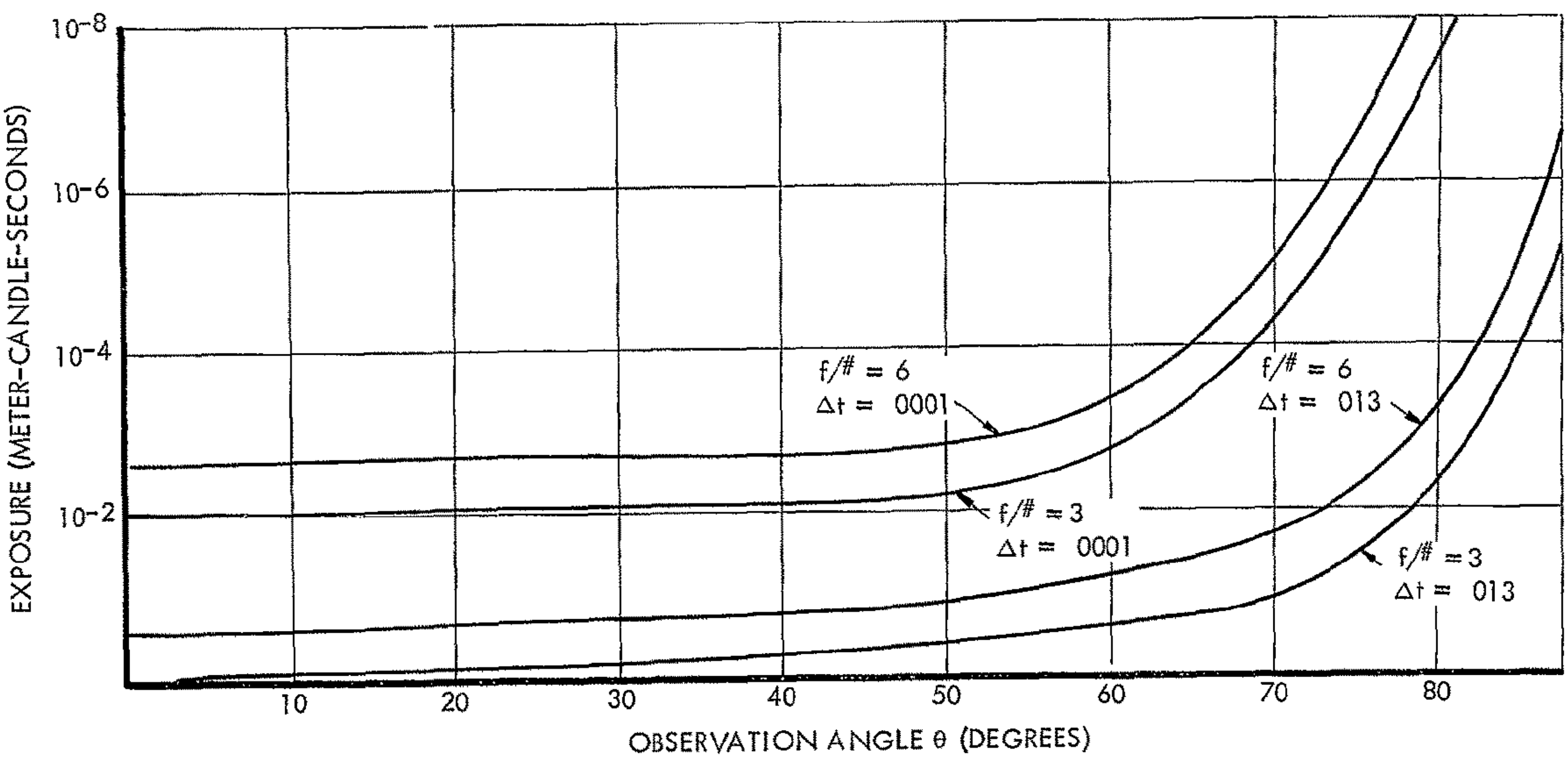

Figure 4-37 Exposure Versus Observation Angle

as the observation angle approaches 90 degrees, long exposure times are indicated even with high quality optics To obtain limiting resolution over the range of observation angles some form of exposure control is indicated

Electrical Bandwidth Limitation The dynamic response of the reading beam of a TV camera imposes a minimum requirement on the electrical bandwidth of the output video amplifier The requirement of converting spatial frequency in the form of resolving power into an equivalent video signal is given by

$$\Delta f = \frac{2\, bAf_r^2}{t_f} \tag{15}$$

where

Δf is the required bandwidth in Hz

b is the blanking factor which is a measure of the part of each scan line which is active It is given by

$$b = \frac{t_f}{t_{f\ (unblanked)}}$$

and is usually designed to give a value of b = 1 23

A is the image area scanned in mm^2

f_r is the resolving power in cycles/mm

t_f is the frame time in seconds.

While this expression appears to establish independent requirements for obtaining a given resolving power, it does not do so Rather, it establishes the minimum electrical bandwidth to obtain a given resolving power for a set of readout parameters, under the assumption that an adequate signal level is reached in the readout beam The implications of signal-to-noise ratio have been discussed previously The implications of electrical bandwidth are fairly straightforward however, if it is assumed that the output signal level is adequate To conserve electrical bandwidth for a given combination of image size and resolving power it is desirable to scan at as slow a speed as possible Limitations on scan time are generally imposed by the storage characteristics of the image surface Thus Vidicons have generally long image storage times while such storage surfaces as Image Orthicons and Plumbicons have very short storage times An Image Othicon with a characteristic readout time of 1/30 sec would require 120 times the bandwidth of a Vidicon with a 4 sec readout time, all else being equal It follows that the combination of high resolution, large storage surface area and required scan time, lead to the selection of Vidicons for the planetary imaging missions This conclusion is further fortified by the fact that there does not appear to be a requirement for very low light level operation where the Image Orthicon with its superior low light level sensitivity would be most useful For planning purposes a Vidicon system will be assumed

Current state-of-the-art in Vidicon technology is shown in Figure 4-38 for so-called 1 inch and 4-1/2 inch tubes In each case the active image area is somewhat less than the available cross-sectional area Typically, the 1 inch Vidicon has an image area of 125 mm^2 while the 4 5 inch Vidicon has an active area of 2500 mm^2 Both Vidicon's have a maximum resolving power of approximately 80 lines per mm after degradation resulting from the camera MTF (but without aperture correction) Assuming a scan time of 4 seconds the bandwidth requirements are

$$\Delta f = \frac{2\ 46 \times 125 \times 6\ 4 \times 10^3}{4} = 0\ 492 \text{ MHz (1 in Vidicon)} \quad (16)$$

$$\Delta f = \frac{2\ 46 \times 2\ 5 \times 10^3 \times 6\ 4 \times 10^3}{4} = 9\ 84 \text{ MHz (4 5 in Vidicon)} \quad (17)$$

Even for relatively slow scan readout, the combination of large area and high resolution lead to wideband video amplifier requirements To obtain the MTF limiting resolution the television line number must, for a square image, have the value

$$N = 2f_r \sqrt{A} \quad (18)$$

This leads to the following requirements

$$N = 2 \times 80 \sqrt{125} = 1850 \text{ lines (1 in Vidicon)} \quad (19)$$

$$N = 2 \times 80 \sqrt{2500} = 8000 \text{ lines (4 5 in Vidicon)} \quad (20)$$

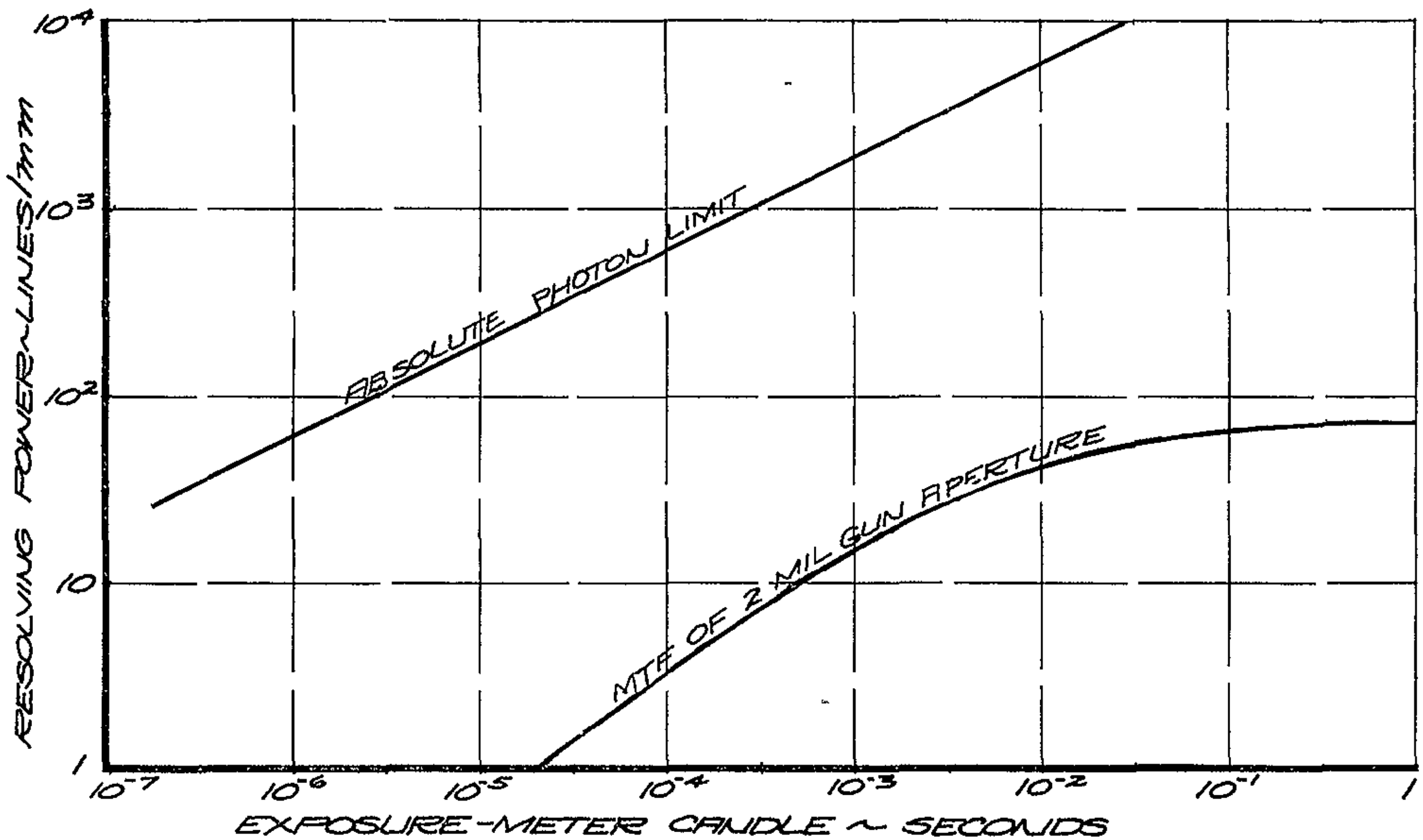

Figure 4-38. Resolving Power of 1-Inch and 4 5-Inch Vidicon Single Exposure Readout ($t_f \pm 4$ Seconds)

The value of 8000 lines appears to be the current projected limit of TV camera technology Conflicting design requirements, image storage technology, circuit limitations and operational degradation combine to limit any projection of the state-of-the-art to camera systems with a maximum of 10, 000 lines It does not appear that any single factor limits attainable performance to this figure but rather a combination of interacting effects produces this result

4 3 2 2 Television Scaling Law

The design of a television system is basically a reconciliation of conflicting requirements among the limited size and spatial resolution of television pickup tubes, high resolution coverage of the object plane and limited available image forming light The reconciliation of the conflicts is not always a straightforward procedure so that a given design may have to be iterated several times before a useful design evolves This follows from the fact that many of the design parameters are not independent so that a change in one area may produce an end result which is unacceptable

A television system consists of three principal parts A light collection or optical telescope sub-system, a camera sub-system consisting of a photo sensitive detector and readout electronics, and a mount to point the aperture of the telescope at the object plane The required scaling law in simplified form would then consist of selecting an optical design from paragraph 4 2 2 in connection with the current TV camera technology discussed in paragraph 4 3 2 1 and then specifying a mount steadiness requirement to prevent resolution degradation during exposure The exposure requirements would then be established from the values given in tables 4-1 and 4-2 with a photometric function selected according to planet type

Such a procedure, while relatively straightforward, would be misleading since it would not account for many of the aspects of TV system performance which affect overall resolution Thus the effects on resolution as a function of exposure would be ignored and performance prediction would be misleading However, the utility of the abbreviated approach is that it permits bounding the detailed approach to ranges of values which are realistic For this reason a complete scaling law for TV systems would be accomplished at two levels The first is a simplified approach based on geometric considerations while a detailed approach based on modulation transfer functions is indicated to permit detailed system design if it is required This will not ordinarily be the case since scaling can be accomplished with first order approximations The detailed approach would be used if a complete specification were to be prepared or if a fundamental question of TV system feasibility in a mission were to arise

<u>First Order Design Procedure</u> The procedure is based on imaging requirements in the form of surface resolution and area coverage for fly-by missions of specific planets using available image forming light Several approaches can be used so that the procedure given is not unique

Starting with the required resolution of the imagery, the surface resolution of a camera system is given by

$$G = \frac{h}{F f_r \quad 25\ 4} \tag{21}$$

where

G is the surface resolution

h is the height above the surface

F is the focal length of the optical system in inches

f_r is the resolving power of the sensor system in lines per millimeter

Surface resolution as a function of various parameters is shown in Figures 4-39 through 4-41 The basic variables are surface resolution, G, as a function of height above the surface, h, with optical system focal length and sensor limiting resolution as parameters Figures 4-39 through 4-41 are plots of surface resolution for optical focal lengths of 6, 12 and 24 inches Several system design constraints are apparent from the figures For fly-by missions, the viewing distances are large so that the attainment of even a one kilometer surface resolution requires a combination of long focal length optics and high sensor resolution

It follows that the optical system would have to have a focal length with a state-of-the-art limited sensor resolution of 80 lines per mm for a one kilometer surface resolution at viewing distances greater than 10^5 kilometers At the other extreme, an upper limit of surface resolution of 100 kilometers permits operation with a much wider range of sensor resolution-focal length combinations with long viewing distances

Several associated system parameters are immediately derivable once a sensor-focal length combination is selected As discussed previously the state-of-the-art in wide spectral band, diffraction limited optics leads to attainable aperture ratios of approximately 3 to 6 This places a design requirement on the aperture to meet surface resolution requirements while making maximum use of the available image forming light, in a first order sense, since once the focal length and aperture ratio are selected the

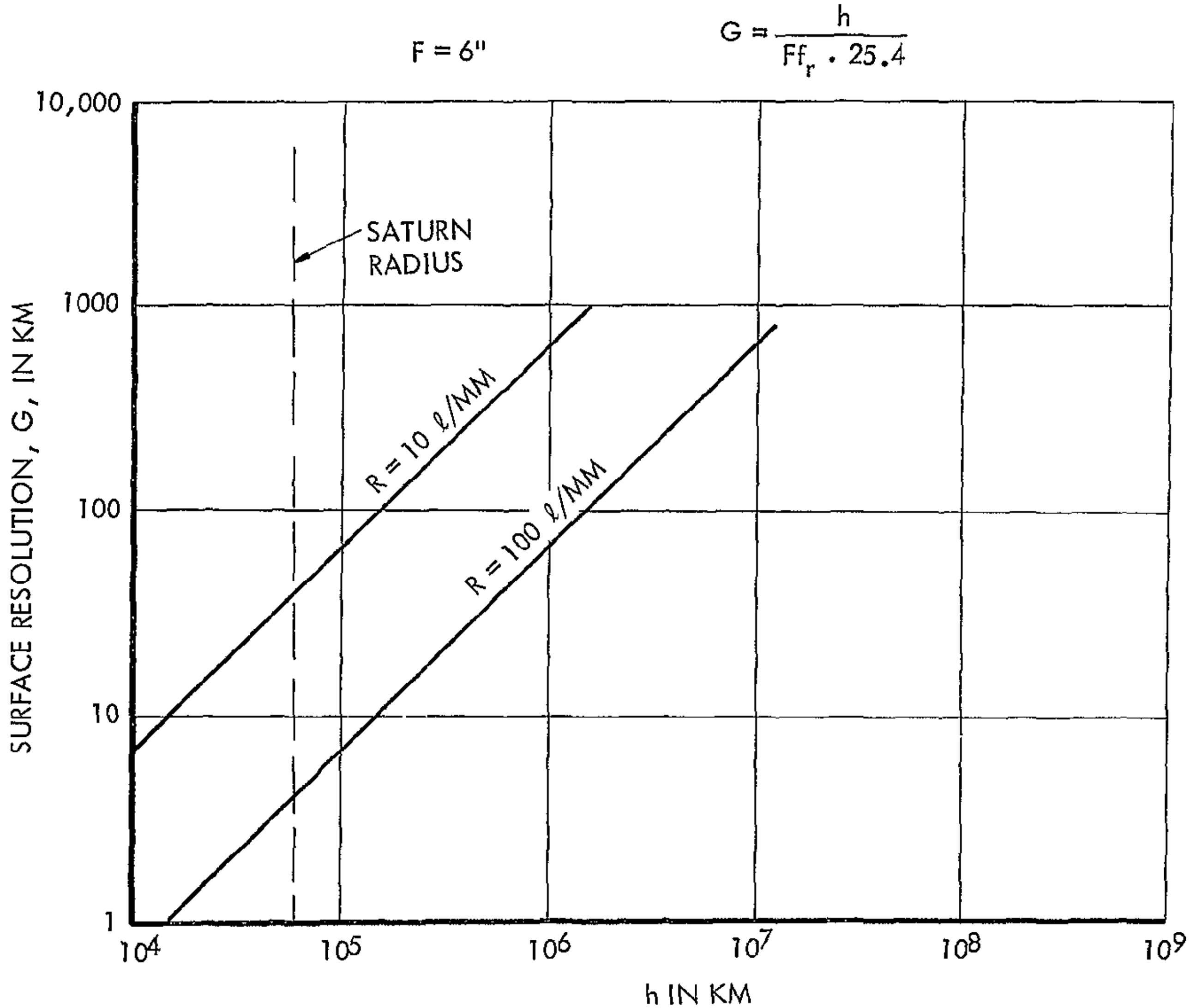

Figure 4-39 Surface Resolution as a Function of Overall Sensor Resolution for a 6-Inch Focal Length Optical System

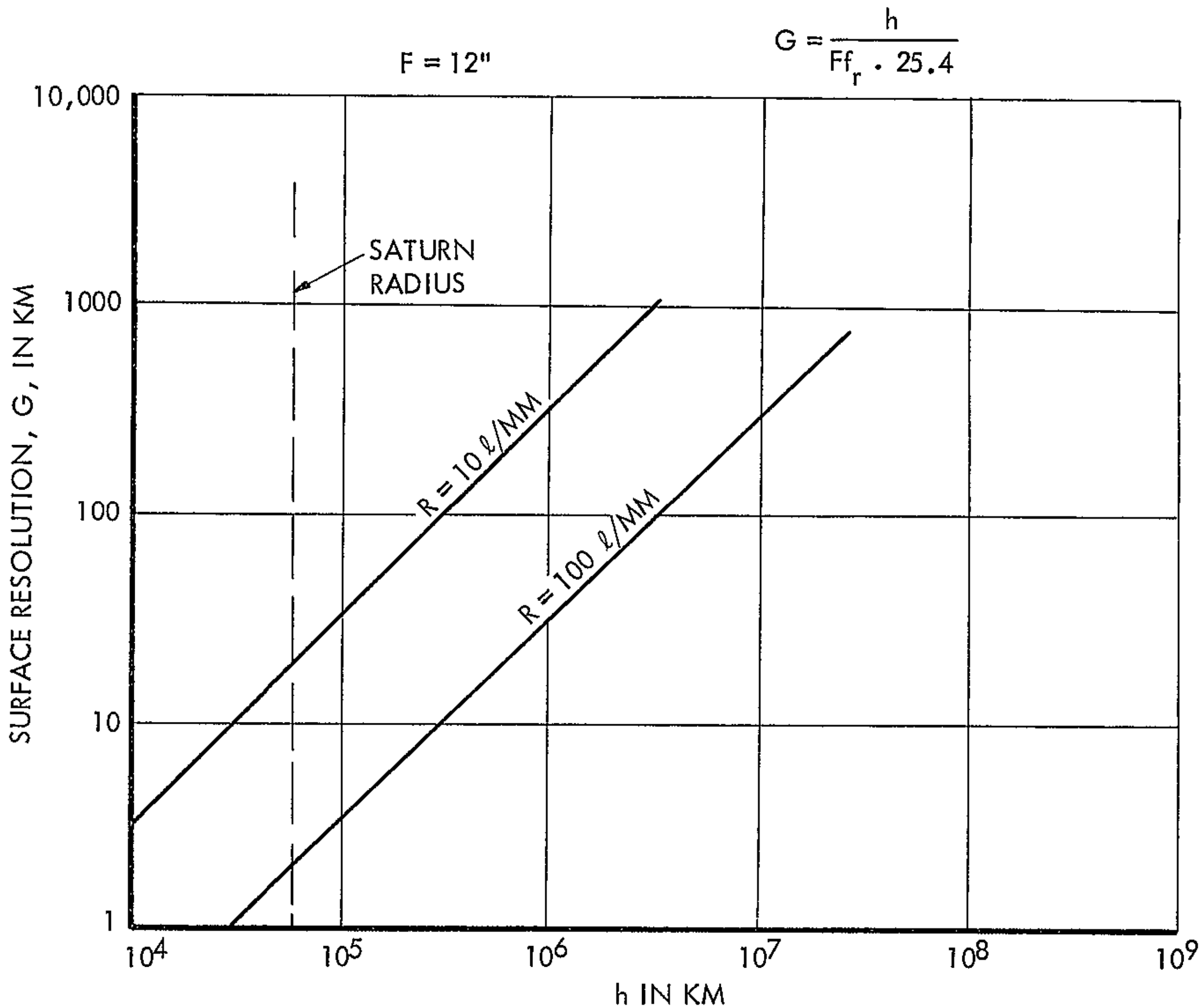

Figure 4-40. Surface Resolution as a Function of Overall Sensor Resolution for a 12-Inch Focal Length Optical System

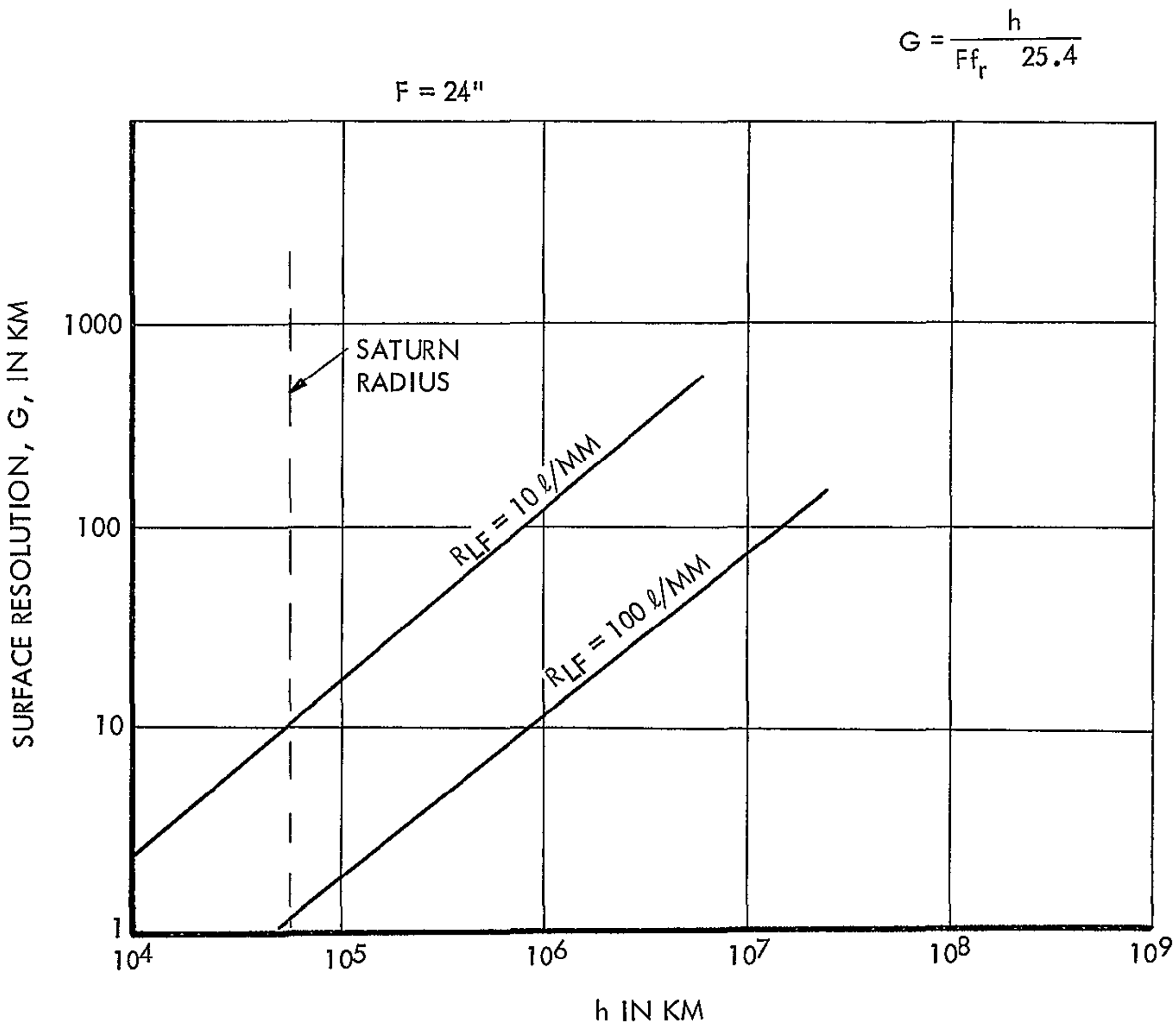

Figure 4-41 Surface Resolution as a Function of Overall Sensor Resolution for a 24-Inch Focal Length Optical System

required aperture is fixed Taking as an example an excellent, diffraction limited f/5 6 lens with a 10 in focal length, an aperture of 1 8 inches is required However, a 240 in focal length optical system of the same quality would require an aperture of 45 inches diameter The range of optical system sizes to meet the surface resolution requirements can therefore be established to be in the range of one to 80 inches depending upon specific mission selections

The attainment of a given surface resolution is not independent of other mission requirements since the surface coverage obtained may not be adequate on a sampling basis or have a sufficient variation in detail to permit interpretation A compromise between surface resolution and surface coverage may be necessary From simple geometry the surface coverage, to a first approximation, is given by

$$L = \frac{\ell h}{f} \qquad (22)$$

for a square format, where

ℓ is the format size length in the same dimensions as f

h is the viewing distance in km

f is the optical system focal length

Practical imaging tube designs range in format size from approximately 0 15 square inches to as much as 4 square inches for high definition state-of-the-art tubes A practical range of linear format dimensions is therefore from approximately 0 5 to 2 inches, it being understood that the larger formats are generally only available in high definition sensors

For long viewing distances surface coverage presents very little difficulty with low resolution coverage Limitations on surface coverage are imposed more by viewing geometry than the inherent limitations of format size or optical parameters in the range of surface resolutions considered for most missions This point is perhaps more obvious from the angle subtended by the disc of a planet with Saturn used as a typical example in a fly-by mission

Since the angle subtended by a planet disc is given by

$$\tan\frac{\alpha}{2} = \frac{R_p}{h + R_p} \qquad (23)$$

where

R_p is the planet radius, and

h is the viewing distance

the angle α is relatively small at long viewing distances when image forming light is available The angle α as a function of h in planetary radii is shown in Figure 4-42 This can be combined with the camera field of view shown in Figure 4-43 Except for the combination of small image format and long focal length, the field of view of the camera and the angle subtended by the disc are in relatively close agreement when best illumination conditions exist A whole range of possible system configurations exist for meeting one or more primary mission objective either partially or fully in a first order sense with the final choice being determined by support requirements and worth

The question of the amount of imagery to be accumulated can have a direct impact on system design in addition to the generation of support requirements From the encounter parameters of a fly-by mission, with Saturn as an example, it can be established that imaging of 100 km surface resolution or better can be obtained at viewing distances of at least 10 Saturn radii to approximately one Saturn radius This permits image data accumulation for a period of approximately 10 hours In the available 10 hours there are basic design choices on the amount of imagery accumulated If, for example, the sensor is optimized to obtain the highest data rate, then 1800 images could be generated with a nominal read-out and recycle time of the imaging system of 20 seconds Since much of the data is redundant it may be more reasonable to reduce the amount of data to the point of minimum redundancy, that is minimum overlap, and thereby reduce overall system complexity Each of these approaches is feasible but the main impact is on support requirements since the sensors can be operated to meet either objective

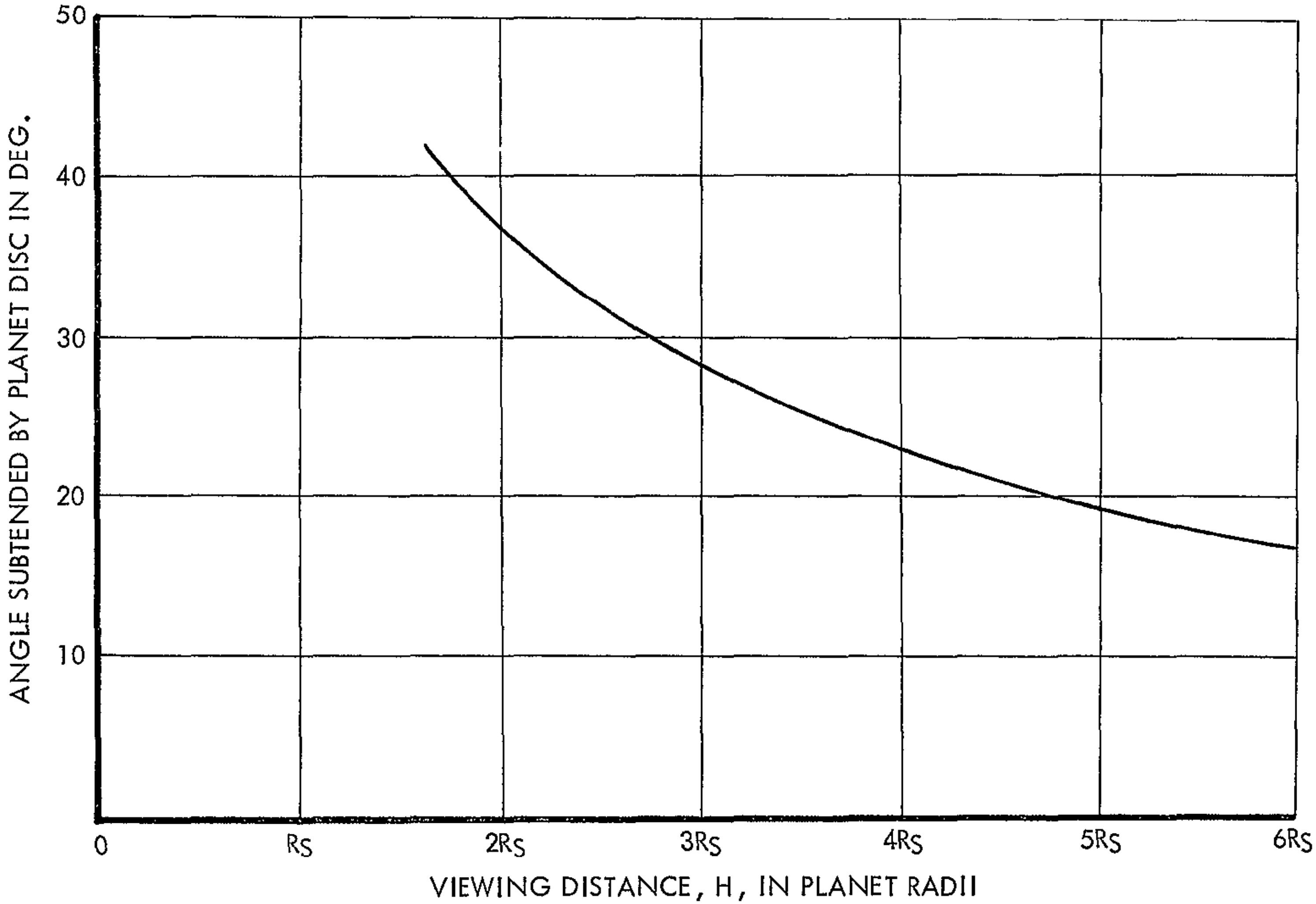

Figure 4-42. Angle Subtended by Planet Disk

$$\theta = 2\ \mathrm{TAN}^{-1} \frac{\ell}{2F}$$

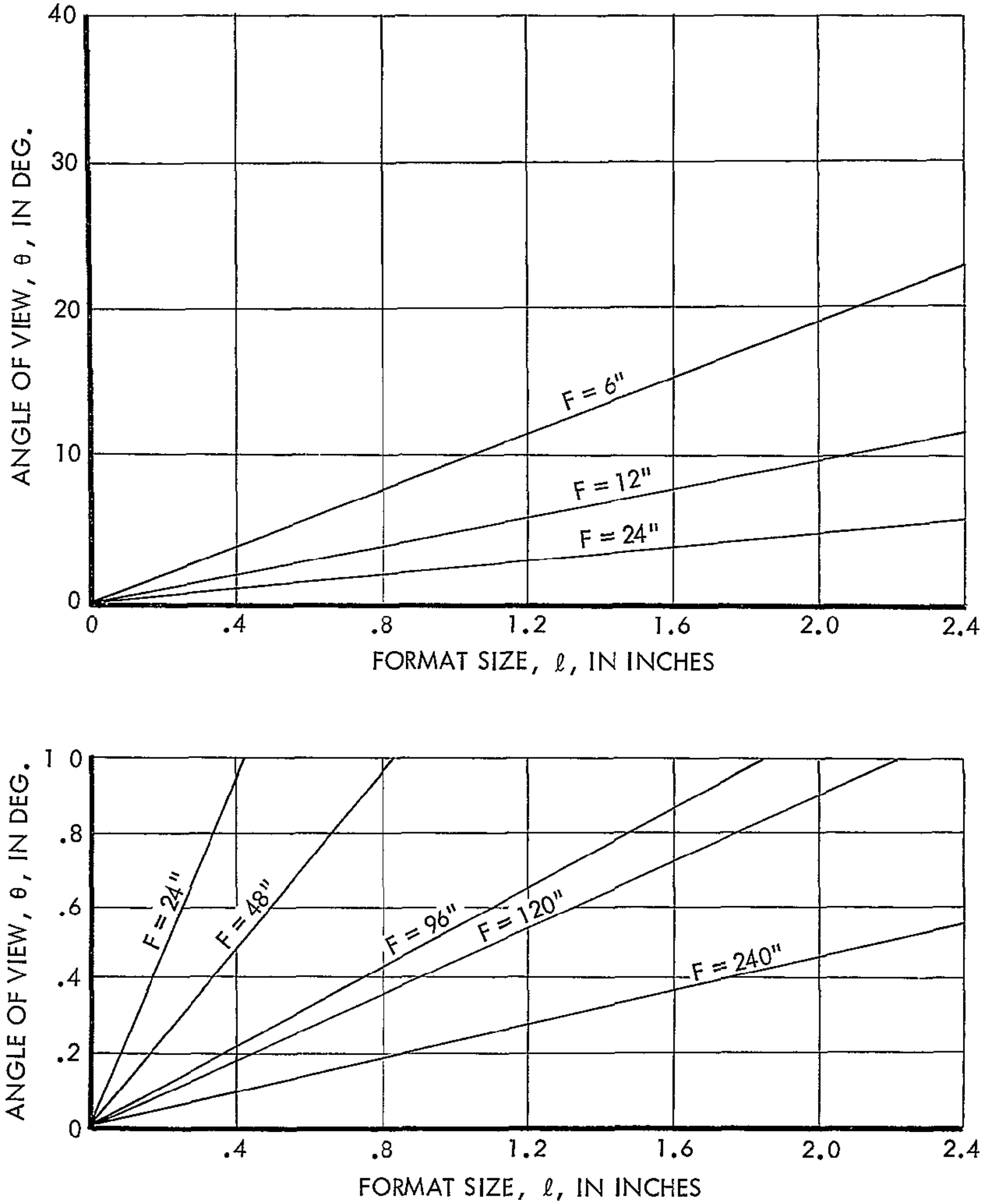

Figure 4-43 Camera Angle of View

4.3 2 3 Support Requirements

For the first order design parameters selected for a given minimum surface resolution, it is necessary to establish support requirements consisting of the following

a Sensor system weight

b Sensor system volume

c Power requirements

d Sensor output data characteristics and rates

e Motion compensation and platform stability requirements

Sensor System Weight A TV sensor consists of essentially two subsystems as follows

1 Television tube and associated electronics, camera controller and data output formatter

2 Image forming optical system

For low resolution, small diameter optics, it is common practice to package the subsystems in a common camera housing A survey of currently available, space-rated TV sensors indicates that, on the average, complete television camera systems are related to TV tube diameter by

$$W = 15\ d$$

where

W is the camera weight in pounds

d is the tube diameter in inches

This expression is useful for systems up to approximately one inch diameter and applies specifically to vidicon systems which are inherently simple For more sophisticated pickup tubes such as orthicons and return beam vidicons, the weight estimate must be increased by 50 percent

For large systems which are packaged in functional form as indicated above, the television tube and associated electronics, as well as the camera controller, represent a small portion of overall system weight compared to the optical system Under the assumption that large diameter tubes will be used with large diameter optical systems, a useful estimate of tube and controller weight can be made by assuming a constant weight of 50 pounds for the tube and 10 pounds for the camera controller Large diameter tubes tend to be heavy because the high quality electron optics are obtained using distributed magnetic focusing which is inherently heavy It should also be borne in mind that large diameter TV sensors are generally much more complex than small diameter vidicons because of the addition of such features as image intensifiers and return beam read-out The electronics of the camera controller may be reduced, but not significantly, by the use of integrated circuits This follows from the fact that the camera controller incorporates such functions as precision frequency generating circuits and constant current control circuits for the electron optics of the readout beam.

When large, separate telescopes are required, the weight scaling given in Table 4-4 is used The basic camera weight does not change because the input optics to the camera are replaced by a field lens to refocus the image plane of the telescope on the TV tube sensitive surface.

For large systems, the total sensor system weight is made up of the sum of the optics, TV sensor, and camera controller The trend in system weight as a function of aperture diameter is shown in Figure 4-44. The dotted line indicates the region where the weight scaling law is questionable. No systems exist in this region of aperture diameters to use as a basis for comparison

Sensor System Volume Television camera system volume is directly correlated with system weight and size For small aperture, complete camera systems, the conversion coefficient is approximately 60 pounds per cubic foot Thus, a 20 pound TV camera occupies approximately one third of a cubic foot or 550 cubic inches

For large diameter, long focal length systems consisting of an optical subsystem, a camera subsystem, and a camera controller, separate volume allowances must be made for each subsystem However, it is common practice to design large optical systems either as a reflective systems or as catadioptric systems with folded optics Folding ratios of four to one are common but the primary optics are designed so that the first pupil or folding point has an "f" number of one to one and one half so that the volume of the primary optics is determined by the diameter of the aperture This results

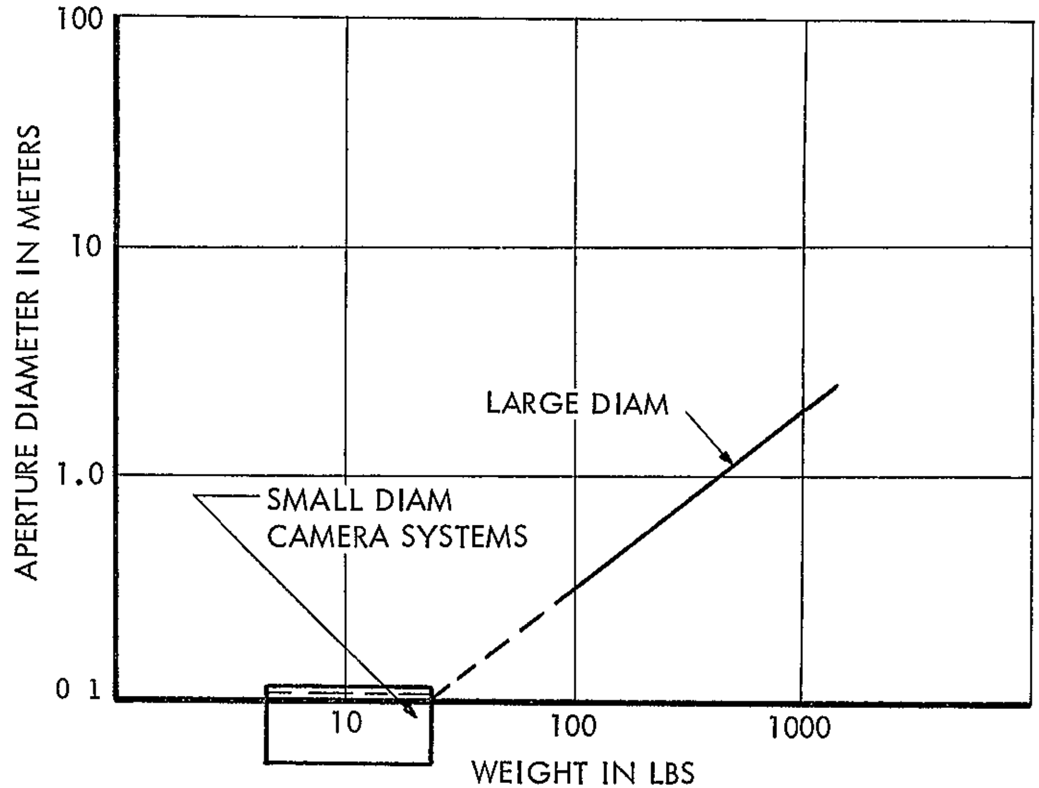

Figure 4-44 TV System Weight as a Function of Optical Aperture Diameter

in a right circular cylinder of diameter approximately ten percent larger than the optical aperture The volume can then be estimated from the expression

$$V_{optics} = 95\ D^3 \tag{25}$$

The television pickup portion of the system is, as before, directly proportional to the weight with a conversion coefficient of 60 pounds per cubic foot

Power Requirements The power required to operate the sensor is basically of two types The electronic circuits associated with camera operation are independent of camera type with the exception of high resolution systems in which extreme care is taken in the electronic design Approximately 5 watts of power are required to operate the electronics including the regulated power supplies In the case of high definition sensors, this figure is doubled so that 10 watts are required

The second principal consumption of power is in TV tube operations Primary power consumption increases in direct proportion to both tube diameter and the quality of the electron optics of the television tube For small, simple cameras, the pickup tube requires approximately the same amount of power as the electronics (that is, approximately 5 watts) but as the tube diameter increases an additional 15 watts per inch of tube diameter is required Thus, for a 1/2 inch tube, 10 watts are required, while for a one inch tube, 15 watts are consumed It is estimated that for a four inch return beam vidicon with high quality electron optics, the power requirement is of the order of 65 watts

Since the principal use of power in high definition systems is in the actual operation of the tube and its associated electron optics, it is doubtful that significant power conservation can be obtained with large scale integrated circuits

Data Output The output from a TV sensor is inherently in analog form For long range communications, it is generally most advantageous to transmit the sensor information in digital form at a rate which may be lower than the sensor output rate These requirements lead to system support requirements which must be selected so as to introduce a minimum loss in information content which is generally specified in terms of loss in resolution An optimum data handling system would thus result in no loss in sensor system resolution but this result can only be obtained with a carefully designed data management and transmission system

Data transmission is not a part of this study so that it is not possible to define a data management subsystem However, data handling requirements can be established in a broad sense based on the characteristics of the sensor output data

As discussed previously, the output analog signal bandwidth required is given by

$$\Delta f = \frac{2bAf_r^2}{t_f}$$

Three characteristics determine the output video bandwidth required, that is the sensor area scanned, A, the resolution of the sensor, f_r, and the readout time, t_f Once the sensor characteristics, that is the resolution and image area, are selected, the only parameter of choice is the readout time, t_f As indicated in Table 4-11, there are characteristic readout times associated with sensor types so that there is not always a wide latitude of choice in selecting a readout time, especially for high resolution tubes To reconcile the conflicting requirements of wide bandwidth and long readout times, it is common practice to select sensors which are compatible with slow scan readout

It is clear from the data in Table 4-11 that a return beam vidicon with an ASOS photosensitive surface offers the best compromise between high resolution and slow scan readout While the capability of slow scan operation may not be the only criterion for selecting a given sensor type, it is obvious that extremely wideband data will be generated by the combination of large image area, high resolution, and fast readout This is evident in Figure 4-45 which is a plot of bandwidth as a function of readout time for several combinations of sensor resolution and scanned area Unless slow scan operation is used, electrical bandwidths of several megahertz are required

As a general rule, thick sensitive surfaces have poor image charge retention characteristics so that it is necessary to scan at a rate which is close to the optimum scan rate If rates either slower or faster than the optimum scan rate are used, then a loss in resolution results Since faster rates are not significant, there is a basic question of the longest storage time which can be used without significant loss in sensor resolution A 10 to one increase in storage time does not significantly degrade sensor resolution so that for a 10 second characteristic time, a maximum readout time of 100 seconds can be used as a bandwidth conservation scheme. This would result in a loss of inherent resolution of 10 to 15 per cent, but will reduce

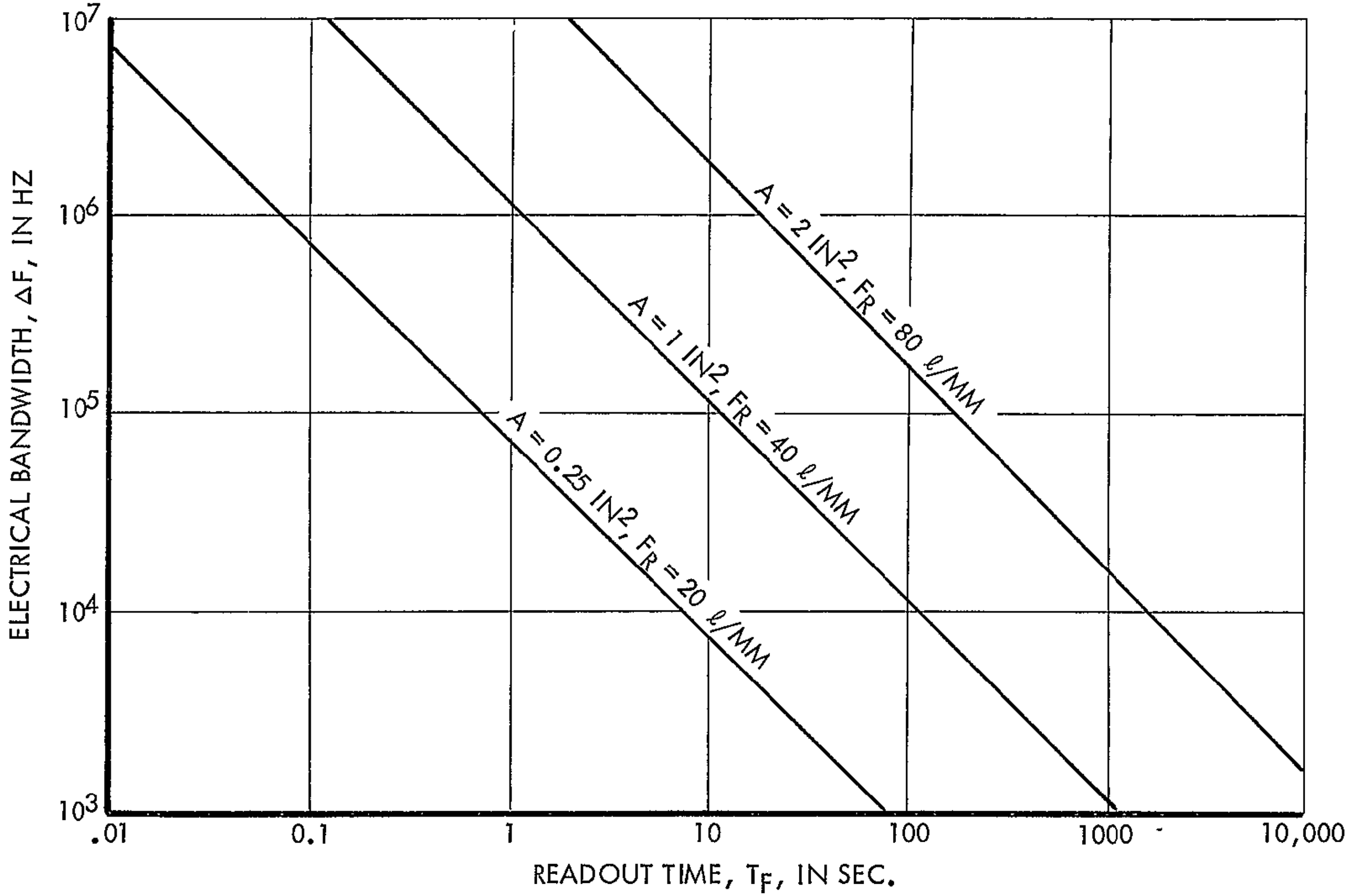

Figure 4-45 Bandwidth Requirements as a Function of Readout Time

the required bandwidth by an order of magnitude. Just what degradation is acceptable is beyond the scope of the scaling law but it is obvious that very wide bandwidth output signals result in very complex data handling systems If digital storage and communication are assumed, it will be necessary to have wide band analog to digital converters for wide band video signals While such devices are feasible, they have limited dynamic range so that it would be necessary to develop a conversion system which meets wideband, high dynamic range requirements.

The bandwidth of the output video signal from the sensor determines the data rate Thus, Figure 4-45 can be used to establish the trend in data rate per image Difficulties arise when a direct conversion from analog bandwidth to bits per second is attempted In data transmission it is common practice to characterize digital systems as bandwidth conservation devices However, from the point of view of data conversion it follows directly that the data rate in bits per second is determined directly by the number of resolution elements in the image and the dynamic range Thus, if there are N TV lines in the image there are N^2 picture elements in a square image If it is required to retain k shades of grey in the image data, then the data rate per image is

$$\text{Data Rate/Image} = G\,N^2 \text{ bits/image} \tag{27}$$

where G = number of binary bits required to represent k shades of grey and if the image is scanned in t_f seconds, then

$$\text{Data Rate} = \frac{GN^2}{t_f} \text{ bits/second} \tag{28}$$

Thus, if a 0 25 in^2 area 500 line TV system is scanned in one second with 64 shades of grey (6 bits) then the data rate is

$$DR = \frac{6 \times 2\ 5 \times 10^5}{1} \text{ bits/second} = 1\ 5 \times 10^6 \text{ bits/second} \tag{29}$$

However, the analog bandwidth of the video amplifier is, from Figure 4-45, approximately 80 kilohertz so that there is not a one to one correspondence between the analog waveform and its digital representation

Image Motion Compensation The requirements for image motion compensation are basic to the generation of imagery of a given resolution. An inherent conflict exists between image motion during exposure and the duration of the exposure time It may be required to have long exposure times and with certain television pickup tubes it is desirable to have continuous exposure On the other hand, there are basic difficulties in obtaining higher and higher levels of image motion compensation which consists of angular motion due to translation of the image sensor plane and the steadiness of the sensor mount during exposure

Linear image motion compensation can generally be accomplished by a single axis correction of the angular motion This leads to requirements for so-called V/H sensors which generate a control signal to maintain a constant look direction for the image plane during exposure This can be accomplished in many ways, either actively or by direct computation Linear motion compensation of as much as 95 per cent is current state-of-the-art so that residual errors are small

A severe limitation is imposed by the random angular motion resulting from uncontrolled and frequently uncontrollable vibrations of the sensor mounting structure If the sensor is mounted on a gimbal to isolate it from the spacecraft, then the limit cycle of the gimbal mount produces residual, random motion of the image plane. Likewise, if the sensor is hard mounted to the spacecraft, then the attitude control system of the spacecraft may have a limit cycle so that the results are not significantly different Any moving parts on the spacecraft will generate motion noise in the sensor during exposure

It is extremely difficult to trade off random motion compensation against resolution at the outset of a system design since it is handled most meaningfully as a modulation transfer function in the sensor system MTF chain As shown in Figure 4-34 in the discussion of the MTF approach to sensor system design, linear image motion has a modulation transfer function which is given in normalized form by

$$T(k) = \frac{\sin \pi a k}{\pi a k} \tag{30}$$

where

a is the magnitude of the uncompensated image motion in the image plane in millimeters

k is the spatial frequency

The quantity "a" is a function of the focal length, f, the angular rate, ω, and the exposure time, Δt_e, in the form

$$a = f \omega \Delta t_e$$

It is first necessary to determine the optical parameters and the exposure time before placing requirements on the linear motion compensation

Experience has shown that random motion is generally the most severe uncompensated motion encountered in imaging sensors As shown in Figure 4-35 random image motion due to mount unsteadiness is given by an MTF in the form

$$T(k) = e \left(2\pi^2 a^2 k^2\right) \qquad (31)$$

where k is the spatial frequency and "a" is the rms value of random image motion in the image plane As before, it is given by

$$a = f \omega \Delta t \qquad (32)$$

but now ω is the rms value of the angular steadiness of the sensor mount

Typical values for ω are in the range of 50 to 500 arc seconds per second which may present difficulties when long focal lengths or long exposure times or both are required It has been estimated that with a sophisticated servo system or an extremely "tight" spacecraft control system, the mount steadiness can be reduced as low as 5 arc seconds per second but this level of control would require significant development

Actual specification of image motion compensation is properly a part of the design procedure since uncompensated motion is a basic quantity to be traded off in the manipulation of MTF's, focal length, and exposure time to arrive at a complete system specification For estimating purposes, the quantity "a" may be used with the requirement that the total motion not exceed one TV line

Since

$$a = f \omega \Delta t \qquad (33)$$

and one TV line represents one half of an optical line pair then "a" in millimeters is given by

$$a = \frac{1}{2f_r} \tag{34}$$

where f_r is the sensor resolution in lines per mm

Therefore, for estimating purposes

$$\omega = \frac{1}{2f_r f \Delta t} \tag{35}$$

This represents the total allowable uncompensated image motion If it is required to specify the motion compensation and mount steadiness separately, the two values of ω are combined as an rss

$$\omega_t = \sqrt{\omega_1^2 + \omega_2^2} \tag{36}$$

where

ω_t is the total allowable angular motion degradation

ω_1 is the uncompensated image translation

ω_2 is the mount steadiness

The two types of motion may be apportioned to remain within the allowed degradation

The first order procedure given above has basic limitations because it is based on the assumption that adequate image forming light is available to obtain the limiting resolution of the TV tube with reasonably short exposure times Furthermore it assumes high scene contrast System degradation can be estimated as a function of exposure or low scene contrast from Figure 4-38 However, if a detailed tradeoff analysis is required, then the procedure given below must be followed It is particularly appropriate for large area, high definiton TV tubes of the RBV type with ASOS photo surfaces where adequate data on tube performance is available It can be used for other TV tube types but it is at best an approximation since it is difficult to predict the quantum limited resolving power function based on manufacturer's data Likewise the modulation transfer function of the electron optics can only be approximated. If no other data are available, then the modulation transfer function of the 2-mil aperture shown in Figure 4-31 should be used Understanding the approximate nature of the approach, the procedure detailed in Figure 4-46 can be followed

FIGURE 4-46

IMAGE FORMING SYSTEM SCALING LAW

I DETERMINE MISSION IMAGING REQUIREMENTS AND LIMITATIONS

1 Planetary mission geometry and dynamics

A Range from spacecraft to planet surface

(1) First encounter (longest range at which imagery is to be obtained)

(2) Minimum altitude at either of the following

(a) Perigee

(b) Terminator is just out of the geometric field of view

B Time available for imaging planet visual surface

C Spacecraft velocity relative to planet visual surface

2 Establish available image forming light level

A Solar constant at planet

B Planetary reflectivity (Albedo)

C Reflectivity model

D Compute available light level as a function of viewing geometry

FIGURE 4-46 (Continued)

3. Delineate imagery requirements

A Visible surface spatial resolution

(1) Best

(2) Minimum acceptable

B Visible surface coverage required

(1) Minimum acceptable

(2) Overlap and nesting requirements

(3) Location preference, latitude, longitude

C. Spectral range if different from visible spectrum

(1) Spectral band(s)

(2) Spectral resolution

(3) Simultaneous versus sequential spectral coverage.

II DEFINE SENSOR SYSTEM REQUIREMENTS

1 First order design procedure (static conditions)

A Assume characteristics of high definition T V. camera (Figure 4-32) to establish resolving power function (f_r)

B Based on available image forming light, compute the required exposure time to meet the resolving power requirements for both high contrast and low contrast scenes

(1) Assume diffraction limited optics and compute the exposure, E, as a function of exposure time, t_e, with aperture ratio, N, as a parameter from the expression

$$E = \frac{B\tau t_e}{4 N^2}$$

FIGURE 4-46 (Continued)

where B is the scene luminance at the planet from I 2 above

τ is the optical transmittance, taken as 0 9 for high quality potics

Use values of N greater than 4 Limit the value of E to twice the mean exposure value indicated in Figure 4-32.

(2) Select values of f_r from Figure 4-32 according to the following criteria

(a) Scene contrast (modulation) expected

(b) Exposure time, t_e Observe that exposure time for single exposure operation (which is assumed) cannot be extended indefinitely due to charge leakage at the photosensitive surface For the data given in Figure 4-32, an exposure time of 2 seconds or less is indicated

(3) Select one or more values of aperture ratio, N, to obtain the selected value of f_r for a range of exposure times, t_e Notice that N and t_e may be traded for a selected value of f_r

(4) Select an image plane format size For the high definition RBV considered, two basic sizes are available

(a) $125mm^2$ (11 2 x 11 2mm) - one inch dia tube

(b) $2500mm^2$ (50 x 50mm) - 4 5 inch dia. tube

Intermediate format sizes could be made available if required but high definition tubes in excess of $2500mm^2$ area are beyond the current state-of-the-art

FIGURE 4-46 (Continued)

(5) Determine the optical parameters of the system

(a) The linear object space surface resolution of an optical sensor is given, to a first approximation, by

$$G = \frac{h}{f_r f}$$

where G is the surface resolution

h is the distance to the object space being imaged

f_r is the sensor resolution in optical line pairs per millimeter

f is the focal length of the optical system in millimeters

Note that G is in the same units as h Determine the required focal length from the required surface resolution, the value of f_r, and the distance to the visual surface Note that the focal length is limited to values less than 4000mm (240 inches)

(b) Combine the value of focal length, f, and aperture ratio, N, from II 1 B.(3) above to obtain the optical aperture diameter

$$D_o = \frac{f}{N}$$

(c) Combine the format size of linear dimension, ℓ, with the focal length, f, to determine the field of view of the sensor

$$\tan \alpha/2 = \frac{\ell}{2f}$$

FIGURE 4-46 (Continued)

and determine the linear surface coverage, L, at a viewing distance h from the geometry

$$L = \frac{\ell h}{f}$$

(6) Design Interaction

(a) Depending upon initial and final viewing conditions, it may be necessary to repeat the design procedure several times to arrive at a tentative design which meets mission requirements in at least one or more major objectives

(b) If a state-of-the-art limited design does not meet mission requirements, the following design choices are available

(1) Reduce viewing distance

(2) If appropriate, use more than one TV camera system to obtain the required combination of surface coverage and surface resolution

(3) Use a combination of TV camera systems with varying fields of view and surface resolution to obtain a compromise between coverage and visual surface resolution

III SYSTEM DESIGN REFINEMENTS

The procedure given in II above does not cover the dynamics of image motion during exposure To a first approximation, motion in the image plane of the instantaneous field of view is given by

$$a = f \omega t_e$$

FIGURE 4-46 (Continued)

where a is the motion of Airy Disc in the image plane

ω is the angular rate of the optical axis in rad/sec

f is the focal length

t_e is the exposure time

Depending upon the value of "a" the resolution of the resulting imagery may be degraded To compute "a" for the selected values of "f" and "t_e" determine "w" as follows

1. The angular rate of the line-of-sight is made up of two parts the linear motion component, and the sensor mount steadiness component The two components, assumed to be independent, are combined by rss to establish a total value of w

2. Linear motion in the image plane during exposure results from an angular rotation of the optical line of sight at a rate given by

$$\omega_1 = \frac{V_H}{h}$$

where V_H is the horizontal velocity of the object plane resulting from

ω_I the spacecraft velocity, and the rotation of the planet

h is the view distance

A large part of the horizontal motion may be removed by image motion compensation (IMC) State-of-the-art limits on IMC are 95 percent compensation with suitable computation and sensing An uncompensated component of linear motion results from a change in viewing distance during exposure when the direction of look is oblique (see the discussion in Ref 11, pp 98-99)

3 Random motion in the image plane during exposure results from sensor mount unsteadiness in the form

$$w_2 = \sigma$$

FIGURE 4-46 (Continued)

where σ is the rms value of the mount steadiness Values of σ may range from 500 arc seconds per second for a conventional sensor mount to as small a value as 5 arc seconds per second for a state-of-the-art projected multiple control loop system with external supervision

If sensor mount steadiness requirements are severe, then a major impact on support requirements results since it may be necessary to mount the complete sensor package on a gimbal structure The trend in power required to support large diameter optics on a gimbal is indicated in Figure 4-8

4 The total uncompensated angular motion is

$$w_T = \sqrt{w_1^2 + w_2^2}$$

5 The value of "a" which results from the angular motion may be used to establish a dynamic value of f_r or the image motion limit may be established so as not to degrade f_r. The criterion used to prevent significant degradation of f_r is

$$a \le \frac{1}{2 f_r}$$

Within state-of-the-art limits, several design choices can be made but if the criterion on "a" is not met then it is necessary to accept the value of "a" as the limiting resolution and reiterate the design beginning with Step II above

IV SUPPORT REQUIREMENTS

Establish the support requirements for the TV system given in Paragraph 4 3 2 3 under "Support Requirements" making certain that, if a gimbal is used to obtain extended exposure time, the power to control the gimbal is included in the Power Requirements Also observe that if more than one camera is used to obtain extended surface coverage, then the support requirements must be multiplied by the number of cameras used

FIGURE 4-46 (Continued)

V MULTI-SPECTRAL IMAGERY

With minor adjustments, the procedure given above can be used to establish support requirements for a TV system when spectral filtering is used The procedure given in Steps I through IV above are to be followed with the following adjustments

1 Recompute the value of the exposure under the assumption that the spectral band-pass filter in each spectral region has a rectangular response characteristic The response of the filter is assumed to be unity over the spectral range The value of the irradiance can be determined from a numerical integration of the solar spectral irradiance (Figure 4-1) integrated over the spectral passband of the filter and scaled to the distance of the planet from the Sun In computing the exposure, decrease the optical transmission to 0 8 to account for filter scattering loss To account for the spectral response of the photodetector (assumed to be ASOS) scale the value of irradiance by the average value at spectral band center of the "standard observer" curve *

VI HIGHER ORDER DESIGN PROCEDURE

The procedure given above is based on the assumption that a relationship between exposure and resolving power has been established For other TV sensor types or for complete specification of the high definition type considered, a more complete system design may be required The procedure is tedious but essentially straightforward provided that an adequate description of the sensor is available It is recommended that references 9 and 11 be followed for the detailed computation required since the procedure given below is based on the procedures developed in the references

The design procedure is summarized below

1 Establish modulation transfer functions for each of the principal components of the camera system to include at least the following (a) Optics, (b) Television tube electron optics, (c) Image motion and

---

* The standard observer curve is well approximated by the shape of the irradiance curve of Figure 4-1 with a scaled value of one at λ = 555 micron. If other photosensitive surfaces are used, perform the numerical integration of the product of the spectral irradiance and the relative spectral response of the photosensitive surface

FIGURE 4-46 (Continued)

mount steadiness If TV tube characteristics are unknown, estimate electron optics MTF Use the standard 2 mil aperture reading beam for conventional tubes or if new developments are indicated, the MTF of either the so-called "super beam" with a 0 7 mil aperture or the high resolution beam with a 1 mil aperture are used It is not recommended that the MTF's for image motion and mount steadiness be included in the design process until exposure time has been established at least tentatively This will require iterative application of this procedure until a suitable composite MTF has been established

2 Determine the image plane illumination available as a function of geometry, spectral bandwidth, and optical parameters This will be a function of exposure time so that several values of exposure time must be selected to feed back into step (1) above for generating motion MTF's Likewise, the dynamic range of the image plane illumination is established in this step to assure compatibility between sensor characteristics and exposure levels

3 Compute the quantum limited resolving power function of the sensor based on the data of step (2) above and the procedure given in Ref 9 This implies one additional exercise of judgment since it is necessary to estimate the object plane contrast Latitude of choice exists but it is common practice to first assume high contrast conditions (that is $m_o = 1$) and then "test" the design for low contrast (that is $m_o = 0\ 1$) However, if a reasonable estimate of scene contrast can be made at the outset then this value should be used in computing the quantum limited resolving power function

4 Graphically establish the system resolving power function by combining the quantum limited resolving power as a function of exposure with the camera system MTF including, as appropriate, the MTF's of image motion and mount steadiness to establish the functional characteristics of the camera

5 Define the optical parameters compatible with sensor requirements to establish field of view, aperture diameter, focal length, format size, etc

6 Establish support requirements based on the system design steps See Para 4 3 2 3

---

* These data are only available for a limited number of tube types If not available, use vidicon or image orthicon data depending upon light sensitivity of photosensor

4 3 3 Scanning Image Forming Systems

4 3 3 1 Design and Performance

Image forming sensor systems based on discrete detectors can have many forms They may range from a large rectangular array of discrete detectors to a single detector which is scanned in one or two dimensions Scanning system configurations have proliferated as a result of the large number and range of functions which scanned systems can be postulated to perform Both object plane and image plane scanners have been proposed but the most common type is the object plane scanner Image plane scanners, while advantageous from the point of view of reduced mechanical scan requirements are generally difficult to mechanize both optically and mechanically They have not found wide application so that object plane scanning is the only type considered as realistic for planetary investigations

Even for object plane scanners, the number of possible detector array-scanner configurations is large Most image forming scanning systems for spacecraft and aircraft use a single axis mechanical scan device which scans transverse to the direction of the velocity vector Several detectors are arranged in a linear array in the direction of motion to reduce scan speed requirements Alternatives to mechanical scan are the so called push-broom configurations in which a linear array of detectors is arranged perpendicular to the direction of motion A two dimensional image is obtained by the forward motion of the vehicle

Push-broom scanners, while conceptually simple, are basically limited by the largest linear array which can be built and the inherently poor spatial resolution The problem is further compounded if the detectors require cryogenic cooling since any temperature gradient across the array could result in false signals or signal loss In addition, since each detector would have a separate output, the stability and matching of the detectors would impose severe design problems As indicated previously, most IR detectors operate stably only when the input is chopped or modulated This implies a-c coupling at the output of the detector and for impedance matching purposes transformer coupling is usually required The overall problem is then one of circuit components limiting the design approach The net result is that the inherent limitations of detector technology generally preclude the use of long linear arrays in a push-broom configuration

The limitations of long linear arrays apply to rectangular arrays of detectors The resolution of a rectangular array is determined by the smallest detector which can be built while the object plane area covered is determined by the largest array area which can be assembled Arrays as large as 100 x 100 elements of detector sizes in the range of 0 1 millimeters are claimed to be feasible but the overall problems of such arrays have not been solved in any real or postulated system It might be assumed that a large array of IR detectors might be useful for planetary investigations to obtain even a crude thermal or spectral radiance map However, the problems of balancing or referencing each detector to a common level and maintaining uniform response of all the detectors preclude active consideration of large detector arrays for planetary investigations

The most frequently used form of imaging with discrete detectors is a mechanical scan system in combination with one or more detectors in a linear array oriented in the direction of vehicle motion The resolution of such systems is still limited by the smallest size detector that can be placed in the image plane A moderately long array in the direction of motion greatly reduces the requirement for high scan speed Up to 10 detectors can be arranged in a linear array and since the detectors are in line with the direction of motion, the effective scan speed requirements are divided by the number of detectors

This approach has other advantages, since any system of discrete detectors which are scanned is limited by the response time of the detector and the information bandwidth of the output amplifier Most currently used detectors have response times of the order of 10 microseconds or less so that response time is generally not a limitation However, if τ is the time available for a resolution element in the object plane to pass through the instantaneous field of view of the optical system at the detector, then the minimum electrical bandwidth without significant signal loss is

$$\Delta f = \frac{1}{2\tau} \tag{37}$$

In terms of the scan rate this can be expressed as

$$\Delta f = \frac{\theta F}{2 \ell} \tag{38}$$

where

θ is the angular scan rate in radians per second

F is the focal length of the optics

ℓ is the detector linear dimension in the same units as F

Since Δf is the approximate noise bandwidth it is advantageous to operate at as low a scan rate as possible to maintain high signal-to-noise ratio

Image forming systems based on discrete detectors are most commonly used in spectral regions where television systems do not perform They are most frequently used in the IR portion of the spectrum as thermal mappers to detect the thermal self emission variations or the reflected solar radiation in the object plane From the system design point of view the two cases are not essentially different but thermal mappers are most frequently described in terms of the minimum detectable temperature difference which the mapper can detect in a given spectral region Performance is then specified either as the minimum detectable temperature difference or as the noise equivalent temperature difference (NEΔT) The NEΔT represents a temperature change in object space which results in a signal-to-noise ratio of one It can be shown that the NEΔT is given by

$$NE\Delta T = \frac{NEP}{W\frac{\partial H}{\partial T}} \qquad (39)$$

where

NEP is the noise equivalent power

W is the instantaneous field of view solid angle of the detector

$\frac{\partial H}{\partial T}$ is the slope of the blockbody radiance curve of temperature T in the spectral region of interest

For mapping an extended object plane which is illuminated by an external source such as solar illumination, which is reflected selectively, a somewhat more involved procedure may be required If the reflection process of the solar radiation is independent of frequency, then the procedure used in describing mapper performance is the same as for thermal mapping The reflected solar radiation can then be considered as a thermal source of equivalent block body temperature equal to the sun, approximately 5000 degK, to establish the spectral content The intensity of the radiation is determined by the distance from the sun, the viewing geometry and a simple reflection coefficient This procedure is probably sufficient for planets without a gaseous atmosphere but care must be exercised when the reflection process is highly spectrally dependent Highly spectrally dependent reflection and transmission processes are characteristics of gaseous atmospheres and are further complicated when particulate matter in the form of dust, aerosols and condensates are present Even crude estimates of system performance are difficult to establish For these reasons the performance is generally estimated in terms of the voltage signal-to-noise ratio in the form

$$\frac{Vs}{Vn} = K \frac{\int_{\lambda_1}^{\lambda_2} D^{*} (\lambda)\ W (\lambda)\ d\lambda}{\left[A_d \Delta f\right]^{1/2}} \tag{40}$$

for detectors which are described by D* and

$$\frac{Is}{In} = \frac{\left[K \int_{\lambda_1}^{\lambda_2} R (\lambda)\ \ W (\lambda)\ d\lambda\right]^{1/2}}{\partial e \Delta f} \tag{41}$$

for detectors which are characterized by a responsivity, R The spectrally dependent function W (λ) is the equivalent signal radiant power which may be an extremely complex function so that the integral of the product of the detector response and the source power require numerical integration

As with any sensing system which results in an image, the question of specifying performance presents certain difficulties Theoretically a mapping system can be described in terms of a modulation transfer function, the scene modulation or contrast and the minimum detectable difference signal-to-noise ratio However, an equivalent resolving power function for a discrete detector imaging system does not have the same meaning as for a continuous system such as TV because the spatial resolution is determined by the smallest detector which can be used The problem is more one of minimum detectable signal-to-noise ratio For visual imagery, this difference is 3 6 so that two resolved areas which exceed a threshold, can be distinguished as different in temperature or different in spectral reflectance if the signal-to-noise ratio differs by at least 3 6 The threshold is partly subjective but a value of 3db is commonly used The number of steps of contrast or reflectance difference which can be distinguished is then a function of the overall signal-to-noise ratio

4 3 3 2 Scanning Imaging System Scaling Laws

The scaling laws for scanning optical systems using point detectors are conceptually similar to non-image forming optical instruments with three different features

1 A scanning mechanism, usually in the form of a scanning mirror, is added to scan the optical aperture of the sensor telescope in a direction transverse to the direction of motion of the spacecraft surface velocity vector

2 The time constant of the detector or detectors is significant because the available observation time is limited by scan velocity The concomitant to this is the bandwidth of the electronics which must be relatively wide to allow contiguous coverage of the object field

3 The resolution, spatial, spectral, or temperature is relatively crude Spatial resolution is limited by the smallest detector size obtainable while spectral and temperature resolution are limited by the integration time Integration time can be increased by using a linear array of detectors oriented in the direction of motion but the longest feasible detector array is of the order of 10 detectors of the photoconductive and photovoltaic type For the visible spectrum this restriction may be alleviated by the use of fiber optics to transmit light from the telescope focal plane to the sensitive surface of the detector However, fiber optics are lossy with typical transmissivities in the range of 0 6 for a one foot fiber length Low light level may therefore preclude the use of fiber optics to obtain a large array of photomultipliers

The optical requirements and/or arrangements of scanning systems are all similar Functional differences are incorporated in the focal area depending upon specific functions A general concept of a scanner is shown in Figure 4-47 To reduce scan speed requirements an array of detectors can be substituted for the detector-filter wheel shown If a linear array of η detectors is used, then the angular scan rate can be divided by η In addition, various optical arrangements can be used to divide the incident flux into spectral bands Dichroic mirrors are commonly used to divide the flux into the visible-UV regions and the IR In addition, a dispersive prism may be placed at the exit aperture to obtain spectral separation in the visible These techniques are exemplified in the Multi-Spectral Point Scanner (MSPS) of the Earth Resources Technology Satellite (ERTS) program A layout of the optical arrangement is shown in Figure 4-47 Light is transferred from the focal plane of the dispersion prism to an array of photomultipliers by means of fiber optics Preliminary characteristics of the instrument which is currently under development by Hughes Aircraft Corp are given in Table 4-12 The MSPS is intended for multispectral mapping of the Earth from an altitude of 500 miles Light levels are high while orbital velocities are intermediate The scan technique used is to oscillate the external mirror at a 15 Hz rate Referencing or gain control is by means of an external

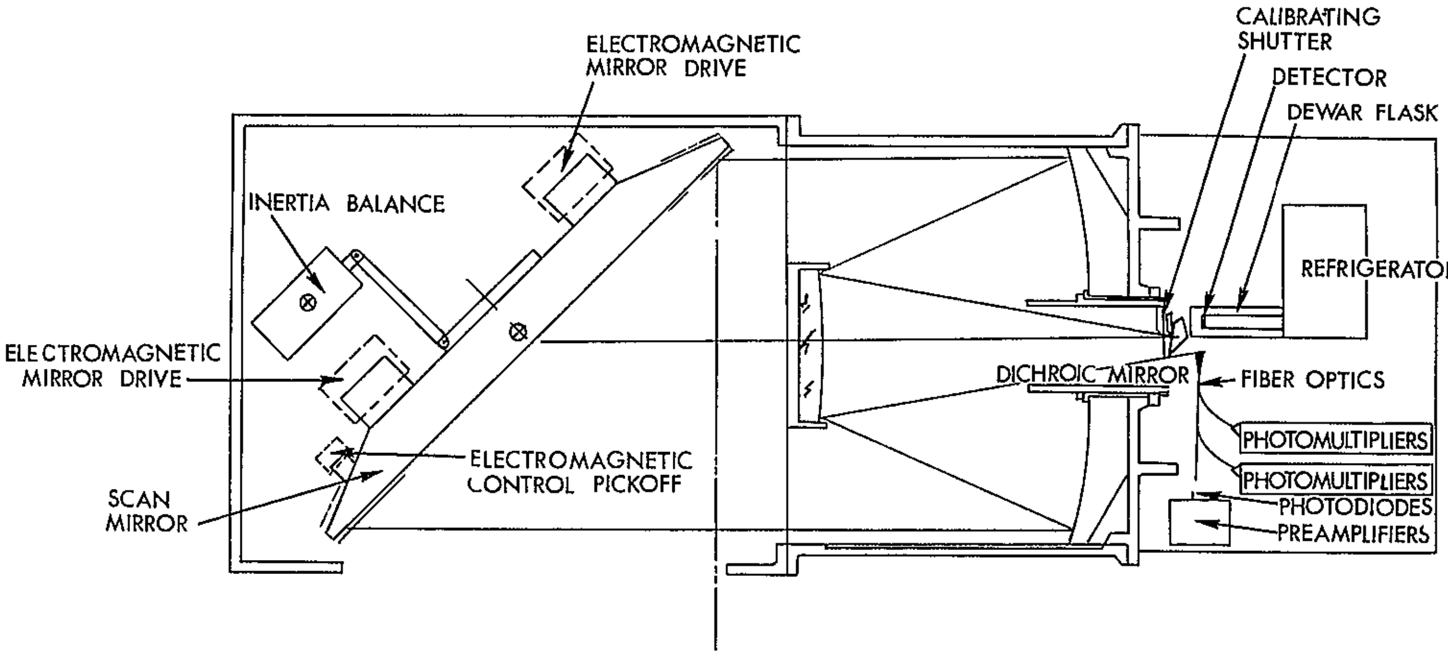

Figure 4-47. Multispectral Point Scanner for ERTS

Table 4-12 Parameters of MSPS for ERTS

Oscillating mirror	Total scan angle ± 3 8 degrees at 15 1 Hz, 13 7 by 9 4 inches Flexure pivots with "speaker coil" drive
Optics	9-inch Cassegrainian with 4-inch secondary mirror, f/3 3
Instantaneous field of view	0 067 milliradian
Spectral bands and detectors	1) 0 5 to 0 6 micron photo-multiplier tubes 2) 0 6 to 0 7 micron photo-multiplier tubes 3) 0 7 to 1 1 micron silicon photodiodes 4) 10 4 to 12 6 micron IR photoconductor
Fiber optics for transmission to detectors	21 ~ 0 002 inch glass fibers
Number of lines scanned/band	7 for bands 1, 2, and 3 2 for band 4
Limiting resolution	~100 feet for bands 1, 2, and 3 ~450 feet for band 4
S/N at 200 feet resol , H=500 nmi	26db at DC spatial frequency ~14 to 18 db (peak to peak/rms)
Noise equivalent temperature	1 degree at 300° K
Temperature for detector	80° K
Weight	~63 pounds for bands 1, 2, and 3 +3 pounds for IR
Power	15 watts, visible +40 watts for IR cooler

mirror which is pointed at the sun The scan mirror "looks" at the reference mirror at the beginning of each oscillation to establish a fixed radiation level at the detectors

Specific scaling laws by function differ principally in the computation of aperture requirements to obtain a given signal-to-noise ratio Since the end result of a scanning system is an image, the requirements for imagery usually impose high signal-to-noise ratio For imagery equivalent to commercial television standards a signal-to-noise ratio of approximately 40 db is required A somewhat lower value of signal-to-noise ratio may still give useful imagery but a minimum value of 20 db is required for interpretation purposes Signal-to-noise ratio calculations, as a function of aperture, are not significantly different for imaging system than those used for spectroscopic computations with the exception that the geometry and scan speed are used in place of the bandwidth to indicate dependence on these parameters However, procedural practices in IR thermal mapper design are usually based on a statement of minimum detectable temperature so that a detailed procedure for thermal mappers is given with appropriate alterations indicated for other spectral regions

Scaling Law for Thermal Mapper The scaling law for thermal mappers is based on the noise equivalent temperature difference NEΔT in a given spectral band at the peak of the blackbody (actually greybody) radiation curve The peak of the thermal radiation can be established from the Stephan-Boltzman radiation law from the known or estimated thermodynamic temperature in the object field The temperatures for the planets are given in Table 4-3

Based on the parameters of the detector and optical system the noise equivalent temperature difference is given by

$$NE\Delta T = \frac{\pi\sqrt{A_d \Delta f}}{\left(\frac{\partial H}{\partial T}\right)_{T,\lambda,\Delta\lambda} A_o \Omega D_\lambda^* \eta} \qquad (42)$$

where

A_d is the area of the detector

Δf is the electrical bandwidth

$\frac{\partial H}{\partial T}$ is the slope of emitted power at a blackbody temperature T, peak wavelength, λ, in the spectral band $\Delta\lambda$ See paragraph 4 2 3

A_o is the area of the collecting optics

Ω is the instantaneous solid angle field of view of the optics

D^*_λ is the specific detectivity of the detector averaged over $\Delta\lambda$

n is the system efficiency

It is customary to express NEΔT in terms of the angular scan speed of the detector and the viewing geometry The bandwidth required is related to the scan speed through the time that it takes one surface resolution element to pass through the field of view of the optics, that is

$$\Delta f = \frac{1}{2t} \tag{43}$$

For a linear array of n detectors the dwell time is multiplied by the number of detectors so that

$$\Delta f = \frac{1}{2nt} \tag{44}$$

For a swath width, W, transverse to the heading direction, a surface resolution, G, a ground speed V_g at an altitude h, the expression for NEΔT can be converted to

$$NE\Delta T = \frac{\pi h^2 \left[\frac{A_d \; W \; V_g}{2n}\right]^{1/2}}{\frac{\partial H}{\partial T} A_o G^3 D^* n} \tag{45}$$

For a given aperture area (A_o), a set of trajectory parameters (V_g, h) and observation requirements (W, G, T,) a detector array of n detectors can be selected to minimize NEΔT The value of n to be used including electronic and optical system losses is of the order of 0 5 For a detector of known dimensions it must be established that the optical system meets the requirement

$$d = N\lambda \tag{46}$$

where

d is the detector linear dimension

N is the optical system aperture ratio

λ is the wavelength of the radiation

This point may seem obscure but it points up the fact that decreasing the ground resolution at a fixed altitude implies decrease in angular resolution or an increase in aperture diameter This procedure cannot be carried out indefinitely without adjusting the optical parameters since for a fixed detector size, ℓ , it follows that

$$\ell = ND_o \alpha \tag{47}$$

where

ℓ is the detector dimension

N is the aperture ratio

D_o is the aperture diameter

α is the angular resolution of the optical aperture

If ℓ is fixed, then the only way to match ℓ to the aperture is through N If N is taken as the aperture ratio of the collecting optics, then extremely long focal lengths would result if the aperture requirements are large to obtain small angular resolution To overcome this limitation it is common practice to use a field lens to reimage the focal plane of the primary optics on the detector The value of N, the so-called "speed" of the optical system, is then understood to be the "f/number" of the field lens There is a basic conflict between spatial resolution determined by the aperture diameter and system sensitivity imposed by the generally large values of N necessary to match the primary optics to the detector

Alternatively, the aperture area required to obtain a given noise equivalent temperature difference at a given surface resolution can be used for scaling purposes In any event, the scaling is accomplished within the state of the art limits given in Table 4-13 The scaling procedure is summarized in Figure 4-48

Table 4-13 State of the Art Limits for IR Thermal Mappers

Aperture Diameter	100 inches
Focal Length	240 inches
Number of Detectors in Linear Array	10
Minimum Detector Size	0 1 mm
Maximum Wavelength	20 μ

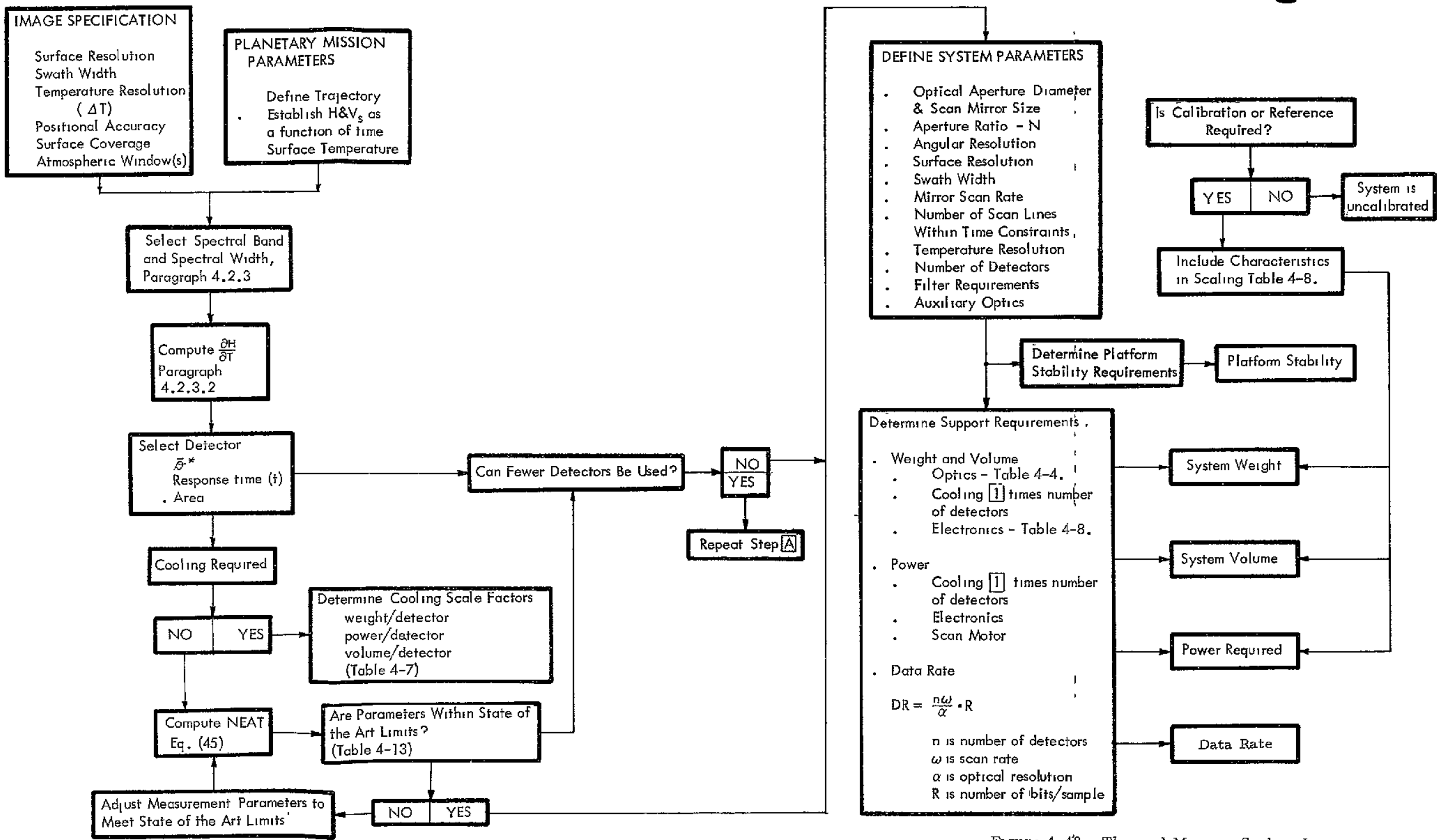

Figure 4-48 Thermal Mapping Scaling Laws

4 3 3 3 Support Requirements

System Weight The weight of the telescope and scanning mirror are determined from the data given in Paragraph 4 2 2 above The weight of the detectors and auxiliary components are determined from Table 4-8 If cooling is required, the scaling factors from Table 4-7 are used

System Volume The volume of the telescope and scan mirror are determined from Paragraph 4 2 2 above The auxiliary components are sized based on the data of Table 4-8

System Power The scan mirror power requirements are determined from Paragraph 4 2 2 above

For the detector array a power consumption of 0 1 watt per detector is required A reference source is generally required so that an additional allowance of 10 watts is made for the source If cooling is required for the detectors, the values given in Table 4-7 are used

Data Rate The data rate of the mapper is determined by the rate at which the instantaneous field of view of the aperture is scanned over the swath width and the dynamic range of the signal In terms of the system parameters this becomes

$$DR = \frac{\omega R}{\alpha} \tag{48}$$

where

ω is the scan rate

α is the angular resolution

R is the dynamic range of the signal

Depending upon the compromise between sensitivity and resolution, the dynamic range is between 4 bits and 6 bits For scaling purposes a dynamic range of 64 shades of grey are assumed so that 6 bits per resolution element are used If more than one detector is used to reduce the scan rate then the data rate becomes

$$DR = \frac{n \omega R}{\alpha} \tag{49}$$

Where n is the number of detectors

Platform Stability The platform stability requirements are determined in the same manner as for TV systems but are computed on the basis of an equivalent exposure time which is given by the dwell time during the scan The stabilization requirements are determined under the assumption that motion in the image plane is limited to one half of a resolution element The uncontrolled angular motion must then be restricted to

$$\emptyset = \frac{\ell}{2\,ft} \tag{50}$$

where

ℓ is the detector size

f is the focal length

t is the equivalent dwell or exposure time

But

$$t = \frac{\alpha}{\omega} \tag{51}$$

where

α is the angular resolution

ω is the scan rate

so that

$$\emptyset = \frac{\ell\,\omega}{2\,f\alpha} \tag{52}$$

4 3 4 Photometers and Scanning Spectrometers for the Visible and Ultraviolet

With suitable adjustments in the orbital parameters and the weight scaling laws for optical systems given in Table 4-4, the procedure given in Reference 2 for UV scanning systems can be used directly to form scaling laws for scanning imaging systems in the visible and UV portions of the spectrum

Several factors lead to specification of required aperture They include, sufficient light gathering for the scan speed dictated by effective ground speed and time available to cover the planet with a given spatial resolution, range from the Sun, light reflected, and the width and central wavelength of the spectral region to be covered

The photometric functions are taken from Reference 2 The aperture size requirement was given in Reference 2, as a function of altitude and surface resolution required

$$r_x = R\Delta\phi \left\{ \frac{\cos \phi}{[(R/R+H)^2 - \sin^2 \phi]^{1/2}} - 1 \right\} \qquad (53)$$

$$r_y = R_s\Delta\phi = \Delta\phi \, R \frac{\sin \gamma}{\sin \phi}, \quad \gamma = \frac{W}{2R} \qquad (54)$$

where r_x and ry are surface resolution values required normal and parallel respectively, relative to the heading direction, $\Delta\phi$ is the angular resolution of the sensor, R is the planet radius, H the altitude, and W is the arc length of a great circle to be covered

If the exit aperture at the image plane is limited by a stop of (δ x) cm diameter, the resolution may be represented by

$$\Delta\phi = \frac{\delta x N}{D_o} \qquad (55)$$

Hence a relation for diameter of the objective mirror follows from the surface resolution and altitude requirement Another relation that would lead to aperture diameter would be light gathering power needed to obtain an acceptable signal-to-noise ratio for a given bandwidth This latter relation is independent of range to the planet for ranges close enough that the image of the planet disk is larger than the exit aperture Therefore, for distant and/or for high speed flyby missions, light gathering requirements may lead to aperture requirements more directly than the resolution requirement Then after determining the aperture required, it may be necessary to adjust mission parameters to obtain the resolution required The light gathering power required is a function also of spectral bandwidth Following Reference 2 (page 57, equation 3-33) the required aperture is

$$Dp = 3 \times 10^{-12} \frac{(S/N)}{\Delta\phi} \sqrt{\frac{\omega}{q \, C_p \, f(i) \, \Delta\phi}} \qquad (56)$$

where

ω is the angular rotation rate of the scan mirror,

q is the photodetector quantum efficiency, (Fig 3-2, Ref 2)

$f(i)$ is the photometric function as a function of solar zenith angle i

C_p is illumination integrated over the bandpass in w/m^2, (see Table 3-1, page 56, Reference 2)

$\Delta\phi$ is the angular resolution, and

(S/N) is the signal-to-noise ratio (10 db for high contrast, 40 db for low contrast targets)

For the planets not covered in Reference 2, follow the procedure given in Section 4 2 2 of this report to determine equivalent values of C_p

4 3 4 1 Support Requirements

System Weight The weight of the telescope and scanning mirror are determined from the data given in Paragraph 4 2 2 above The weight of the detectors and auxiliary components are determined from Table 4-10

System Volume The volume of the telescope and scan mirror are determined from Paragraph 4 2 2 above The auxiliary components are sized based on the data of Table 4-10

System Power The scan mirror power requirements are determined from Paragraph 4 2 2 above

For the detector array, a power consumption of 0 1 watt per detector is required

Data Rate The data rate of the mapper is determined by the rate at which the instantaneous field of view of the aperture is scanned over the swath width and the dynamic range of the signal In terms of the system parameters this becomes

$$DR = \frac{\omega R}{\alpha} \quad (57)$$

where

ω is the scan rate

α is the angular resolution

R is the dynamic range of the signal

Depending upon the compromise between sensitivity and resolution, the dynamic range is between 4 bits and 6 bits For scaling purposes a dynamic range of 64 shades of grey is assumed so that 6 bit per resolution element are used If more than one detector is used to reduce the scan rate then the data rate becomes

$$DR = \frac{n \omega R}{\alpha} \quad (58)$$

where n is the number of detectors

Platform Stability - The platform stability requirements are determined in the same manner as for TV systems but are computed on the basis of an equivalent exposure time which is given by the dwell time during the scan The stabilization requirements are determined under the assumption that motion in the image plane is limited to one-half of a resolution element The uncontrolled angular motion must then be restricted to

$$\phi = \frac{\ell}{2\, ft} \quad (59)$$

where

ℓ is the detector size

f is the focal length

t is the equivalent dwell or exposure time

But

$$t = \frac{\alpha}{\omega} \quad (60)$$

where

α is the angular resolution

ω is the scan rate

so that

$$\phi = \frac{\ell \omega}{2 f \alpha} \quad (61)$$

Logic for Estimation of Size of Photometric Systems - A logic flow diagram for the design of visible and UV photometric sensor systems is presented in Figure 4-49

Entry to the logic system begins with specification of surface resolution and planet coverage requirement goals The nominal required optics size versus bandpass relations are computed for the mission Surface resolution versus areas of the planet covered are tabulated and compared with the input goals

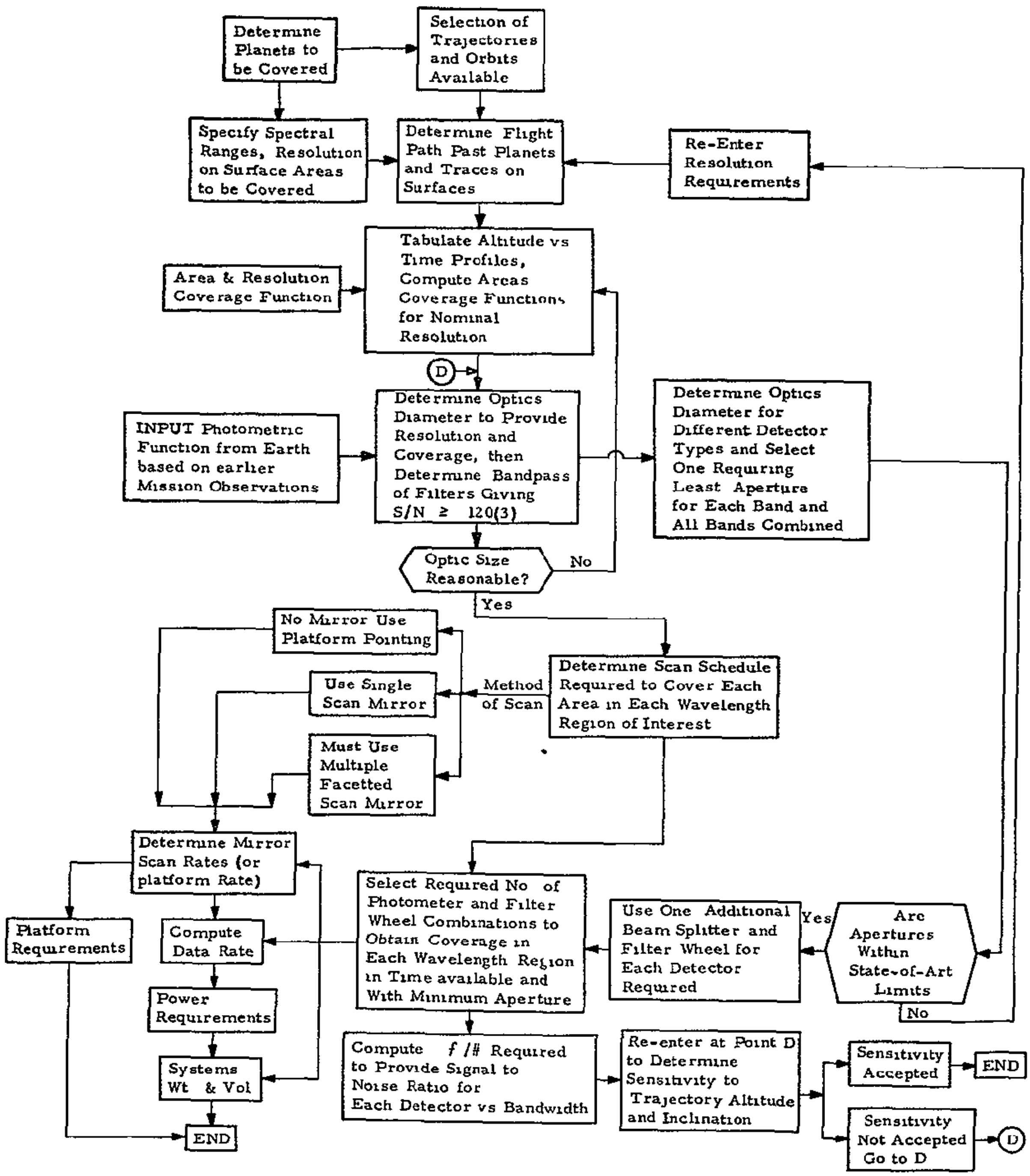

Figure 4-49 UV and Visible Photometer Design Logic Flow Diagram

4 4 ACTIVE OPTICAL INSTRUMENTS

4 4 1 Introduction

Active optical instruments could conceptually encompass as many instrument types as are available in active microwave sensors However, the state-of-the-art of coherent electromagnetic energy generation in the optical spectrum limits the types of instruments used to essentially "range only" devices which are essentially laser radar or "lidar" The closest approximation to a lidar in the microwave region is the radar scatterometer However, there are significant differences in both technologies so that the design procedure for laser systems is generally a mixture of pulsed radar transmitter system design and passive optical receiving system design

4 4 2 Lidar Systems

While advances in laser technology have been rapid, the following significant features differentiate between radar and lidar technology

1 There are no satisfactory duplexing or diplexing techniques available at optical frequencies so that separate transmitting and receiving apertures are required for lidar

2 No satisfactory coherent modulation-demodulation techniques such as frequency or phase modulation are available at optical frequencies Therefore, pulse compression techniques for improved range resolution cannot be used

3 While the carrier frequency of lasers is coherent, the modulation is basically non-coherent amplitude modulation and the detection is non-coherent envelope detection

4 The duty cycle of lasers is low so that pulse repetition rates are generally in the range of one in 10 second to one per second Likewise, while efficiency per pulse has been improved markedly, high PRF operation is basically confined by heat transfer limitations

The basic similarity between lidar and radar is that system design is based on a set of deterministic equations with external constraints in the form of required functions such as range and/or range resolution or in system limitations such as peak and average power capabilities The scaling of lidars then follows a straightforward procedure with few design iterations required

4 4 2 1 Design and Performance

A lidar consists of a pulsed laser and a sensitive receiver mounted in close proximity The laser emits a pulse of monochromatic radiation of duration τ (sec), wavelength λ (microns), power P_t (watts), and a field beamwidth θ_r (radians) A small fraction of the outgoing beam is directed with a beam splitter for monitoring and timing purposes. Radiation back-scattered from aerosols, atmosphere, etc , is collected by a telescope with effective aperature A_r and acceptance angle θ_r The output of the telescope is passed through a narrow-band filter (of bandwidth $\Delta\lambda$) to the cathode of a photomultiplier or solid state detector The output of the detector, when properly calibrated, gives information on the properties of the medium which backscatters the pulsed radiation

It may be concluded from the considerations set forth in the rest of this section, that the best lidar system performance under sunlight conditions is obtained by maximizing E_L and A_r, minimizing θ_t, keeping θ_r nearly equal to θ_t, choosing the largest pulse width τ consistent with acceptable range resolution, and matching the receiver video bandwidth to the pulse

The intensity I_r of the backscattered laser light is given by

$$I_r = \frac{E_L \beta C}{2R^2} \tag{1}$$

where E_L is the laser energy, β the backscatter coefficient, $C = 3 \times 10^8$ m/sec is the speed of light and R is the range The backscatter coefficient β is a complicated function of the molecules, aerosols, dust particles, etc , in the scattering volume and an estimate of its magnitude is required For estimating purposes, the nominal value for earth-clouds of $\beta = 10^{-3} m^{-1}$ steradian^{-1} will be used

It is interesting to note that the intensity of the backscattered light is proportional, not to the intensity of the laser beam, but to its total energy E_L This result is true for extended targets which fill the instantaneous field of view of the receiving optics It differs from the usual $1/R^4$ radar equation because most targets are point reflectors with small angular extent in the radar case

Receiver sensitivity is an important factor in overall lidar design The type of receiver depends upon the wavelength to be detected For ruby (λ = 0 694 microns) or Neodymium (λ = 1 06 microns) photo-multipliers appear to be the best choice Many types are available, but RCA types 7265 and 7102 (or equivalent) appear to be nearly optimum for ruby and neodymium respectively The maximum sensitivity of these tubes is given in Table 4-14 CO_2 lasers (λ = 10 6 microns) on the other hand must be detected by other means To obtain maximum sensitivity, a cooled solid state detector is required The nominal sensitivity of such a device is given in the table in terms of responsivity

Background noise is mainly a result of sunlight reflected from the planet Since a narrow bandpass filter is used in the receiver, only that part of the reflected spectrum which falls within the passband of the filter need be considered The maximum intensity I_s of the reflected light is given by the relation

$$I_s = \frac{\Phi(\lambda)\rho\Omega_r\Delta\lambda}{4} \qquad (2)$$

Where $\Phi(\lambda)$ is the differential spectrum of the sun at the planet (watts/m^2 -Å), ρ the reflectivity of the planet (approximately equal to the albedo), Ω_r solid angle field of view of the receiver telescope, and $\Delta\lambda$ the width of the filter For any meaningful results, $I_s < I_r$ For design purposes a value of

$$\frac{I_r}{I_s} > 10 \qquad (3)$$

is used to obtain good signal/noise ratio

Spatial resolution is determined by the divergence angle θ_t and θ_r of the transmitter and receiver respectively If these are nearly the same, as efficient design would dictate, the length, r, of the detected area is given by

$$r = R\ \theta_r \qquad (4)$$

where R is the range to target

In practice, the laser far-field divergence angle is too large for the missions under consideration, being 1-5 milliradians The situation can be improved by the use of a beam-expanding telescope For a telescope of magnification M, the resulting improvement in θ_t is by the factor 1/M Practical considerations limit M to 20 or less, which results in $\theta_t \leq 0$ 2 milliradians

Table 4-14 Detector Types for LIDAR

Detector Type	Wavelength	Sensitivity	Noise Equiv Power
PM tube, S-20	0 694	2 6 x 10^5 amp/watt	**1 pw
(RCA 7265)		260 volt/watt	(25°C)
PM tube, S-1	1 06	340 amp/watt	55 pw
(RCA 7102)		*0 34 volt/watt	(25°C)
Solid State	10 6	0 01 volt/watt	0 1 pw
			(at 77°K)

*using a load resistor of 1000 ohms
**dark current 10^{-6} amps

Altitude resolution is determined by the laser pulse length τ In order to obtain high total energy E_L, τ must be as large as possible, while for good resolution τ must be as small as possible, clearly a compromise is in order The altitude resolution Δh is given by

$$\Delta h = (1/2)\ C\ \tau \tag{5}$$

4 4.2 2 Scaling Laws and Support Requirements

System Mass and Energy The total weight of a lidar system as a function of laser energy may be obtained by extrapolation from known systems Such an extrapolation is presented in Table 4-15 Figure 4-50 presents the data from Table 4-15 in graphical form, and suggests a power-law type of extrapolation formula This law is not expected to hold over more than the range indicated At the low energy end, some leveling off would occur since total systems of mass much less than 10 kg are impractical The other end of the energy scale (lasers producing greater than 10,000 joules) cannot be predicted at this time In the specified ranges, the following formulas give the estimated system mass, excluding primary power supply, of the Neodymium-YAG and CO_2 lidar systems, respectively

Table 4-15 Estimated Lidar Weights and Powers

Laser	E_L (Joule)	Weight (kg)	Efficiency (percent)	Average Power (watts)	
				1 shot/10 sec	1 shot/100 sec
1970 Nd-YAG	1	10	1	1	0 1
1973 Nd-YAG	100	50-100	2	500	50
1978 Nd-YAG	1000	250-500	5	2000	200
1970 CO_2	10	50-100	20	5	0 5
1973 CO_2	1000	250-500	25	400	40
1978 CO_2	10,000	500-1000	30	3300	330
1970 Ruby	0 1	23	0 01	100	10

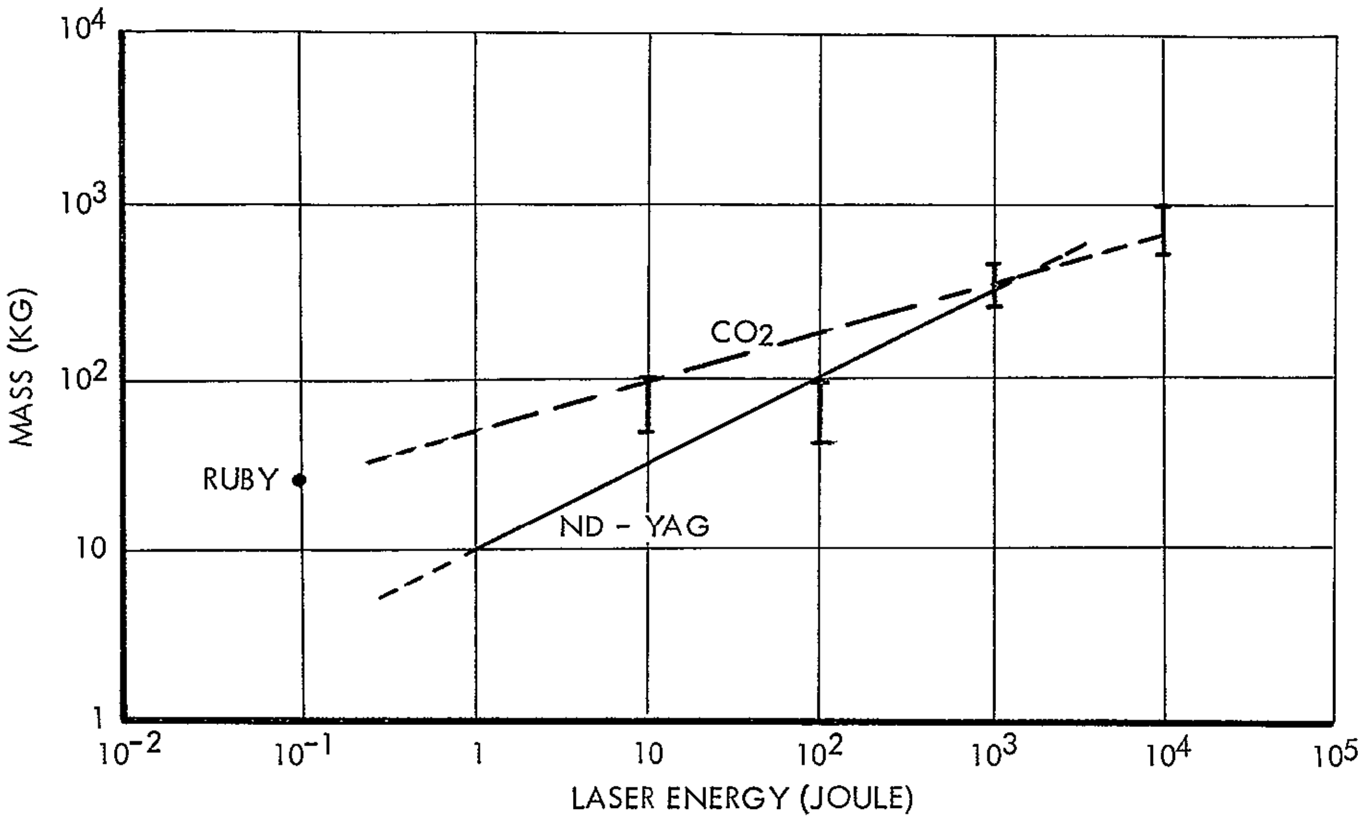

Figure 4-50 Projected LIDAR System Mass and Energy

$$M_{nd} = 10\ E_L^{1/2}\ (\text{kg}) \tag{6}$$

$$M_{CO_2} = 75\ \left(E_L/10\right)^{1/2} (\text{kg}) \tag{7}$$

where E_L is the laser energy in joules, no extrapolation formula is given for ruby because the ruby system, in spite of the higher receiver sensitivity, does not compare favorably with the other two

<u>System Volume</u> May be estimated by using the same density (mass/volume) as existing systems

System Operating Power P_o is a function of laser energy E_L, number of pulses per second N, and overall efficiency η It can be expressed by the ratio

$$P_o = \frac{E_L}{\eta} N \tag{8}$$

Values for E_L are given in Table 4-15

Data Rate The data rate of a lidar is inherently low due to the low pulse recurrence frequency, but the analog bandwidth at the output is wide to accommodate the narrow pulse To prevent multiple and sidelobe returns the receiver is gated on for a time T_R and the output is sampled at a rate equivalent to the range resolution $\tau/2$, that is

$$\text{Sample Rate} = \frac{T_R}{\tau/2} = \frac{2\,T_R}{\tau} \tag{9}$$

where

T_R is the time the receiver is gated on

τ is the transmitted pulse duration

If a dynamic range of 20 db is built into the receiver, then four bits per sample are required Therefore, the data rate per sample is

$$\text{Data Rate per sample} = \frac{2\,T_R}{\tau} G = \frac{8\,T_R}{\tau} \text{ (20 db dynamic range)} \tag{10}$$

where G is the number of bits per sample If p is the pulse recurrance rate in pulses per second then

$$\text{Data Rate} = \frac{2\,T_R}{\tau} G\ p \text{ bits/sec} \tag{11}$$

Platform Stability The primary requirement for platform stability results from the requirement for the receiving aperture to be aligned with the direction of transmission during the transmit time of the transmitted pulse If θ_r is the "beamwidth" of the receiving aperture, then significant loss in power will result in the receiver moves by one half beamwidth during the pulse travel time The angular rate of the platform must then be less than

$$\theta \leq \frac{C\theta_r}{4R\,max} \tag{12}$$

where C is the velocity of light

θ_r is the receiving aperture "beamwidth"

R max is the longest range which the Lidar is capable of measuring

Experiment Design Procedure Based upon the previous sections, the ruby laser system should be dropped from further consideration because of its low efficiency Unless a technical breakthrough occurs in ruby laser technology, the weight required to get a backscattered return equal to or greater than the background power is prohibitive This leaves the Neodymium-YAG and the CO_2 laser systems to be considered.

The logical procedure necessary to design a system for a particular mission follows, after which an example for a Jupiter fly-by is calculated

Step 1 Get minimum range, R min, from orbit data

Step 2 Calculate θ_r from Equation (4) and the required spatial resolution

Step 3 Obtain differential solar constant $\Phi_S(\lambda)$ and albedo for the planet under consideration

Step 4 Use Equation (2) to calculate background intensity I_s

Step 5 From Equation (1) calculate the laser energy E_L based upon $I_r = 10\,I_S$

Step 6 Establish a pulse length τ consistent with altitude resolution [Equation (5)] and laser energy requirement

Step 7 Calculate mass of laser system from Equation (6) or (7)

Step 8 Determine noise equivalent power P_n (Table 4-14)

Step 9 Calculate required receiver aperture area assuming $I_r A_r = 10 P_n$

Step 10 Calculate the data rate (Equation (11))

Step 11 Calculate the platform stability requirements (Equation (12))

Example Jupiter flyby

1 Let $R_{min} = 40,000$ km $= 4 \times 10^9$ cm

2 For Jupiter $\Phi(1\ 06\mu) = 2\ 4 \times 10^{-7}$ watt/cm^2 - Å

and $\rho = 0\ 51$

Let $\theta_r = 2 \times 10^{-4}$ radians, $\Delta\lambda = 10$ Å

Then from Equation (2)

$$I_s = \frac{2\ 4 \times 10^{-7}\ (2 \times 10^{-4})^2 \times 10}{4} = 2\ 4 \times 10^{-14}\ \frac{\text{watt}}{\text{cm}^2}$$

3 From Equation (1)

$$E_L = \frac{2R^2 I_r}{\beta C} = \frac{20R^2 I_s}{\beta C} = 25 \text{ joules}$$

4 From Equation (4)

$$r = R\theta_r = 4 \times 10^4 \times 2 \times 10^{-4} = 8 \text{ km}$$

5 From Equation (5)

$$\tau = 10^{-3} \text{ sec}$$

$$\Delta h = 1/2C\tau = 1\ 5 \times 10^8 \times 10^{-3} = 1.5 \times 10^5 \text{ m}$$

$$= 150 \text{ km}$$

6 $E_L = 25$ joule Equation (6),

$$M = 10\ (25)\ 1/2 = 50 \text{ kg}$$

7 $I_r = 10\ I_s = 2\ 4 \times 10^{-13}$ watt/cm^2

Equiv noise power P_n (Table 4-14) = 55 pw = $5\ 5 \times 10^{-11}$ watt

$I_r A_r = 10\ P_n n$

$$A_r = \frac{10P_n}{I_r} = \frac{10 \times 5\ 5 \times 10^{-11}\ \text{watt}}{2\ 4 \times 10^{-13}\ \text{watt/cm}^2} = 2300\ \text{cm}^2$$

4 5 ACTIVE MICROWAVE SYSTEMS

4 5 1 Introduction

Radar systems are generally designed to meet a specific function which can be described in at least semi-quantative terms Thus search radars are designed to detect specific types of targets with the radar design selected based on describable target parameters such as size or equivalent radar cross-section, speed, altitude, range, etc The more specific the radar requirements are, the more straightforward the radar design approach can be made However, when radar for a range of variables is required, then it is difficult to select a single radar approach which is optimum in every sense Mission planning must then have available a fairly wide range of alternatives so as to select a system which most closely approaches mission needs For this reason the basic design data are presented in the form of tradeoffs with attendant limitations imposed either by the state-of-the-art or inherent features of the design approach

Discussed below are some of the more useful techniques available for a variety of operating regimes which are applicable to ground mapping radar Three basic techniques are discussed First is conventional, non-coherent ground mapping using available radar systems Second are so-called coherent systems, and third are high or fine resolution data processing ground mapping radar systems All of the radars are assumed to be of the side-looking type so that a valid basis of comparison can be established although this restriction is not necessary for non-coherent radars Also the design approach and scaling laws can be applied to the design of scatterometers when angular resolution precludes operation as a mapping system

4 5 2 Non-Coherent Mapping Systems

The limitations of conventional radar ground mapping systems in obtaining high resolution are well known The resolution is limited by three basic factors

1 The attainable azimuth resolution is limited by that obtained from realistic antenna size in terms of wavelength

2 The minimum pulse width of the transmitted pulse which must be of finite duration

3 Geometric factors which affect both range resolution and azimuth resolution

The limitations can be overcome to a certain degree by judicious selection of operating frequency, ground illumination geometry, and operating regime but there are inherent limitations to conventional radar which, at best, limit its use to applications requiring crude resolution

4 5 2 1 Azimuth Resolution

The azimuth resolution of a conventional radar is limited by the radiation pattern of the antenna A satisfactory measure of resolution is the 3 db beamwidth in radians, β_a, of the antenna and this is, for a rectangular aperture, given by

$$\beta_a = K \frac{\lambda}{D} \tag{1}$$

where

K is a proportionality factor generally taken as 1 2 for conventional linear arrays

λ is the operating wavelength

D is the length of the antenna aperture in the same units as λ

For a fixed aperture length, D, it is obvious that decreasing the wavelength will improve angular resolution This cannot be carried on indefinitely, however, because of two factors First there is a limit to the attainable tolerances to which an antenna structure can be built and deployed in space so that state-of-the-art in antenna manufacturing techniques limit both the upper useful frequency for a given aperture size and the azimuth beamwidth at a fixed frequency for increasing aperture size Even with state-of-the-art improvement it is difficult to postulate an antenna with a gain in excess of 60 db and since gain and beamwidth are related by

$$G = \frac{3 \times 10^4}{\beta^2} \tag{2}$$

where β is the beamwidth in degrees It appears that a beamwidth limitation for a 60 db gain is of the order of

$$\beta = \sqrt{\frac{3 \times 10^4}{10^6}} = 1.73 \times 10^{-1} \text{ degrees} = 3 \text{ milliradians} \qquad (3)$$

The 60 db limitation applies basically to an aperture such as a parabolic antenna or a rectangular antenna with height and width approximately equal In this configuration a maximum dimension of 400 wavelengths (λ) is considered a maximum On the other hand a very long, narrow antenna might have a length of 800 λ, with 1000 λ considered the theoretical limit In no event, however, is the gain of feasible antennas expected to exceed 60 db for space deployable antennas

The equivalent antenna size as a function of wavelength is shown in Figure 4-51. Aperture sizes of 100 feet or less indicate systems operating at frequencies above S-band, that is wavelengths less than 10 cm, to obtain the best angular resolution Somewhat more realistic values of attainable angular resolution as a function of wavelength are presented in Figure 4-52 for an assumed antenna efficiency of 60 percent and a maximum gain of

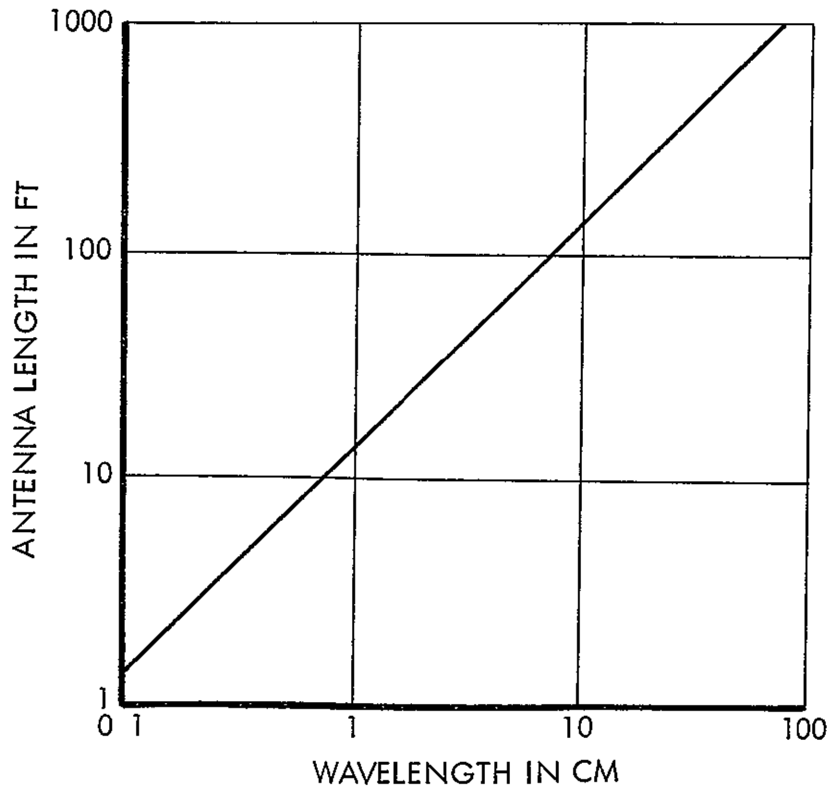

Figure 4-51 Maximum Realistic Antenna Size as a Function of Wavelength

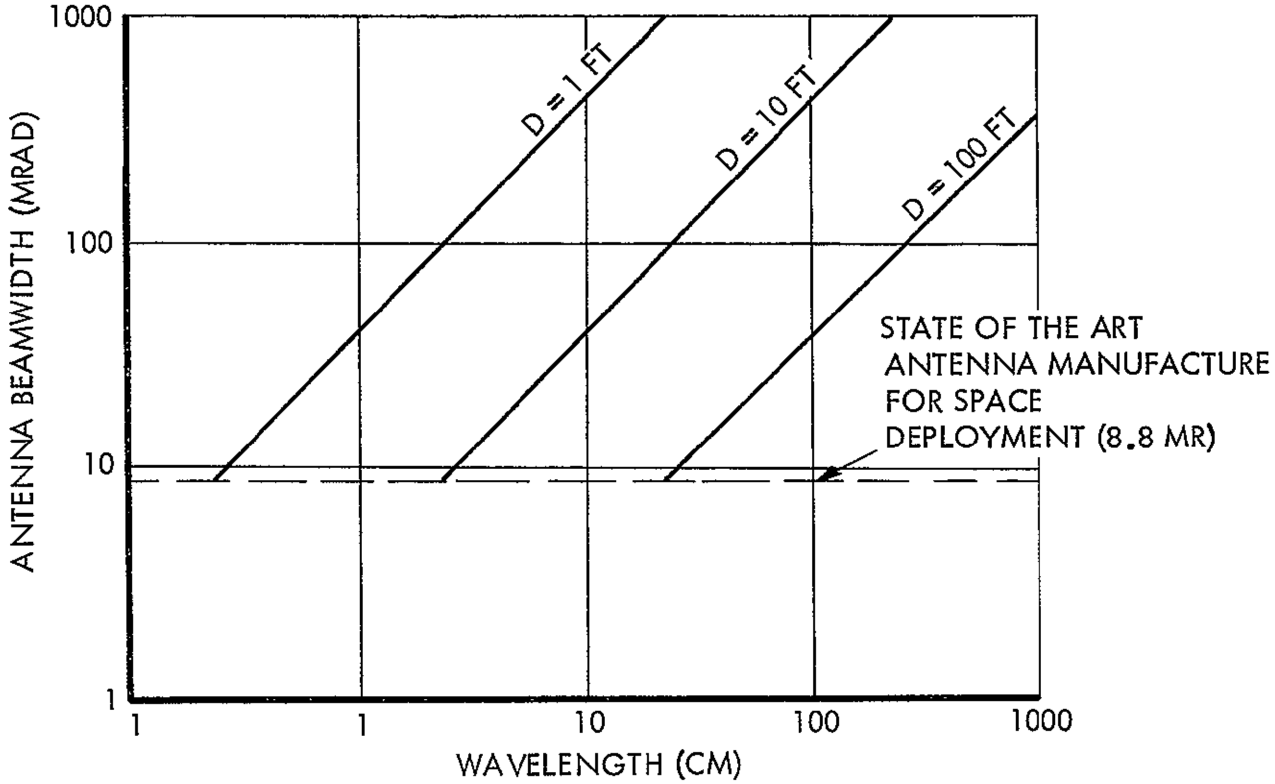

Figure 4-52. Antenna Beamwidth as a Function of Wavelength for Various Aperture Lengths

50 db It is clear from the figure that even at high frequencies the attainable angular resolution is greatly limited by antenna technology

There is a second limitation on attainable azimuth resolution which is more general than antenna design limitations Radar resolution at a given altitude is degraded in azimuth ground resolution since

$$r_a = R \beta_a \tag{4}$$

where

r_a is the azimuth ground resolution

R is the slant range to the ground patch being illuminated by the radar

β_a is the antenna azimuth beamwidth

This expression can be rewritten in terms of the azimuth aperture size, D_a, and wavelength since

$$\beta_a = 1\ 2 \frac{\lambda}{D_a} \tag{5}$$

so that

$$r_a = 1\ 2 \frac{R\lambda}{D_a} \tag{6}$$

furthermore, from the viewing geometry for an operating altitude H and an elevation angle, γ, from the vertical, the slant range is

$$R = H \sec \gamma \tag{7}$$

so that the azimuth ground resolution is given approximately by

$$r_a \approx \frac{1\ 2\ \lambda H \sec \gamma}{D_a} \tag{8}$$

The approximation results from the assumption of a flat surface The flat surface approximation is useful because it does not introduce appreciable error especially for viewing angles less than 60 degrees, for altitudes which are a small fraction of the planetary radius, and results in major mathematical simplifications

It is clear from the expression for azimuth ground resolution that the geometry always introduces degradation since it is directly proportional to both altitude and the secant of the viewing angle The degradation can be partly overcome by using both higher frequencies and larger apertures but for reasonable aperture sizes the resolution is still low This can be seen from Figure 4-53 which is a plot of ground resolution for a variety of parameters Even for a millimeter wave system, large antenna sizes must be used to obtain reasonable resolution at ranges in excess of 200 nmi

Range Resolution The problem of attaining range resolution with a conventional radar is not nearly so severe as azimuth resolution Range resolution is a function of transmitted pulse width in the form

$$r_r = 1/2\ C\tau \tag{9}$$

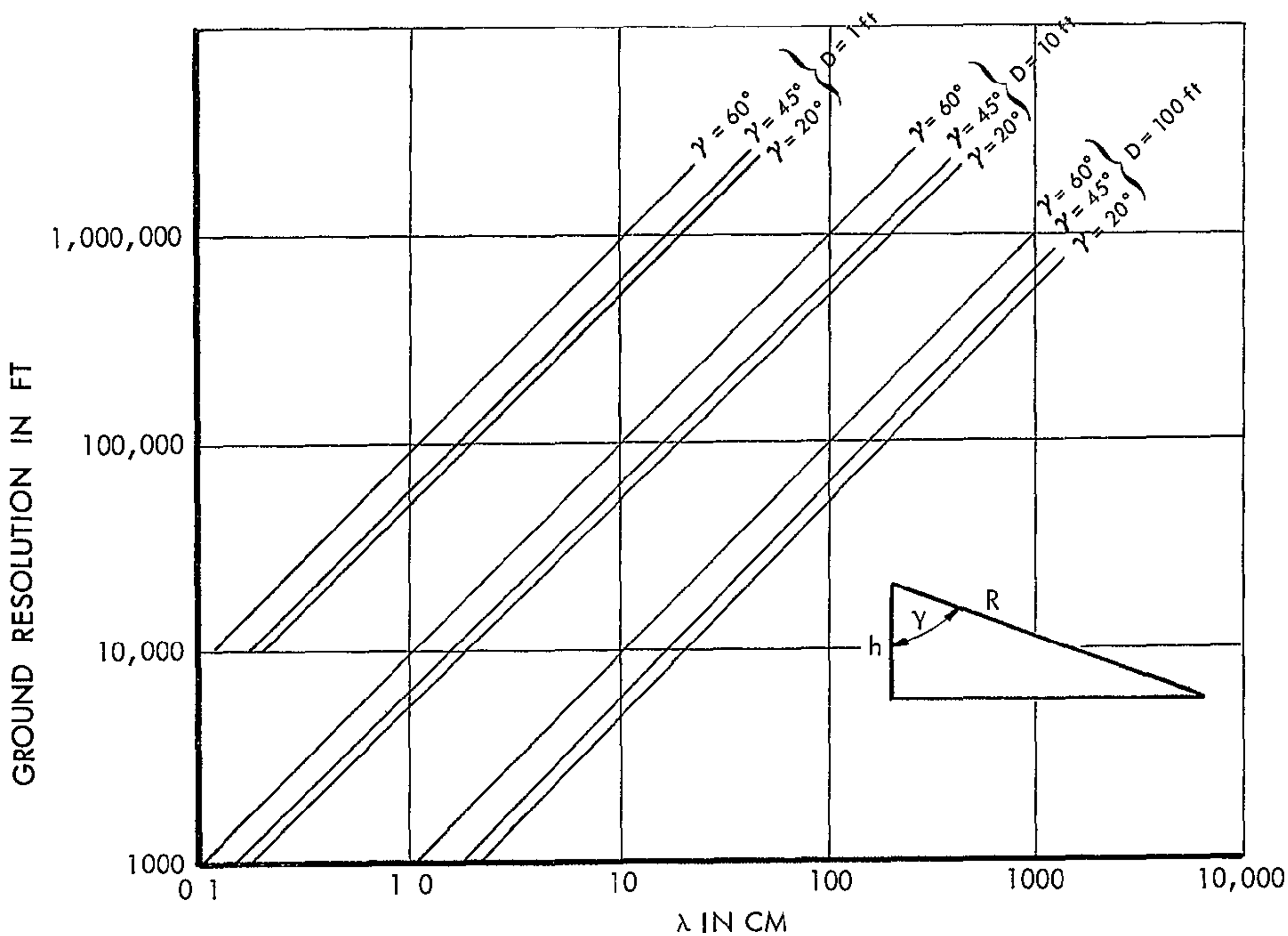

Figure 4-53. Ground Resolution Versus Wavelength for Various Antenna Diameters at an Altitude of 200 n m

where

r_r is the range resolution

C is the velocity of propagation (3×10^8 meters/sec)

τ is the transmitted pulse width

However, in ground mapping, the viewing geometry also degrades resolution in the range direction since from the geometry shown in Figure 4-54 it can be seen that the instantaneous return from the ground is a function of the viewing angle so that

$$r_r = 1/2 \ C\tau \csc \gamma \tag{10}$$

which is shown plotted in Figure 4-55 for a range of pulse widths and viewing angles

It appears from the figure that very high range resolution can be obtained for reasonable viewing angles There are limitations which preclude

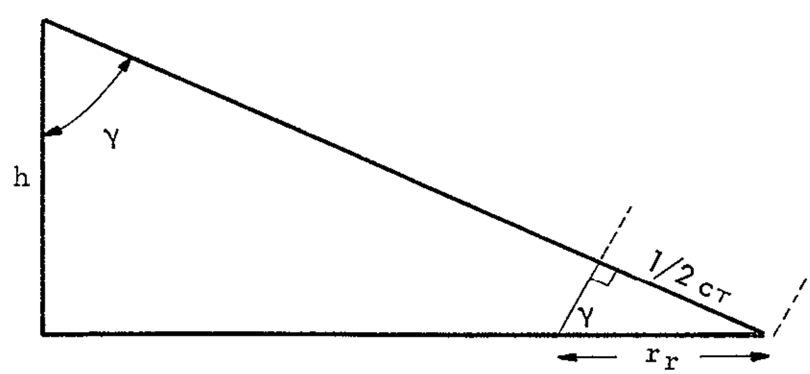

Figure 4-54 Instantaneous Return From a Pulse of Duration τ

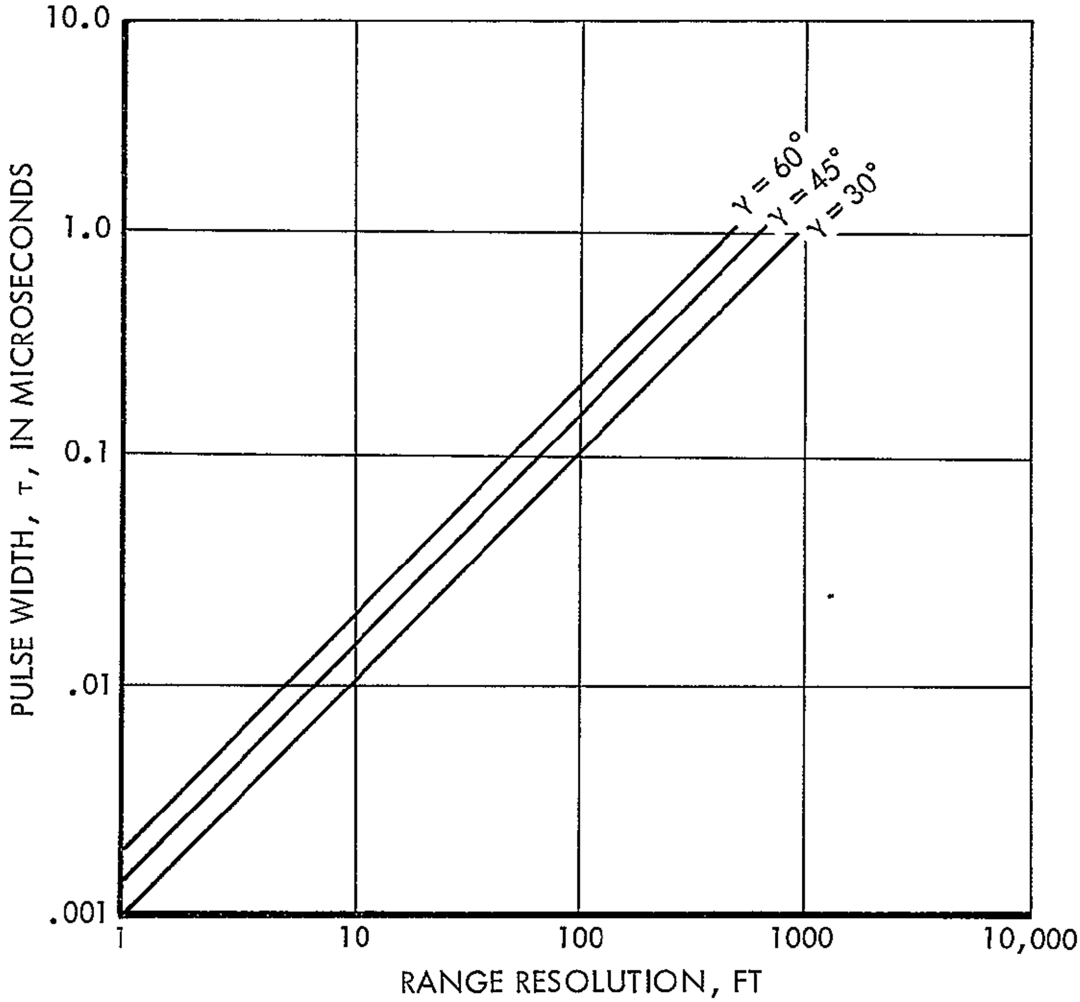

Figure 4-55. Range Resolution as a Function of Pulse Width

the use of shorter and shorter pulses First it is necessary that any transmitted pulse must be long relative to the period of the transmitted frequency Otherwise it is not possible to define a carrier frequency A useful rule is that

$$f_c \tau = 10 \tag{11}$$

where f_c is the carrier frequency Therefore to use extremely short pulses higher and higher carrier frequencies are necessary The limitations on carrier frequency are discussed below but it is apparent that a very short pulse such as one nanosecond requires a carrier frequency in the X-band region or above

A somewhat more severe restriction results from the transmitter bandwidth requirement for transmitting short pulses The pulse bandwidth is given by

$$B = \frac{1}{\tau} \tag{12}$$

Thus, for a one nanosecond pulse an instantaneous bandwidth of approximately 1000 megahertz is required The difficulties of designing transmitters with such wide instantaneous bandwidths generally lead to low power devices

From signal detection theory it is well known that the primary criterion for reliable signal detection is directly dependent on average transmitted power But, average transmitted power is given by

$$P_{av} = \frac{P_t \tau}{T} = P_t \tau \,(PRF) \tag{13}$$

where

P_{av} is average transmitted power

P_t is peak transmitted power

τ is the transmitted pulse duration

T is the interpulse period

PRF is the pulse repetition frequency

5 ⊕

It is obvious that for a given pulse width, τ, average power can be increased either by increasing the peak power or by increasing the PRF For very high frequencies the peak power is severely limited by the state-of-the-art in high power amplification devices This limitation has led to the development of pulse compression techniques which are discussed below under coherent radar systems The other method of obtaining short pulse-high power operation is to increase the PRF However, increasing the PRF leads to additional limitations since as the PRF is increased there is a decrease in the maximum unambiguous range to which the radar system can map

Basically the time available for mapping unambiguously is the interpulse period, T, but since the pulse must travel to the target and return, the maximum unambiguous range is given by

$$R\ max = 1/2\ CT = \frac{C}{2(PRF)} \tag{14}$$

where C is the propagation velocity It can be seen that increasing the PRF severely reduces the available mapping range

Along these same lines there is an additional restriction imposed when the radar is operated at orbital altitude where velocities are high The PRF must be sufficiently high that at least one pulse return is received from each resolution element For a target at range R, the target is in the antenna beamwidth for a time determined by the antenna velocity so that

$$\frac{V\ T}{2} = \beta_a\ R \tag{15}$$

where

- V is the antenna beam velocity with respect to target
- T is the interpulse period
- β_a is the antenna azimuth beamwidth
- R is the target range

It follows that

$$PRF \geq \frac{2\ V}{\beta_a\ R} \tag{16}$$

In a realistic case, the PRF is selected to obtain multiple hits per beamwidth so that the minimum PRF is selected according to the criterion

$$(\mathrm{PRF})\ \mathrm{min} = \frac{m V}{\beta_a R} \tag{17}$$

where m is an integer in the range of 2 to 10

By substituting β_a and R in terms of antenna aperture and geometry the minimum PRF can be expressed as

$$(\mathrm{PRF})\ \mathrm{min} = \frac{m D_a V \cos \gamma}{1.2 H \lambda} \tag{18}$$

To illustrate the implication of minimum PRF, the minimum PRF is shown plotted in Figure 4-56 for a value of m = 5 and orbital altitudes of 200 and 400 nmi and antenna velocities of 24,000 and 22,000 feet per second, respectively It can be seen from the figure that the narrow beamwidth associated with large antennas require PRF's of the order of 1000 pps which in turn limit the width of the ground swath which can be mapped in the range direction For example, with a PRF of 1000 pps the maximum unambiguous range of the radar is only 80 miles This does not imply that such a PRF cannot be used from orbital altitude but rather that the maximum ground swath length in the range direction is 80 miles This can be seen from the illumination geometry shown in Figure 4-57 For an elevation beamwidth, β_e, the restriction on PRF is such that the pulse return from point 2 must be at a shorter range than R_1 before the succeeding transmitted pulse arrives at point 1 This can be accomplished by restricting the elevation beamwidth, β_e, of the antenna so that the ground swath length, W projected on R_2 is not greater than the difference between R_2 and R_1

The companion restriction on antenna elevation beamwidth for a given PRF can be derived from the illumination geometry From Figure 4-57 it can be shown that the swath length, W, is given by

$$W = H \left[\tan \left(\gamma + \frac{\beta_e}{2}\right) - \tan \left(\gamma - \frac{\beta_e}{2}\right) \right] \tag{19}$$

This expression is plotted in Figure 4-58 for an orbital altitude of 200 nmi and a range of values of beamwidth and elevation angle Curves of the type shown in Figure 4-58 can be used in two ways If a PRF is selected from

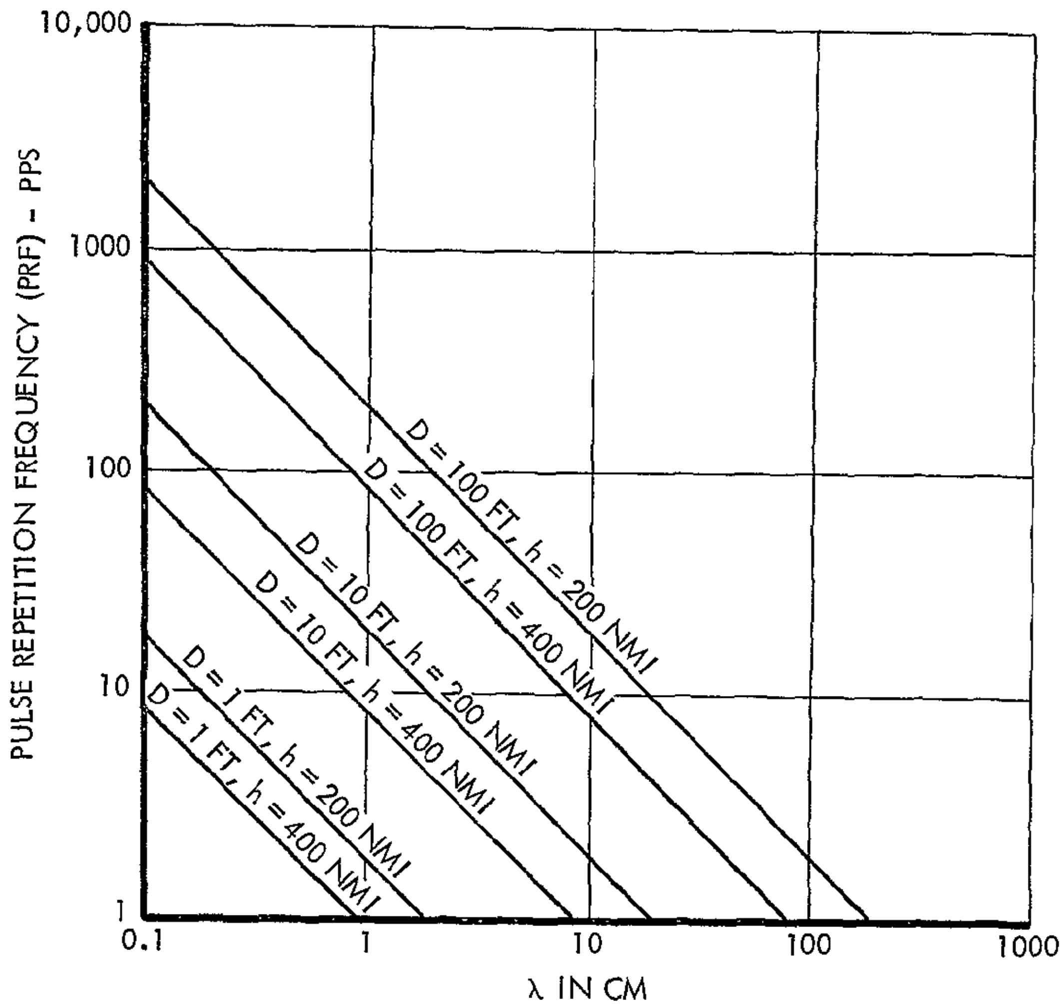

Figure 4-56 PRF Requirements From Orbital Altitude

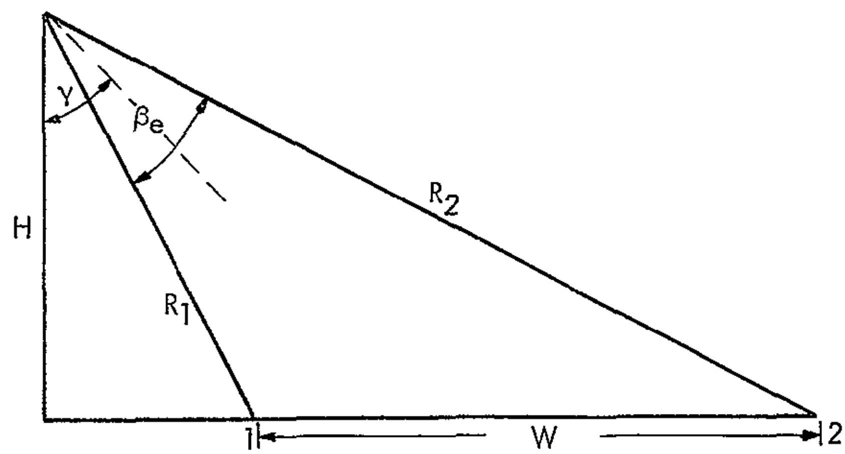

Figure 4-57 Ground Illumination Geometry

optimum average power considerations, the equivalent swath width from the figure can be used to determine the required combination of elevation look angle for the antenna and the elevation beamwidth Conversely, at a given elevation angle, the resulting swath length and antenna elevation beamwidth combination may be determined

<u>Realizable Resolution</u> It is clear from the discussion above that conventional pulse radar systems are basically low resolution mapping devices at all except very short ranges The basic limitation is in azimuth resolution since antennas of finite size result in essentially limited beamwidth reduction capability There is no advantage in using a combination of very high frequency such as millimeter waves and large antenna sizes since the current state-of-the-art in antenna manufacturing tolerances limits the electrical length of antennas to something less than 1000 wavelengths for long linear arrays, and 400 wavelengths for antennas having approximately equal length and width

In the range dimension, improved resolution can be obtained by using very short transmitted pulses But this approach implies very high frequency operation where peak power generation capabilities are limited If the PRF is increased to maintain average power while reducing peak power, then a range ambiguity problem is introduced resulting in the requirement for reducing the ground swath length illuminated by the radar

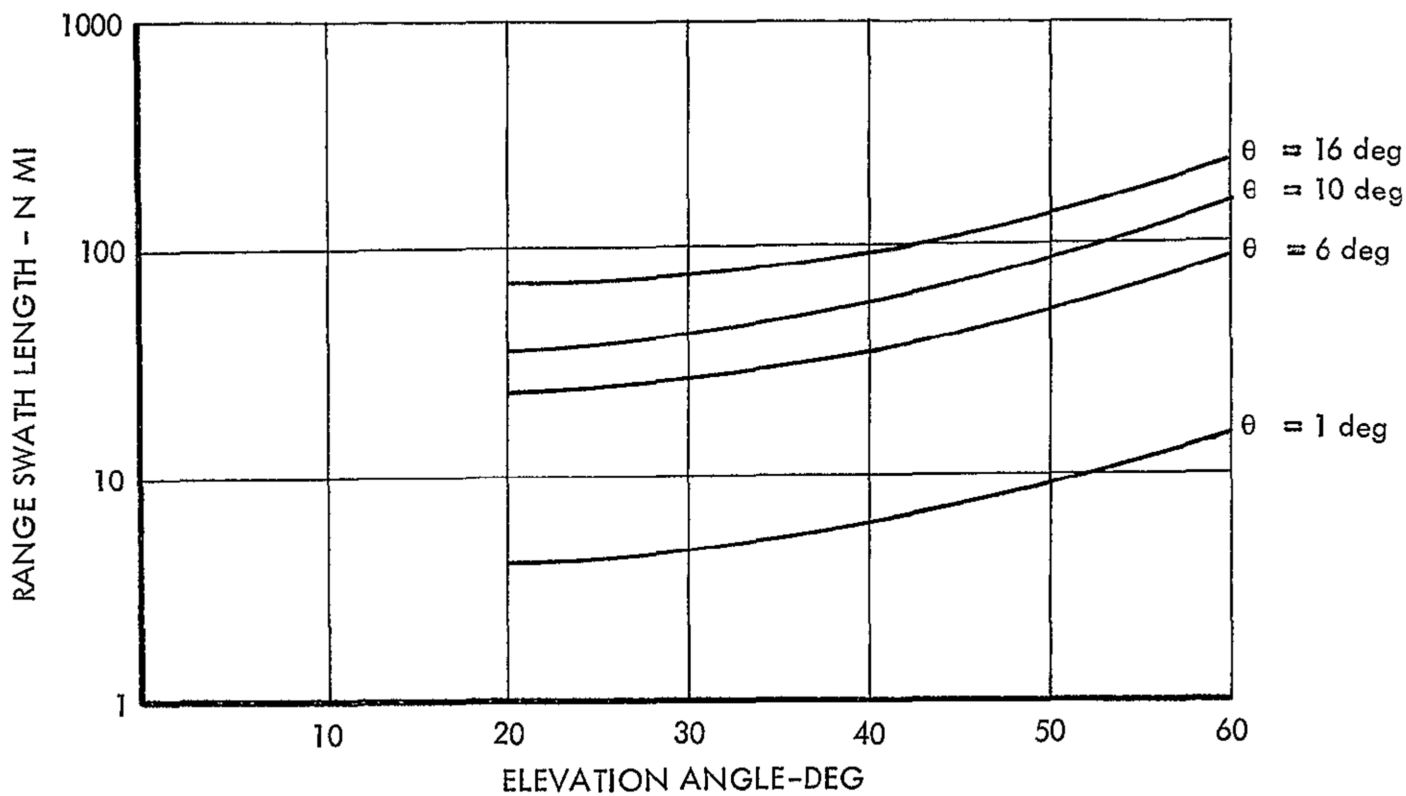

Figure 4-58. Range Swath Length as a Function of Elevation Angle for a Range of Antenna Elevation Beamwidths at an Altitude of 200 n m

The question arises naturally as to the best tradeoff between azimuth and range resolution It is not obvious that equal range and azimuth resolutions are advantageous The introduction of distortion in the imagery may actually be useful if it is understood Under these circumstances a somewhat improved range resolution could be obtained with conventional pulse radar The resulting imagery would generally not be useful for mapping but it could have important uses in scatterometry

In general, however, it is common practice to design mapping radars with essentially equal range and azimuth resolution This amounts to degrading range resolution below its potential

System Characteristics To demonstrate the characteristics of a typical pulse radar for ground mapping it is assumed that the radar would be operated in a space environment at an altitude of 200 nmi This case is chosen since it implies a payload limited system and represents a minimum altitude which a flyby mission might attain

If ground resolution is selected arbitrarily, then the limit on the attainable angular resolution of microwave antennas may be exceeded It is assumed that range and azimuth ground resolution are equal in the ground mapping system If, for example, a ground resolution element of 1000 ft by 1000 ft is assumed, then for an orbit altitude of 200 mi and a look angle of 45 degrees off the nadir, an angular resolution of approximately 0 6 mr is required But this implies an antenna length of 2000 λ which is well beyond the state-of-the-art

For illustrative purposes an angular resolution of 0 6 mr can be used but it is to be understood that such a system is beyond the state-of-the-art in antenna design Alternatives to the 0 6 mr angular resolution are first to assume that a state-of-the-art improvement can be postulated resulting in an angular resolution equivalent to the best ground based antennas, that is an antenna beamwidth of 3 3 mr, or, more conservatively, to accept the resolution attainable with an 8 8 mr beamwidth for realistic space deployable antennas The resolution attainable for a 3 3 mr beamwidth is thus 5 5×10^3 ft while for the 8 8 mr beamwidth the resolution is 1 47×10^4 ft It follows that once the geometry for observation is selected, the best attainable ground resolution in the azimuth direction is imposed by the state of the antenna art and cannot be selected arbitrarily For illustrative purposes, an azimuth resolution of 3.3 mr will be used in spite of the fact that it results in a surface resolution which is 5500 ft

For space deployable antennas, it is assumed that a reasonable antenna dimension is in the range of 25 to 50 feet in the azimuth direction From Figure 4-53, it can be seen that a range of frequency selection exists to obtain a resolution of 5500 ft Selection of an operating wavelength of

3 ft can impose a requirement for an antenna which is approximately 40 ft long Since adequate high power transmitting equipment exists in this region, an operating wavelength of 3 cm will be used

Transmitted Power Requirements Of particular concern in spacecraft operated radar systems is the required power to obtain a given ground resolution This can be obtained from the familiar radar equation once the parameters of the radar system are defined. In general the power received by a radar from a transmitted pulse is

$$Pr = \frac{P_t G^2 \lambda^2 \sigma L}{(4\pi)^3 R^4} \tag{20}$$

where

P_t is the transmitted peak power

G is the antenna gain

λ is the operating wavelength

σ is the radar equivalent cross-section

L is the system losses, including atmospheric if any

R is the slant range to the target

The antenna gain cannot be specified until the length of the ground swath in the range dimension has been established From Figure 4-56 a PRF of approximately 100 pps is indicated so that an interpulse period of 1 0 milliseconds is acceptable The problem of range ambiguities is alleviated by the low PRF so that the range swath length is limited mainly by transmitted power considerations To conserve transmitted power a swath length of 100 miles is assumed From Figure 4-58, an elevation beamwidth of 15 degrees is indicated for an elevation look angle of 45 degrees and a ground swath length of 100 miles Since the antenna gain in terms of beamwidth is given by

$$G = \frac{2\ 5 \times 10^4}{\beta_a \ \beta_e} \tag{21}$$

where β_a and β_e are in degrees and the assumed antenna efficiency is 55 percent For a 3 3 mr (0 189 deg) azimuth beam width and a 15-degree elevation beamwidth the resulting gain is 39 5 db

Of actual significance is not so much the received power, as such, but the signal-to-noise ratio For reliable ground mapping a minimum signal-to-noise ratio of 10 db is required The system noise power is given by

$$N = \overline{NF}\ K\ T\ B \tag{22}$$

where

$\overline{NF}$ is the system noise figure

K is Boltzman's constant (1 38 x 10^{-23} watts/deg k-cps)

T is the system reference noise temperature (300°K)

B is the system bandwidth

The system bandwidth is taken as the reciprocal of the transmitted pulse width From Figure 4-55 for a range resolution of 5500 feet at an elevation angle of 45 degrees the pulse width is 9 microseconds The required bandwidth is then 0 11 megahertz

A limitation of short wavelength operation is the attainable noise figure. Current state-of-the-art in receiver design is indicated in Figure 4-59 From the figure it can be seen that a receiver noise figure of 8 db is the best attainable at a 3 centimeter wavelength The resulting noise power is

$$N = 6\ 3 \times 1\ 38 \times 10^{-23} \times 3 \times 10^{2} \times 0\ 11 \times 10^{6} \tag{23}$$

$$= 2\ 87 \times 10^{-15} \text{ watts}$$

For unity signal-to-noise ratio we have by direct substitution

$$\frac{P_r}{N} = 1 = \frac{P_t G^2 \lambda^2 \sigma L}{(4\pi)^3 R^4 2\ 87 \times 10^{-15}} \tag{24}$$

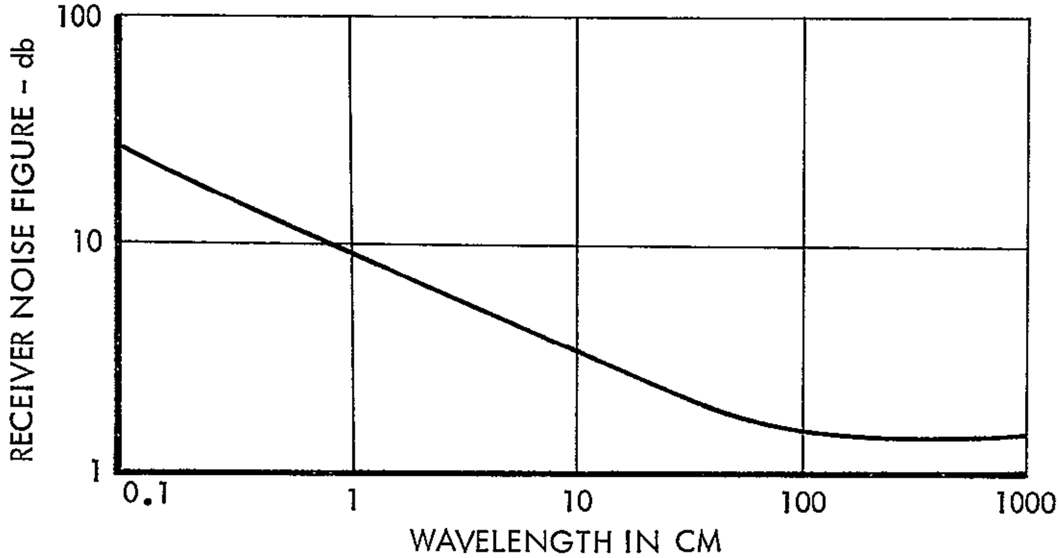

Figure 4-59. Best Obtainable Noise Figure
as a Function of Wavelength

From the geometry the maximum range is 330 miles or $6\ 1 \times 10^5$ meters. The losses are the result of atmospheric attenuation, if any, and the internal losses in the transmission systems An assumed loss of 4 db is used so that

$$L = 4\text{db} = 0\ 4 \tag{25}$$

The radar equivalent cross-section is composed of two basic factors The first is the geometric area of the ground resolution patch which is simply the product of the range and azimuth resolution elements The second part is the backscatter coefficient The backscatter coefficient is difficult to define theoretically since the surface of planets is a combined specular and diffuse scatterer of microwave energy For this reason, the backscatter coefficient is usually determined empirically from measurement The backscatter coefficient is frequency dependent and very little data exists in the 3 centimeter wavelength portion of the spectrum To maintain a measure of conservatism a backscatter coefficient of -40 db will be used Therefore

$$\sigma = r_a r_r \delta \tag{26}$$

where

r_a is the azimuth ground resolution = 5500 feet (1680 meters)

r_r is the range resolution = 5500 feet (1680 meters)

δ is the backscatter coefficient = -40 db = 10^{-4}

Solving the unity signal-to-noise equation for P_t we obtain

$$P_t = \frac{(4\pi)^3 \times R^4 \times 8 \times 10^{-15}}{G^2 \lambda^2 \sigma L} \tag{27}$$

The values to be substituted in this expression are summarized below

$(4\pi)^3 = 1\ 984 \times 10^3$

$R^4 = (6\ 1 \times 10^5 \text{ meters})^4 = 1\ 38 \times 10^{23} \text{ m}^4$

$G^2 = (8\ 8 \times 10^3) = 7\ 8 \times 10^7$

$\lambda^2 = (3 \times 10^{-2})^2 = 9 \times 10^{-4} \text{ m}^2$

$\sigma = 2\ 83 \times 10^2 \text{ m}^2$

$L = 0\ 4$

If these values are substituted into the expression for the peak power we obtain

$$P_t = 10^5 \text{ watts}$$

This value is unrealistic when a detection criterion of 10 db is applied since the peak power requirement then becomes one megawatt

The difficulty can be alleviated in several ways but the most straightforward method is to reduce the length of the ground patch illuminated in the range direction Doing so increases the gain of the antenna by reducing the elevation beamwidth If, for example the length of the ground swath is reduced from 100 to 50 miles then from Figure 4-58 the elevation beamwidth required is approximately 6 degrees The resulting antenna gain would be

2 2 x 10^4 and would result in a reduction in required power of approximately 4 db The peak power requirement for unity signal-to-noise would be

$$P_t = 4 \times 10^4 \text{ watts}$$

and for a 10 db signal-to-noise ratio would be

$$P_t = 4 \times 10^5 \text{ watts}$$

400 kilowatts of peak power at 3 cm still presents a difficult problem and is generally indicative of why long range non-coherent mapping systems have not found wide use in space

On the other hand, the average transmitted power is relatively low since

$$P_{av} = P_t \ \tau(\text{PRF}) \tag{28}$$

where

P_t is the peak transmitted power = 400 kilowatts, τ is the transmitted pulse width = 9 x 10^{-6} sec, PRF is the pulse repetition frequency = 100 pps

so that

$$P_{av} = 360 \text{ watts}$$

The total power consumption by the radar is determined primarily by the transmitted power requirements In the microwave portion of the spectrum transmitter efficiency is generally low so that an efficiency in the range of 15 to 18 percent overall can be expected Under these circumstances, the total power required by the radar is 2120 watts for a transmitter efficiency of 17 percent

Antenna The antenna aperture size is 40 feet long by 1.2 feet high It would weigh approximately 250 pounds

Transmitter The transmitter, including the high voltage power supply would occupy approximately 4 cubic feet and would weigh approximately 225 pounds

<u>Receiver and Synchronizer</u> Receiver and synchronization circuits represent a very small portion of the size and weight penalty of the overall radar system. Approximately 20 pounds and 0.5 cubic feet are the penalties of the receiver-synchronizer.

<u>Non-Coherent Radar Data</u> The output of the radar is essentially a video waveform of moderate bandwidth. If all of the target information in the waveform is retained, then the dynamic range of the output signal may be 35 db to cover a range of backscatter coefficients from 0.3 to 0.0001. The output of the radar may be directly modulated onto a carrier, in either analog or digital form, or it may be recorded in either analog or digital form for delayed transmission. The data rate is determined by three principal factors: the ground resolution of the system, the pulse repetition frequency and the length of the ground swath in the range direction. In addition, the information generation rate requires the consideration of the amount of contrast or dynamic range of the signals (shades of gray) which must be preserved for imagery generation.

The number of resolution elements per transmitted pulse is simply the swath length, W, divided by the ground resolution, r_a. For a 50-mile swath length and a 5500-foot resolution, this is simply

$$N_p = \frac{W}{r_a} = \frac{3.04 \times 10^5}{5.5 \times 10^3} \simeq 55 \text{ samples} \qquad (29)$$

and for a PRF of 100 pps this becomes

$$N/\text{sec} = 5.5 \times 10^3 \text{ resolution elements/sec}$$

This is a relatively modest rate but it is misleading unless consideration is given to the dynamic range of the received signals. Without any form of compression the dynamic range of the received signals is approximately 35 db. However, for ground mapping operation it would be difficult to design a linear receiver with a 35 db response range without gain control. But gain control is, in effect, dynamic range compression and it is common practice in radar receiver design to compress the signal dynamic range to approximately 15 to 20 db at the output of the radar receiver. To accommodate a 20 lb dynamic range (100 to 1 signal variation) a seven bit binary number would be required. However, if the information content is restricted to 64 shades of gray a six bit number would suffice and the bit rate from the radar would be

$$\text{Bit rate} = 6 \times 5.5 \times 10^3 = 3.3 \times 10^4 \text{ bits/sec}$$

4.5 2 2 Scaling Law Development

The utilization of non-coherent imaging radar is practically completely precluded by the unattainability of the required antenna lengths to achieve even the minimum required resolution for the missions under consideration Antenna dimensions on the order of (5000λ) or more would be necessary for even the least demanding Jupiter and Saturn swingbys (Mission 7) For completeness, however, a scaling law procedure is given in Figure 4-60.

4 5 3 Coherent Mapping Systems

4 5 3 1 Design and Performance

The limitations of conventional pulse radar in attempting to obtain high resolution ground mapping result primarily from the nature of the transmitted signal, the limitations on the construction of large aperture antennas and the basic conflict between a narrow pulse, that is high resolution, transmitted signal and the requirement for relatively high average power These limitations are basic and even with major advancements in the state-of-the-art it is difficult to postulate significant improvements in resolution performance based on brute force techniques.

To overcome the limitations of conventional radar, a fundamental change in system design is necessary The approach is to design a radar which is coherent, that is, one in which the phase of the transmitted signal is controlled to the extent that the received signal contains both phase and amplitude information Coherency is essential to obtaining improvements in both azimuth and range resolution since it permits the application of techniques for resolution improvement in two dimensions based on the vector nature of the detected signals

The major difference between conventional and coherent radar systems is in the way that the received signals are used In order to exploit the capabilities of coherent radar it is generally necessary to preserve the form of the received signals over a sufficiently long time span to permit the combination of many returns to form an estimate of target location This implies some form of data processing and it is the nature of the processing requirements which add appreciably to the complexity of coherent radar

Implicit in the coherent radar approach is the capability of performing coherent integration with an attendant improvement in signal-to-noise ratio From signal detection theory it can be shown that if n target returns are summed (integrated) coherently, then signal power increases as the square of the number of pulses integrated Noise power on the other hand, being essentially a random process in wideband radar systems, increases only linearly as the number of pulses integrated As a consequence, the signal-to-noise ratio for a coherent system has a theoretical advantage over a non-coherent system

Two basic approaches are used to obtain high resolution with a coherent radar From a theoretical point of view the approaches are quite similar but from a practical mechanization point of view they are markedly different. Range resolution improvement is obtained by coding the transmitted waveform in such a way that the time duration of the transmitted pulse is extended in time to increase average transmitted power and then, based on the known modulation characteristics of the transmitted signal, compressing the received signal in time to obtain the equivalent of a narrow transmitted pulse. A common form of pulse compression signal design is frequently referred to as "CHIRP" and is discussed briefly below.

Improved angular resolution with coherent radar is frequently referred to as "synthetic aperture" which consists essentially of accumulating target data over many interpulse periods. For a coherent system the target returns have a vector form, that is, they contain amplitude and phase information The separate target returns are combined vectorially to produce the equivalent of an antenna aperture which is many times the length of the physical aperture, thus a synthetic aperture is generated The application of synthetic aperture theory is based on the change in Doppler frequency as the physical aperture is moved past the target Therefore the theory is based on the translation of the physical aperture past a target to generate a Doppler history The requirement and capabilities of synthetic aperture radar are discussed below

In the discussion that follows it is assumed that a square resolution element is required although, as discussed previously, it is not essential to the radar that this restriction apply

<u>Pulse Compression</u> It can be shown from very basic theory of signal modulation that if a pulsed transmitter is modulated so as to generate a signal spectrum which is equivalent to the spectrum of an unmodulated pulse of duration τ then the resulting spectrum can be used to reconstruct a pulse whose equivalent duration is τ. This technique, commonly called pulse compression, is extremely useful in high resolution radar systems since it permits the transmission of low peak power, "long pulses" which can be compressed to the equivalent of a narrow pulse of very high peak power

The requirements for a pulse compression radar are fairly stringent since not only must the system be coherent but there must be a careful match between the transmitter and receiver characteristics to effect pulse compression To understand why this is so, consider the mechanization requirements for effecting pulse compression. The most commonly used pulse compression technique is characterized by a transmitter waveform which is linearly frequency modulated for a time duration, T, where T is the real transmitted pulse width The transmitted waveform is shown in Figure 4-61 in idealized form The time duration of the pulse, T, is generally selected to be much longer than the resolution requirements of the radar. The frequency excursion during the pulse, however, is selected to be large since it can be shown that the effective pulse width, τ, after suitable processing in the receiver is given by

$$\tau = \frac{1}{\Delta} \tag{30}$$

where τ is the effective pulse width for resolution and Δ is the frequency excursion of the linear FM during the pulse time, T Further it can be shown that there is a relationship between τ, Δ, and T which defines the pulse compression ratio, c_p, in the form

$$\frac{T}{\tau} = T\Delta = c_p \tag{31}$$

The compression ratio, c_p, is frequently referred to as the dispersion factor Values of c_p of the order of 100 are well within the capabilities of current CHIRP radar systems For illustrative purposes, a value of c_p of 100 will be used to illustrate the capabilities of pulse compression radar systems

The generation of the transmitter waveform presents certain practical mechanization difficulties but it is in the area of receiver design that a large amount of complexity is added to the radar In order to effect pulse compression it is necessary for the receiver to accept all frequency returns resulting from the frequency modulation of the transmitted pulse over a time duration T and effectively delay the frequencies by an amount equivalent to their time of occurrence within the transmitted pulse width, T This requirement is illustrated graphically in Figure 4-62(a). The envelope of the receiver response is shown in Figure 4-62(b) and is given analytically by the absolute value of

$$E = \sqrt{c_p}\ \frac{\sin \pi\Delta t}{\pi\Delta t} \tag{32}$$

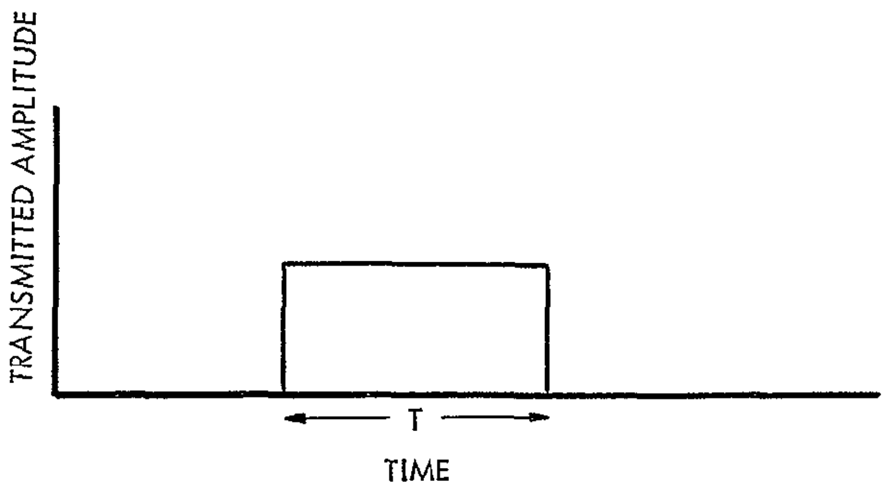

(a) TRANSMITTED PULSE AMPLITUDE

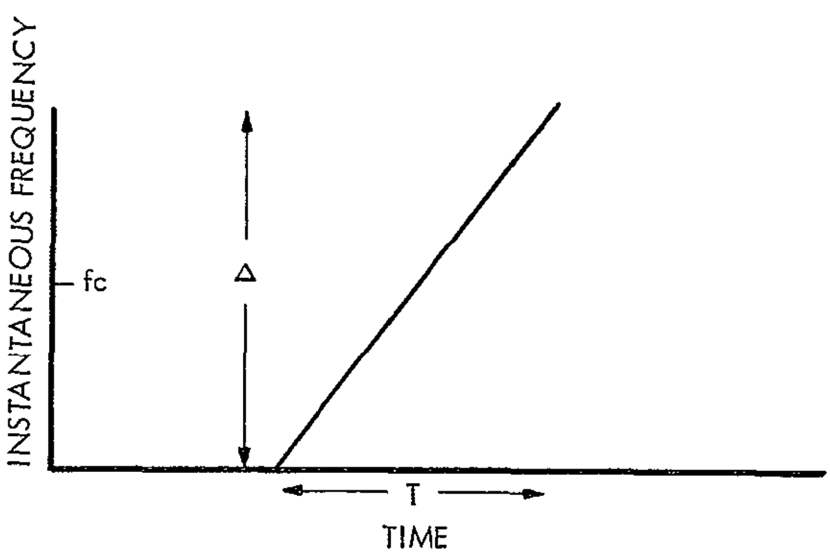

(b) LINEAR FREQUENCY MODULATION VS TIME AND THE FREQUENCY EXCURSION Δ

Figure 4-61 CHIRP Transmitted Waveform

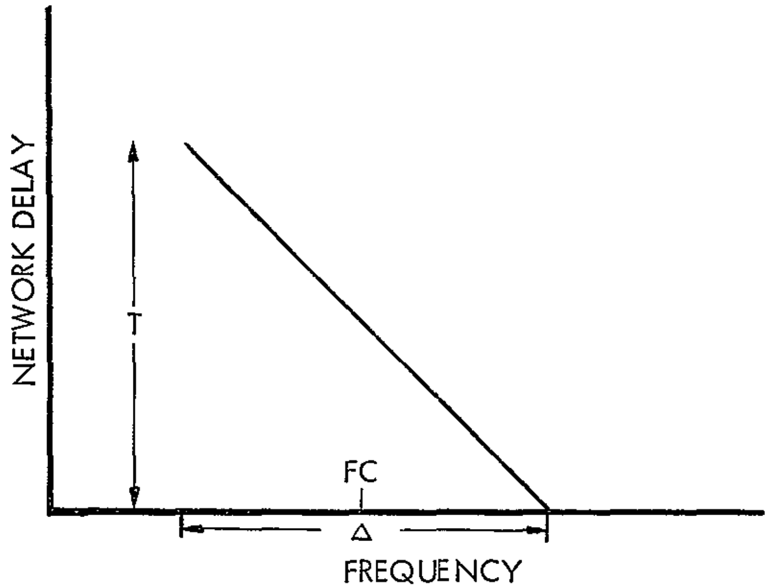

(a) REQUIRED RECEIVER DELAY RESPONSE FOR CHIRP

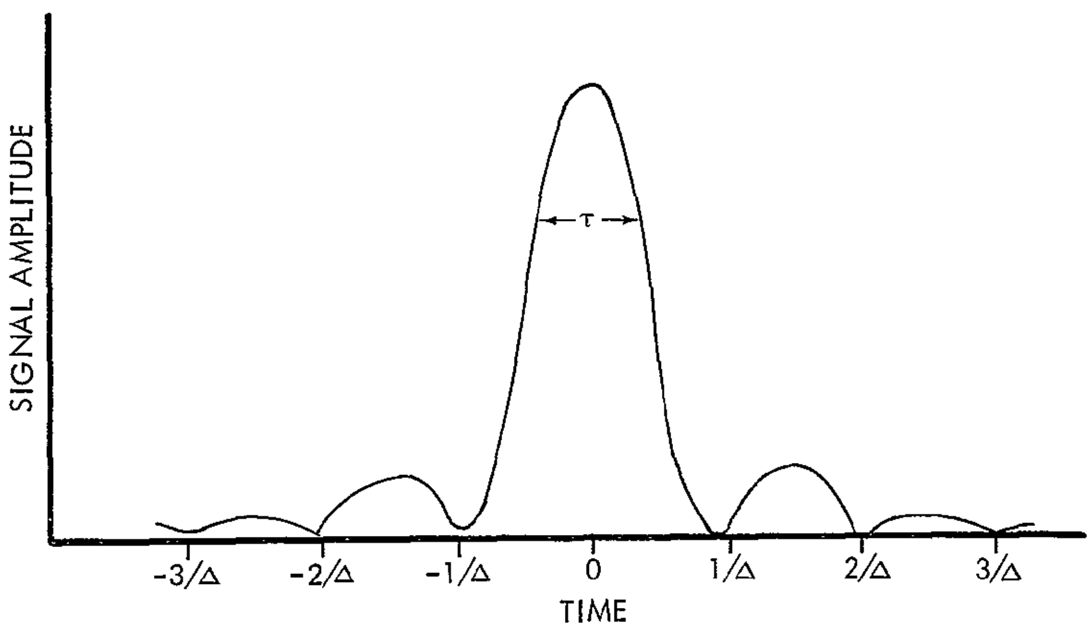

(b) TIME RESPONSE OF RECEIVER WITH DELAY CHARACTERISTIC OF (a) TO A LINEAR FM CHIRP SIGNAL

Figure 4-62 Receiver Response

where

c_p is the dispersion factor

Δ is the frequency excursion of the transmitted pulse

t is the time.

There are several significant features of Figure 4-62(b) which bear on system design. The collapsed pulse width, τ, is defined as the 3 db width of the main lobe of the sin x/x function and is of the order of $1/\Delta$ Secondly, the collapsed pulse amplitude is proportional to the square root of c_p This implies that the CHIRP average pulse of duration T can be compressed to a narrow pulse of equivalent average power during the pulse resulting in an effective peak power directly proportional to the dispersion factor c_p The third significant feature is the appearance of "so-called" time sidelobes which are in effect spurious target responses. The appearance of the time sidelobes is the direct consequence of the equivalence of the mathematical theory of pulse compression and aperture antennas A change in the symbology of the mathematics of pulse compression can convert it directly to the equivalent of the mathematics of antenna array design This point is significant since it permits the application of highly developed antenna theory to pulse compression receiver design especially in the area of sidelobe suppression It can be shown that by proper weighting of the frequency response of the receiver, the time sidelobes of the compressed pulse can be suppressed to insignificant levels with typical suppression values of 25 to 30 db below the main lobe response This is accomplished at the price of slight increases in the collapsed pulse width but the equivalent pulse width is still essentially equivalent to the reciprocal of the frequency excursion, Δ.

To illustrate the usefulness of pulse compression, consider the difficulty of obtaining 100 ft ground resolution with a conventional pulse system From Figure 4-56 it can be seen that a 0 1 microsecond pulse width is required If a dispersion factor of 100 is assumed, then the actual transmitted pulse using CHIRP would be 10 microseconds Furthermore for equal average power, the peak power in the conventional case would be of the order of 1 26 megawatts as discussed previously for orbital altitudes but with a dispersion factor of 100 the peak power requirements would be reduced to 12 6 kilowatts Therefore, high resolution has been obtained using pulse compression with significant reduction in peak power requirements The reduction has been obtained, of course, at the expense of a relatively large increase in complexity The point to be made, however, is that with suitable radar design many of the limiting factors such as peak power generation can be alleviated with suitable design approaches

Angular Resolution The improvement of the angular resolution of a mapping radar system implies the use of techniques other than straightforward improvement of radar state-of-the-art technology The limitations inherent in conventional techniques are quite clear so that an alternate approach is indicated If, for example, data on a target can be accumulated over a time period, it should be possible to combine the data in such a way that target resolution is improved While this approach is readily envisioned, it is somewhat more difficult to postulate what properties of the target can be used in accumulating a history such that when the individual target measurements are combined they will result in increased knowledge of the target properties such as size, shape, and location.

It has been shown that of all the target properties which a radar might measure, the single most useful feature is the variation in the Doppler frequency of a target as an antenna of finite beamwidth is moved past the target The Doppler history of the target, if properly accumulated, can be used to reconstruct the target with a level of resolution equivalent to an antenna of length equal to the time that the target is illuminated by a real aperture

This approach has led to the development of side-looking radar carried in a moving vehicle since the side-looking configuration generally optimizes the amount of time that the target is illuminated while the vehicle motion causes a variation in Doppler frequency as the antenna is moved past the target. Such systems are frequently designated as synthetic aperture systems since the Doppler data gathering process may continue as long as the target is illuminated by the real aperture

It should be understood that such an approach is truly a data processing radar since two essential steps must be followed in sequence It is first necessary to accumulate the Doppler history of a target and then process the Doppler data to reconstitute a high resolution image Many difficulties associated with high resolution radar design arise from the data processing requirements However, for an unmanned spaceborne system it is postulated that the radar processing will be accomplished on the ground and the spaceborne portion of the system consists only of the sensing elements.

The mechanization for azimuth resolution improvement is based on the detection and recording of the Doppler velocities generated by the linear motion of an antenna past fixed surface targets For a fixed antenna beamwidth, the Doppler velocity generated by a fixed target and an antenna linear velocity V can be expressed in terms of the Doppler frequency as

$$f_D = \frac{2\mu}{\lambda} \tag{33}$$

where μ is the radial velocity component of the fixed target toward the antenna As can be seen from the geometry in Figure 4-63 the radial component of the velocity results in a Doppler frequency given by

$$f_D = \frac{2V \sin \alpha}{\lambda} \tag{34}$$

for an antenna velocity, V, and a target lying within the beamwidth of a side-looking antenna For an antenna of fixed aperture length the total Doppler bandwidth generated by the target is nominally that range of frequencies generated between the half-power beamwidth points of the antenna pattern Also because the beamwidth is generally a small angle, the target angle, α, is also small so that

$$f_D = \frac{2V\alpha}{\lambda} \tag{35}$$

and from the geometry the Doppler spectrum width is given by

$$\Delta f_D = \frac{2V}{\lambda}\left[\frac{\beta_a}{2} - \left(-\frac{\beta_a}{2}\right)\right] = 2V\frac{\beta_a}{\lambda} \tag{36}$$

where β_a is the antenna azimuth beamwidth

Also since

$$\beta_a = 1\ 2\frac{\lambda}{D_a} \tag{37}$$

it follows that

$$\Delta f_D = 2 \times 1.2\frac{V}{D_a} \tag{38}$$

This expression implies that, for a fixed velocity, large antenna sizes restrict the Doppler bandwidth which in effect reduces the number of samples which can be used to obtain improved resolution As discussed below, this expression contains the basic fact that resolution of a data processing radar is, at least in theory, limited primarily by the antenna aperture length and in the

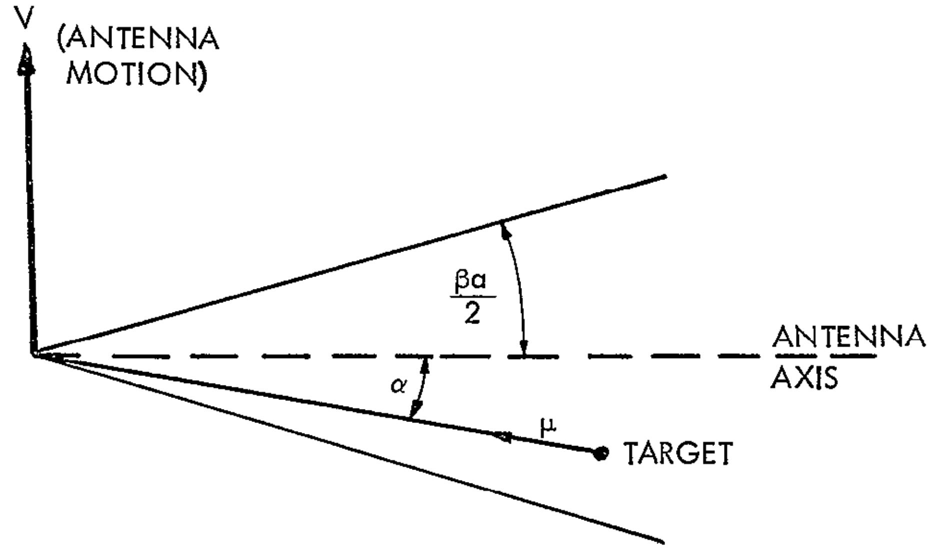

Figure 4-63 Target Doppler Geometry for a Moving Antenna

limit is established by one half the aperture length High resolution therefore requires small apertures to obtain sufficient Doppler bandwidth for processing

Of equal significance, however, is the corollary requirement for detecting all Doppler frequencies over the Doppler bandwidth of interest It is a well known fact of sampling theory that in order to measure frequency unambiguously it is necessary to have at least two samples per cycle In a sampled data system such as a pulsed radar this requirement imposes a restriction on the minimum PRF which can be used to determine the Doppler frequencies over a given bandwidth Δf_D It follows therefore that

$$PRF \geq \frac{2 \times 2\ 1\ 2V}{D_a} = \frac{4V\beta_a}{\lambda} \tag{39}$$

In a more general way, it can be shown that

$$PRF = \frac{2MV\beta_a}{\lambda} \tag{40}$$

where, depending upon the type of data processing used, M may have a value of either 1 or 2

If the PRF serves as a measure of the maximum unambiguous Doppler frequency which is used in the data processing, then it follows from the geometry that an effective array length is generated which is equivalent to the time that the fixed target is in the beam. For a target at range R this is equivalent to a length, ℓ , given by

$$\ell = R\beta_a \tag{41}$$

where β_a is the azimuth beamwidth of the real antenna But the length ℓ is equivalent to an effective beamwidth of

$$\beta_{eff} = \frac{k\lambda}{\ell} \tag{42}$$

and an equivalent ground resolution r_a given by

$$r_a = R\beta_{eff} = \frac{kR\lambda}{\ell} \tag{43}$$

also since

$$\ell = R\beta_a \tag{44}$$

it follows that

$$r_a = \frac{kR\lambda}{R\beta_a} = \frac{k\lambda}{\lambda/D} = kD \tag{45}$$

which states that the equivalent ground resolution is limited ultimately by a single parameter, the antenna physical length, D Furthermore it follows that resolution is independent of the geometry and operating frequency under the assumption that the full Doppler spectrum width is used This has implications in the data processing system since the full Doppler spectrum width which is generated by a target is not independent of range so that the processing must be adjusted as a function of range to incorporate longer lengths of ground trace as the range increases This procedure is frequently referred to as focusing the synthetic aperture, and the high resolution radar is referred to as a focused system

A coherent Doppler mapping system can be operated in an unfocused mode such that the Doppler information which is processed is an inverse function of range Resolution improvement is obtained, but it is no longer independent of range. It can be shown that in an unfocused mode of operation the ground resolution is proportional to the square root of range rather than directly proportional to range so that resolution improvement over a conventional system is obtained. For discussion purposes, it is assumed, however, that a focused data processing scheme will be used and azimuth ground resolution is essentially independent of range

In addition to the minimum PRF imposed by the maximum Doppler frequency requirement, there is also a maximum PRF imposed by the mapping length in the range direction. As discussed previously, in order to map a length W in the range direction unambiguously, it is necessary that the interpulse period of the radar meet the criterion

$$T \geq \frac{2W \sin \gamma}{C} \tag{46}$$

where

γ is the elevation angle of the antenna beam

W is the swath length in the range direction

C is the velocity of propagation

Therefore, the PRF must be

$$PRF \leq \frac{C}{2W \sin \gamma} \tag{47}$$

The PRF is thus constrained to lie within the limits

$$\frac{2MV\beta_a}{\lambda} \leq PRF \leq \frac{C}{2W \sin \gamma} \tag{48}$$

or in terms of the azimuth aperture length, D_a,

$$\frac{2kMV}{D_a} \le PRF \le \frac{C}{2W \sin \gamma} \tag{49}$$

For the best theoretical resolution, it follows that

$$D_a \ge \frac{2kMV}{PRF} \tag{50}$$

with a minimum ground resolution given by

$$r_a = kD_a = \frac{V}{PRF} \tag{51}$$

where k has the value of approximately 1/2.

The constraints on resolution, aperture size, and range swath length are shown plotted in Figures 4-64, 4-65 and 4-66 respectively for an orbital altitude of 200 miles and an antenna velocity of 24,000 feet/second Consideration of the data in the figure indicates that there are no basic limitations on attainable ground resolution imposed by either the antenna azimuth dimension or the PRF. However, it should be borne in mind that once a particular system parameter is selected, very little latitude remains for trading-off other system parameters If, for example, an antenna azimuth size is chosen, then the best ground resolution and range swath length are constrained by the PRF Even cursory consideration of the data in the figures, however, indicates that unless very high resolution is sought, say of the order of 5 to 10 feet, then a large amount of latitude is available in selecting system parameters For these reasons system design is more highly restrained by hardware parameters when such requirements as transmitted power are considered.

<u>System Characteristics</u> Transmitted Power Requirements In deriving the requirements for a spaceborne high resolution radar the following assumptions are made

Required ground resolution r_a = 100 ft

Maximum antenna dimension D_a = 50 ft

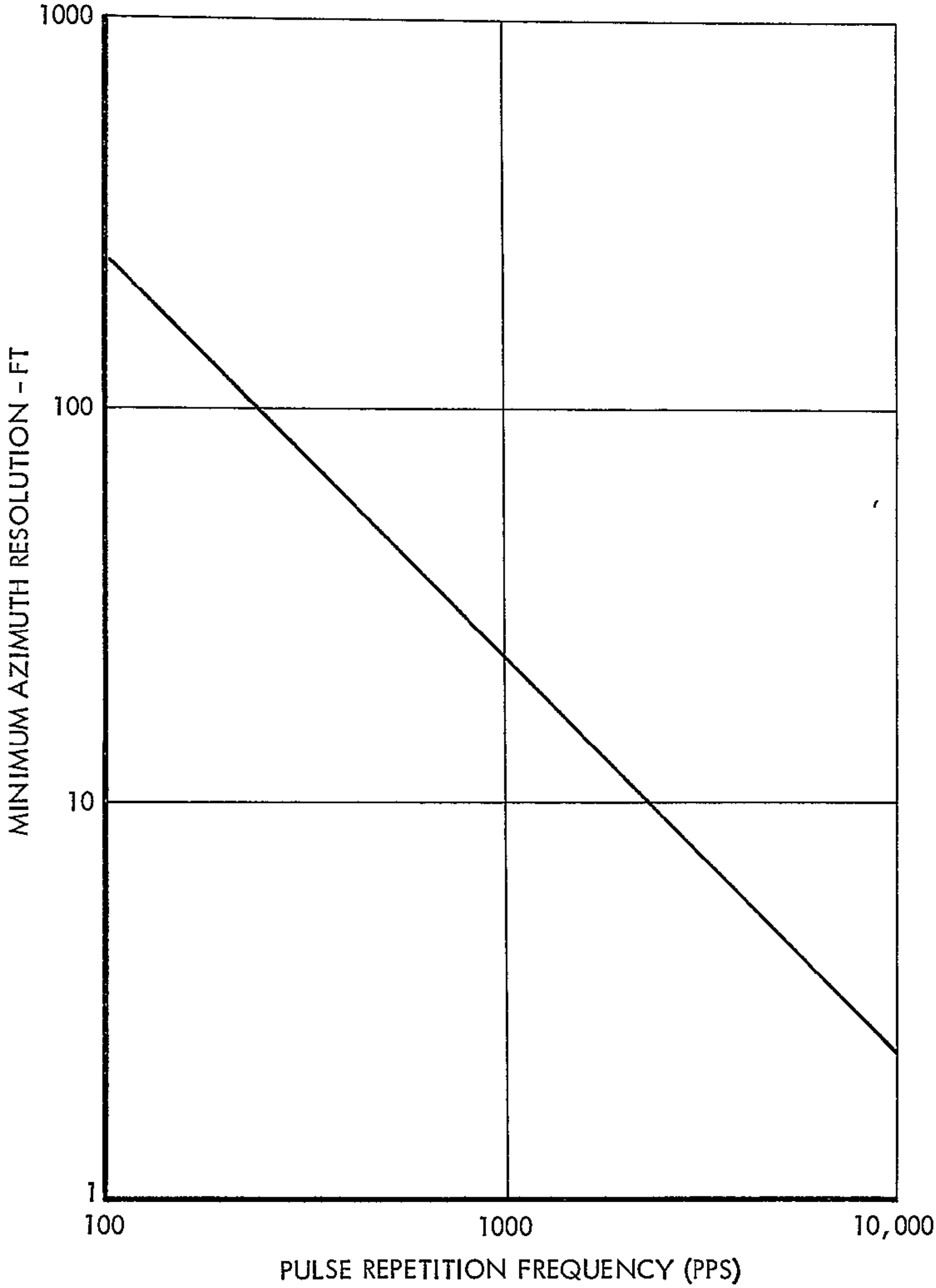

Figure 4-64 Minimum Azimuth Resolution Based on System Constraints

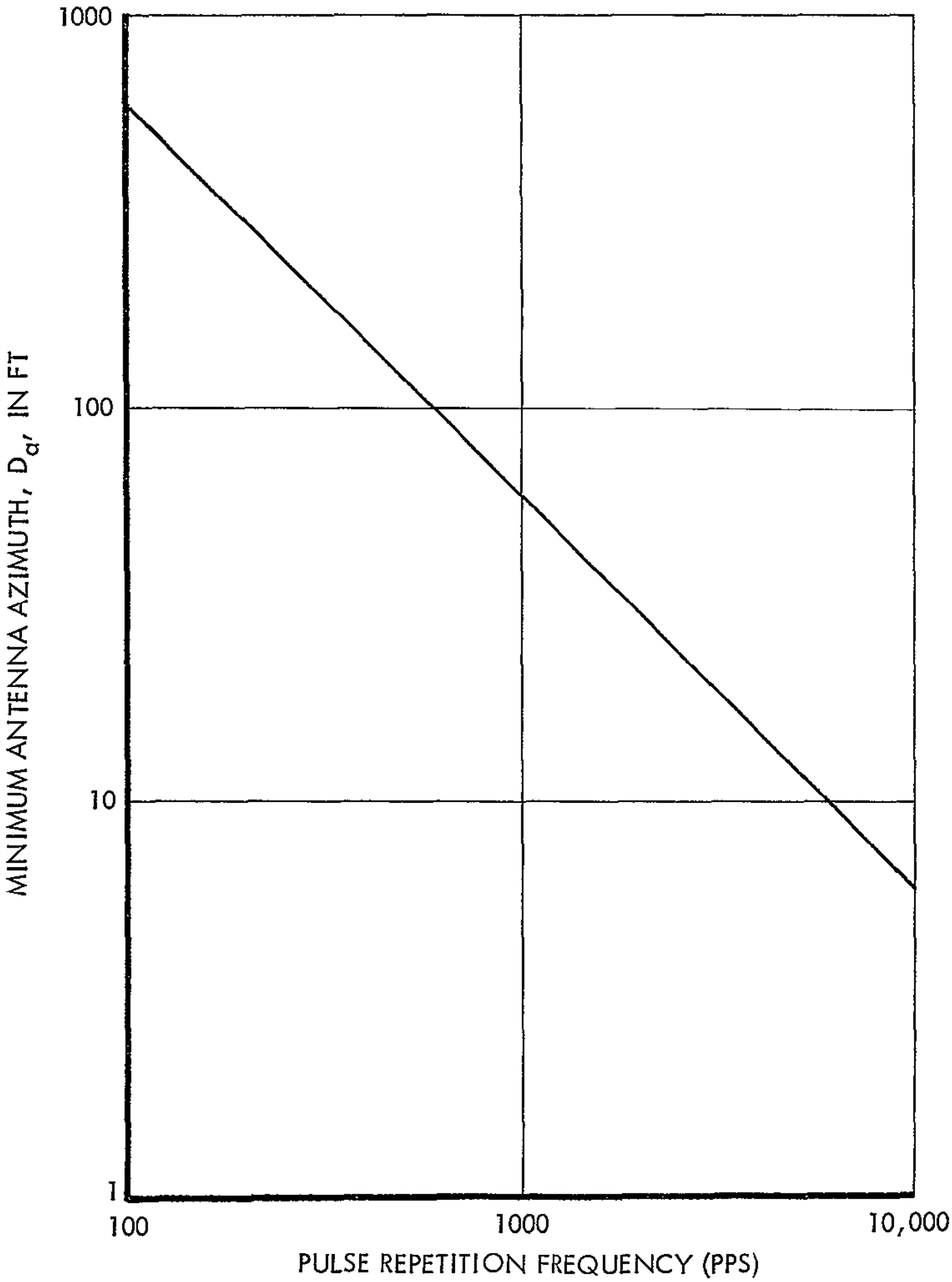

Figure 4-65 Minimum Antenna Aperture

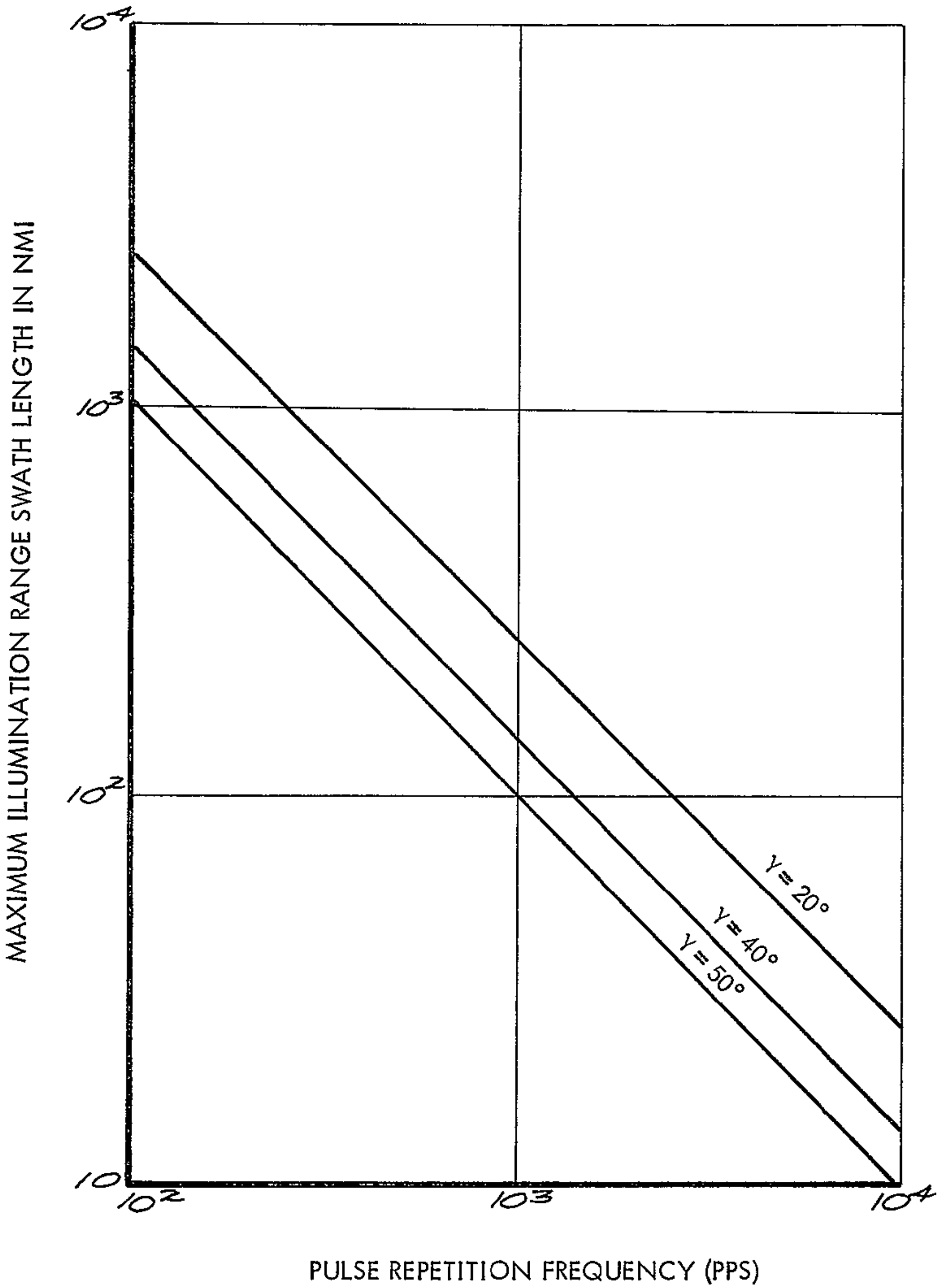

Figure 4-66 Maximum Illuminated Swath Length as a Function of Elevation Angle

Orbital altitude H = 200 nmi

Orbital velocity V = 2.4×10^4 ft/sec

Range swath length W = 100 nmi

Antenna elevation angle = 45 deg

Pulse compression ratio P_c = 100

Operating frequency - (X band) λ = 3 cm

Minimum radar backscatter coefficient δ = - 40db

The procedure for determining transmitter power requirements are essentially the same as in the non-coherent case except that pulse compression and coherent integration are assumed. For coherent integration the number of pulses integrated is, from the geometry, given by

$$m = \frac{R\beta_a \, (PRF)}{V} \tag{52}$$

If this expression is substituted into the expression for received power there results

$$P_r = \frac{P_t G^2 \lambda^2 L \sigma m}{(4\pi)^3 R^4} = \frac{P_t G^2 \lambda^2 L \beta_a \, (PRF) \sigma}{(4\pi)^3 R^3 V} \tag{53}$$

but

$$\beta_a = 1.2 \frac{\lambda}{D_a} \tag{54}$$

so that

$$P_r = \frac{P_t G^2 \lambda^3 L \, 1.2 \, (PRF) \sigma}{(4\pi)^3 R^3 V D_a} \tag{55}$$

For a ground resolution of 100 feet, the minimum PRF is, from Figure 4-64, approximately 250 pps However, from Figure 4-66 a ground swath length of 100 nmi permits a PRF of approximately 1200 pps so that the larger value of PRF is chosen

The received power is computed with the peak transmitted power as a parameter Since

$$\sigma = r_a \; r_r \; \delta \tag{56}$$

where

$r_a = r_r = 100$ ft (the ground resolution)

$\delta = 10^{-4}$ (-40 db backscatter coefficient)

so that

$$\sigma = 1 \text{ ft}^2 = 0\ 093\text{m}^2$$

There is negligible atmospheric transmission loss at X-band, so that the system losses are assumed to be -4 0 db or

$$L = 4 \text{ db} = 0\ 4$$

The antenna gain is given by

$$G = \frac{2\ 5 \times 10^4}{\beta_a \; \beta_e} \tag{57}$$

and

$\beta_a = 14$ deg

$\beta_e = 15$ deg (from Figure 4-58)

so that

$$G = 1\ 19 \times 10^4$$

$$G^2 = 1.42 \times 10^8$$

also

$$R = 322 \text{ mi} = 6 \times 10^5 \text{ meters}$$

$$R^3 = 2.16 \times 10^{17} \text{ m}^3$$

If these values are substituted into the expression for received power we obtain

$$P_r = 4\ 3 \times 10^{-21}\ P_t \text{ watts}$$

System noise power is given by

$$N = \overline{NF}kTB \tag{58}$$

which is computed as previously except that at X band

$$\overline{NF} = 8 \text{ db} = 6\ 3 \text{ (from Figure 4-59)}$$

and the system bandwidth which must be wide enough to permit a dispersion factor of 100 in the pulse compression circuits while obtaining an effective pulse width of 0 1 microseconds for 100 ft ground resolution The actual transmitted pulse width is 10 microseconds long but the modulation on the pulse imposes a bandwidth of

$$B = \frac{1}{\tau} = 10 \text{ megaHertz} \tag{59}$$

where τ is the compressed pulse width The noise power is therefore

$$N = 6\ 3 \times 1.38 \times 10^{-23} \times 3 \times 10^2 \times 10^7 \text{ watts}$$

$$N = 2.6 \times 10^{-13} \text{ watts}$$

For unity signal-to-noise ratio

$$P_t = \frac{2\ 6 \times 10^{-13}}{4\ 3 \times 10^{-21}} = 6\ 05 \times 10^7 \text{ watts}$$

and for a 10 db signal to noise ratio the transmitted peak power becomes

$$P_t = 6\ 05 \times 10^8 \text{ watts}$$

Even with a dispersion factor of 100 the peak power required is only reduced to

$$P_{t_c} = 6.05 \times 10^6$$

which is excessive In order to reduce the peak power level it is necessary to reduce the swath length in the range direction If the range swath length is reduced to 10 miles then the elevation beamwidth of the antenna would be reduced from 15 deg to 2 deg This would reduce the peak power requirements by approximately 20 db so that

$$P_{t_c} = 6\ 05 \times 10^4 \text{ watts}$$

which is marginal for state-of-the-art of X band transmitters

For a 200-nmi orbit the average power required for a 100-foot ground resolution is

$$P_{av} = P_t\ T\ (PRF) \tag{60}$$

where T is the duration of the uncompressed pulse The average power therefore is

$$P_{av} = 725 \text{ W}$$

The average power penalty is higher in the coherent radar case but the resolution improvement is approximately one and one half orders of magnitude.

Radar Data Output The output of the radar system is wideband, pulse compressed, bipolar video which, for optimum signal detection, contains both in-phase and quadrature signal components The in-phase and quadrature components require dual output channels so that it is desirable to combine the two signals in a quadrature combiner to form a single vector signal This would add complexity to the radar but would simplify the data processing

One of the most difficult design tasks in the high resolution radar is the preservation of signal information content from the output of the radar to the input of a ground-based data processing system By their very nature the high resolution signals are wideband since it is necessary to preserve a signal bandwidth equivalent to the pulse width required for a 100-foot ground resolution Since this requires a 0 1 microsecond pulse, the bandwidth of the information in the high resolution video signals is of the order of 10 megaHertz

The wideband signal can be modulated directly in analog form onto a carrier if real time data transmission is postulated However, it is more reasonable to expect that a digital recording system would be used since analog recording at 10 megaHertz would impose a severe system penalty Even so, a wideband digital recording system with a dynamic range suitable for converting all signals in the expected range of ground signals presents a difficult design task

There are few alternatives available which would result in significant compression of the raw data output from the radar This follows from the fact that the output data is generally meaningless when interpreted on a pulse by pulse basis since the information is only useful when it is combined with information from preceding and/or following range scans of the radar One obvious, although not attractive, approach is to process the radar data on-board the spacecraft and then transmit only those high resolution images which contain significant information This approach would result in an enormous increase in system size, weight, power consumption and complexity

<u>Data Rate</u> As discussed previously in the noncoherent radar case, the data rate is determined by the ground resolution of the radar, the pulse repetition frequency and the length of the ground swath in the range direction For a 10 nmi swath length and a 100-foot ground resolution, the data per transmitted pulse is

$$N_p = 6\ 08 \times 10^2 \ \frac{\text{resolution cells}}{\text{pulse}} \qquad (61)$$

For a PRF of 1200 pps this becomes

$$N = 7\ 3 \times 10^5 \text{ resolution cells/second} \qquad (62)$$

If, as previously, a six-bit binary word were used to represent the dynamic range of signals, then most of the significant information would be lost This follows from the fact that a true vector signal is generated and a wider dynamic range is necessary From practical considerations a 12-bit word is postulated so that the bit rates becomes

$$\text{Bit rate} = 12 \times 7\ 3 \times 10^5 = 8\ 8 \times 10^6 \text{ bits/sec}$$

or approximately 10 megabits per second

4 5 3 2 Scaling Law Development

The discussion presented above gives a general approach to radar system design based on specific parameter definition A more general scaling law approach is developed to estimate support requirements when a radar can be demonstrated to be feasible

Geometry Consider a sidelooking antenna such that the sidelook plane is the plane normal to the satellite's flyby orbital plane and through the current local vertical to the, assumedly, spherical planet of radius R_p (Note that this definition places the sidelook plane normal to the tangent to the orbit of periapse only, so that for an orbit of eccentricity $\varepsilon > 0$, there will be a non-zero doppler component due to the spacecraft velocity for true anomaly, $\emptyset \neq 0$)

Let the antenna dimension in the sidelook plane, that is, the antenna height, be denoted by D_r, and the antenna length, the dimension parallel to the orbital plane, by D_a the respective 3 db beamwidths are then

$$\beta_r = \frac{K_{D_r} \lambda}{D_r} = \frac{1\ 25\ \lambda}{D_r} \tag{63}$$

$$\beta_a = \frac{K_{D_a} \lambda}{D_a} = \frac{\lambda}{D_a} \tag{64}$$

Where

λ = transmitted wavelength

K_{D_r} = Antenna pattern factor in sidelook plane

K_{D_a} = Antenna pattern factor in plane normal to sidelook

Antenna gain is maximized by choosing illumination tapers as small as possible consistent with the maximum first sidelobe level permissible In the sidelook plane, suppression of the altitude return requires sidelobes of at most, say, -25 db so that $K_{D_r} = 1\ 25$, while in the direction of the orbit a sidelobe level of -13 db is acceptable (uniform illumination) so that $K_{D_a} = 1\ 0$

The antenna area is

$$A_{Ant} = D_r \quad D_a \tag{65}$$

The antenna gain

$$G = \frac{4\pi}{\beta_a \; \beta_r} = \frac{4\pi \cdot D_a \cdot D_r}{\lambda^2 \, K_{D_a} \; K_{D_r}} = \frac{4\pi \, D_a}{\beta_r \, \lambda} \tag{66}$$

Referring to Figure 4-67, the following relations will be useful The depression angle at the far beam edge, α, from the local horizontal at the spacecraft is constrained by the horizon limit, $\emptyset_h$, such that $\alpha > \alpha_h$ and

$$\alpha_h = \arccos \left[\frac{1}{1 + H/R_p} \right] \tag{67}$$

where H is the altitude above the planet surface Further, the grazing angle at the far beam edge, $\psi 2$, is defined by the depression angle as

$$\psi_2 = \arccos \left[(1 + H/R_p) \cos \alpha \right] \tag{68}$$

The distance to the planet at the far beam edge, the maximum range within the beam is

$$R_2 = R_p \, (\tan \alpha \cos \psi_2 - \mathrm{Sin}\, \psi_2)$$

$$= R_p \left[(1 + \frac{H}{R_p}) \, \mathrm{Sin}\, \alpha - \left\{ 1 - (1 + \frac{H}{R_p})^2 \cos \alpha^2 \right\}^{\frac{1}{2}} \right] \tag{69}$$

The swath length, W, defined as the distance along the great circle arc in the sidelook plane over which resolved imagery is to be obtained,

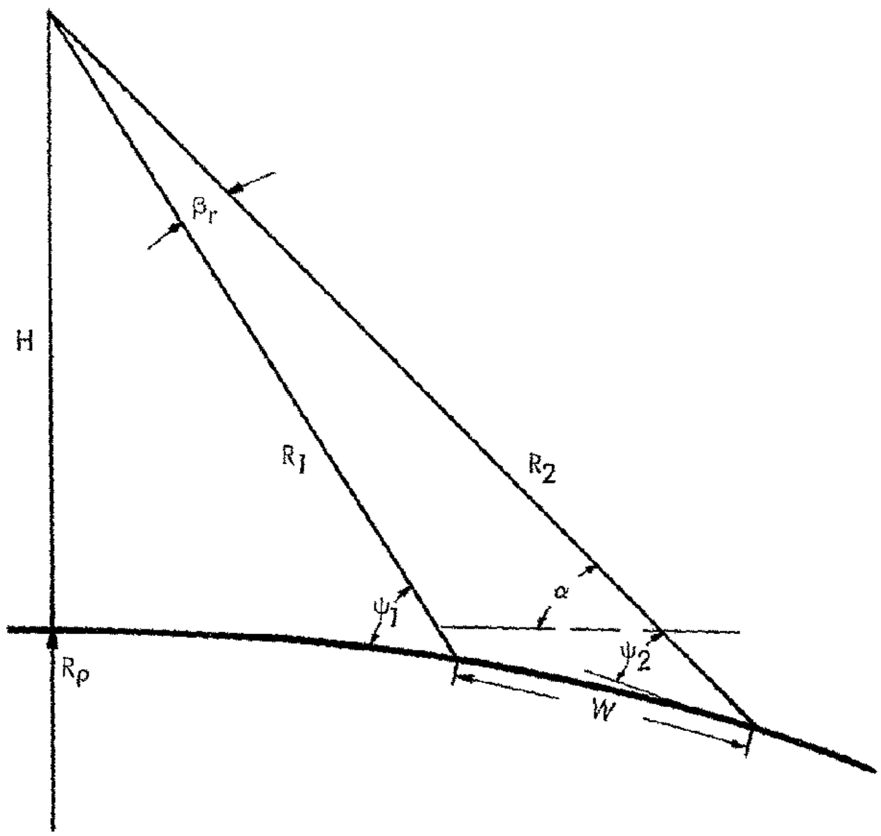

Figure 4-67. Geometry in Sidelook Plane for Mapping Radar

constrains the sidelook beam width, β_r, and conversely An exact relation defining β_r as a function of W, H, and R_p is given by

$$\beta_r = \arctan \left[\frac{W \sin (\psi 2 + \frac{W}{2 R_p})}{R_2 - W' \cos (\psi 2 + \frac{W}{2 R_p})} \right] \tag{70}$$

where W′ is the chord of W

However, for the problems at hand, β_r will, of necessity, be a small angle and similarly, $W \ll R_2$, permitting a simpler and more useful approximate scaling relation, namely

$$\beta_r \approx \frac{W}{R_2} \sin \psi_2 \tag{71}$$

Ground-Imposed Relations Let the ground resolution dimension required be denoted by r_h, and stipulate that this resolution requirement be the same in the sidelook direction as in the direction of the orbital path

Referring to Figure 4-68 the conditions imposed by the resolution geometry are as follows

The synthetic aperture length, D_{sa}, is related to the resolution in the direction of travel by

$$r_h = \frac{R_2 \lambda}{2 D_{sa}} \tag{72}$$

That is to say that the minimum value of D_{sa} is given by the resolution required at the far edge of the swath The resolution in the sidelook direction must be achieved by pulse width control so that the ground distance encompassed by the processed pulse width satisfies the relation

$$r_h \geq \frac{C \tau'}{2 \cos \psi_1} \tag{73}$$

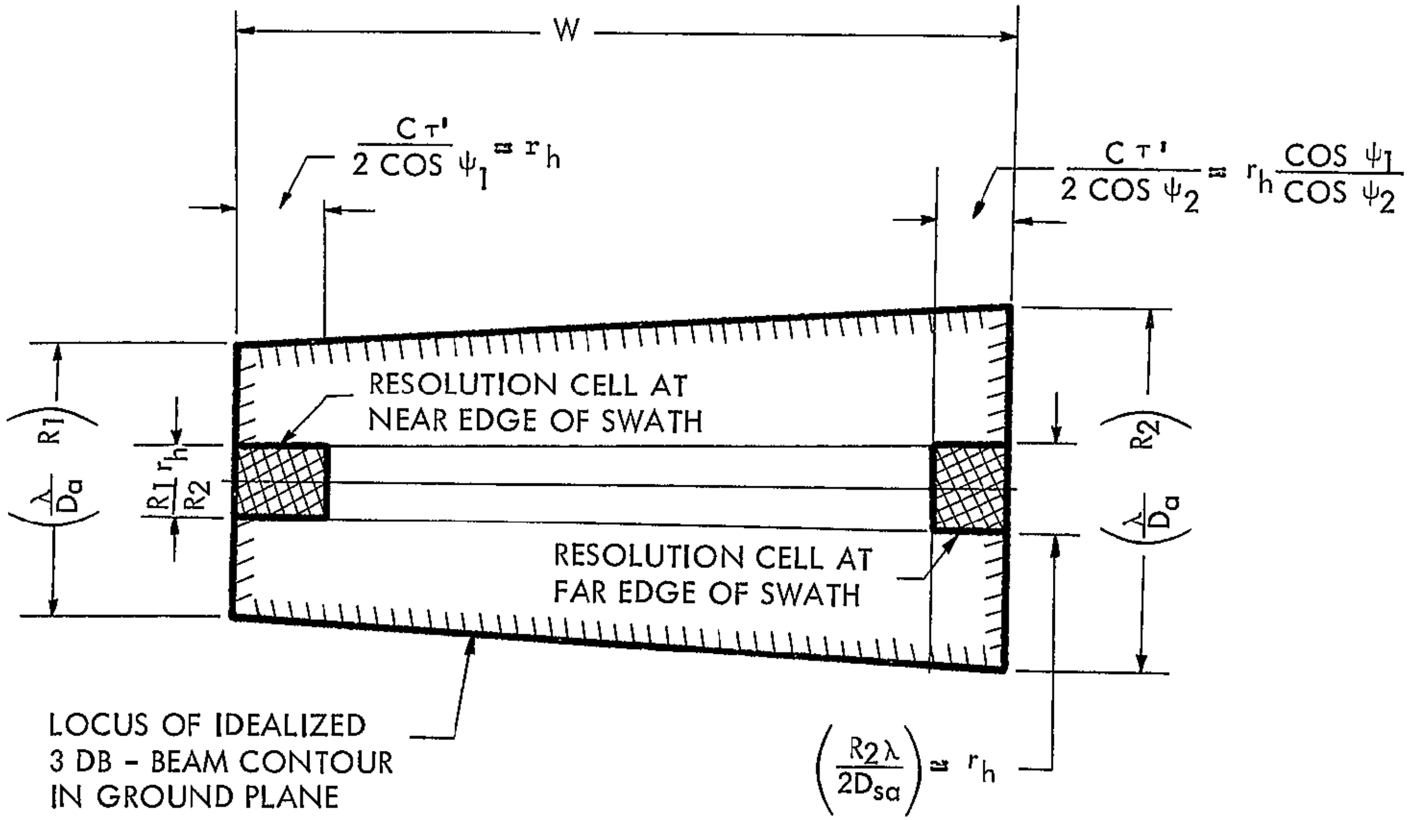

Figure 4-68 Resolution Geometry

where τ' is the processed pulse width (on receive) and ψ_1 is the minimum incidence angle, which occurs at the near edge of the swath

Again, for the conditions permitting Equation (71),

$$\frac{\cos \psi_2}{\cos \psi_1} \approx 1, \tag{74}$$

making the resolution degradation over the swath width negligible such that

$$r_h \approx \frac{C\ (\tau')\ \max}{2 \cos \psi_2} \tag{75}$$

(Note that the utilization of pulse compression techniques permits the transmitted pulse width, τ, to be $(c_p\ \ \tau')$ where c_p is the compression ratio This technique will yield higher transmitter duty cycles and the attendant reduction in peak power transmitted

The pulse repetition rate, P, is directly constrained by the stated problem geometry due to the imposition of, at least, range unambiguity over the swath width, that is

$$\frac{1}{P} \geq \frac{2\ (R_2 - R_1)}{C} \tag{76}$$

more exactly if the transmission time is taken into account,

$$\frac{1}{P} \geq \tau + \frac{2\ (R_2 - R_1)}{C} \tag{77}$$

A more useful form of (77) is obtained by substituting

$W \cos \psi_2 \approx (R_2 - R_1)$, and making use of (75) results in

$$P \leq \frac{C}{2 \cos \psi_2\ (W + c_p\ r_h)} \tag{78}$$

In general, set $P = P_{max}$ permissible by (78) in order to minimize the required transmitted peak power [see Equation (102)] and to optimize the transmitter duty cycle. A further simplification in this relation obtains, for $(cp \gamma r_h) << W$, a condition which will practically always be met if a synthetic aperture is required in the first place. Then

$$P_{max} \approx \frac{C}{2 \cos \psi_2 W} \qquad (79)$$

Antenna Dimension Scaling Laws. The antenna length, D_a, that is, its dimension in the direction normal to the sidelook plane, has a lower limit imposed by the relations of the physical antenna pattern to the pattern of the synthetic antenna. In particular, the doppler ambiguity restriction is

$$D_a \geq \frac{K_{d_a} \quad 2 V_h}{PRF} \qquad (80)$$

A second restriction arises from angular ambiguity caused by the relative position of the synthetic aperture sidelobe with respect to the physical antenna's main lobe. This ambiguity is eliminated by the restriction

$$D_a \geq \frac{4 V_h}{PRF} \qquad (81)$$

Since $K_{D_a} < 2$, [see equation (64)], equation (81)) represents the dominant restriction. Here, V_h is the planet's surface velocity normal to the sidelook plane within the beam. For scaling purposes, it will be convenient to set

$$(V_h)_{max} \approx V_s (0) \qquad (82)$$

where V_s (0) is the velocity of the subsatellite point at periapse. (This substitution will be valid whenever the planetocentric angle, γ_2, between the local vertical and the swath edge, remains small for swingby orbits, in attaining a fixed minimum incidence angle, (ψ_2) of say, $\psi_2 = 45°$.)

An obvious and trivial upper bound on the antenna length is

$$D_a < D_{sa} \qquad (83)$$

This relation, however, in conjunction with (72) results in a lower limit on the attainable resolution, namely

$$r_h \geq \frac{D_a}{2} \tag{84}$$

For the missions under consideration, the resolution requirements as well as the limitations on transmitted power, [see Equation (96)], and the antenna lengths due to the state-of-the-art, dominate r_h minimum far above the limits of (84) In particular, an upper limit on antenna dimension (in any direction) is

$$(D_r)_{max} = (D_a)_{max} = 1000\ \lambda \tag{85}$$

Scaling laws defining the antenna height, D_r, and minimum antenna length $D_{a\,min}$ as a function of spacecraft altitude and swath length, W, are then defined as

$$D_r \approx \frac{1\ 25\ \lambda\ R_2}{W \sin \psi_2} \quad (1000\ \lambda) \tag{86}$$

from (63) and (71), and from (77) and (81)

$$\frac{8\ V_h\ W \cos \psi_2}{C} \leq D_a < (1000\ \lambda) \tag{87}$$

(Note that the term on the left is independent of λ) Several other useful scaling laws for the antenna dimensions obtained directly from the above as

$$(D_a)_{min} = \frac{10\ \lambda\ V_h \cdot R_2}{D_r \cdot C \quad \tan \psi_2} \tag{88}$$

and the minimum antenna area, (A_{ant}), as a function of the problem geometry only, by

$$(A_{ant})_{min} = (D_a)_{min}\ D_r = \frac{10\ \lambda\ V_h\ R_2}{C \tan \psi_2} \tag{89}$$

Expression (89) can be used as a means of direct elimination of coherent radar utilization for a given planet orbit, regardless of any power, resolution or mapped-area-extent trade-offs, by the imposition of a maximum antenna area (or weight) due to, say, logistic requirements In the absence of such limitations, there still exists the previously stated restriction of (85)

$$(A_{Ant}) < 10^6 \lambda^2 \tag{90}$$

Note also that receiver bandwidth constraints, due to (80), and antenna size constraints, due to (86) and (87), readily restrict the choice of the incidence angle, ψ_2, to the neighborhood of $\pi/4$

Radar System Characteristics The required average transmitted power, P_{av}, is a function of the problem geometry, resolution, and extent of area mapped It is likely the most important parameter in the scaling laws since it defines the input power required from the spacecraft as well as the size and weight of the radar transmitter Again, determination of a $(P_{av})_{min}$ for a given planet flyby permits direct assessment of the feasibility of utilization of coherent mapping radar for the mission phase, given a maximum available input power

The radar equation is

$$P_{av} = P_t \tau (PRF) = P_t \quad c_p \tau' (PRF) \tag{91}$$

$$= \frac{\tau' (PRF) \quad R_2^4 \cdot (4\pi)^3 \quad (S/N) \quad K \cdot T \quad B \cdot (\overline{NF}) (L_{RF}) (L_{atm})}{m \quad \sigma_2 \quad G^2 \quad \lambda^2}$$

where

P_{av} = average transmitted power (watts)

P_t = peak transmitted power (watts)

τ = transmitted pulse width (seconds)

c_p = pulse compression ratio

(PRF) = pulse repetition frequency

τ' = τ / c_p

R_2 = range to far edge of mapped swath

σ_2 = equivalent radar cross section of resolution cell at R_2

m = number of pulses coherently integrated, which is the number of pulses transmitted during the time interval corresponding to the generation of the synthetic aperture length, D_{sa}

λ = transmitted wave length

G = antenna gain

(S/N) = signal-to-noise ratio

K = Boltzmann constant

T = noise temperature (°K)

$(\overline{NF})$ = receiver noise figure

(L_{RF}) = RF-Loss factor

(L_{atm}) = atmospheric loss factor

B = receiver bandwidth (H_z)

The receiver bandwidth for a matched system is $B = 1/\tau'$ The signal-to-noise ratio is customarily set at (S/N) = 10 The RF-loss factor, $(L_{RF}) = 4$(6 db)

The term σ_2 can be written as

$$\sigma_2 = r_h^2 \delta \tag{92}$$

that is, the resolution cell size multiplied by a backscatter coefficient, δ In the absence of detailed information on radar reflectivity for the outer planets, a conservative constant value of $\delta = 5 \times 10^{-4}$ (-33db) is assumed

The number of pulses integrated, m, can be expressed as

$$m = (PRF) \quad t_1 = p \frac{D_{sa}}{V_h} = \frac{(PRF)\,\lambda \cdot R_2}{2\,V_h \quad r_h} \tag{93}$$

where t_1 is the integration time

Here, Equation (9) is used in substituting for D_{sa}

The noise temperature term, T, will be written as

$$T = (200°K) \quad K_T$$

where K_T is a dimensionless temperature coefficient for a given planet, such that

Planet	K_T
Mercury	3 0
Venus	3 5
Jupiter	1 0
Saturn	1 0
Uranus	1 0
Neptune	1 0
Pluto	1 0

(94)

See Reference (2) Figure 8.11

The receiver noise figure ($\overline{NF}$) can be defined as an empirical fit to the state-of-the-art attainable as a function of wavelength only Use of the data in Figure 4-59 results in the relation

$$(\overline{NF})_\lambda = 10^{[\,35(1 + \log_{10}\lambda)]} \quad (\lambda \text{ in meters}) \tag{95}$$

The atmospheric loss factor (L_{atm}) can, for power scaling purposes, be assumed as follows

The beam incidence angle, ψ_2, will be, at least, ($\pi/4$). Then with λ in meters,

$$(L_{atm}) = \exp\left(\frac{9}{\lambda^2 \; 10^4}\right) \quad \text{for Venus (See Reference (2) Page 270)}$$

$$\approx \exp\left(\frac{37}{\lambda^2 \; 10^4}\right) \quad \text{for Jupiter, Saturn, Uranus, Neptune (See Reference (2) Page 271)}$$

$$\approx 1 \quad \text{for Mercury, Mars and Pluto}$$

A simplification, which causes no appreciable uncertainty in power scaling, is to set

$$(L_{atm}) \approx 1 \text{ for } \lambda \geq 0.1 \text{ meters for any planet}$$

The power relation can now be restated, by substitution of (66), (92), (93), and (94) as

$$P_{av} = \left[5.56 \times 10^{-15} \; (\overline{NF}) \; (L_{atm}) \; K_T \; (\text{joules})\right] \frac{\beta_r^2 \;\; R_2^3 \cdot V_h}{D_a^2 \;\; r_h \;\; \lambda} \tag{96}$$

This expression determines power requirements for a given swingby geometry, with ground resolution as the tradeoff parameter since the antenna properties are already constrained by (63) through (89) Substitution of (71) permits restatement of (96) in terms of the swath length, W, as

$$P_{av} = \left[5.56 \times 10^{-15} \; (\overline{NF}) \; (L_{atm}) \; K_T \; (\text{joules})\right] \frac{R_2 \;\; W^2 \;\; V_h \sin^2\psi_2}{D_a^2 \;\; r_h \;\; \lambda} \tag{97}$$

Finally, introducing the ratio (Da_{min}/Da) that is, trading off antenna length beyond the minimum required for power and using (87) for substitution in the above, results in a particularly elegant power relation namely

$$P_{av} = \left[8\ 7 \times 10^{-17}\ (NF)\ (L_{atm})\ K_T \left(\frac{Da_{min}}{Da}\right)^2\ (joules)\right] \frac{R_2 \tan^2 \psi_2\ C^2}{\lambda\ \ r_h\ \ V_h} \qquad (98)$$

Note that this expression defines the transmitted power required as a function of the problem geometry at periapse independently of swath length with ground resolution, r_h, as the only parameter and with antenna length as a trade-off In applying this relation, care must be taken with respect to the upper bounds of D_a of $D_{a(max)} \leq 1000\,\lambda$, see (87) and any other limit on D_a imposed by logistic considerations

The required peak transmitted power, P_t, is

$$P_t = P_{av} \frac{1}{d_c} \qquad (99)$$

where d_c is the transmitter duty cycle By definition

$$d_c = c_p\,\tau'\,(PRF) \qquad (100)$$

Substitution of (75) and (78) then permits duty cycle definition as a function of swath length and resolution as

$$d_c = \frac{c_p r_h}{W + c_p r_h} \qquad (101)$$

So that necessity of pulse compression (if any), as a function of an upper limit on P_t, can be established by inspection of

$$P_t = P_{av} \left[\frac{W}{c_p r_h} + 1\right] \qquad (102)$$

The input power (P_{in}) to the coherent radar transmitter, assuming a transmitter and power supply efficiency of 0 20, is estimated as

$$P_{in} = 5 P_{av} \tag{103}$$

(Here, any constant load, independent of transmitted power, has been neglected as compared with the P_{av} required for the transmitter)

A suggested scaling utilization of the relations (91) through (103) is

Impose on upper bound on P_{in} and P_t The former results in a limiting P_{av}, the latter in a definition of the pulse compression ratio

Let the resolution, r_h, cover the span between the desired and the minimum required values for the given mission This defines the tradeoff bounds for D_a and λ when used in conjunction with the antenna scaling laws The swath length tradeoffs can be kept independent of this procedure by virtue of (98)

<u>Effects of Extension of Radar Map Area in Direction of Orbit on Power Requirements.</u> The required increase in both average transmitted power and peak power, over that required in the neighborhood of periapse, when extending the mapped swath in the direction of the spacecraft path can be defined as follows

Consider a sidelooking radar system at a fixed depression angle, α, with respect to the orbital plane of the satellite for a given flyby orbit about a (assumed spherical) planet of radius R_p

Let $\emptyset$ denote the true anomaly angle of the satellite. Then the satellite altitude from the planet surface as a function of $\emptyset$, denoted by H ($\emptyset$), is

$$\frac{H(\emptyset)}{R_p} = \frac{H(0)}{R_p}\left[\frac{(1+\varepsilon) + \varepsilon(1-\cos\emptyset)}{1+\varepsilon\cos\emptyset}\right] \tag{104}$$

where

$H(0)$ = altitude at periapse

ε = orbit eccentricity (for swingby, by definition, $\varepsilon > 1$)

The maximum range to the planet surface, $R_2(\phi)$, that is the distance in the sidelook plane to the far edge of the mapped swath is

$$\frac{R_2(\phi)}{R_p} = \left\{ \left(1 + \frac{H(\phi)}{R_p}\right) \sin\alpha - \left[1 - \left(\frac{1+H(\phi)}{R_p}\right)^2 \cos^2\alpha\right]^{\frac{1}{2}} \right\} \tag{105}$$

The power ratio, for constant S/N and a fixed transmission format, as a function of true anomaly only, becomes

$$\frac{P(\phi)}{P(0)} = \left[\frac{R_2(\phi)}{R_2(0)}\right]^4 \frac{\sigma_2(0)}{\sigma_2(\phi)} = \left[\frac{R_2(\phi)}{R_2(0)}\right]^3 \frac{\cos\psi_2(\phi)}{\cos\psi_2(0)} \tag{106}$$

Using the relations (68), (69), and the above, yields the power ratio, as a function of the orbit parameters only, as

$$\frac{P(\phi)}{P(0)} = \left[\frac{1+\varepsilon}{1+\varepsilon\cos\phi}\right]^4 \left[\frac{\sin\alpha - \left\{\left(\frac{R_p}{R_p+H(0)}\right)^2 \left(\frac{1+\varepsilon\cos\phi}{1+\varepsilon}\right)^2 - \cos^2\alpha\right\}^{\frac{1}{2}}}{\sin\alpha - \left\{\left(\frac{R_p}{R_p+H(0)}\right)^2 - \cos^2\alpha\right\}^{\frac{1}{2}}}\right]^3 \tag{107}$$

This rather unwieldy expression is actually a simple function of the angle ϕ only, since the depression angle α is a constant, fixed by the choice of $\psi_2(0)$, [see Equation (68)] and ε, H (0) and R_p are constants of the given periapse geometry

The suggested use of (107) is the determination of a limiting true anomaly to which mapping is extended Let $|\phi_{Lim}|$ denote the absolute value of the determined angle Then the planet area mapped as a fraction of the total planet surface is

$$A_{(map)} = \frac{2\ W\ \left|\phi_{Lim}\right|}{R_p\ 4\pi} \tag{108}$$

In general, the maximum ratio of $P(\emptyset)/P(0)$ which defines $|\emptyset_{Lim}|$ by (97) should not exceed a value of 2 0, since a trade-off with extension of the swath width to achieve a given $A_{(map)}$ will result in smaller power requirements than extension of $\emptyset_{Lim}$ beyond power ratios of, say, 2 0, (see Equation (97))

4 5 3 3 Support Requirements

Power The required power input to the radar from the spacecraft during the operation of the radar is

$$P_{in} = 5\ P_{av} \tag{109}$$

Here a transmitter efficiency of 1/5, and a negligible constant load has been assumed

Energy The total required energy for a given swingby imaging mission is

$$E = 5\ P_{av}\ t\ (\emptyset_{lim}) \tag{110}$$

where $t\ (\emptyset_{lim})$ is the time in orbit between periapse and the true anomaly $(\emptyset_{lim})$ corresponding to a maximum permissible power ratio (See Equation (107))

Antenna Weight Antenna weight can be conservatively estimated to be $6K_g/\text{meter}^2$ of antenna area

Weights as low as $1/2\ K_g/\text{meter}^2$ could be achieved with thinly coated, inflatable types of antennas However, for the high power densities required in the missions under consideration here, the use of this type antenna is precluded

At best, a minimum weight of $3\ K_g/m^2$ may be assumed.

Transmitter and Power Supply Weight An empirical relation representing a fit to a few existing, low power, systems is given in Reference 2, Page 276 as

$$M_T = 13\ 6 + 9\ 1\ \ell n_e \left[\frac{P_t\ \lambda}{100}\right] \text{Kg} \tag{111}$$

for $P_t\ \lambda$ in units of watt-meters

The systems used in obtaining this empirical expression all exhibited duty cycles on the order of 1/1000 and average transmitted power levels of less than 10 watts. It is expected that (111) does not yield good weight estimates for high power systems ($P_{av} > 1000$ watts). It furthermore does not reflect any effect of duty cycle on weight and is unduly affected by λ

An alternative empirical expression which has been found to fit a fairly diverse set of high power systems in the wavelength band between 3 to 12 cm is

(Power in Watts)

$$M_T\ (K_g) = \frac{P_{av}}{78 \sqrt{d_c}} = \frac{\sqrt{P_{av} \quad P_t}}{78} \tag{112}$$

(Here d_c can be expressed as a function of resolution and swath width by (101)

<u>Data Acquisition Rate</u> A lower bound as data acquisition rates can be established as

$$(DR)_{min} = G_c \frac{W \cdot V_h}{r_h^2} \tag{113}$$

where G_c is the number of bits per sample, ($W \ V_h$) is the mapped area per unit time, and (r_h^2) is the max resolution cell area

This lower bound on data rate can only be attained if a radar data processor aboard the spacecraft performs the coherent integration function permitting a single data entry per resolution cell The data acquisition rate required when no coherent integration is provided by an on-board processor is then given by

$$DR = \frac{n \quad V_h \quad W}{r_h^2} G_c \tag{114}$$

Here n represents the (redundant) number of pulses transmitted during the time which the sidelook plane travels a distance r_h on the planet surface at the far edge of the swath, i e ,

$$n = (PRF)\frac{r_h}{V_h} \qquad (115)$$

Substituting Equation (79) for (PRF), results in

$$n = \frac{C\, r_h}{V_h \quad 2W \cos \psi_2} \qquad (116)$$

Since $\cos \psi \approx \frac{\sqrt{2}}{2}$, and $C = 3 \times 10^8$ m/sec the data rate requirement for coherent imaging radar is, by substitution into (114)

$$(DR) = \left[2 \times 10^8 \frac{G_c}{r_h} \text{bits/sec}\right] \qquad (117)$$

(with r_h in meters)

Usually $4 \leq G_c \leq 7$ bits

Note that this data acquisition rate requirement is inversely proportional to the ground resolution dimension only and independent of the extent of the area mapped per unit time

This relation should be interpreted as the data rate required for a system where peak power has been minimized by maximizing the repetition rate Thus, a trade-off exists between the required data rate and the peak power as a function of the PRF for a given coverage and resolution

Antenna Pointing and Stability Requirements A necessary condition imposed on the antenna pointing stability is that a given mapped element must remain within the locus of the 3db-beam contour on the planet surface for, at least, the integration time interval (See Figure 4-68)

Let θ represent the angular velocity vector of the antenna as a rigid body, with respect to an inertial frame

Let θ_p represent the component in the direction normal to the orbit plane

θ_y the component along the local vertical

θ_R the component along the local horizontal in the plane of the orbit

Then, for the sidelook geometry defined in Paragraph 4.5 3 2 ideally

$$\theta_p = \emptyset \quad \theta_R = \theta_y = 0 \tag{118}$$

where $\emptyset$ is the true anomaly angle of the spacecraft

Let $\delta(\theta)$ denote the error in the angular rate components so that

$$\begin{aligned} \delta(\theta_p) &= \left| \theta_p - \emptyset \right| \\ \delta(\theta_R) &= \left| \theta_R \right| \\ \delta(\theta_y) &= \left| \theta_y \right| \end{aligned} \tag{119}$$

The stability condition then requires that

$$\begin{aligned} \delta(\theta_p) &\le \frac{\beta_a}{2\ (t_1) \sin\alpha} \\ \delta(\theta_y) &\le \frac{\beta_a}{2\ (t_1) \cos\alpha} \\ \delta(\theta_R) &\le \frac{\beta_r}{2\ (t_1)} \end{aligned} \tag{120}$$

The integration time, t_1, for the synthetic aperture is given in terms of the problem geometry and resolution by (93) as

$$t_1 = \frac{R_2}{2V_h \quad r_h} \tag{121}$$

Substituting (121) and (63) and (64) respectively, the stability requirement becomes

$$\delta(\theta_p) \le \frac{r_h \quad V_h}{R_2 \quad D_a \quad \sin\alpha}$$

$$\delta(\theta_y) \le \frac{r_h \quad V_h}{R_2 \quad D_a \quad \cos\alpha} \qquad (122)$$

$$\delta(\theta_R) \le \frac{1\ 25\ r_h \quad V_h}{R_2 \quad D_r}$$

Scaling Law Application The steps in estimating system parameters and support requirements are given in Figure 4-69 Caution must be exercised in using the Figure however, since inconsistencies may be introduced unless the restrictions imposed in the text are taken into account

Implication of Mission Requirements A summary of the minimum antenna area and the minimum input power required in utilizing a coherent, synthetic aperture, radar in the neighborhood of periapse for the planetary missions considered is given in Table 4-16

Here, use has been made of Equations (89), (98) and (103) for a baseline wavelength $\lambda = 0\ 1$ meters The minimum power input computed reflects a ground resolution of 10^3 meters and antenna lengths of $D_a = (D_a)_{min}$ The scaling of both parameters listed in this table for $D_a > D_{a_{min}}$ is an increase in required area proportional to $D_a / D_{a_{min}}$ and a decrease in input power in the ratio

$$\frac{(D_{a_{min}})^2}{D_a}$$

The effect of ground resolution on the power values listed in the table is simply a multiplier of $1000/r_h$ with r_h in meters

Table 4-16 Prime Power and Antenna Area Requirements for Selected Planetary Missions

Mission Number	Planet	Periapse Altitude Km	Periapse Ground Speed Km/Sec.	P_{in} (kw) for r_n=1 km D_a=D_a min.	Min. Antenna Area (M^2) for = 0.1 m
1	Mercury	2200	6.4	2.67	60
2	Mercury	2200	6.9	2.5	63
3	Venus	6100	4.6	11.5	112
4	Venus	6100	4.0	13.5	97
5	Venus	1200	10.3	1.0	50
	Mercury	2200	5.2	3.3	48
6	Venus	2000	10.1	1.83	81
	Mercury	2200	5.4	3.2	50
7	Jupiter	42000	17.5	6.0	2900
	Saturn	60000	9.4	16.0	2300
8	Jupiter	260,000	11.2	185.0	38,000
	Saturn	121,000	7.5	37.5	4,000
9	Jupiter	190,000	3.9	118.0	3,000
	Uranus	50,000	7.2	17.0	1,500
	Neptune	22,300	11.4	5.0	1,000
10	Jupiter	277,000	6.5	107.0	7,200
	Uranus	8,300	20.4	1.0	700
	Neptune	22,000	11.5	5.0	1,000
11	Jupiter	104,000	4.0	65.0	1,660
	Saturn	260,000	3.3	185.0	3,600
	Pluto	6,000	12.0	13.3	290
12	Jupiter	440,000	8.7	12.4	15,500
	Saturn	360,000	3.0	300.0	4,300
	Pluto	6,500	11.0	13.3	260

The data in the table can be used to screen each of the missions for mapping radar suitability both from the point of view of power requirements and antenna area and/or weight

The procedure given in the text has been applied to Mission 7 for a Saturn swing-by The trade-off's are indicated in Figure 4-70 for a distance of closest approach of one planet radius The same data is cross-plotted in Figure 4-71

Table 4-17 Definition of Terms for Coherent Imaging Radar

$A_{(Ant)}$	Antenna area
$A_{(map)}$	Mapped area as fraction of planet surface area
B	Receiver bandwidth
C	Velocity of light
c_p	Pulse compression ratio
d_c	Transmitter duty cycle
D_a	Antenna length - (dimension in orbital plane)
D_r	Antenna height - (dimension in sidelook plane)
D_{sa}	Length of synthetic aperture
DR	Rate of data acquisition
ϵ	Orbit eccentricity
G	Antenna gain
G_c	Gray code (bits)
H	Altitude of spacecraft above planet surface
K	Boltzmann's constant ($1\ 38 \times 10^{-23}$ joules/°K)
K_{Da}	Antenna pattern factor normal to sidelook plane

Table 4-17 Definition of Terms for Coherent Imaging Radar (Cont)

K_{Dr}	Antenna pattern factor in sidelook plane
K_T	Noise temperature coefficient for given planet
L_{atm}	Atmospheric loss power factor
L_{RF}	RF-loss power factor
m	Number of pulses transmitted during time interval corresponding to travel of synthetic aperture length
M_{Ant}	Antenna weight
M_T	Weight of transmitter including power supply
$(\overline{NF})$	Receiver noise figure
PRF	Pulse repetition frequency
P_{av}	Average transmitted power
P_{in}	Input power
P_t	Peak transmitted power
r_h	Ground resolution dimension
R_2	Scaling range - distance from spacecraft to far edge of swath
R_p	Planet radius
S/N	Signal-to-noise ratio
t_i	Integration time - travel time corresponding to length of synthetic aperture
T	Input noise temperature
V_h	Velocity of planet surface within beamwidth in direction normal to sidelook plane with respect to sidelook plane

Table 4-17 Definition of Terms for Coherent Imaging Radar (Cont)

V_o	Orbital velocity of satellite at periapse
V_s	Velocity of subsatellite point
W	Swath width - length of surface element in sidelook plane over which resolved imagery is obtained
α	Depression angle of antenna, angle between local horizontal plane of subsatellite point and LOS from antenna to far edge of swath in sidelook plane
β_a	3db - beamwidth normal to sidelook plane
β_r	3db - beamwidth in sidelook plane
Δf_D	Doppler spread over 1/2 β_a
$\delta (\Delta f_D)$	Uncertainty in Δf_D due to antenna stabilization errors
δ	Back scatter coefficient
θ_p	Angular rate of antenna about normal to orbit plane
θ_R	Angular rate of antenna about local horizontal at spacecraft in orbit plane
θ_y	Angular rate of antenna about local vertical
λ	Transmitted wavelength
σ_2	Equivalent radar cross section of resolution cell at far edge of swath
τ	Transmitted pulse width
τ'	Received (compressed) pulsewidth
$\emptyset$	True anomaly angle of spacecraft with respect to periapse for given planet orbit
ψ_2	Beam incidence (grazing) angle at far edge of swath

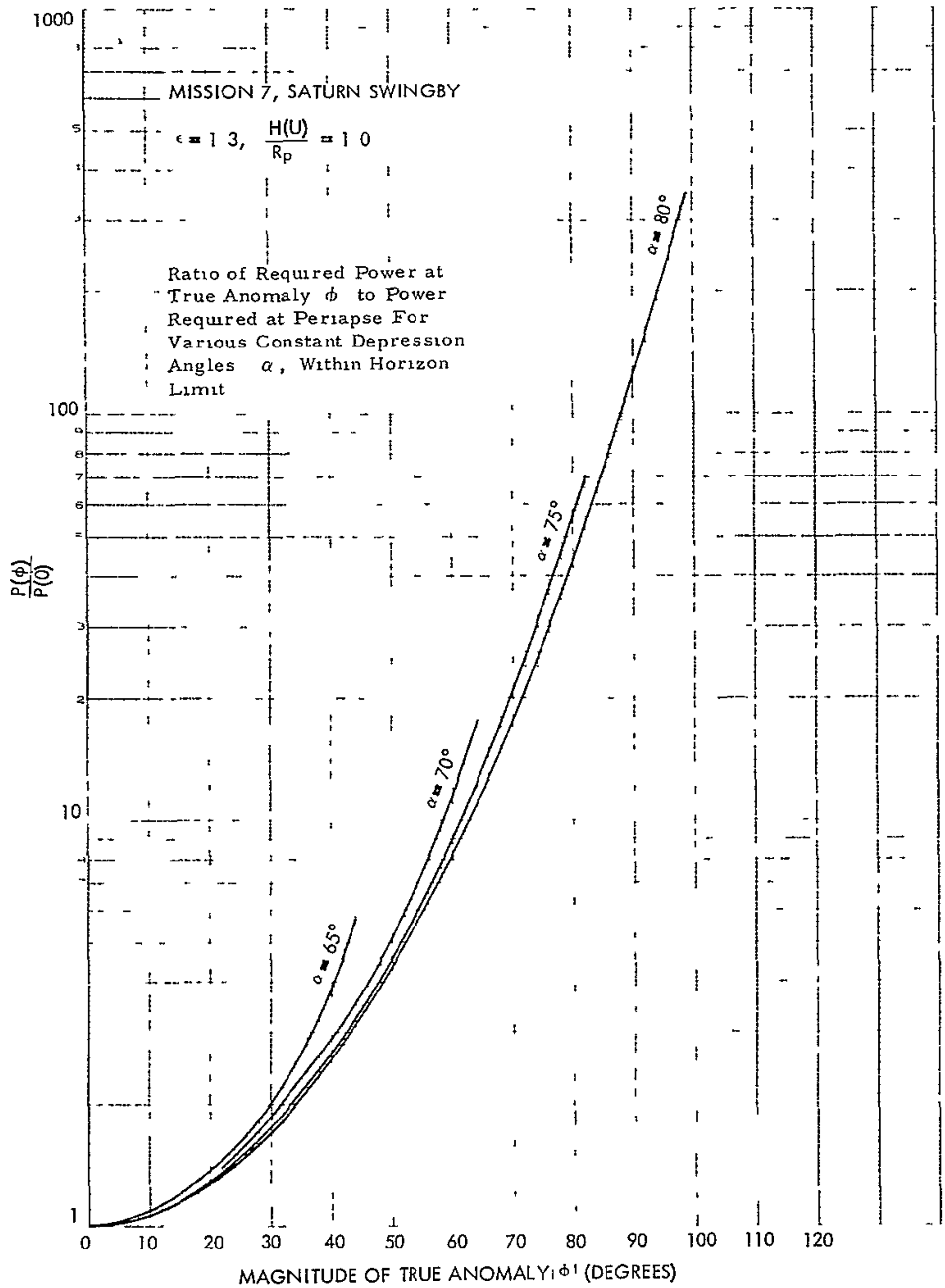

Figure 4-70 Coherent Mapping Radar Tradeoff for Mission 7 - Part I

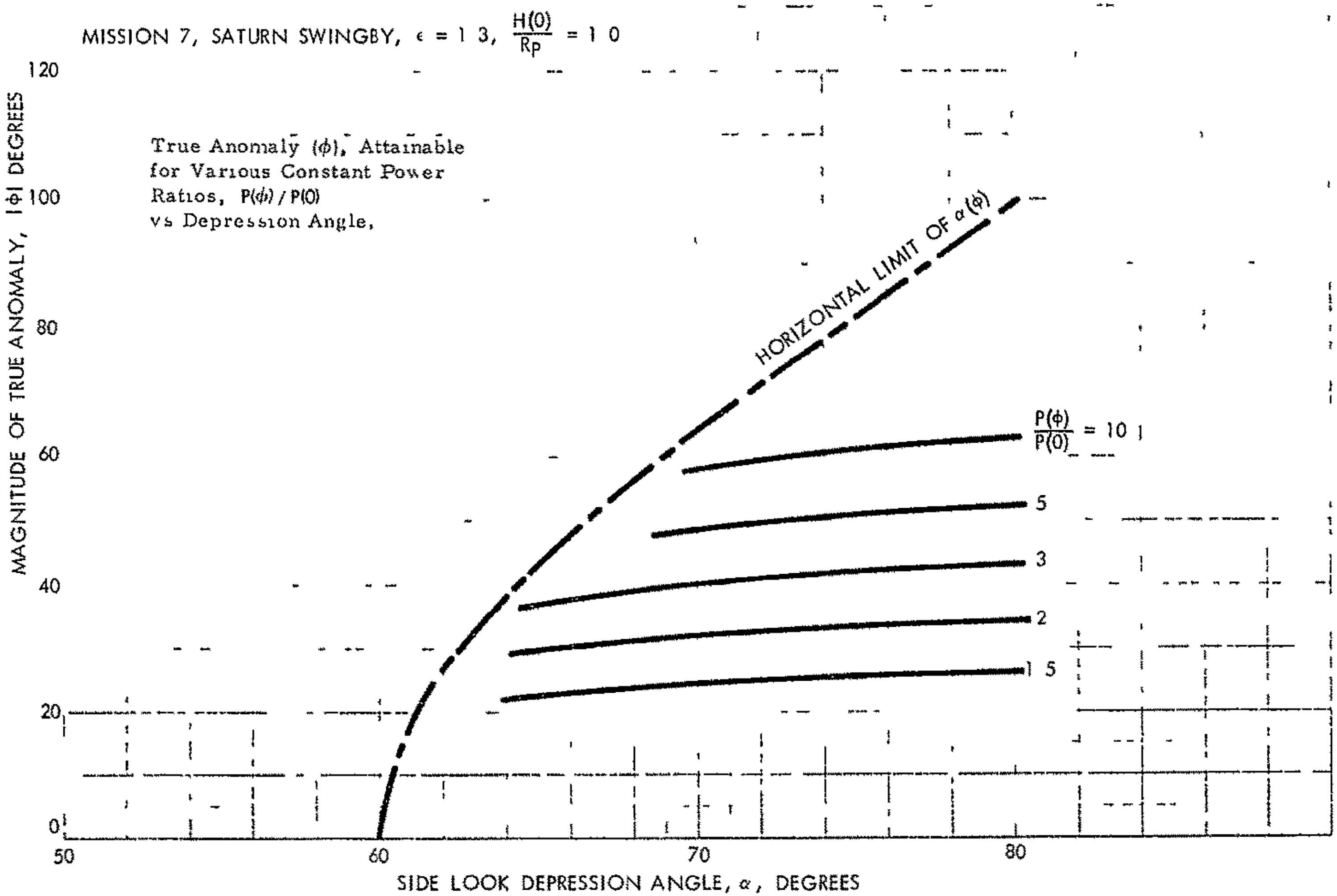

Figure 4-71 Coherent Mapping Radar Tradeoff for Mission 7 - Part II

4 6 SEMI-ACTIVE AND PASSIVE MICROWAVE INSTRUMENTS

4 6 1 Introduction

The design of semi-active and passive microwave instruments for planetary exploration are all quite similar This follows from the fact that the instrumentation on the spacecraft consists of a receiver and a receiving antenna with minor modifications to perform a variety of functions depending upon measurement experiments. The instruments which fall into this classification are the following

a Two-frequency occultation experiment

b Measuring radiometer

c Mapping radiometer

d Microwave spectrometer

These experiments all require an antenna and receiver on the spacecraft with significant increases in support requirements to mechanize antenna scanning for the mapping radiometer case

The two-frequency occultation experiment is only one of several microwave occultation experiments which might be postulated It is included because it imposes support requirements on the spacecraft to receive a signal of known characteristics from the earth It can be extended to include occultation of radio stars if there is a favorable geometry for conducting such an experiment The alternative of placing a microwave source on the spacecraft for measuring the effects of occultation at the earth is not included since it is a trivial extension of the communications problem from spacecraft to earth The communications area is not part of the sensor support requirements study so that the spacecraft to earth occultation experiment is more a by-product of the communications problem and should be considered with it

Microwave spectrometers are a special case of measuring radiometers in which RF bandwidth is traded against integration time The scaling law given below is for a measuring radiometer in which the basic support requirement results from the antenna The electronic support requirements are essentially trivial when compared with the size and weight of the antenna A microwave spectrometer would use the same antenna with an electronic package which has the same support requirements as the radiometer but would differ from it in bandwidth and local oscillator tuning characteristics

Although not explicitly described in the study, it is fairly obvious that many of the functions of microwave instruments described separately could be performed by a single instrument It would be necessary to time share the functions of occultation measurements with temperature measuring and mapping radiometry, but at least formally the same antenna-receiver combination could be a multifunction device

The design of semi-active and passive microwave instrumentation is essentially deterministic once a set of measurement parameters has been defined For this reason, the tradeoffs which are open to selection are readily summarized in the form of nomograms. This approach has been used in establishing scaling laws for microwave instruments Nomograms have been developed to permit rapid assessment of the implications of changes in significant system parameters

They have been established to cover the range of parameters most likely to be encountered in planetary exploration In addition, where meaningful limitations on the state-of-the-art exist, the limitations have been taken into account in establishing the range of operation of the parameters affected

4 6 2 Two-Frequency Earth Occultation Experiment

Occultation of a radio signal by the atmosphere of a planet allows determination of the total density from refraction and phase shift (retardation) measurements. If two substantially different frequencies are employed, the resulting dispersion data permit separation of ion and electron from neutral atomic and molecular densities To determine the bi-frequency phase shift, a coherent transponder, at one of the frequencies, (usually not the basic spacecraft communications frequency) is required The times of entrance and exit also give a measurement of the planetary radius Additional uses of the coherent transponder, to determine plasma densities in the interplanetary medium, to measure planetary distances, and to observe general relativistic effects near the sun and major planets, are outside the scope of the study

4.6.2.1 Design and Performance

To establish the total sensor requirements, design parameters and performance data are developed for spacecraft antennas at both frequencies, as well as for the coherent transponder Usually, one of the antennas is the high-gain communications antenna, and is more than sufficient for the occultation experiment A single-frequency occultation experiment requires no *ad hoc* sensor equipment

4.6.2.2 Scaling Law Development

A two-frequency experiment is assumed. Both transmitters are on Earth with the corresponding receivers on the spacecraft or one transmitter can be located on Earth with the corresponding receiver on the spacecraft and the communications transmitter on the spacecraft used as the second transmitter.

The scaling laws for the Earth Occultation experiment give the error in measuring the gas refractive index and the electron density as a function of spacecraft trajectory and equipment parameters. The results are presented both in the form of equations suitable for numerical analysis and nomographs to allow a rapid analysis and tradeoff study. The geometry of the experiment is shown in Figure 4-72. A planet of radius r is assumed with an atmosphere of depth h. The spacecraft at point P receives energy from a source on the Earth. The distance is sufficiently large that the rays can be assumed to be parallel. The spacecraft has a velocity V normal to the Earth spacecraft line. The closest approach to the planet of a ray joining the spacecraft and the Earth is denoted by ρ.

Note that the analysis ignores the bending of the ray paths due to the presence of the atmosphere. It is shown in References 13, 14, and 15, that the bending is small and will not significantly affect the error analysis.

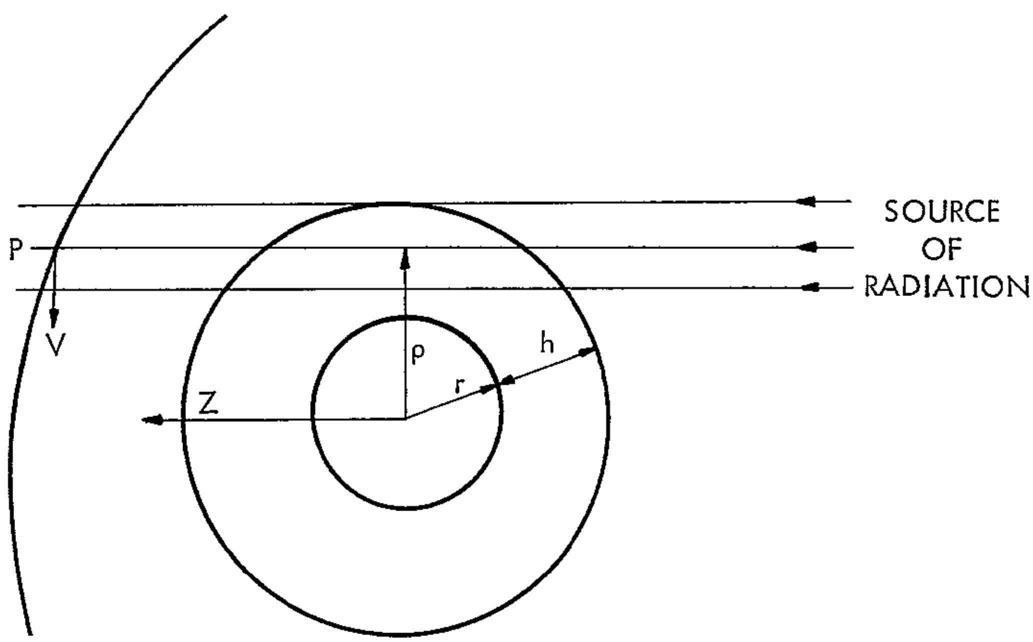

Figure 4-72 Two Frequency Occultation Geometry

The analysis is valid in either case. Assume a planet with both a neutral gaseous envelope and an ionosphere Let the operating wavelength λ, be sufficiently small that the ionosphere has negligible effect The phase path increase in cycles $\phi_1 = \phi_1(\rho)$ is given by

$$\phi_1(\rho) = \frac{1}{\lambda_1}\int_{-\infty}^{\infty} \Delta\mu \; dz \tag{1}$$

where the refractivity $\Delta\mu$ is given by

$\Delta\mu = \Delta\mu(\rho) = (\mu_G - 1) \times 10^6$ = the refractivity, where

$\mu_G = \mu_G(\rho)$ = the gas refractive index

and

z = the coordinate through the center of the planet parallel to the unbent rays

A second wavelength λ is used so that the ionospheric phase shift is significant, $\lambda_2 > \lambda_1$ The phase path increase in cycles, $\phi_2 = \phi_2(\rho)$ is given by

$$\phi_2(\rho) = \frac{1}{\lambda_2}\int_{-\infty}^{\infty} \Delta\mu \; dz + \frac{1}{\lambda_2}\int_{-\infty}^{\infty} \Delta\mu_e \; dz \tag{2}$$

where

$\Delta\mu_e = \Delta\mu_e(\rho) = (\mu_e = 1)\, 10^{+6}$ = the refractivity

$\mu_e = \mu_e(\rho)$ = electron refractive index

The relation between $\Delta\mu_e$ and the electron density is given by

$$\Delta\mu_e = \frac{40\ 3}{f^2} N$$

where

N = electron density in electrons/m^3

f = frequency in Hertz

40 3 is a dimensional constant

Assume an error in the gas refractivity $\Delta\mu$ and the electron concentration N Error terms will be denoted by prefixing the quantities with δ Since the integral is a linear function of the corresponding error in the phase path, an increase in ϕ_1 (ρ) will be given by

$$\delta\phi_1 = \delta\,\phi_1\,(\rho) = \frac{1}{\lambda_1}\int_{-\infty}^{\infty} \delta(\Delta\mu\,)\,dz \tag{3}$$

In practice, the measurements are not instaneous Each determination of ϕ_1 (ρ) will occupy a time $\Delta\ t_1$ Thus each measurement will give the average phase path length increase The average is taken over an altitude interval $\Delta\ h_1$ given by

$$\Delta\ h_1 = \Delta\ \rho_1 = V\ \Delta\ t_1 \tag{4}$$

We define h, the depth of the atmosphere, by letting h be the greatest altitude where ϕ_1 (ρ) differs from zero by a measurable amount

The number of intervals is given by $n = h/\Delta\ h_1 = h/\Delta\ \rho_1$ During the experiment we obtain n values of ϕ_1 (ρ_1), $i = 1$, n. From these values we will obtain n values of $\Delta\mu$ (ρ_j), $j = 1$. n by replacing the simultaneous integral equations by an n by n matrix equation and performing an inversion. Since the error analysis does not require an inversion we need only estimate the error in ϕ_1 (ρ_1).

If the value of $\Delta\mu$ (ρ_1), $i = 1$ n is in error by $\delta\Delta\mu$, then the average error in ϕ_1 (ρ) will be given by

$$\delta\ \phi_1\ (\rho) = \frac{Z_{av}}{\lambda_1} \quad \frac{\delta\,\Delta\mu}{\sqrt{h}}$$

Where $z_{av} = (rh)^{1/2}$, the average path length Thus

$$\delta \phi_1(\rho) = \frac{\delta \Delta\mu}{\lambda_1} \left[\frac{\Delta h_1}{h}\right]^{1/2} (rh)^{1/2}$$

$$\delta \phi_1 (\rho) = \frac{\delta \Delta\mu}{\lambda_1} (r\Delta h_1)^{1/2} \tag{5}$$

Let S/N be the power signal-to-noise ratio at the receiver output. The presence of noise will also introduce an error in the measurement We assume a sufficient signal strength for equality between the two sources of error Thus

$$\delta \phi_1 (\rho) = \frac{1}{2\pi}\sqrt{N/S} = \frac{1}{2\pi}\sqrt{\frac{KTB_1}{A_1 \zeta_1}} \quad \text{Hz}$$

where

K = Boltzmann's constant (1 38 x 10^{-23} joules/°K)

T = The receiver noise temperature in °K

B_1 = the receiver bandwidth in Hz

A_1 = the receiver antenna aperture in m^2

ζ_1 = the power flux density of the source at wavelength λ_1 in $\frac{\text{watts}}{m^2}$

From Eq (4) we obtain

$$\frac{1}{\Delta t_1} = \frac{V}{\Delta h_1}$$

Equating B_1 and $\frac{1}{t_1}$ we obtain

$$\delta \phi_1 (\rho) = \frac{1}{2\pi} \sqrt{\frac{KTV}{A_1 \zeta_1 \Delta h_1}} \tag{6}$$

Let

$$\zeta_1 = \frac{P_1 \Gamma d_1^2}{R^2 \lambda_1^2} \tag{7}$$

where

$P_1 \Gamma$ = the transmitter power in watts attentuated by the intervening atmosphere

d_1 = the transmitter antenna aperture in m

R = the distance from the transmitter to the receiver in meters

$$\delta \phi_1(\rho) = \frac{1}{2\pi} \sqrt{\frac{KTVR^2 \lambda_1^2}{A_1 P_1 \Gamma d_1^2 \Delta h_1}} = \frac{\delta \Delta\mu}{\lambda_1} \left(r \Delta h_1\right)^{1/2}$$

or

$$\Delta\mu = \frac{R}{2\pi \Delta h_1 \frac{b_1}{\lambda_1} \quad \frac{d_1}{\lambda_1}} \sqrt{\frac{KTV}{r P_1 \Gamma}} \tag{8}$$

where we have set

$$A_1 = D_1^2$$

with D being the diameter of the second antenna in m

We next consider Eq. (2). Since $\lambda_2 > \lambda_1$ and $\Delta\mu < \Delta\mu_e$ we neglect the first integral and obtain

$$\phi_2(\rho) = \frac{1}{\lambda_2}\int_{-\infty}^{\infty} \Delta\mu_e \, dz \text{ cycles}$$

and

$$\delta\phi_2(\rho) = \frac{1}{\lambda_2}\int_{-\infty}^{\infty} \delta\Delta\mu_e \, dz \text{ cycles}$$

By the same argument as for the first equation, we obtain

$$\delta\phi_2(\rho) = \frac{\delta\Delta\mu_e}{\lambda_2}\left(r\Delta h_2\right)^{1/2} \tag{9}$$

Next we use the relation between $\Delta\mu_e$ and N to obtain

$$\delta\Delta\mu_e = \frac{40\ 3}{f^2}\,\delta N = \frac{40.3\,\lambda^2}{C^2}\,\delta N$$

hence

$$\delta\phi_2(\rho) = \frac{40\ 3\,\lambda\,\delta N}{C^2}\left(rh_2\right)^{1/2} \tag{10}$$

Again using the signal-to-noise argument we obtain

$$\delta\phi_2(\rho) = \frac{1}{2\pi}\sqrt{\frac{KTVR^2\lambda^2}{A_2P_2\Gamma d_2{}^2\Delta h_2}} \tag{11}$$

As before, let $A_2 = D_2^2$ and solve for δN

$$\delta N = \frac{C^2}{40.3\lambda^2} \quad \frac{R}{\Delta h_2 \; {}^{D_2}/_{\lambda_2} \cdot {}^{d_2}/_{\lambda_2}} \sqrt{\frac{KTV}{rP_2\Gamma}}$$

$$\delta N = \frac{C^2 \times 10^{-6}}{40.3\,\lambda^2} \quad \delta\,\Delta\mu \qquad (12)$$

The factor 10^{-6} is a dimensional constant Eqs. (8) and (12) give the final solutions

The parameters in the equations have the following bounds

$$P_1\Gamma,\ P_2\Gamma = 10^2 \text{ to } 10^6 \text{ watts.}$$

Higher powers are difficult to achieve and lower powers would not be sufficient

$$D/_{\lambda},\ d/_{\lambda} = 30 \text{ to } 300.$$

The lower bound would not be sufficient and the upper bound is difficult to achieve even under controlled conditions This is especially true on the spacecraft where a steerable antenna has been assumed. In addition, a dual frequency receiving antenna on the spacecraft would make the attainment of a 300 wavelength aperture difficult

$$T = 100 \text{ to } 10^4 \text{ °K}$$

The lower bound corresponds to a parametric amplifier. The upper bound corresponds to a very poor superheterodyne receiver.

$$\lambda_1 = 3\text{m to } 3 \text{ cm}$$

$$\lambda_2 = 30 \text{ m to } 30 \text{ cm}$$

The values of λ_2 encompass the wavelengths where ionospheric effects are significant and λ_1 is smaller than λ_2 by a factor of at least 10.

$$\Delta h = 1 \text{ to } 10 \text{ km}$$

The lower bound is smaller then can be achieved in practice The upper bound represents a value of little interest

Eqs (8) and (12) can be solved analytically or by the use of the three nomographs shown in Figures 4-73, 4-74 and 4-75 To illustrate the use of these nomographs we consider an example The distinction between solutions of Eqs (1) and (2) is dropped in the example

Use Figure 4-73

Step 1 -

Choose $T = 10^3$ and $P\Gamma = 10^5$ This gives a point P_1 on reference line number (1).

Step 2 -

Choose $D/\lambda = 100$ and draw the line joining this point with P_1, where this line crosses reference line number (2) defines a point P_2

Step 3 -

Choose $d/\lambda = 100$ and connect the point with P_2, where this line meets the β_3 axis, point p_3, defines the solution to the equation

$$\beta_3 = \left[\frac{K\ T}{P\ \Gamma (d/\lambda)^2\ (D/\lambda)^2}\right] = 3\ 72 \times 10^{-17}$$

Next the value of β_3, found using Figure 4-73, is entered on the β_3 scale in Figure 4-74 Choose $\Delta h = 1$ km and connect $\beta_3 = 3\ 72 \times 10^{-17}$ with $\Delta h = 1$ km This gives the solution to the equation

$$\beta_4 = \frac{\beta_3}{2\pi\Delta h} \times 10^6 = 5\ 93 \times 10^{-15}$$

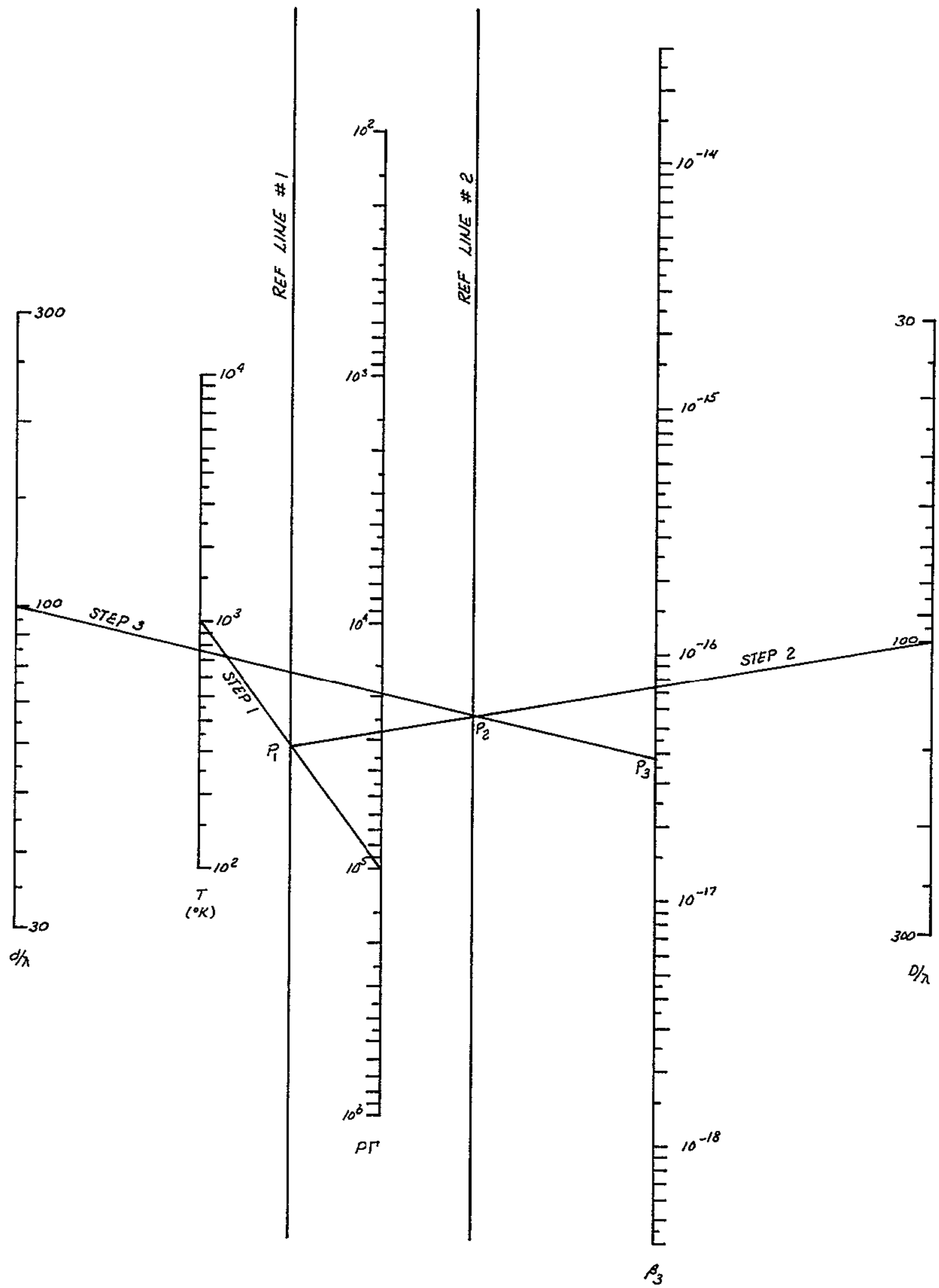

Figure 4-73 β_3 Nomogram

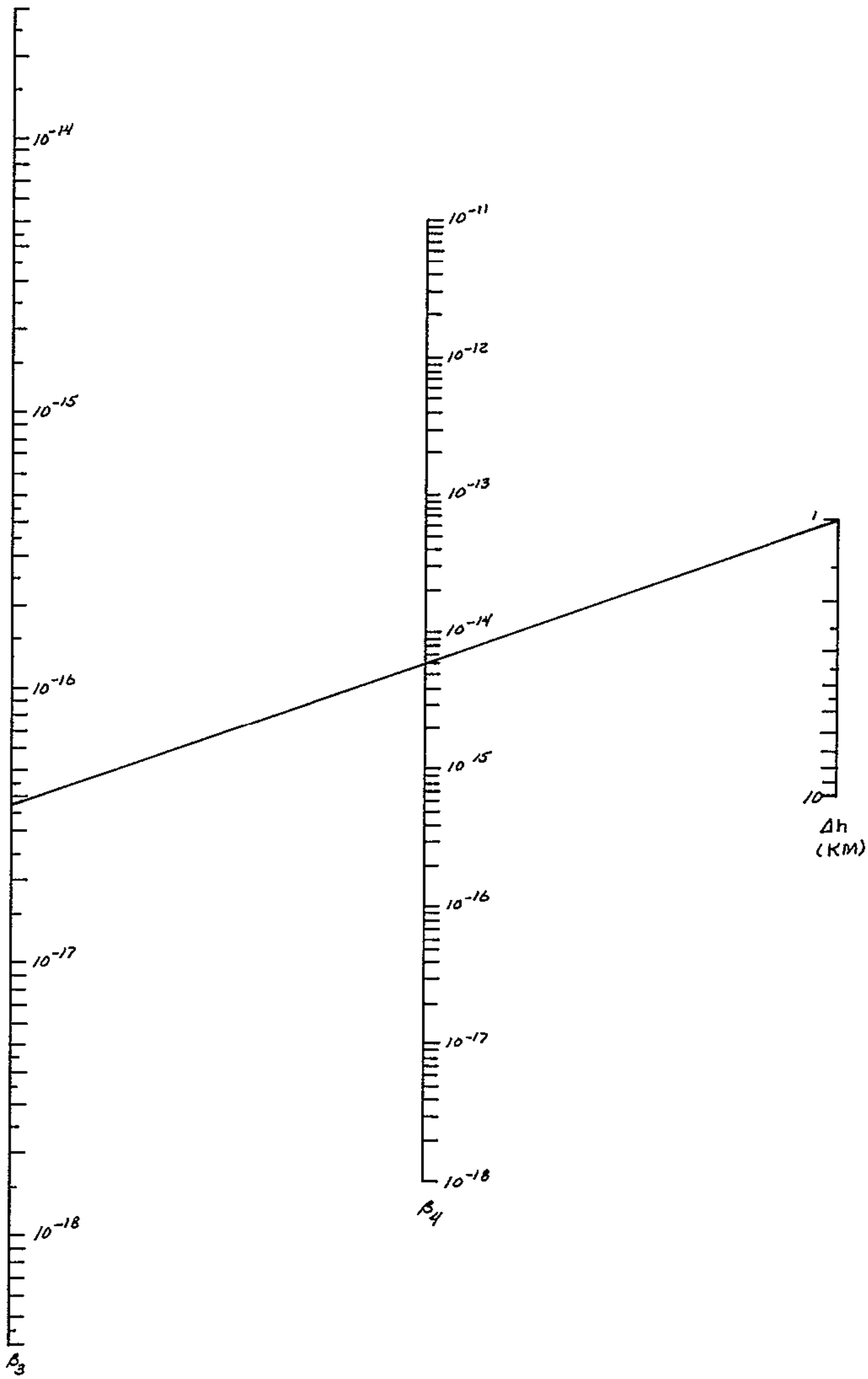

Figure 4-74 β_4 Nomogram

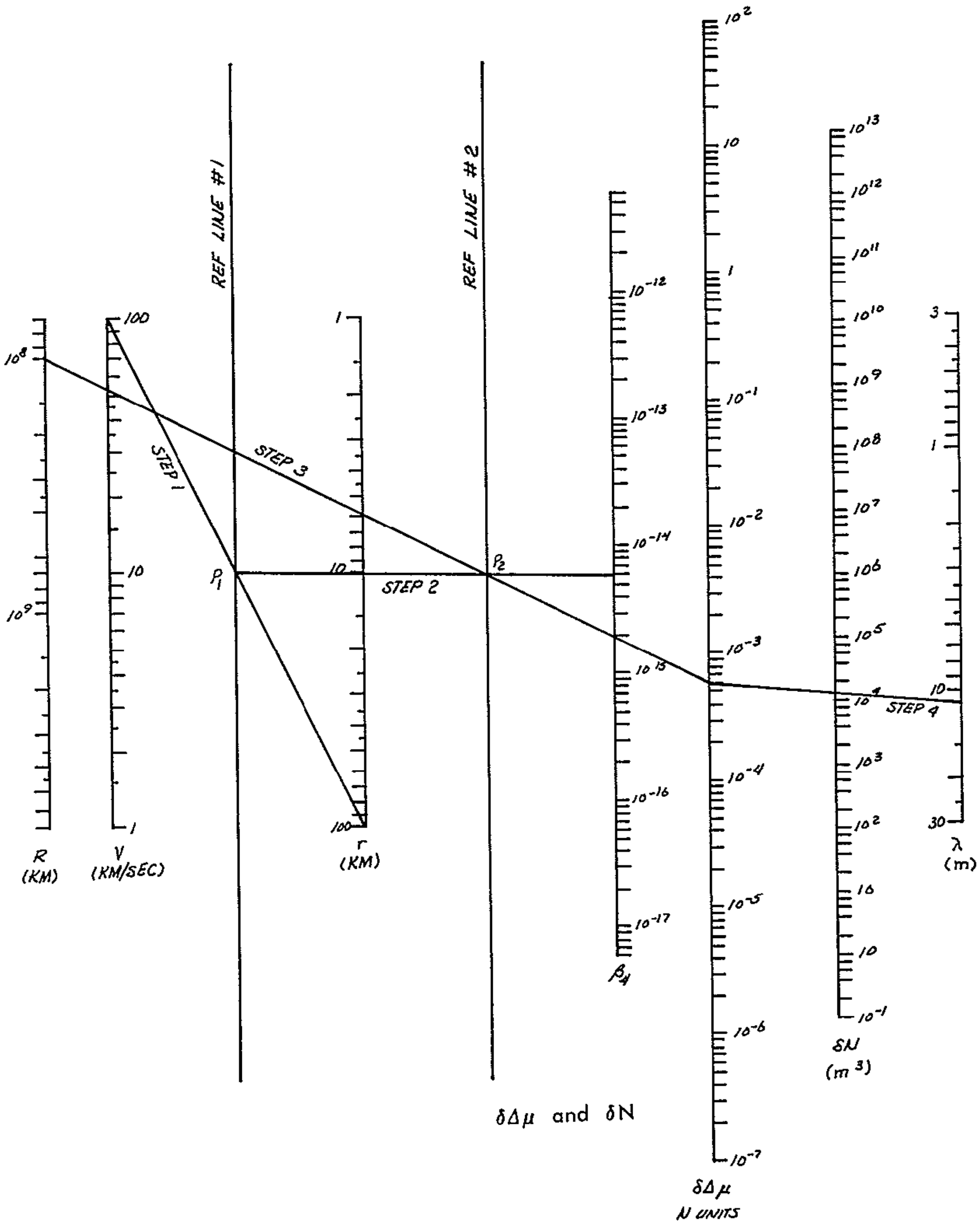

Figure 4-75 Error Nomogram for $\delta\Delta\mu$ and δN

The value of β_4, found using Figure 4-74, is entered on the β_4 scale in Figure 4-75

Step 1 -

Connect $V = 100$ km/sec with $r = 100$ km The line crosses reference line number (1) at point P_1

Step 2 -

Connect point P_1 with the point on the β_4 axis previously entered. The line crosses reference line number (2) at point P_2

Step 3 -

Connect point P_2 with $R = 10^8$ km Extend the line to the $\delta\Delta\mu$ axis Obtain $\delta\Delta\mu = 5\ 93 \times 10^{-4}$

Step 4 -

Connect $\delta\Delta\mu = 5\ 93 \times 10^{-4}$ to $\lambda = 10$, obtain $\delta N = 1\ 32 \times 10^4\ m^{-2}$

Step (3) gives the solution to the equation

$$\delta\Delta\mu = R \sqrt{\frac{V}{r}}\ \beta_4$$

Step (4) gives the solution to the equation

$$\delta N = \frac{C \times 10^{-6}}{40\ 3\ \lambda^2}\ \delta\Delta\mu$$

4 6 2 3 Support Requirements

System Weight The dominant factor in weight for the occultation experiment is the antenna While a steerable antenna is probably required, it does not appear that high angular rates will be encountered, especially during measurements Therefore, a not too rigid structure appears feasible and a weight scaling factor 1 5 kg/square meter of aperture area is adequate, that is

$$M_{ant} = 1.5\ D^2\ kg \qquad (13)$$

where

D is the aperture diameter (assumed parabolic)

M is the antenna weight in kg

The receiver weight is relatively modest since the receiving functions are unsophisticated unless it can be established that the receiving antenna must track the ground station signal From a rudimentary consideration of the geometry this does not appear to be required so that a nominal weight of 2 kg per channel can be assigned as the weight penalty for the receiver

System Volume. Under the assumption that a parabolic antenna is used, then the launch volume of the antenna is the significant parameter Current practice in deployable antennas is such that the aperture can be folded for launch to 0 1 its deployed diameter However, the feed portion is difficult to fold so that the launch volume of the antenna is determined by the focal length of the antenna For most parabolic antennas an f /number of 0 45 or less is used so that in the launch configuration the volume is

$$V = f\left(\frac{D}{10}\right)^2 = 4\ 5 \times 10^{-3}\ D^2$$

where f is the focal length, and D is the deployed aperture diameter

System Power Under the assumption of a non-steerable antenna, a nominal value of 5 watts can be assumed as the power required to operate the dual receiver

Data Rate As indicated in the discussion of the nomographs, the number of measurement samples is determined by the height resolution which the experiment is trying to achieve For an atmosphere - ionosphere height of, h, and a resolution of Δ h then

$$\text{number of measurement samples} = \frac{h}{\Delta h}$$

The total amount of data is determined by the component of spacecraft velocity perpendicular to the direction of propagation of the source radiation, V, and the integration time selected so that

$$n = \frac{h}{\Delta h} = \frac{h}{V \Delta t_1} \qquad (15)$$

where

n is the number of samples

h is the altitude

V is the spacecraft velocity

Δt_1 is the integration time

Since each measurement is a phase comparison measurement, it is ambiguous every 2π radians Therefore, if the phase comparison is to be established to $\Delta\phi$ degree, then the dynamic range of each measurement must encompass

$$G = \frac{360}{\Delta\phi} \text{ increments} \tag{16}$$

Under the assumption of one bit per increment the total data is

$$D = \frac{h \times 360}{V \Delta t_1 \Delta\phi} \tag{17}$$

and if the measurement requires T seconds the data rate is

$$DR = \frac{360\, h}{V \Delta t_1 \Delta\phi T} \frac{\text{bits}}{\text{sec}} \tag{18}$$

Stabilization Requirements. To prevent signal loss during reception, the spacecraft antenna must be kept pointed at the earth based source to within a small fraction of the antenna beamwidth during the measurement time, T A tenth of the beamwidth is considered adequate to prevent signal loss so that the antenna must be pointed with an accuracy of $0\ 1\ \theta$ where θ is the antenna beamwidth The maximum error of 0.1θ implies a stabilization of

$$\theta T = 0\ 1\ \theta \tag{14}$$

where

θ is the drift rate

T is the measurement time

θ is the antenna beamwidth

so that

$$\theta_{max} = \frac{0.1\,\theta}{T} \tag{20}$$

4 6 3 Radio Polarimetry Experiment

Measurements of the rotation of the plane of polarization of electromagnetic radiation passing through an ionized medium determines the total ion density in the beam column (Faraday effect) If a polarized radio signal is used during earth occultation, the ion density in the planetary atmosphere can be calculated as a function of altitude This experiment can be substituted for, or added to, the second occultation frequency To observe low ionospheric densities (e g , at Mercury), the data must be corrected for rotation due to the interplanetary plasma

4 6 3 1 Design and Performance

The equipment for the polarization experiment is the same as that for a single-frequency radio occultation, with added provision for a plane- or circularly-polarized signal If circular polarization is used, the angle must be synchronized with timing pulses

4 6 3 2 Scaling Law Development

The scaling law for polarimetry is based on the earth occultation experiment The Polarimetry experiment gives the phase error in radians as a function of the system parameters The equation is derived, as were equations (6) and (7), in the Earth Occultation experiment description In radians the phase error is given by

$$\delta \phi = \left(\sqrt{\frac{KT}{P\Gamma (d/\lambda)^2 \quad (D/\lambda)^2}} \right) \left(\frac{R}{\lambda} \sqrt{\frac{V}{\Delta h}} \right) \qquad (21)$$

The first term is the quantity β_3, found from Figure 4-73 in the Earth Occultation section Thus only one additional nomograph is required for this experiment The nomograph is shown in Figure 4-76 To illustrate the solution of the equation using the nomographs, we enter $\beta_3 = 3\ 72 \times 10^{-17}$ (found using Figure 4-73 of the Earth Occultation section) on the β_3 scale of the nomograph

Step 1 -

Choose $V = 10$ km/sec, $\Delta h = 10$ km Join these points with a line This line crosses reference line number (1) at the point P_1

Step 2 -

Connect the point P_1 with the value of β_3 previously entered This line crosses reference line number (2) at P_2

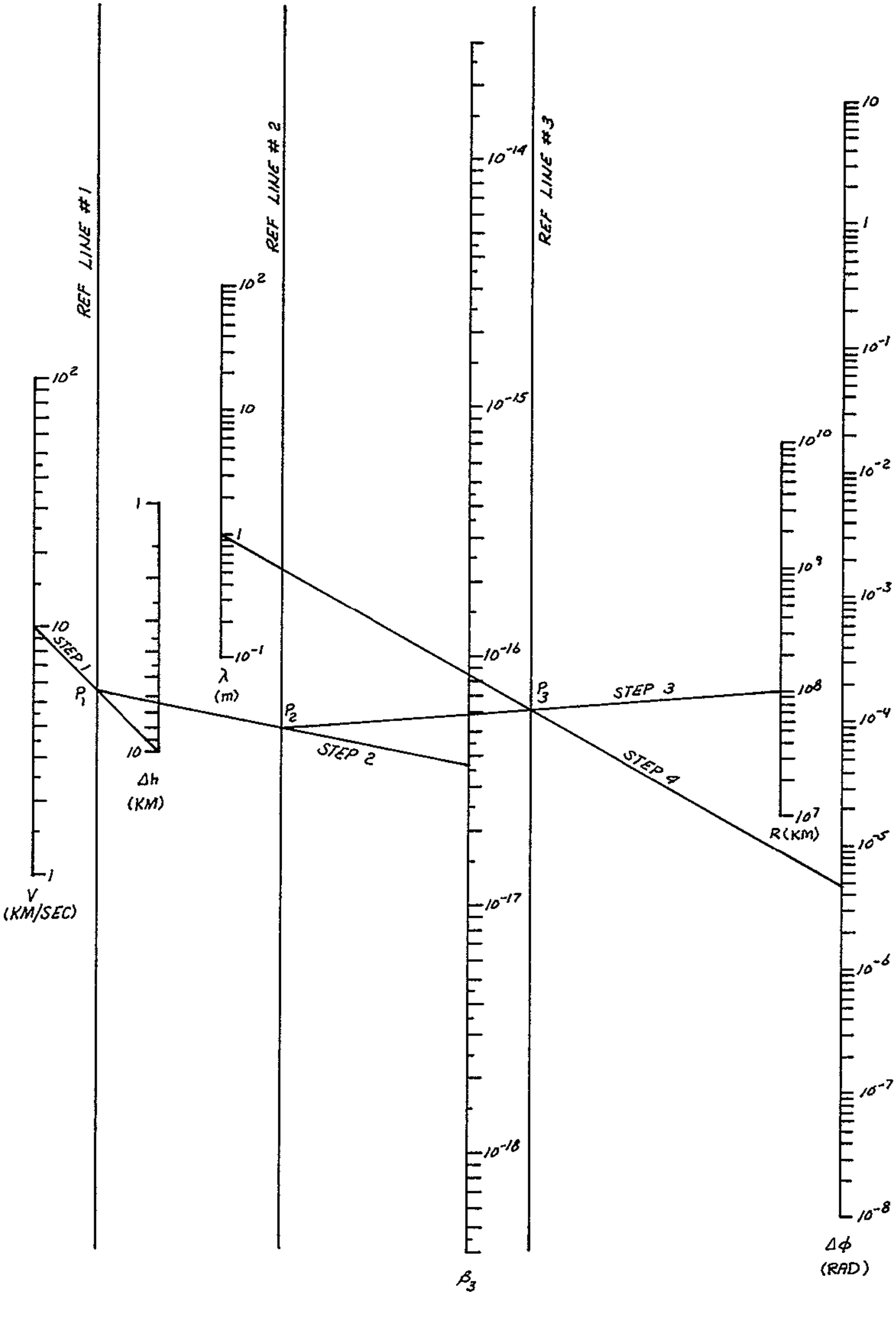

Figure 4-76 Phase Variation Nomogram

Step 3 -

Connect P_2 with $R = 10^8$ This line crosses reference line number (3) at P_3

Step 4 -

Connect $\lambda = 1$ m with P_3 Extend the line to the $\Delta\phi$ scale This gives the solution $\Delta\phi = 3\ 72 \times 10^{-6}$ radians

4 6 3 3 Support Requirements

The support requirements for the Polarimetry experiment are the same as the support requirements for the Earth Occultation experiment given above

4 6 4 Microwave Radiometer

4 6 4 1 Scaling Law Development

This section presents the scaling laws that relate the sensor performance to the orbit parameters, the signal characteristics, and the sensor parameters The results are presented in the form of nomographs The final result is an expression giving the maximum altitude of operation versus the signal characteristics and known orbital parameters

Intermediate steps in the solution give the temperature resolution, the linear resolution, and the angular resolution of the sensor The minimum detectable signal or temperature resolution is derived in Reference 16 In slightly different notation, it is given by

$$\Delta T_{min} = \left(\frac{B_F}{K_1 B_H}\right)^{1/2} \left[T_A' + T_L + (F - 1) T_o\right] \qquad (22)$$

where

B_F = the post detection bandwidth

B_H = the predetection bandwidth

T_A' = the apparent antenna noise temperature due to the background This varies from planet to planet and with the operating wavelength

T_L = the contribution to the temperature by the system losses

F = the system noise figure

T_o = noise figure reference temperature

= 290^oK (by definition)

K_1 = a constant

= 1/2 for an unmodulated radiometer such as is used for imaging

= 1/8 for a Dicke radiometer with square wave modulation and demodulation such as is used for temperature measuring

The first step in determining the temperature resolution is to simplify the expression for the composite system noise temperature

The composite noise temperature is given by

$$T_C = T_A' + T_L + (F - 1)\, T_o \tag{23}$$

Set

$$T_A = T_A' + T_L \tag{24}$$

Then define

$$F_R\, T_o = T_A + (F - 1)\, T_o \tag{25}$$

F_R can be called the effective noise figure

The value of F_R for chosen values of F and T_A can be obtained from Figure 4-77

Next calculate the relation between post detection noise bandwidth and the integration time Assume a simple RC integrator, hence the relation between the two is

$$B_F = \frac{1}{4\,\tau_1} \tag{26}$$

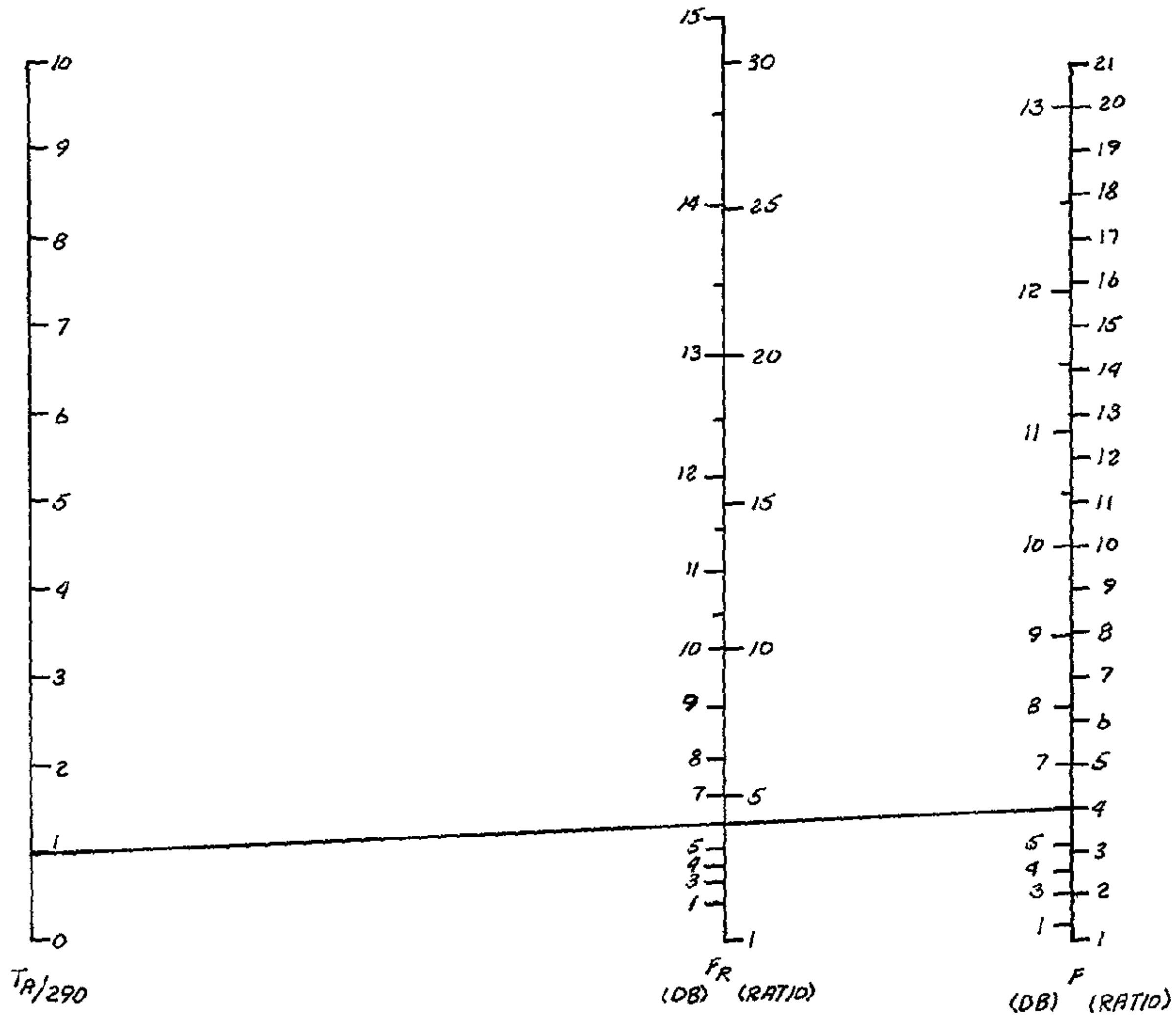

Figure 4-77 Effective Noise Figure Nomogram

where

τ_1 is the time constant of the RC integrator in seconds

The minimum data rate required to transmit the received data back to earth is 2 2 B_F

Next calculate the available integration time It is assumed that the integration time τ_1 is equal to the least time required to move one-half a resolvable unit on the surface At a distance h_o the linear resolution ΔL_o is given by

$$\Delta L_o = h_o \beta \tag{27}$$

where

$\beta \approx \lambda/D$ = the 3 db beamwidth of the antenna

D = the antenna diameter

λ = the operating wavelength

Note that aperture weighting can be introduced by defining an equivalent antenna diameter, i e , if $\beta = 1\ 2\ \lambda/D$ then define $D' = \frac{D}{1\ 2}$ then $\beta = \frac{\lambda}{D'}$

If V_g is the ground speed when the spacecraft is at altitude h_o, then

$$\tau_1 = \frac{h_o \beta}{2\ V_g} \tag{28}$$

If the planet's rotation can be neglected, the lowest value for τ_1 occurs when the true anomaly is zero Then h_o is the minimum altitude and V_g is a maximum In this case $h_o = h_\rho$, $V_g = V_\rho$, the values at periapse If the planet's rotation cannot be neglected, it is necessary to find the minimum value of h_o/V_g The value of h_o and V_g that makes the ratio a minimum is to be used in the calculation of τ_1 The values of h_o and V_g for which the ratio is a minimum can be determined from the trajectory parameter ρ

The values of τ_I for the values of D/λ, h_o and V_g can be determined from Figure 4-78 This figure also gives the linear resolution ΔL_o for any altitude, it is only necessary to interpret the scale h_o as the instantaneous altitude above the planet

The radiometer sensitivity ΔT_{min} in degrees Kelvin is found from Figure 4-79 This nomograph requires the value of F_R found from Figure 4-77, the value of τ_I found from Figure 4-78 and the system bandwidth B_H in Hz This figure is from Reference 17 The range on the various scales has been chosen to exceed the achievable state-of-the-art range in the variables, as were those in the previous two nomographs The state-of-the-art in the next few years, and practical considerations, impose the following limits

$D/\lambda < 300$, since antennas with larger diameters can be erected only in a controlled environment

$B_H \leq 1\ f_o$,

where f_o is the center frequency of the band

It is difficult to design components that operate well over a bandwidth larger than $1\ f_o$ System losses in particular become excessive

By reducing B_H to a small fraction of f_o and using a tuned local oscillator, the system can be used as a microwave spectrometer of essentially low resolution

$\tau_I \leq 20$ sec, since too large an integration time can cause errors due to equipment instabilities

The other limit on these variables and limits on the remaining variables are set by the desire to achieve a desired linear and temperature resolution

The equation solved in Figure 4-79 is

$$\Delta T_{min} = \left(\frac{2}{B_H \tau}\right)^{1/2} F_R\ T_o \tag{29}$$

The factor of two results from assuming a Dicke radiometer with square wave modulation and demodulation

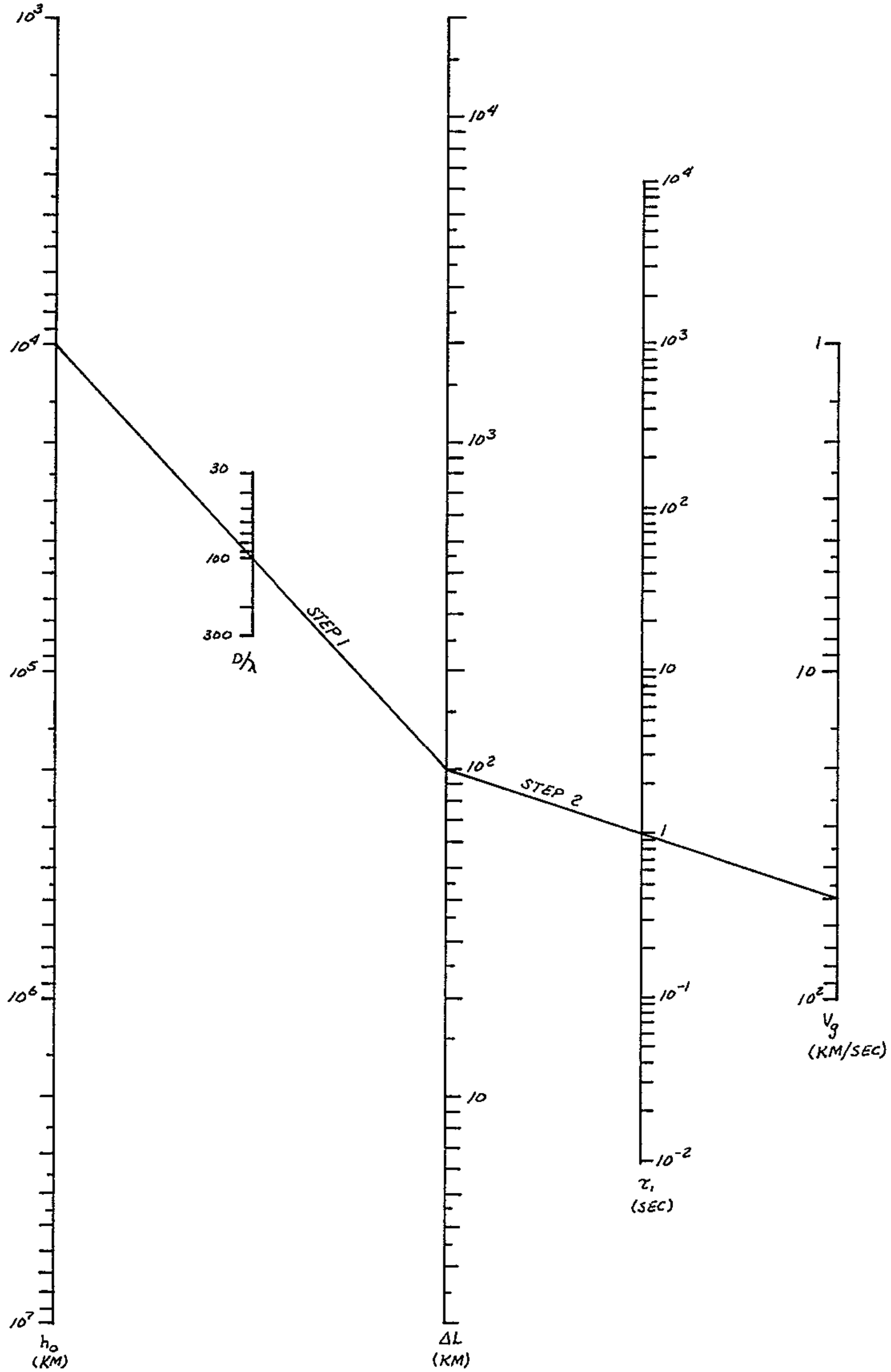

Figure 4-78 Integration Time Nomogram

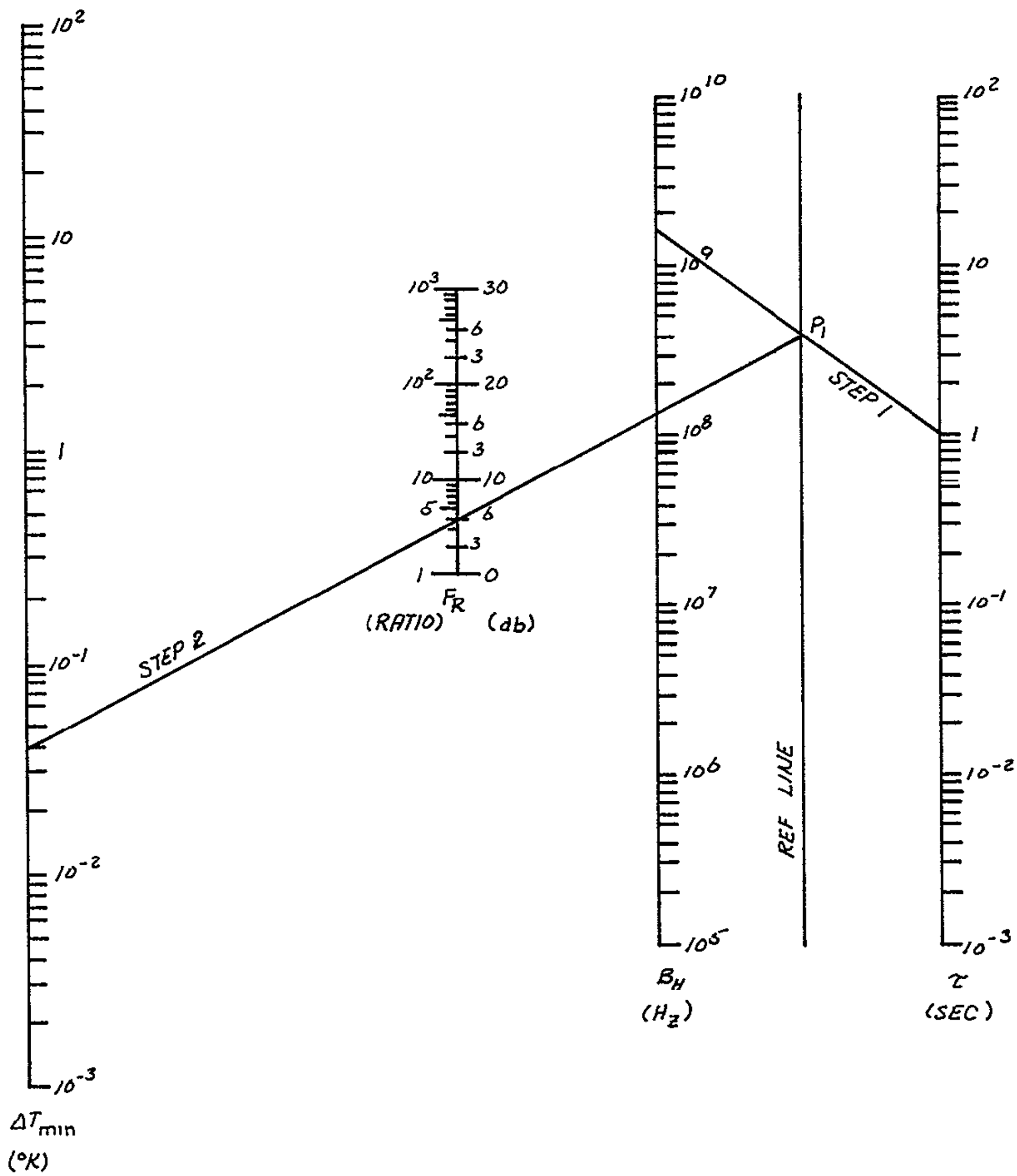

Figure 4-79 Radiometer Sensitivity Nomogram

Given a temperature variation T_T at the target area, calculate the variation seen by the radiometer which will be denoted by ΔT_A

The relation between the two quantities is given by

$$\Delta T_A = \frac{\Omega T}{\Omega A} \quad T_T \Gamma \tag{30}$$

where

Ω_T = solid angle subtended by the target

Ω_A = solid angle subtended by the antenna beam

Γ = the power transmission coefficient of the atmosphere if an atmosphere is present

Set $\Omega_A = \beta^2$ and $\Omega_T = A_T/h^2$, where A_T is the target area which will be approximately $(\Delta L \rho)^2$

$$(\Delta L \rho)^2 = (h_o \beta)^2, \tag{31}$$

This is the smallest antenna beam intercept It occurs at periapse for any planet

$$\Delta T_A = \frac{h_p^2}{h^2} \quad T_T \Gamma \tag{32}$$

Let S/N denote the signal-to-noise power ratio We wish to choose the system parameters so that

$$\Delta T_A = (S/N) \quad \Delta T_{min} \tag{33}$$

Equating the two expressions for ΔT_A gives

$$\frac{h}{h_p} = \sqrt{\frac{T_T \Gamma}{(S/N)\ \Delta T_{min}}} \tag{34}$$

Let

$$T_\ell = \frac{T_T \Gamma}{(S/N)} \tag{35}$$

denote the effective target temperature Then

$$\frac{h}{h_p} = \sqrt{\frac{T_\ell}{\Delta T_{min}}} \tag{36}$$

The value of T_ℓ can be found from Figure 4-80 Since the value of the atmospheric attenuation for the planets with a dense atmosphere is unknown, this figure also can be used in a tradeoff study to determine what surface temperature variation can be measured with a given signal-to-noise ratio for any value of Γ

The value of T_ℓ obtained from Figure 4-80 and the value of T_{min} obtained from Figure 4-79 are used in Figure 4-81 to obtain h/h_p

4 6 5 Imaging Radiometer

4 6 5 1 Scaling Law Development

The equations developed in paragraph 4 1 for the Measuring Radiometer hold, with the exception of Equation (28), for the imaging radiometer

The time τ_1 given by

$$\tau_1 = \frac{h_p \beta}{2 \, Vg} \tag{37}$$

must now be interpreted as the time available to map a strip of length W normal to the projection of the velocity vector on the surface To simplify the discussion we neglect both the curvature of the planet and the change in the resolvable unit size with scanning

Let ϕ be the total scan angle

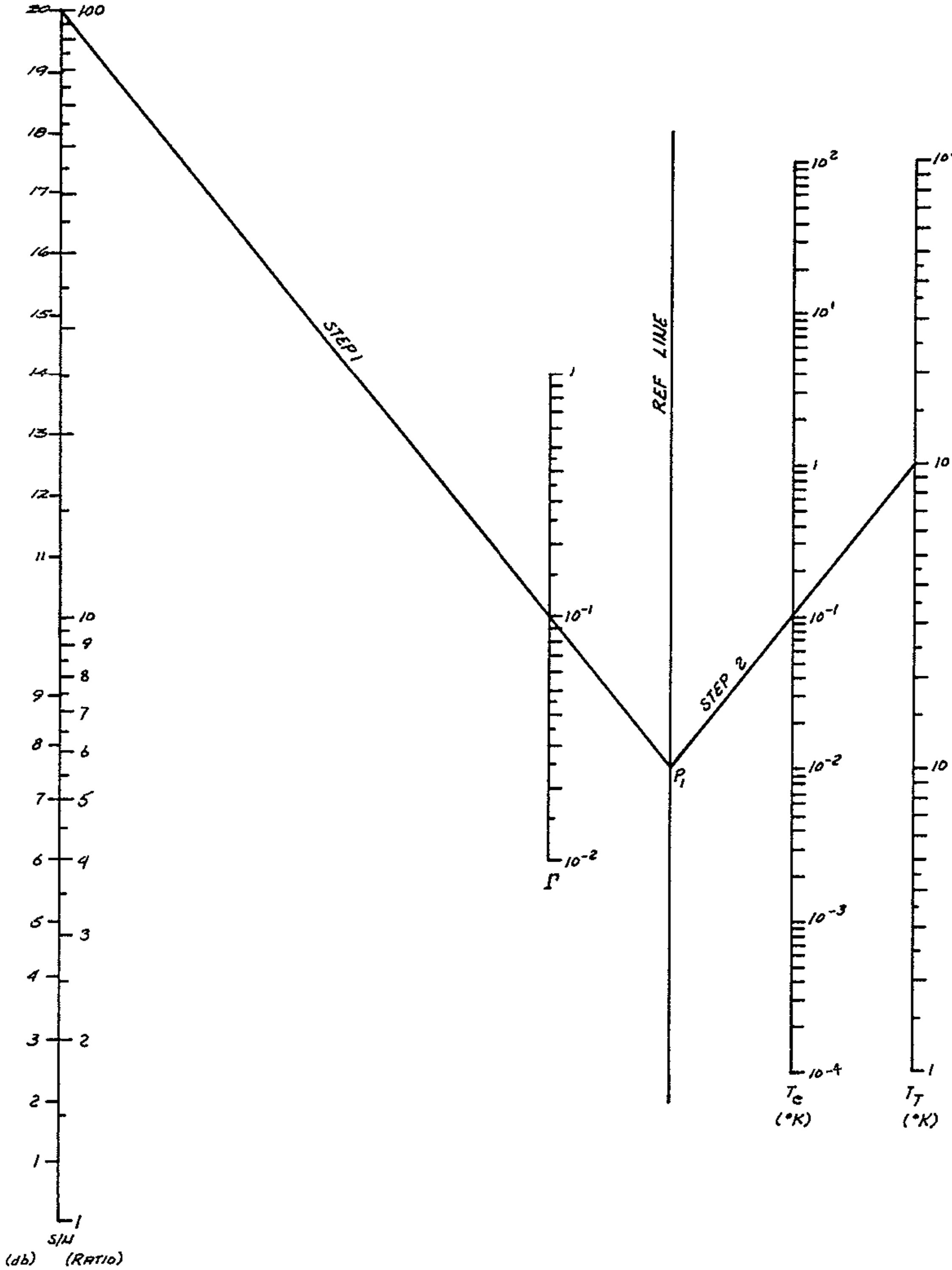

Figure 4-80 Scaled Target Temperature Nomogram

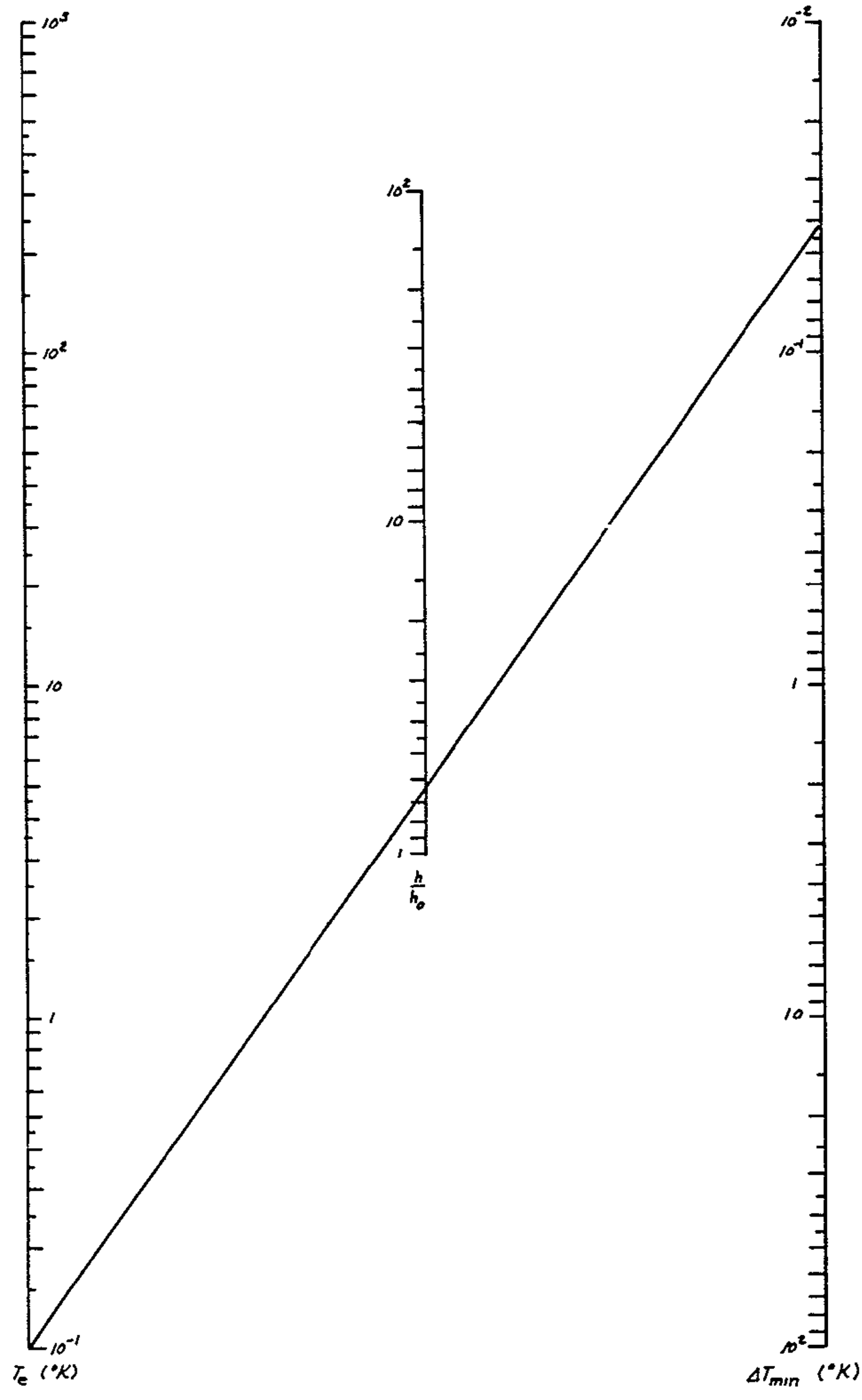

Figure 4-81 Height Scaling Nomogram

Define the strip width W by

$$W = h_p \phi \tag{38}$$

where h_p is the altitude at periapse

Thus at altitudes higher than h_p we use data from less than the maximum scan angle

The number, n, of resolvable units per strip is given by

$$n = \frac{W}{\Delta L_p} \tag{39}$$

where ΔL_p is the linear resolution obtained from Figure 4-78 by setting $h_o = h_p$

The integration time τ_2 is then obtained from Figure 4-82 The relation between τ_1 and τ_2 is given by

$$\tau_2 = \frac{4\tau_1}{n} \tag{40}$$

The factor of 4 appears since the imaging radiometer has a different radiometer constant than a measuring radiometer With this factor included, the radiometer sensitivity ΔT_{min} is found using Figure 4-79 The remaining nomographs in Section 4 3 are then used to obtain the ratio h/h_p

The data rate required for the imaging radiometer using this formulation is given by

$$n^2 = \frac{2\ 2}{4\tau_1} \tag{41}$$

so the data rate is higher than that of the measuring radiometer by a factor of n^2

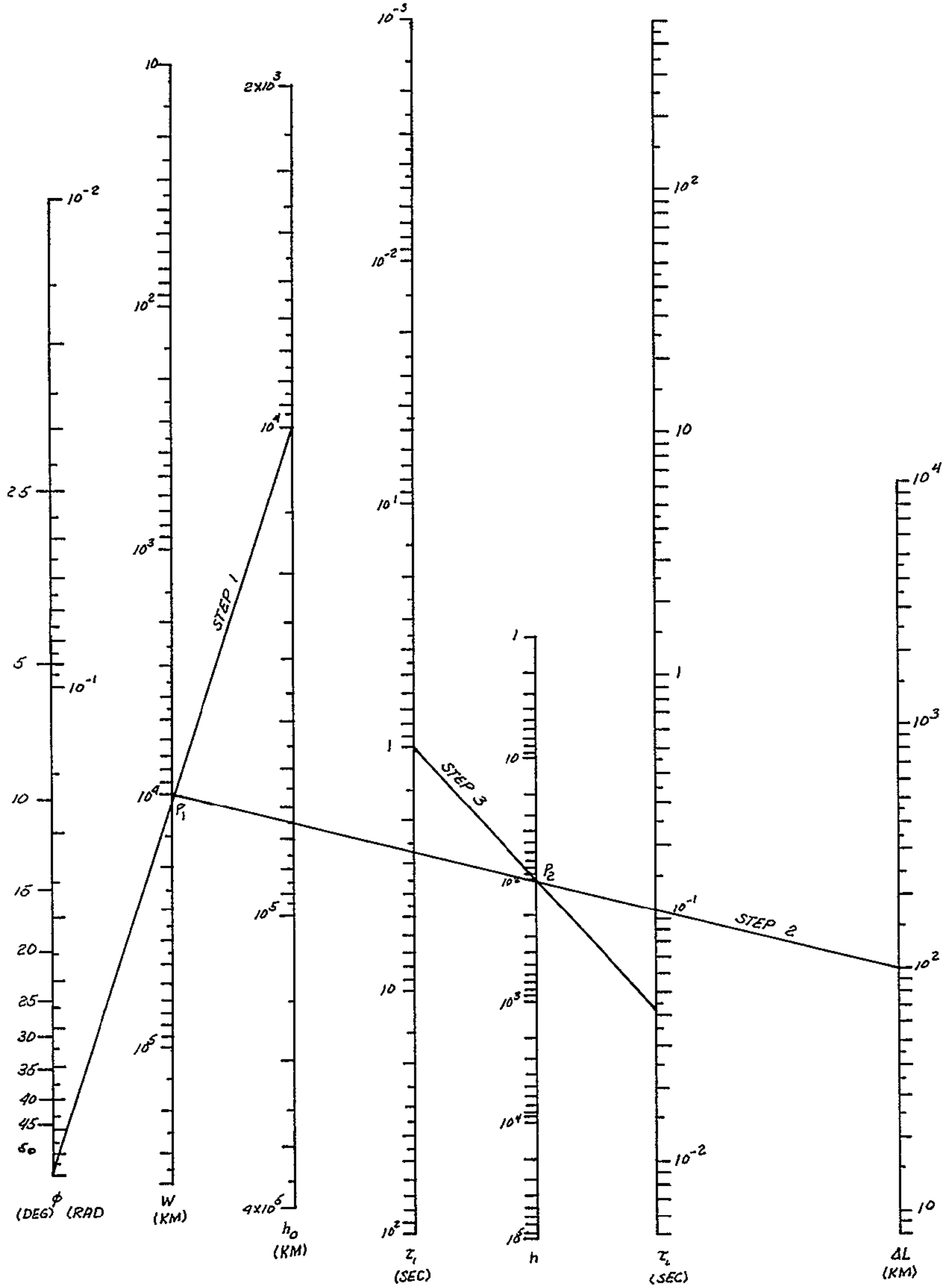

Figure 4-82 Imaging Radiometer Integration Time Nomogram

The above basic description neglected the effects of surface curvature and beam scanning The time required to scan the beam can be made negligible using phase scanning New developments in ferrites has resulted in the production of phase scanned antennas with nanosecond beam switching times Thus all but a negligible portion of the available time can be used to sample the terrain

As to the effects of surface curvature, a more exact calculation of the shape of the resolvable unit will result in a lower value for n

If n is fixed by the phase shift network, this will result in fewer than n independent resolvable units giving a lower linear resolution If ϕ is less than a radian, i e , the half scan angle is less than 30 deg , this effect is not significant

An example of the use of the nomographs is given below The numbers chosen have no significance

1 Use Figure 4-77

Let $T_A = 290$ k so that $\frac{T_A}{T_o} = 1$

Let F = 4

Obtain $F_R = 4$ or $F_R = 6$ db

2 Use Figure 4-78

Step 1

Let $h_o = 10^4$ km, let $D/\lambda = 10^2$

Obtain $\Delta L = 10^2$ km

Step 2

Choose $V_g = 50$ km/sec

Obtain $\tau_1 = 1$ sec

3 Use Figure 4-79

Step 1

Enter τ_1 = 1 sec on the τ scale

Connect to $B_H = 1\ 7 \times 10^9$ Hz The intersection of the connecting line with the reference line gives the point P_1

Step 2

Enter $F_R = 4$

Connect P_1 with $F_R = 4$ and extend line to intersect ΔT_{min} scale Read $\Delta T_{min} = 4 \times 10^{-2}$ °K

4 Use Figure 4-80

Step 1

Choose S/N = 100, $\Gamma = 10^{-1}$

Connect the two points and extend to the reference line to obtain the point P_1

Step 2

Choose $T_T = 10^2$ °K

Connect P_1 and $T_T = 10^2$ °K to obtain $T_\ell = 1$ °K

5 Use Figure 4-81

Enter $T_\ell = 1$ °K, $\Delta T_{min} = 4 \times 10^{-2}$ °K

Obtain $h/h_o = 5\ 0$

For the imaging radiometer, the sequence of steps is

A, B, B1, C, D, E

For Step B1, use Figure 4-82

Enter $\Delta L = 10^2$ km and $\tau_1 = 1$ sec from Step B

Step 1

Choose $\phi = 1$, $h_o = 10^4$ km, obtain $L = 10^4$ km

Step 2

Connect $L = 10^4$ km and $\Delta L = 10^2$ km, obtain $n = 10^2$

Step 3

Connect $\tau_1 = 1$ with $n = 10^2$ and extend the line to intersect with τ_2 at $P_3 = 4 \times 10^{-2}$

This value is then entered for τ in Step C

4 6 6 <u>Radiometer Support Requirements</u>

The support requirements developed below are an extension of the support requirements developed in Section 7 of Reference A

4 6 6 1 Passive Microwave Support Requirements

Antenna Size and Weight

This is the dominant support requirement, by far, for all applications of passive microwave systems For parabolic antennas, mechanically positioned (for scaling purposes $A_{ant} = D^2$ where D is the antenna diameter in meters), the antenna weight is

$$M_{ant}\,(kg) = \psi_A D^2 \qquad (42)$$

where

ψ_a is the mass/unit area,

For the problems at hand it will be useful to set

$$1\ 5\,\frac{kg}{m^2} < \psi_A \leq 6\,\frac{kg}{m^2} \tag{43}$$

Here the upper limit (See Reference 1, Page 232) is to be used for antennas subjected to high mechanical scanning rates with a scan flyback time $t_f << 1$ sec, and which require great dimensional stability because of small operating wavelength, say, $\lambda < 3$ cm These conditions, will be encountered in imaging radiometer experiments with small $\Delta(\phi)$

The lower density limit of 1 5 Kg/m^2 appears to be a reasonable estimate of the attainable state-of-the-art for the subject time period for antenna applications where deformation due to angular acceleration requirements is minimal and the operational band is such that $\lambda > 3$ cm These conditions correspond to experiments of occultation, polarimetry, and temperature measurements in fixed or near-fixed directions

Electrically Scanned Array Antennas Again, for scaling purposes, the antenna dimensions are L by L. The number of elements in the array of length L is given by

$$N = \frac{L}{\lambda}(1 + \phi) \tag{44}$$

where

λ = wavelength

ϕ = extent of scan angle

The weight/element can be estimated to be of the form

$$M/_{element} = K_1 + K_2 L \lambda \tag{45}$$

Here K_1 accounts for the element module weight which is independent of length, such as the phase shift and isolation amplifier required for each element, while $(K_2 L_1 \lambda)$ represents the length and diameter of the waveguide times a density constant An empirical fit (in metric units) for K_1 and K_2 to state-of-the-art systems is

$$M/_{element}\,(Kg) = 0\ 05 + 3\ \lambda\ L$$

The Antenna Weight then becomes

$$M_{ant} = (M/_{element}) \quad N \tag{46}$$

$$M_{ant} = \left[\frac{L}{20\lambda} + 3L^2\right] (1 + \phi), (\phi \text{ in radians}) \tag{47}$$

This relation is an empirical, valid for 0 005 < λ < 0 3 m

The antenna dimension, L, obtains, for imaging radiometry experiments directly as

$$L = \lambda (\Delta \phi) \tag{48}$$

where

$\Delta\phi$ is the required angular resolution

For occultation applications, D^2 or L^2 defines the aperture area on receive, and can be established as a tradeoff against the power requirement imposed on the ground (Earth) transmitter

Power Requirements Antenna Power Requirements For mechanically scanned antennas, a relation which defines the required power for scanning is derived in Reference 2 as

$$P_A(\text{watts}) = \frac{40\, M_{ant}\, D^2 \phi^2}{t_f^3}$$

where

t_f is the scan flyback time in seconds

ϕ is the scan angle in radians

and acceleration is obtained with a 25% efficient electric motor This equation can be used as a valid estimate for small antennas (D < 2 meters)

It leads to exorbitant power demand for high speed electrically driven antennas The cross-over point for other types of drives is generally 25 watts of power For larger antennas a much lower power demanding mechanization results from the use of hydraulic drives and accumulators which permit the cyclic conversion of pressure energy to kinetic energy and conversely

The required input power for systems of this type is small, say on the order of 10-50 watts

Power Requirements Electrically Scanned Arrays   The power required for each phase shifter module is estimated as

P_A/element = 0 2 watts, so that the total power becomes

$P_A = 0\ 2\ N = 0\ 2\ (1 + \emptyset)\frac{L}{\lambda}$ watts

Power Requirements Microwave Receiver Power   For $\lambda > 3$ cm, an almost negligible power input of, 3 to 5 watts (See Ref 2, Pg 227) is indicated

For short wavelengths, $\lambda < 3$ cm, as much as 25 watts may be required

Platform Stability   The platform stability required is most severe in imagery experiments

Then a necessary condition can be stipulated as follows   Consider that the flyback time is small in comparison to the dwell (integration time)   Then for a resolution dimension ΔL, from an altitude h, the required angular stability is

$$\theta' < \frac{\Delta L}{h \Delta t} \tag{49}$$

then, with equal resolution in any direction,

$$\Delta t = \frac{\Delta L}{V_h} \tag{50}$$

so that

$$\theta' < \frac{V_h}{h} \text{ rad/sec} \qquad (51)$$

where the velocity of the subsatellite point can be substituted for V_h

Data Acquisition Rates The dominant data rate for passive microwave experiments arises in imaging radiometry applications

With the antenna angular resolution given by $(\Delta\phi)$, and assuming the flyback time to be small in comparison with the scan time t_s, the number of elements mapped per unit time multiplied by a grey code, G_c, represents the minimum data rate Within a scan angle ϕ there are $\phi / \Delta\phi$ elements so that

$$DR = \frac{\phi}{\Delta\phi \, t_s} \qquad (52)$$

Since

$$t_s = \left[\frac{V_h}{h \Delta\phi}\right]^{-1} \qquad (53)$$

$$DR = \frac{V_h \phi}{(\Delta\phi)^2 h} G_c \qquad (54)$$

where

V_h is the subsatellite point velocity

h is the altitude

$\Delta\phi$ is the angular resolution

G_c is the number of bits/sample, usually $4 \leq G_c \leq 7$

4 7 PARTICLES AND FIELDS SENSORS

4 7 1 Introduction

A wide variety of highly developed and specialized types of particle and field sensors have been flown in Earth orbit and on interplanetary missions In the early space program, particles and fields dominated the space science programs The size, power, and telemetry requirements for particles and fields instruments vary only approximately with objectives Scaling laws could be written for limited ranges of various objective requirements for each sensor type, but would be of limited value. Scaling factors are indicated in tabular form, due to the large variety of sensor types and special features of current instruments A quasi-historical approach to sensor sizing is taken, attempting to show general trends for the sizes of these sensors versus requirements instead of arithmetical scaling laws

4 7 2 Magnetometers

Five basic types of magnetometers are being considered for use or have been used in space They are the search coil, flux gate, proton precession, Hall-effect, and the optically pumped rubidium vapor, cesium vapor, and helium vapor magnetometers These magnetometers can be built to measure various ranges of field strengths, and to determine one or more components of the field or the field magnitude with or without indication of direction Factors that may lead to magnetometer sizing include measurement precision requirements for accuracy of field strength and direction, frequency response, range of sensitivity, lifetime and degree of freedom from interfering spacecraft induced fields

Table 4-18 presents a description and lists some of the factors leading to sizing for each of the magnetometer types flown At the present time, only flux gate and optically pumped magnetometers are considered as flight-proved on interplanetary missions A search coil magnetometer was used on Pioneers 1, 2, and 5, Explorer 6, EGO, and POGO On Pioneer 5 the spacecraft spin was used to permit measurement of the resultant of the two field components perpendicular to the spin axis The third component could have been measured with the addition of a motor driven coil The coil fixed on the spacecraft measures the ambient field, unaffected by fixed spacecraft fields which rotate with the coil, hence produce no contribution. But the motor driven coil would be sensitive to spacecraft fields To determine the spacecraft fields perpendicular to the spin axis, a pair of motor driven coils would have to be used Slip rings may also be needed These motors, of course might produce some permanent fields if electrical, but not if gas driven The reliability of motor and slip ring mechanical systems for long duration missions, which may be a problem, and accuracy limitations, have lead to use of other magnetometers on interplanetary spacecraft

Due to the above problems and limitations, in addition to the emphasis away from particle and fields on Mars and Venus missions, the search coil magnetometer has not been used on interplanetary flights since Pioneer 5 Nevertheless, there may be an important role for the search coil magnetometer on missions to Mercury or to the outer planets which could have strong fields If the planet is assumed to have a low field but has a strong one instead, the flux gate or optically pumped instruments might be driven off scale, whereas the spin coil magnetometer could be designed to cover a wider range of ambient conditions as a backup sensor Fixed search coils also could be used to measure changing fields independent of the spacecraft and its own changing fields The spacecraft spin-axis could be changed by 90° to permit measurements of other axes The pair of spin coils could be spun up on command when required

The weight, volume, and power requirements for search coil magnetometers of the above types are summarized in Table 4-19 The weights and sizes are based on Pioneer 5 state-of-the-art with additional feature constraints estimated as indicated Recent developments in electronics might lead to somewhat smaller coils and electronics than indicated in Table 4-19 which should be viewed as upper estimates of instrument sizes

4 7 2 1 Flux Gate Magnometers

Following the Pioneer 5 mission, flux gate magnetometers came into use in Earth orbit, and on Mariner 2 The flux gate magnetometer consists of a primary and secondary coil wound on a pair of cores of Permalloy or similar material A high frequency (20 to 60 kHz) signal, sufficient to saturate the core, is impressed on the primary The secondary coils are wound in opposite directions so that zero output results if there is no external field An external field produces an assymetry in the hysteresis loop, leading to a field dependent output signal in the form of the amplitude of the second harmonic of the driving signal Components are measured separately by three magnetometers mounted orthogonally in a rigid cruciform

The Mariner 2 magnetometer had two output scales, 0 to ±64 (±0 6 gamma precision) and 0 to ±320 (±0 25 gamma precision) Auxiliary coils were used to cancel spacecraft fields, and to provide a calibration check each 15 77 hours The problem of picking up a stray field on the spacecraft or by the magnetometer cores has been dealt with on later Pioneer flights by flipping the units by 180° If no stray field exists, no change in indicated field magnitude would result

Magnetic cleanliness may be something of a problem for long duration space missions Mariner-4 (with the helium vapor sensor) had a 140 gamma permanent field at launch No one knows for sure if the same field existed

Table 4-18 Basic Magnetometer Types, Description, and Sizing

Magnetometer Type	Flights	Mass (kg)	Volume of		Power		Reference	Measurement		Range (gamma)	Precision (bit)	Outputs	Max. Sampling Rate (s)	Bit Rate (b/s)
			Sensor (cm3)	Electronics (cm³)	Cont. (w)	Peak (w)		Advantage	Limitation					
3-axis search coil	Explorer 6 OGO-1 Pioneer	1	60	540	1.2	1.2	Smith	External field only	Changes only	-	8	B_x B_y B_z	1	72
3-axis flux gate with coil flipper to permit deter. of nullfield several times per flight	Mariner 2 Explorer OGO-E IMP D,E Pioneer C,D Pioneer 6	2.1			6		Coleman Cahill Heppner Sonett Ness	Components only	Can pick up a bias field of unknown magnitude	$\pm$ 64 $\pm$ 320 $0.1-10^5$ + 64	$\pm$ 0.6 10 8	B_x B_y B_x, B_y, B_z	1	30
Proton Precession	Vanguard III							Scaler field magnitude	Measures higher fields, slow response for weak fields	10^4-10^5				
Cesium Vapor	OV-1-10						AF S/C	Lower power than rubidium	Less accurate than rubidium and helium	10-50,000				
Rubidium vapor with Helmholtz coils	Explorer OGO, IMP	1.4	2100	2360	3.5		Ness		Less accurate than helium	0.05 to 10,000	7 cps/ gamma 10 bit	B_x, B_y, B_z Total	1	40
Hall Effect	-	-	-	-	-	-	-	-	-	-	-	-	-	-
Helium vapor with Holmholtz coils	Mariner 4	3.4	1500	2360	7.0	10 w 10	Norris JPL TR	Measures nulling currents in 3 sets coils		0.25 to	23 cps/ gamma 10 bit	B_x, B_y, B_z	1	30
	Modified Mariner 4 applicable to TOPS							Total field higher accuracy than rubidium		0.1-360 360-36000	$\pm$ 0.1 10 bit	B_x, B_y, B_z Total	1	40

Current and power for high fields are excessive.

Table 4-19 Search Coil Magnetometer Design Constraints

Magnetometer Type	Mass (kg)			Volume $(cm)^3$			Data Outputs	Precision Each Chan (bit)	Typical Sample Rate (s)	Typical Total Data Rate (b/s)	Power Estimates (w)
	Sensor Head	Electronics	Total	Sensor Head	Electronics	Total					
Single fixed coil	0 09	0 5	0 5	20	380	400	B_x at 1 HZ 10 100 1000	8	1	32	1
2 fixed orthogonal coils	0 18	0 6	0 8	40	450	500	B_x at 1 10 100 1000	8	1	64	1 2
3-axis set of fixed orthogonal coils	0 27	0 7	1 0	60	540	600	B_x at 1 Hz 10 100 1000	8	1	72	1 4
Single fixed coil plus synchronous motor driven spin coil at 144 rpm (based on 2400 Hz power)	0 38	0 6	1 0	70	480	550	B_x at 1 Hz 10 100 1000 $\left[B_y^2 + B_z^2\right]^{1/2}$ at 1 10 100	8	1	56	2
Two synchronous electric motor driven orthogonal spin coils	0 58	0 6	1 2	100	600	700	$\left[B_x^2 + B_y^2\right]^{1/2}$ at 1 Hz 10 100 $\left[B_y^2 + B_z^2\right]^{1/2}$ at 1 10 100	8	1	48	3
2 synchronous motor driven orthogonal spin coils plus fixed coil for 3rd axis measure ment in stationary state output propor tional to field changes only	0 67	0 8	1 5	120	680	800	B_x at 1 Hz 10 100 1000 $\left[B_x^2 + B_y^2\right]^{1/2}$ at 1 10 100 $\left[B_y^2 + B_z^2\right]^{1/2}$ at 1 10 100	8	1	80	3 2

Pertinent Reference D L Judge M G McLeod and A R Sims The Pioneer I Explorer VI and Pioneer V High Sensitivity Transistorized Search Coil Magnetometer IRE Trans SET 6 114 September 1960 at planet encounter Although the 140 gamma bias was found to be stable in time, small oscillatory changes might be indistinguishable from the weak planetary field and solar environmental fluctuations

The instrument weight and power for an inner or outer planet mission should range from 1 4 to 2 1 kg and 3 5 to 6 watts, including the flipping system Scaling with field strength over 0 1 to 10^5 gamma is not significant

4 7 2 2 Helium and Alkali Vapor Magnometers

Helium, rubidium, and cesium vapor optically pumped magnetometers have been used almost as extensively as flux gate magnetometers for measurements in space Whereas the flux gate magnetometer is used to measure field components, the optically pumped magnetometers measure only the total field

To obtain field direction or to measure field components, with an optically pumped magnetometer, the sensor vapor cell is surrounded with three sets of orthogonal Helmholtz coils used to null out the external field and/or field components The Mariner 4 helium magnetometer used a servo system to vary nulling currents on the three sets of coils to produce a zero internal field The values of the nulling currents were transmitted For future flights, the total field could be transmitted also, then the current in each set of coils could be nulled to zero and currents transmitted, then the total scaler field could be transmitted A further possibility would be to use an optically pumped magnetometer for total field measurements and three orthogonal flux gate magnetometers for field components

For Jupiter, Saturn and possible other missions, high magnetic fields might be encountered The Mariner 4 type of low-field magnetometer would have to be modified for wide range environments If a set of Helmholtz coils is used to null the field, currents and instrument power required will depend on external field and on coil diameter The field at the center of a pair of Helmholtz coils is approximately equal to

$$B = 2 \frac{\mu_o \; Ni}{a} \tag{1}$$

where

μ_o = 12 57 x 10^{-7} webers - amp^{-1} - $meter^{-1}$ (10^{-4} gauss = 1 w/m^2)

N = Number of turns of 30 or 40 gauge wire (1000 typical)

i = Current in amps

a = Coil radius (0 05 to 0 08 meters typical)

If the external field were 360 gammas (the maximum value measurable by the Mariner 4 helium magnetometer) then the current in each coil would have to be

$$i = \frac{(360)\ (10^{-5}\ \text{gauss}/\gamma)\ (10^{-4}\ \text{w/meters}^2\text{-gauss})\ (0\ 06\ \text{meters})}{(12\ 57\ \times\ 10^{-7}\ \text{w/amp meters})\ (1000\ \text{turns})}$$

= 17 microamps in each coil

If the external field were 360,000 gammas then the currents would have to be 17 milliamps Number 30 wire has a resistance of about 0 1 ohm per foot at 25° C The length of wire required for the 6 Helmholtz coils would be equal to 6 (1000 turns) (0 38m/turn) (3 28 ft/m) or about 7500 feet and would have a D C resistance of 750 ohms A potential of about 13 volts would drive these coils Hence, coil power requirements for a Jupiter mission do not appear to be significantly different than for the Mariner 4 instrument

Minor temperature control problems were encountered on Mariner 4 The tested temperature range was from -45° to +45°C By encounter, the temperature was 6°F below the design range The temperature dropped on occultation, as expected Were more power available for heating, a constant temperature could have been maintained, as it may have to be for an outer planet mission Cooling may be required for a Mercury or close-in Solar probe Power estimates for cooling or heating may be developed in scaling law form, but no information is available at this time upon which to base it

The optically pumped magnetometers for an outer planet mission would be the same as presently designed except possibly for dual lamp units for increased reliability and lifetime

4 7 3 Charged Particle Spectrometers

A large variety of charged particle spectrometers have been flown for measurement of cosmic rays, solar corpuscular radiation, trapped radiation, and solar plasma Table 4-20 presents a summary of spectrometer types used, showing typical weight, volume, power requirements The sizes are roughly proportional to the particle energy, or to particle range in the detection media The solar plasma spectrometers use electrostatic means to capture the lowest energy particles and count them in a current mode The plasma energies range from 10eV to 10keV for protons, electrons, or heavier particles Predominantly protons have been measured on interplanetary missions Low energy ionospheric electrons have been measured around the earth

Table 4-20 Selected Charged Particle Spectrometer Descriptions

	Sensor Type	Flown On	Approximate Values for Sensor			Reference
			Mass (kg)	Dimensions (cm)	Power (w)	
1	Geiger-Mueller Tubes With Varied Shielding	Mariner 2, 4 Pioneer	1 0	8 x 16 x 30	0 4	1, 2
2	Ion Chamber & GM Tube	Mariner 2, 4	1 2	20 x 20 x 16	0 5	1, 2
3	Proportional Counter Telescope	Pioneer 5	1 to 5		~1	
4	Semiconductor Telescope	Mariner 4	1 2	16 x 16 x 16	0 6	(2) Simpson
5	Plastic Phosphor Scintillator Telescope	Explorer 12 Imp, etc	0 9	10 x 12 x 12	~2	(5) Ludwig
6	Cerenkov-Scintillator Telescope	Balloons	>2		>2	(3) McDonald
7	Magnetic Analyzer	Explorer	>2			(4) Walt
8	Bubble Chamber		Variable,	>20		
9	Spark Chamber	Balloons	Variable,	>20		
10	Electrostatic Analyzer	Mariner 2 Pioneer 6	2 2	20 x 20 x 10	1	(1) JPL TR-32-315
11	Faraday Cup Analyzer	Mariner 4 Explorer, etc	2 9	16 x 16 x 10	2 9	(2) JPL TR-32-883

Predominantly protons have been measured beyond the geomagnetosphere using ion chambers, Geiger-Mueller counters, proportional counters, scintillators, and semiconductor particle spectrometers Cosmic ray particle measurements have been proposed using larger instruments which include, bubble chambers, spark chambers, large solid and gaseous Cerenkov spectrometers, and magnetic analyzers Nuclear emulsions have not been proposed for unmanned spacecraft beyond Earth orbit

Except for the high cosmic ray energies, charged particle spectrometer sizes and weights run between 0 9 and 10 kg The weights depend on detector type and collimation angle Omnidirectional detectors and spectrometers do not need much collimation, but to define narrow angles of sensitivity, collimators must have thicknesses larger than the particle ranges (except where the particle flux remains small enough that coincidence counting can be used without much collimation)

Shielding plus collimation may be needed for outer planet missions to prevent rapid damage to semiconductors and other detectors from absorption of intense fluxes of trapped radiations The amount of shielding required for adequate protection in the trapped radiation belts of Jupiter is not presently known, but estimates may be made of the expected range of shielding, assuming available models for the trapped environments

4 7 3 1 Electrostatic Spectrometers

The overall size of a charged particle spectrometer varies according to particle energy, range, or radius of curvature depending on how the energy is measured Low energy particles in the eV to keV range are detected by deceleration in an electrostatic field followed by detection of the remaining current The electrostatic spectrometer must be long enough to permit the maintenance of a uniform potential of a few kilovolts in a vacuum, and must have an entrance aperture large enough to collect a detectable current The size of the plasma spectrometer for an OPM mission should be on the same order as those used for Pioneer and Mariner missions shown in Figures 4-83, 4-84, 4-85, and 4-86 The weight, volume, power, and data rates given in Table 4-21 need not be different for missions in deep space

4 7 3 2 Semiconductor Charged Particle Spectrometers

For energies of protons, electrons, alphas and slightly heavier ions, energy and flux are measured by determining the total energy deposited in a silicon semi-conductor junction, for particles with ranges up to about 5 mm in silicon For higher energies, a series of semi-conductors with absorbers in between are used to determine flux versus energy from the rate of energy loss in each detector in the series Thus the size of this type of spectrometer is determined by the particle range and flux to be detected, and the collimation angle established by the shielding

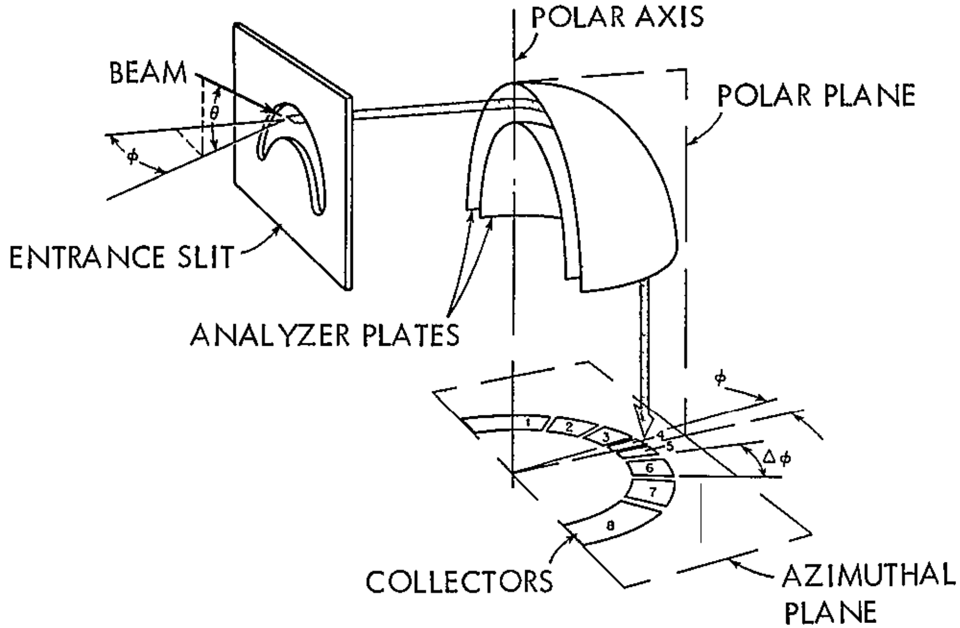

The spherical electrostatic analyzer can measure flux azimuth using segmented collectors. Spectral analysis is accomplished by stepping the voltage applied across the concentric surfaces.

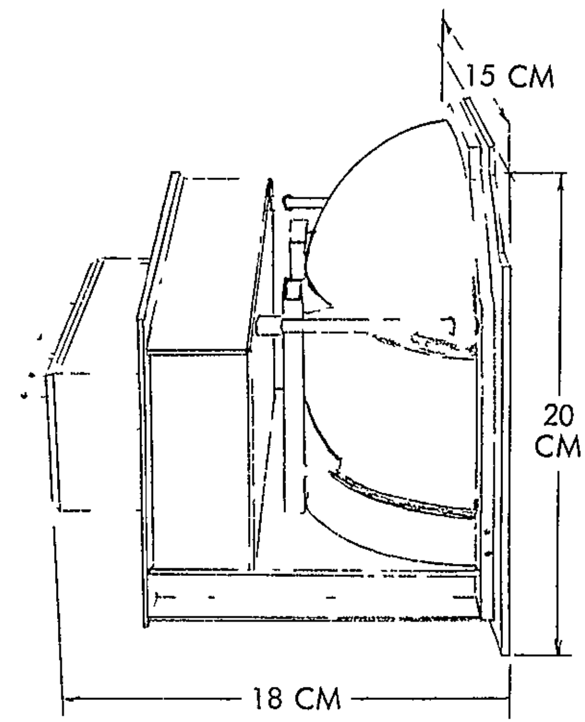

Figure 4-83 Ames Research Center Plasma Spectrometer for Pioneer 6 and 7

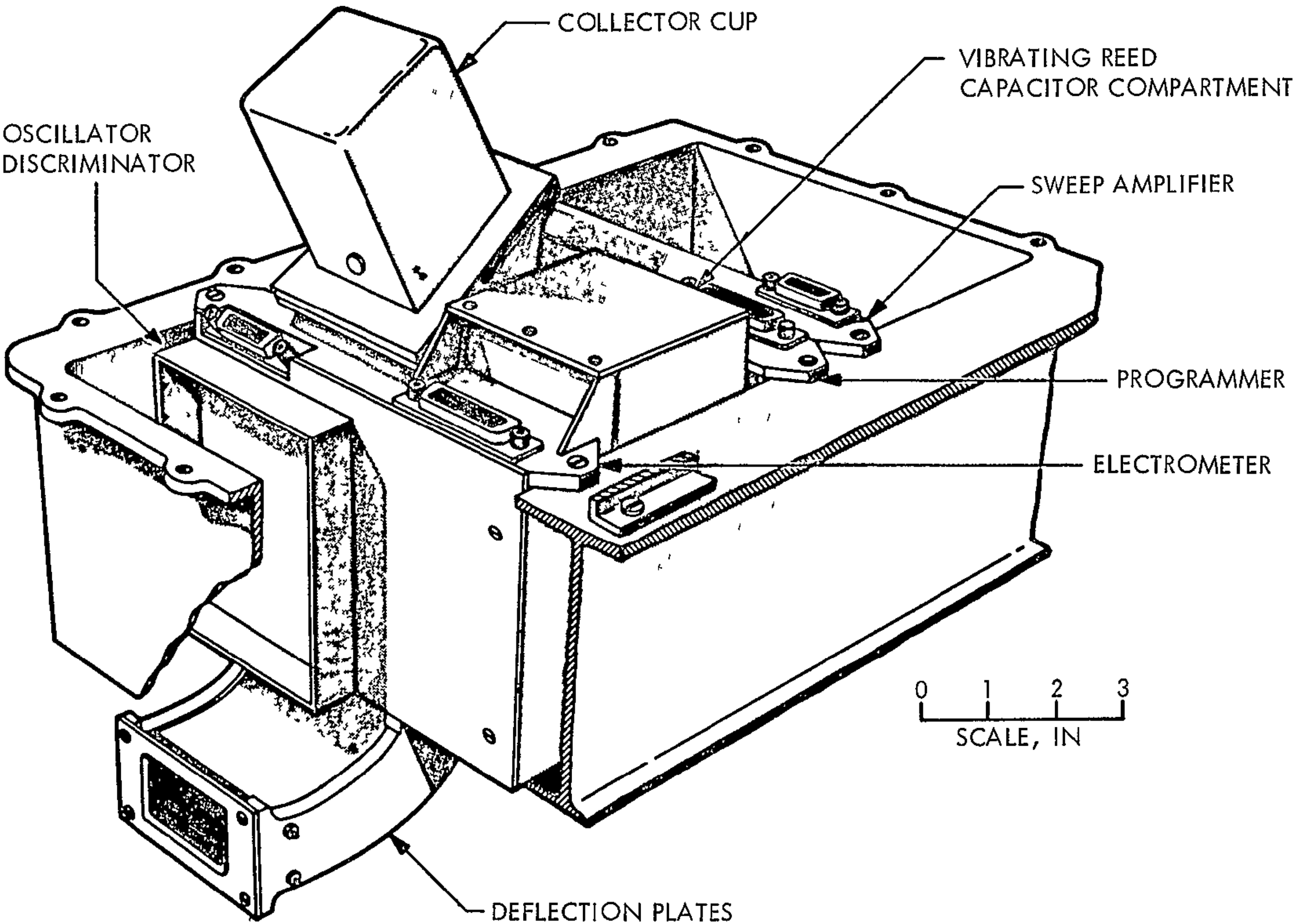

Figure 4-84 Mariner II Solar Plasma Spectrometer Experiment Assembly

Space Division
North American Rockwell

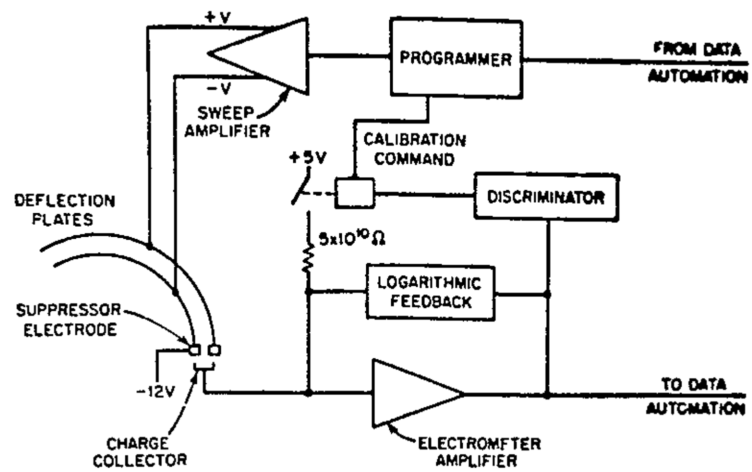

Figure 4-84a Mariner II Plasma Spectrometer Block Diagram

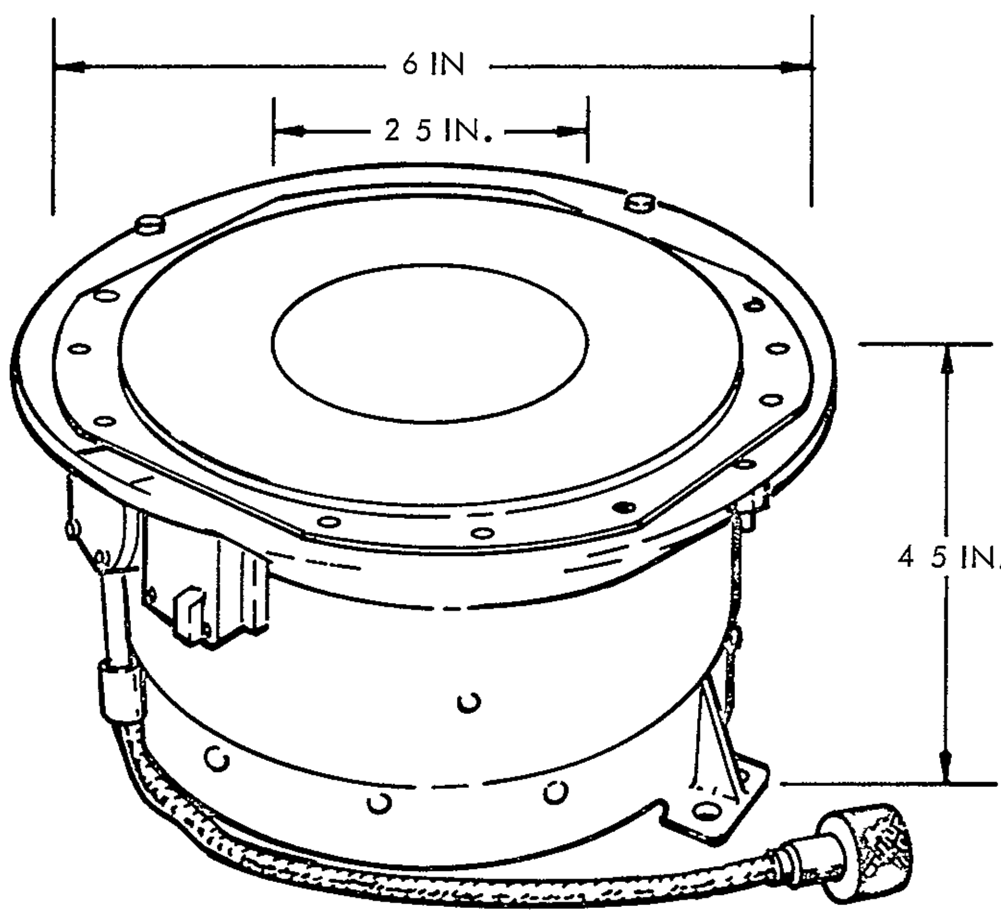

Figure 4-85 Mariner IV MIT Solar Plasma Faraday Cup Sensor Head

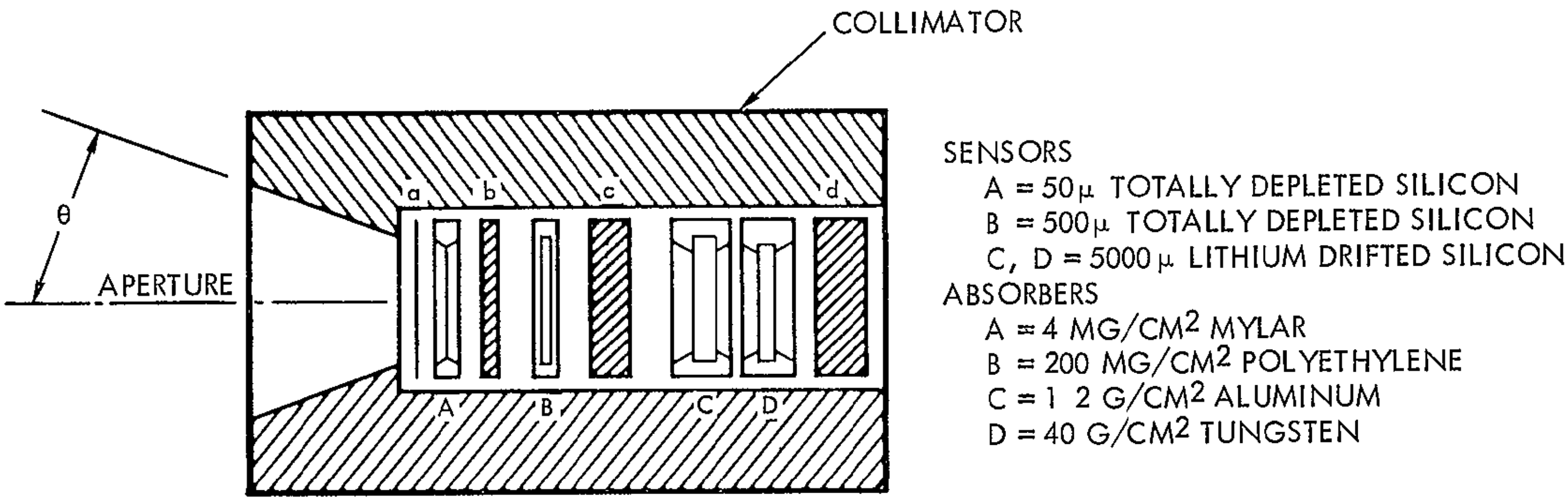

Figure 4-86. Representative Charged Particle Spectrometer

Table 4-21 Plasma Spectrometer Constraints

Spacecraft	Responsible Agency	Type	Mass (kg)	Dimension Sensor (cm)	Power (w)
Pioneer Imp	Ames (J W. Wolfe)	Spherical Plate Electrostatic Spectrometer	1 4 0 9		0 3
Imp	MIT (H Bridge)	Faraday Cup Spectrometer	2 2		1 5
Ranger 1, 2 Mariner 2	CIT (C Snyder, M Neugebauer)	Cylindrical Plate Electrostatic Spectrometer	2 2	16 x 24 x 12	1 0
Mariner 4	MIT & CIT (H Bridge, C Snyder)	Faraday Cup Spectrometer	2 9	16 Dia x 10 (Sensor) 5 x 16 x 16 (Electronics)	2 65 - 2 9

The shield mass used for collimation of relativistic particle energies can weigh more than the sum of all other parts of the spectrometer, especially for collimation angles less than 90 degrees The mass of sensors for particles greater than a few keV and less than that which can penetrate 5 mm of silicon (or thickest silicon semiconductor detector available) depends primarily on the mass of the magnetic core memory bank for storing counts in each resolved energy interval The range of weights varies according to the number of energy channels provided and the required sampling rate which is related to detector required area Such detectors are described in Figure 4-22 This spectrometer is of the dE/dx x E type The energy deposited in the first detector is proportional to the rate of loss of energy of the particle For particles stopping in the second detector, the output pulse height is proportional to total energy This type of detector covers the proton energy range from 10 keV to 300 MeV and comparable ranges for alphas and electrons The weight of the detector is mostly the weight of the collimator The collimator thickness is on the order of 10 to 20 g/cm^2 thick in all directions In the entrance angle portion of the collimator, the length of the aperture will depend on collimation angle as shown in Figure 4-22 The mass of the detector parts are estimated below for an upper energy E (MeV) limit of protons

Mass in Grams

Detector Unit

$$\pi\ (1\;5\ \text{cm})^2 \left(3\;2 \times 10^{-3} E^{1\;76}\right)$$

Rear Cap of Aluminum

$$\pi \left(1\;5 + \frac{3\;24 \times 10^{-3} E^{1\;76}}{2\;7}\right)^2$$

Cylindrical Portion of Collimator

$$\pi \left[\left(1\;5 + \frac{3\;2 \times 10^{-3} E^{1\;76}}{2\;7}\right)^2 - (1\;5)^2\right] \left[6\;4 \times 10^{-3} E^{1\;76}\right]$$

Entrance Aperture Cone

$$\pi \left[\left(1\;5 + \frac{3\;2 \times 10^{-3} E^{1\;76}}{2\;7}\right)^3 \tan\left(\frac{\pi}{2} - \phi\right) - \left(3\;2 \times 10^{-3} E^{1\;76}\right)\left(1\;5 \times 3\;2 \times 10^{-3}\right) E^{1\;76} - \frac{1}{3}\left(1\;5 + \frac{3\;2 \times 10^{-3} E^{1\;76}}{2\;7}\right) \tan\left(\frac{\pi}{2} - \phi\right) + \frac{1}{3}(1\;5)^2 \tan\left(\frac{\pi}{2} - \phi\right)\right]$$

The above collimator basic thickness of 10 g/cm^2 may be taken to be the range of the highest energy non-relativistic particle to be detected The proton range, R_{Al}, in aluminum as a function of energy can be given as

$$R_{Al} = 3\ 2 \times 10^{-3} E^{1\ 76} \quad (2)$$

where R_{Al} is the range in g/cm^2 of aluminum and E is the kinetic energy in MeV valid from about 5 to 150 MeV

4 7 3 3 Cosmic Ray Spectrometers

For protons with energy greater than about 100 MeV (Range equal to 10 g/cm^2), coincidence counting alone may be used to establish collimation angle, but unless the particle is stopped in the last detector, there would be no accurate way to determine the particle energy except to use a number of thick detectors in parallel and to use thicker collimators The collimator thickness for 300 MeV would be 68g/cm^2 and would increase exponentially with energy Also, the probability of inelastic scattering becomes large Hence for protons above 150 MeV, other detection methods are used. These include the Cerenkov detector, spark chamber, and bubble chambers of large volume

The Cerenkov detector has been used in a gas or solid form, for protons from 100 to 1000 MeV and heavier particles It consists of a scintillation medium that is insensitive to low energy particles Lucite is a common Cerenkov phosphor The flashes of light which are energy dependent are detected by a photomultiplier, usually in coincidence with a second scintillator to help define angle and particle type The size of the Cerenkov detector is a function of the particle range in plastic plus the photomultipliers The mass, volume and power are given in Table 4-22

4 7 3 4 Bubble Chambers and Spark Chambers

The spark chamber consists of a stack of parallel plates charged with high voltage and separated by an inert gas When a high energy particle traverses the stack, a spark is produced between the plates, marking the path of the particle

The bubble chamber consists of a tank of liquid gas such as hydrogen When a high energy particle passes through the liquid, bubbles are formed, marking the path

Table 4-22 Cerenkov Spectrometer Sizes

	Diam (cm)	Length (cm)	Mass (kg)	Vol (cc)	Pwr (w)
Entrance Scintillator	2K	$\frac{2\pi K}{37}$	$\frac{2\pi K^3}{37}$ (3 67)	$\frac{2\pi K^3}{32}$	2
Cerenkov Detector	2K	2K	$2\pi K^3$		2
Light Pipes	2K by 5 to 7 5 cm at window	2K	$\frac{2\pi K^3}{3}$		

NOTE $K = 1\ 6 \times 10^{-3} E^{1\ 76}$

The size of these devices range from a liter to tanks as large as wanted to increase the capture rate for cosmic rays The cosmic rays lose about 2 Mev per g/cm^2 per nucleon due to ionization Thus a 1 GeV proton would travel about 70 meters in liquid hydrogen, or about 2 meters in aluminum unless absorbed inelastically.

Heavy devices of this type are being flown on balloons, but have not been used in space as yet The dimensions can be proportional to the radius of curvature of the highest energy particle to be detected in a magnetic field produced across the instrument The instruments have also been used without magnetic fields to measure angular distributions, and high energy particle interactions with matter

Particle energy, charge, and mass can be determined in a bubble chamber or spark chamber as small as 10 to 30 cm square, if the chamber is placed between the pole pieces of a strong and uniform magnetic field The magnet will weigh more than the chamber and will require more power. Due to the strong magnetic field, these instruments are incompatible with magnetometer experiments The field must be strong enough to cause the particle to follow a path through the chamber with enough curvature that the momentum per unit charge can be measured Ion density along the path plus energy loss rate - dependent pulses in guard counters may be used to determine particle mass, charge, and energy per nucleon

A simplified diagram of a typical spark or bubble chamber is given in Figure 4-87

Considering a square chamber of length d (cm), the weight of the instrument will be approximately

$$M \geq \rho steel \left(d \times \frac{2d}{5} \times \frac{d}{5}\right) + \rho steel \left(\frac{d}{5} \times d^2\right)$$

$$\geq \frac{8}{5}\left[\frac{2}{5}d^3 + d^3\right] = \frac{8d^3}{5} \ (1\ 4)$$

$$\geq 2\ 24d^3 \text{ grams} \qquad (3)$$

If a magnetic field of B = 1000 gauss were produced across the chamber, then the radius of curvature R (meters), of charged particles would be given by

$$R = \frac{\sqrt{E_k{}^2 + 2m_oC^2E_k}}{300ZBec} = 56.5 \text{ meters for 1 GeV proton} \qquad (4)$$

where

E_k = kinetic energy in MeV

m_oC^2 = 938 MeV for protons

Z = charge of the particle

e = electron charge

c = speed of light

B = magnetic field in gauss

The approximate current required to produce the field B is given for 10^3 gauss by approximately

$$i = \frac{Bd}{uoM} = 30 \text{ amp} \qquad (5)$$

where

d = 0 3 meter is the length of chamber.

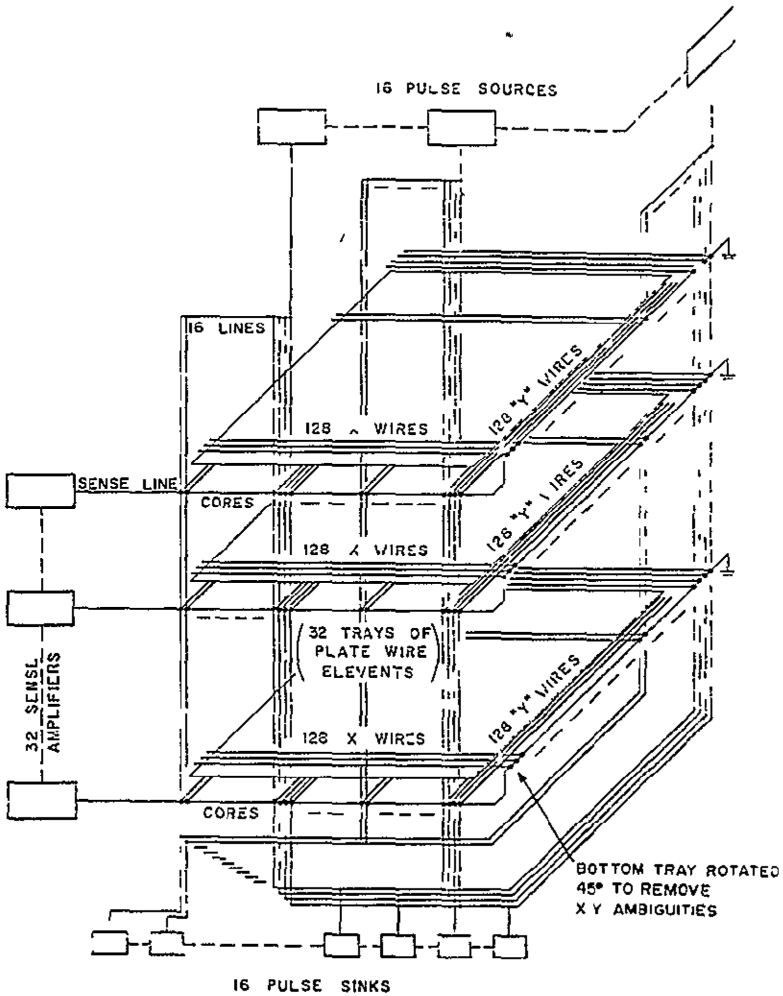

—Arrangement of wires and wire trays in the Goddard double spark chamber The beryllium-copper wires are 0 015 centimeter in diameter The active area of each tray is about 15 x 15 centimeters (Courtesy of T L Cline)

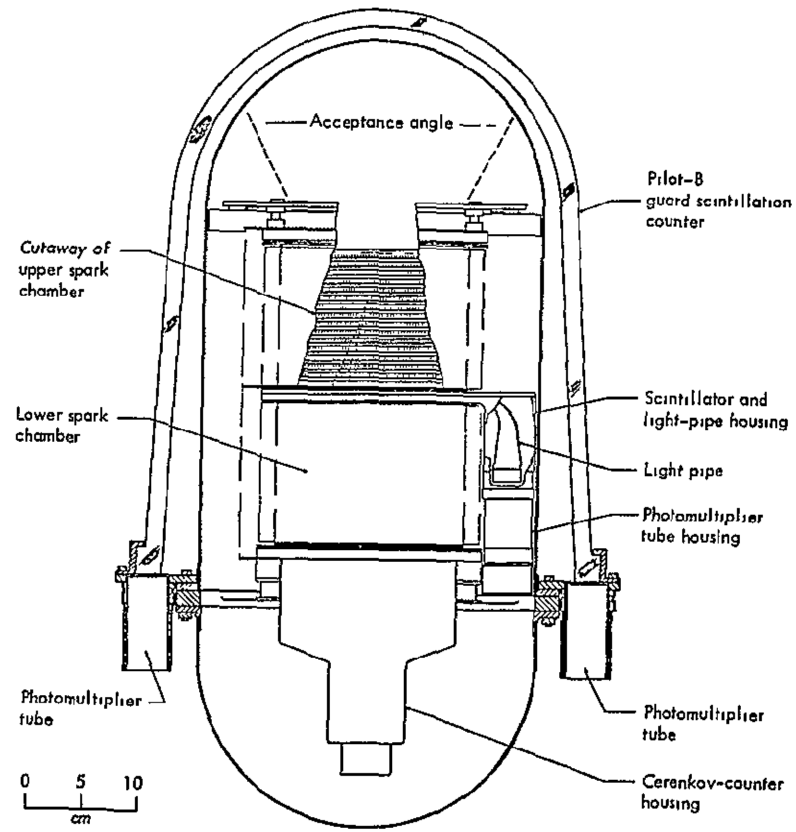

—Cross section of the Goddard double spark chamber (Courtesy of T L Cline)

Figure 4-87 Cross Section of Goddard Double Spark Chamber and Wiring Arrangement

4 8 SCALING LAW APPLICATION METHODOLOGY

4 8 1 General

The scaling laws just presented are generally procedures whereby one may calculate the support requirements of sensors that meet specified measurement requirements The relationships contained in these laws are usually functions in which both independent and dependent variables are continuous within domains restricted by physical and technological limitations The laws themselves do not contain specific values of support requirements but are tools for the determination of such values

To apply a scaling law, the sensor measurement requirements must be evaluated at one or more points on a trajectory, as described in Sections 3 4 1 and 3 4.2 The trajectory must encounter a planet to which the observation requirements are relevant, and the planetary region to be viewed must satisfy conditions of geometric visibility and illumination Conditions of distance, viewing angle, etc , are considered as parts of many scaling laws The sensor capabilities and support requirements usually vary from point to point on a trajectory When the observation requirements do not include area, latitude, or longitude coverage, the capabilities and support requirements depend only on the location of the individual trajectory points In this case, points P_1 and P_4 in Figure 4-88 bound a trajectory segment on which a sensor can (subject to state-of-the-art and geometric limitations) satisfy or exceed the marginal observation requirements Points P_2 and P_3 bound a smaller segment on which the same sensor can satisfy or exceed the optimal observation requirements At P_o, the capability of any sensor is maximum, and the support requirements of a sensor just able to meet the optimal (or marginal) observation requirements are minimized

If the observation requirements include area, latitude, or longitude coverage, usually they cannot be satisfied at any one point but only over a segment of the trajectory This situation is shown in Figure 4-89 P_1 and P_4 now bound the segment over which the sensor must be used in order to satisfy the optimal requirements P_2 and P_3 now bound the segment from which the marginal requirements can be satisfied The support requirements must be sufficient for use of the sensor throughout the entire segment. These support requirements are usually established by one of the end points P_1 or P_4, or P_2 or P_3

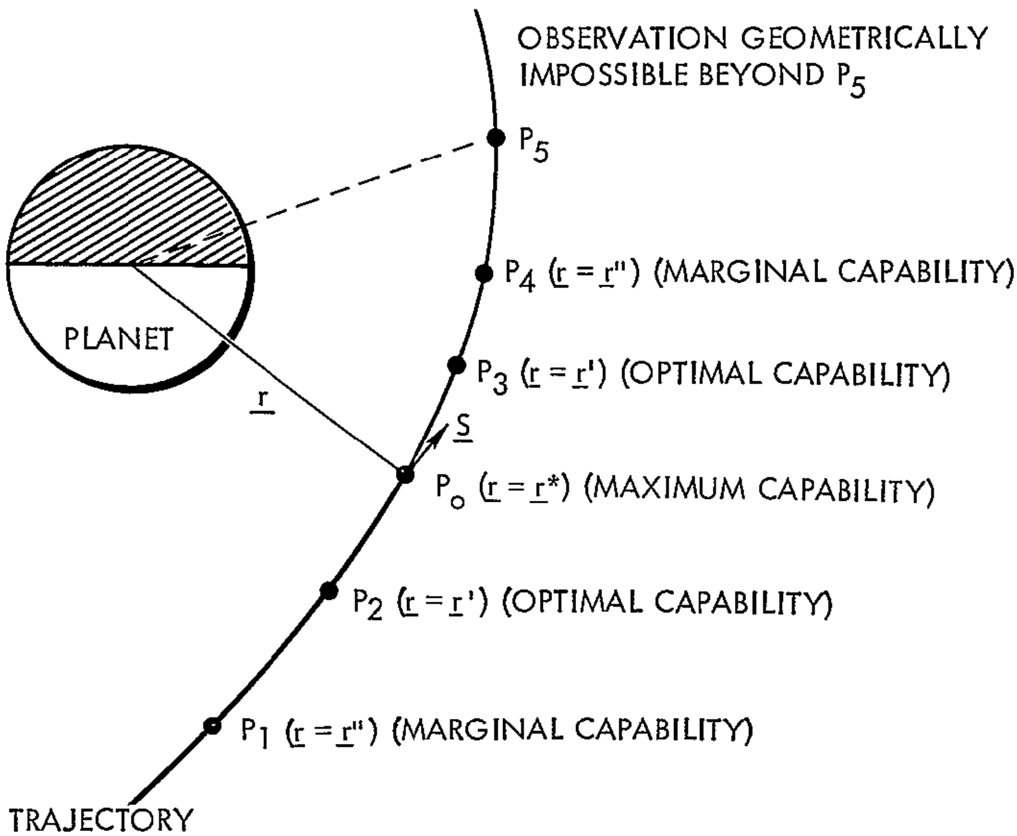

Figure 4-88 Measurement Capabilities of Trajectory Points

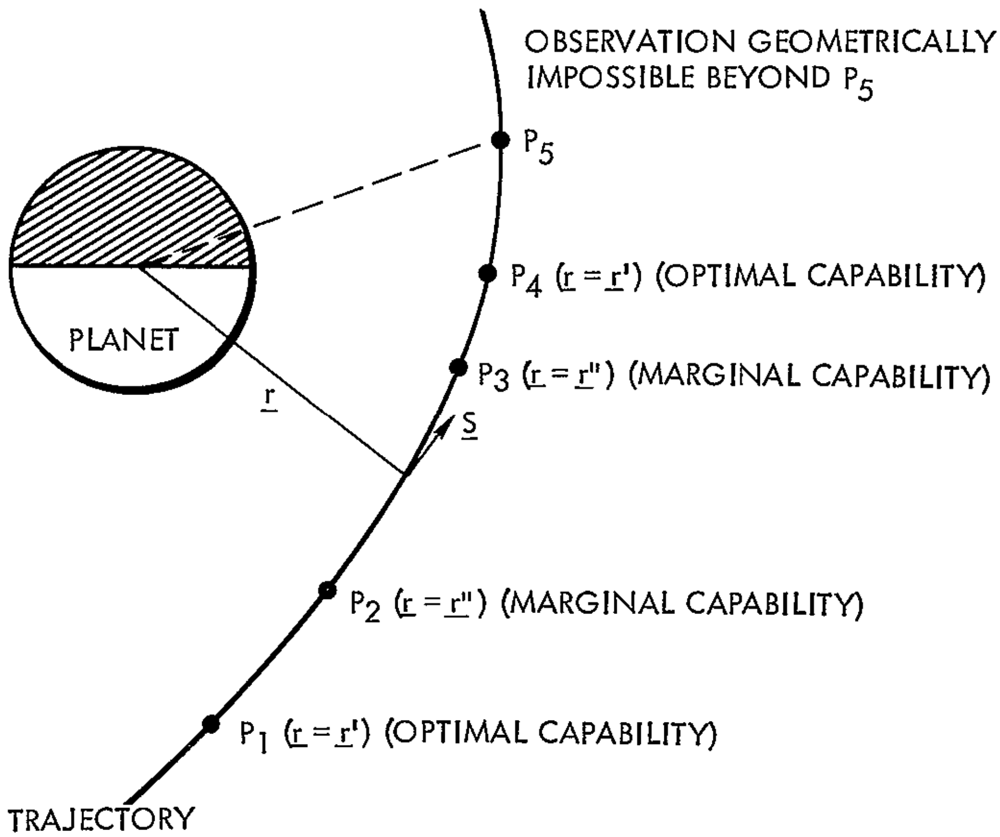

Figure 4-89 Measurement Capabilities Along a Trajectory Segment

To apply some scaling laws, it is necessary to select options in the synthetic design logic or to assume fixed values of certain design or operation parameters

For example, the viewing direction may be constrained to the nadir, or the sensor aperture angle may be fixed Details of these procedures, and data values, are presented in connection with specific scaling laws, or as part of the support requirement evaluation

The calculation of optimal and marginal measurement requirements at any given trajectory point was described in Section 3 1 2 The worth of a measurement capability at a point is simply that of the corresponding quality or quantity of the observation That is,

$$(b_m) = w\,(a_i) \tag{1}$$

where the measurement parameter value

$$b_m = f_{im}\,(a_i,\ P_k) \tag{2}$$

The measurement parameter worth is denoted by u to denote a generally different functional form than the observation worth w In equation (2), the P_k are the trajectory parameters involved in transformation of the i th observation requiremeter parameter to the m th measurement requirement parameter The transformation is expressed by the function or operator F_{im} To evaluate the optimal and marginal measurement requirements with respect to the entire encounter trajectory, find the maxima and minima of

$$b'_m = f_{im}\,(a'_i,\ P_k) \tag{3}$$

and

$$b''_m = f_{im}\,(a''_i,\ P_k) \tag{4}$$

for all points P_k If $b'_m > b''_m$, the overall optimum is the maximum of Equation (3) and the overall marginal value is the minimum of Equation (4) If $b'_m < b''_m$, the optimum is the minimum of Equation (3) and the marginal value is the maximum of Equation (4) The maxima and minima satisfy

$$\frac{\partial}{\partial \underline{s}} b'_m (a'_i, P_k) = 0 \tag{5}$$

and a similar equation in a_i'' Maxima and minima can be distinguished by the signs of the second derivatives The vector $\underline{s}$ is of unit length, tangent to the trajectory defined by

$$\underline{r} = \underline{r}(P_k, t) \tag{6}$$

in the sense of increasing time in the (K +1) dimensional space of t and the K trajectory parameters P_k We can write Equation (6) as

$$r = \sum_{k=1}^{K} h_k(t)\, \underline{r}_k \tag{7}$$

where $\underline{r}_k$ is a unit vector in the direction of P_k Then

$$\underline{s} = \frac{1}{|\underline{r}|} \frac{\partial \underline{r}}{\partial t} = \frac{1}{|\underline{r}|} \sum_{k=1}^{K} \underline{r}_k\ \partial h_k(t)/\partial t \tag{8}$$

At the point r' at which the maximum capability b_m^* is attained

$$\left. \frac{\partial u(b_m)}{\partial b_m} \right|_{\underline{r} = \underline{r}'} = 0 \tag{9}$$

Therefore,

$$\prod_{i=1}^{I_j} \left. \frac{\partial w(a_i)}{\partial a_i} \right|_{a_i = a_i'} \left[\partial b_m (a_i, \underline{r}')/\partial a_i \right]^{-1} = 0 \tag{10}$$

I_j is the number of observation requirement parameters associated with the j th observation objective

In practice and in the SERA computer program, the $\underline{r}'$ and $\underline{r}''$ are located by inspection of values of $b_m(a_i')$ and $b_m(a_{i''})$ at selected points The portion of the trajectory on which the optimal measurement requirements are attainable (subject to sensor limitations) is bounded by two values of $\underline{r}'$, one on either side of a point $\underline{r}^*$ at which requirements in excess of optimal are attainable The marginal measurement requirements are attainable on a segment bounded by two values of $\underline{r}''$

The next problem is to evaluate the worth of a sensor which partially satisfies measurement requirements arising from J distinct observation objectives Support of the same objective at two different planets or missions is counted here as support of two distinct objectives Normalize the previously defined worth functions to the worth w_j of fully satisfying the jth objective,

$$w_{ij}\ (a_i) = w_j\ w\ (a_i) \tag{11}$$

$$u^*h_j\ (b_m) = w_j\ u\ (b'_{mj}) \tag{12}$$

where b'_{mj} is the value of b'_m with respect to the jth objective Suppose a sensor has a set of measurement capability parameter values N_{mj} (corresponding one-to-one to the measurement requirement parameters) Let the worth of the sensor with respect to the mth measurement parameter be

$$\Upsilon_m = \sum_{j=1}^{J} u^*_{mj}\ (b_m) = \sum_{j=1}^{J} w_j\ u\ (b'_{mj}) \tag{13}$$

Considering all M measurement parameters, the overall worth of attaining the set of parameter values $(m_1, m_2, \quad, m_M)$ with respect to the jth objective is,

$$u^*_j = \frac{\sum_{m=1}^{M} u^*_{mj}\ (bm)}{\sum_{m=1}^{M} u^*_{mj}(b'mj)} = \frac{\sum_{m=1}^{M}\sum_{i=1}^{I_j} w_{ij}\ (a_i)}{\sum_{m=1}^{M}\sum_{i=1}^{I_j} w_{ij}\ (a'_i)} \tag{14}$$

Summing over all J objectives,

$$u^* = \sum_{j=1}^{J} u^*_j \tag{15}$$

The total worth of the sensor is

$$\Upsilon = \frac{\sum_{m=1}^{M} \Upsilon_m}{\sum_{m=1}^{M} \Upsilon'_m} = \frac{\sum_{m=1}^{M} \sum_{j=1}^{J} w_j \, u(b_m)}{\sum_{m=1}^{M} \sum_{j=1}^{J} w_j \, u(b'_{mj})} \tag{16}$$

4 8 2 Computer Program for Support Requirements

The third module of the SERA computer program uses scaling laws to evaluate sensor support requirements at selected points on planetary encounter trajectories Inputs to the SERA-3 module include the observation requirements read and stored by SERA-1 (Reference 1), trajectory data read by SERA-2 (Table 3-9), and measurement requirements calculated by SERA-2 As additional data in SERA-3, the sensor type whose scaling laws are to be applied is identified, various design procedure options are selected, and certain operation or design parameters may be fixed SERA-3 then calls a subroutine to apply the indicated set of scaling laws at each selected trajectory point As the individual laws in the set are applied, design parameter and support requirement values are compared to state-of-the-art limits If any limit is exceeded, calculation proceeds to the next trajectory point If the measurement capability of a sensor within state-of-the-art limits is poorer than the marginal requirement at a given point, the computations are completed at this point but the sensor worth is zero with respect to this measurement parameter

Calculations of sensor worth incorporate Equations (1), (2), (3), (4), (11), (12), and (13) Location of $\underline{r}'$ is limited to identification of that selected trajectory point at which the measurement capability is nearest optimum (i e , greatest if larger values of b_m represent improvement)

The selection is restricted to twenty points per problem (four points per output page) When the observation requirements involve consideration of sensor capabilities throughout a trajectory segment (Figure 4-89), usually only the two end points need be specified as inputs to SERA

Subroutines have been written for the ultraviolet spectrometer and laser radar Subroutines for other sensor types will be added later Laws for particle and field sensors are evaluated manually, since the support requirements are essentially independent of the trajectory

A detailed SERA users manual appears in the Appendix. Flow diagrams, lists of variables, program and subroutine listings and storage maps, and additional output samples are included

The first section is produced by SERA-1 and is explained in Reference 1 which is the source of this part of the example This first section traces each observation requirement back to the observation objective, scientific or technological knowledge requirement, and space exploration goal that they support Each relevant observation requirement parameter is identified, and its functional form and maximum value of the worth of the parameter are indicated

The second section, produced by SERA-2, contains two types of information concerning measurement requirements The first type represents the envelope of measurement requirements over all supported observation objectives The second type gives the measurement requirement parameter values associated with each individual objective At the programmer's option, both, either, or neither of these types may be printed

The first type (multiple-objective) of output includes the following information

1 Identification of mission and planet

2 Identification of observation technique (corresponding to one or more candidate sensor types)

3 Identification of observation objectives, including page citations of Reference 1

4 Names and values of mission and experiment parameters that are held constant in this problem

5 Special characteristics of selected trajectory points (See Section 6 2 1 for selection criteria)

6 Values of variable trajectory parameters at each point

7 Name, optimal value b'_m, marginal value $b''m$, and optimal worth $u(b'_m)$ of each relevant measurement requirement parameter, at each point Here b'_m represents the most stringent value of b'_{mj} at the given point If increasing b_m represents greater stringency, b'_m is the largest b'_{mj} b''_m is the least stringent of the b''_{mj} at the given point

8 The total optimal worth $\sum_{m=1}^{M} u\,(b'_m)$ at each point

The second type of SERA-2 output is similar, except in items (7) and (8) the optimal value b'_{mj}, the marginal value b''_m, the optimal worth $u(b'_{mj})$, and the total optimal worth

$$\sum_{m=1}^{M} u\,(b'_m)$$

are given for each individual observation objective The functional form of $u(b_{mj})$ is also given, it is the same as the form F_{ij} of the corresponding observation parameter worth function $w(a_i)$ When several objectives are considered together, F_{ij} may depend on j and no form can be specified for $u(b'_m)$

The output of SERA-3 repeats the identification of mission, planet, observation objectives, and measurement requirements Here, optimal and marginal measurement requirement parameter values are calculated at each selected trajectory point, as in SERA-2 In addition, overall optimal and marginal values are determined for the entire set of 1 to 20 selected points, subject to overriding values at any point considered in previous problems That is, SERA-3 determines an overall optimum

$$B'_m = \max\,(b'_{mp}, b'_{mq}) \tag{17}$$

and an overall marginal

$$B''_m = \min (b''_{mp}, b''_{mq}) \tag{18}$$

where max represents the largest value of the arguments, min represents the smallest value, the index p refers to the four points in one subset (p=1, 2, 3, 4) and q indicates any other single points of the other subsets up to 20 points in all

Equations (17) and (18) are written for the case where increasing b_m represents a more stringent requirement If the reverse is true,

$$B'_m = \min (b'_{mp}, b'_{mq}) \tag{19}$$

$$B''_m = \max (b''_{mp}, b''_{mq}) \tag{20}$$

The next part of SERA-3 output gives the sensor capability values as determined by the scaling law or from the measurement requirements The scaling law takes precedence over the measurement requirements, that is, if the scaling law leads to a lesser capability than the requirements, the scaling law capability is printed Sensor state-of-the-art limitations are bounds on the capability values computed by the scaling law The maximum worth values

$$\Upsilon_m = \sum_{m=1}^{M} \Upsilon_m$$

are shown Finally, values of coefficients in the scaling law are given, and the sensor support requirements are evaluated The functions in which these coefficients appear are shown as part of the scaling law descriptions in Section 4 0 The support requirements are expressed at each selected trajectory point, and also at the points corresponding to the optimal and marginal sensor capabilities

4 9 FUTURE DEVELOPMENTS

The current state-of-the-art in sensor system technology represents a very high stage of development, but significant shortcomings become apparent when available technology is postulated for long-duration space exploration missions In many instances, the ability of sensors to accomplish the required scientific measurements for planetary investigations is limited as much by the conditions under which the sensor is used as by the physical processes of sensing While increased sensor performance is always desirable, it is frequently the case that performance is limited by factors which are not truly sensor limits but rather external conditions such as payload limits, environmental constraints, conditions of use, or perhaps even economics

For these reasons, it is very difficult to postulate realistic future sensor capabilities without reservation The discussion of future developments is intended, therefore, mainly to indicate what current limits exist, and present trends in research and development which might be useful in improving remote sensor capabilities in the area of planetary scientific exploration

The discussion is limited to electromagnetic sensors and is organized in the same manner as the scaling law development section, i e , passive and active optical sensors, and passive and active microwave sensors

4 9 1 Passive Optical Instruments

The limitations of passive optical instruments are in the areas of primary optical size and quality, detector sensitivity and, depending upon whether the sensor is image forming or non-image forming, in post-detection or pre-detection information processing For convenience, the discussion given below is presented according to the functional component of the sensor system Thus primary optics limitations are presented first, followed by a discussion of detector technology, auxiliary optical components such as filters and diffraction gratings, and finally image forming systems

4 9 1 1 Primary Optics

As discussed previously, there are no overriding reasons why the best earth-based optical telescopes cannot be configured for deployment in a space environment The limitations are primarily economic and the development schedule From a theoretical point of view the advantages of such an approach may be difficult to justify since the advantages to be gained from a telescope as large as the 200-inch diameter telescope of Mt Palomar are not obvious This follows from the fact that large-diameter earth-based telescopes serve the two primary purposes of increasing the collected energy and increasing the angular resolution Both of these factors are related to the geometry of viewing for planetary surface investigations so that by moving the primary sensor operation close to the planet, the equivalent of the largest earth-based telescope or better can be obtained with appreciably smaller diameter optics

Therefore, if the sensor aperture is to be brought into the vicinity of the planetary surface, that is within several planetary radii, it does not appear that very large diameter optics can be justified for planetary investigations Just what upper limit is likely to be used is conjectured, but when such factors as booster diameter and payload limits are considered, it does not appear likely that aperture diameters in excess of 100 inches will be postulated in the immediate future

Rather than larger diameter systems, it appears that emphasis will be placed on improving optical quality and increasing the available field of view of large diameter optics Much work has been done in the field of catadioptric optical systems but the refractive corrective components still limit the attainable aperture ratios of such systems to the range of f/numbers from approximately three to six Since high speed, wide angle optical systems are highly desirable for remote planetary sensing, it appears that useful improvements can be made in this area Two areas of particular concern are improving the "figure" of the refractive correcting components and the smoothness of the primary reflecting mirror surface Both of these improvements are intimately associated with the limitations in optical manufacturing techniques and the ability to launch and use the optical system in the dynamic environment of space

Optical manufacturing techniques have improved to the point where surface quality controlled to one fortieth of a wavelength is within the state-of-the-art This level is of course attainable only in a laboratory environment but is indicative of the fact that little or no improvement is required in this area

Of more concern for space applications are the degradations which result from launch and deployment dynamics as well as from the varying thermal environment to which the telescope is subjected in space The degradations which result from these effects, while theoretically controllable, have resulted in the limitations on attainable f/number to the region of three to six depending upon the degree of optimism used in estimating field degradation Means of controlling the degradations are of two types The first and perhaps most important is the selection of the optimum materials for primary optical components Material selection for primary mirror fabrication for large telescopes for space deployment is generally limited to various types of glass and beryllium The figures of merit used in material selection are generally a strength factor and a thermal stability factor If light weight is the primary criterion then beryllium is selected because it has good thermal characteristics, but if overall weight is not the primary criterion then several other materials are available which have improved thermal characteristics but are both expensive and difficult to manufacture Among these are silicon and several varieties of sintered materials, such as sintered aluminum, which have excellent overall strength and thermal stability characteristics However, the difficulty with the more exotic materials is that they have not been developed to the point where large optical mirror blanks have been formed so that they are at best only postulated for large mirror applications They do have highly desirable characteristics, however For example, silicon has a strength figure of merit very close to beryllium but a thermal stability merit factor which is an order of magnitude better than beryllium If silicon were postulated for the primary optical mirror of the telescope, then it appears that a diffraction-limited optical system with f/number in the range of 1 5 to 2 would be reasonable

The second effect which limits the performance of large diameter optics is the maintenance of optical alignment and focus over the total range of operating environments As discussed previously, large diameter optical systems have generally been proposed only for manned systems since a human operator could then perform the function of alignment and maintenance of focus This is not meant to imply that an automatic system to perform the same functions could not be developed It is obvious, however, that an automatic alignment and focusing system would add a high level of complexity to the telescope with attendant impact on reliability and operating life While such an approach is feasible, it is probably unlikely in the near future

In summary, it does not appear likely that optical apertures in excess of 100 inches can be postulated for planetary exploration It appears that optical technology will be applied to improving attainable optical quality to extend current capabilities close to diffraction-limited performance in the f/number region of 1.5 to 2

4 9 1 2 Detectors

Detectors for non-imaging passive optical instruments have been discussed previously as IR detectors and visible-UV detectors The same classification is used here

IR Detectors As discussed previously, IR detectors of the discrete type are of two general classes, those which have spectrally dependent detection characteristics such as photo-conductive and photo-voltaic cell photon detectors and those which are spectrally independent such as thermocouples and bolometers Primary emphasis in IR detector development technology has been in the area of photon detectors although there are obvious applications for spectrally independent response characteristics in such fields as spectroscopy From Table 4-6, it can be seen that photon detectors generally have detectivities which may be several orders of magnitude better than the best bolometer so that photon detectors are more widely used

The technology of photon detectors for the infrared is highly developed As indicated in Table 4-7, the performance of IR detectors is close to the theoretical limit of ideal detectors so that very little improvement in detection capability can be expected in the near future Steady, minor improvements can be expected as manufacturing and quality control procedures improve so that peak D·'s as large as 10^{12} may be postulated for the near and intermediate IR However, other developments indicate that for the near IR the application of photodiodes and avalanche multiplication photodiodes is highly likely with resulting D·'s in the range of 10^{14} It can be expected that continuing efforts will be made to extend the application of avalanche multiplication techniques into the intermediate IR region so that some improvement in D can be expected in this region

A current limitation in IR detector technology is, of course, in the long wavelength portion of the spectrum Three effects are apparent in the long wavelength region which is considered to extend from approximately 30 microns to beyond 100 microns The first effect is that photon detectors, even when operated at liquid helium temperatures (4 2 deg K), have longwave cutoffs of D: in the region of 50 microns It is, therefore, usually necessary to use cooled bolometer detectors in the long wavelength region The second effect which becomes apparent in the long wavelength region is that phenomena in this spectral region have low thermodynamic temperatures Therefore, the background which the detector "sees" must be kept low to prevent masking of the effect to be measured by the blackbody radiation of the background This imposes the requirement for cooled optics and spectral filters to reduce direct thermal radiation to the detector from its immediate surroundings The third effect is the necessity of incorporating detector and optical cooling mechanisms in the design

Developments in long wave detectors and cooled optical components are such that longwave IR measurements are relatively routine on a laboratory basis so that future developments can be expected to be concentrated on the development of suitable cooling techniques The difficulty arises from the duration of the missions for planetary investigations Mission duration generally precludes the use of conventional laboratory techniques in which pre-cooled liquids and solids are used to obtain temperatures close to absolute zero

Much emphasis has been placed on the development of closed-cycle cryogenic coolers for IR detectors but current technology limits the usefulness of such techniques to temperatures in the range of 80 deg K Unless a major breakthrough is made in this area, it is not expected that any significant improvement will be made in the area of closed-cycle cooling systems

Because of the limitations of closed-cycle cooling systems, recent emphasis has been placed on the development of passive cooling systems for long duration space missions From a theoretical point of view, radiative cooling by passive techniques can be used to obtain detector operating temperatures near absolute zero However, practical thermal designs to accomplish this have not been developed Current technology in passive cooling permits detector operating temperatures in the range of 150 deg K to be predicted for moderate heat loads It appears that continued research in this area will result in passive cooling techniques which produce detector operating temperatures in the range of 80 deg K, although the time span for obtaining this result is highly dependent on the level of research pursued

Considering current technology and known planned research, it does not appear that longwave IR systems for planetary investigations can realistically be predicted beyond 50 microns in the immediate future

Visible and U V Detectors The impetus of research in detector technology in the visible and UV portions of the spectrum has been mainly in the area of developing cell detectors to replace the photomultiplier. Three techniques have been pursued The first is basically an extension of the silicon photodiode used in the near IR region into the visible and near UV portions of the spectrum While this approach offers a decrease in complexity over the photomultiplier, it does not have equivalent sensitivity so that it is unlikely that it will replace the photomultiplier

Along the same lines, efforts have been made to develop photoconductive detectors for the UV While demonstrable on a laboratory basis, it does not appear that solid-state detectors for the UV will be competitive in the immediate future

A solid-state detector which does appear to be competitive with the photomultiplier is the avalanche photodiode Like the photomultiplier, it has internal gain so that it is competitive sensitivity-wise but exhibits a short wavelength cutoff near 0 3 micron so that it is not useful in the UV As with any new development, there are limitations in avalanche diodes with the principal one being the critical voltage on the diode at which breakdown occurs The voltage operating point must be set with a high level of precision to obtain useful operation Therefore, while it appears that these devices offer a major simplification over a photomultiplier, in actuality they may impose operating requirements which are difficult to meet It does not appear likely that these devices will replace photomultipliers in the near term but continued development may make them competitive

Developments in photomultipliers are principally in the area of extending spectral response to shorter wavelengths

Detectors for the visible and ultraviolet have in the past decade undergone a revolution in noise reduction so that extremely low light levels can be measured Little additional improvement in this area can be expected but systems for improving quantum efficiency will continue to be effective However, quantum efficiencies exceed 20 percent for most of the ultraviolet and visible so improvements of this sort will be limited to factors of 2 or 3 Dark currents can be limited to 1 count per second or less in the visible and near UV and 1/100 or less for the vacuum ultraviolet

4 9 1 3 Auxiliary Optical Components

The state-of-the-art in auxiliary optical components, such as filters, diffraction gratings and beamsplitters, is highly developed It is not expected that significant improvements will be obtained in such areas as filters since the basic problem is not one of actual component design but rather available light for measurement For many spacecraft applications, total throughput of light is the limiting factor in visible and ultraviolet spectrometer design The best way to improve light sensitivity for such components as gratings is, at the present time, to increase the effective aperture of the instrument by increasing the grating size and number of lines per mm At present, spectrometers are being designed with gratings having 3600 lines/mm and areas of 100 square cm Slow, moderate improvement in such gratings will take place in the future, but no breakthrough is presently foreseen However, new slit coding techniques such as "Hadamard transform spectroscopy" are just being tried for opening the effective aperture of a spectrometer without increasing grating or prism size If these schemes work, an order of magnitude improvement in sensitivity, for cases of a diffuse source and no rigid angular resolution requirement, will be achieved

Improvements in spectroscopy can be expected if efforts to extend the concept of the Michelson Interferometer spectroscope to the visible and UV portion of the spectrum are successful Fourier Transform Michelson Interferometers are being developed for the visible and near ultraviolet but are limited in resolution under spacecraft conditions of vibration However, laser reference techniques may be used to reduce this effect so that interferometers may become important in this field This area could represent a major breakthrough in visible and ultraviolet spectroscopy, but this is not yet firmly established

4 9 1 4 Image Forming Optical Sensors

Image forming optical sensors, while of many possible types, are restricted to television systems and arrays of discrete detectors because they are the most likely candidates for planetary exploration

Television Systems As discussed previously, it can be shown that the inherent resolution of photosensitive surfaces for TV pickup tubes is equal to or better than the resolution of high-definition aerial reconnaissance photographic film The two detection systems for image formation do not have equivalent performance, however, because of the inherent limitations of TV systems The limitations are basically imposed by the modulation transfer function of the camera reading beam and the associated limitations on electron optics, and the maximum surface area of the photosensitive surface which can be read out before the charge on the detector surface is neutralized by leakage

Current technology in return beam vidicon design, using highly sophisticated electron optics, predicts a limiting resolution of 10,000 TV lines on a 2500 mm^2 sensitive surface area This is equivalent to a limiting resolution of 100 line pairs per millimeter and appears to represent an upper limit on TV camera resolution for the immediate future

The limiting resolution of 100 lines per mm presupposes that the read-out time of the photosensitive surface is optimum For the case of large surface area, this implies a very large video bandwidth which may be difficult to accommodate in an unmanned spacecraft The alternative is to use a slow scan read-out as a bandwidth conservation technique This leads inevitably to a conflict between attainable resolution and read-out time It is, therefore, in the area of slow scan readout techniques for high definition photosensitive surfaces that future development efforts can be expected to be concentrated

An alternative to slow scan for bandwidth conservation is the development of wideband, large dynamic range recording techniques, either digital or analog, with subsequent processing to remove redundancy While this approach has much promise, it does not appear likely that it can be implemented for spacecraft use on a near term basis It is an area where future development effort is most likely to be concentrated so that the time frame in which it may become available is difficult to estimate

Arrays of Detectors The availability of large arrays of discrete detectors, especially for the IR portion of the spectrum, is highly doubtful in the immediate duture It is obvious that a large rectangular array of detectors is advantageous for image formation in the IR portion of the spectrum since the performance of IR TV pickup tubes does not appear to be satisfactory However, the difficulties of building large arrays of discrete detectors of small size have not been overcome Steady improvements in detector manufacturing techniques can be expected but the overall complexity of such an approach places their utility for long duration space missions in doubt

4 9 2 Active Optical Instruments

The state-of-the-art of active optical instruments has been discussed previously because the inherent limitations of optical transmitters limit the application of the technique to low duty cycle, pulsed transmitters While steady improvement in coherent optical sources (lasers) can be expected, it does not appear likely that coherent transmitter technology will improve in the near term to permit use of active optical systems equivalent to ground mapping microwave radar

4 9 3 Passive and Active Microwave Systems

Microwave sensor technology is highly developed and in many areas the technology is approaching limiting physical bounds For these reasons, it is not expected that any dramatic improvements will be obtained in the immediate future Rather, it is expected that improvements in performance will result from improved processing of measured data

For the most part, the limitations and projections on the state-of-the-art for microwave sensors have been discussed previously The principal area in which significant developments can be expected on a near term basis is in the area of millimeter wave technology Principal improvements are expected in the areas of receiver technology Current millimeter wave receivers have noise figures in the range of 15 to 20 db Steady improvement can be expected in this area but it is unlikely that noise figures of less than 10 db will be obtained on a near term basis

Continued improvement can be expected for spaceborne antenna systems, although it appears unlikely that antenna gains in excess of 60 db will be obtained in a space environment The areas of improvement will be principally in the development of low-sidelobe antennas and fast switching of beam position in array antennas Where sidelobe requirements indicate very low levels, it is expected that antennas with 35 db sidelobes can be developed Improved response-time microwave switching techniques could result in beam switching times approaching one nanosecond, although the requirement for such fast switching may be difficult to establish

PRECEDING PAGE BLANK NOT FILMED

REFERENCES

1 Observation Requirements for Unmanned Planetary Missions, North American Rockwell Corp , NR-SD 70-24 (March 1970) NASA CR 73458, 73459

2 Klopp, D Orbital Imagery for Planetary Exploration (Vol 4) IITRI (Sept 1969), NASA CR 73453

3 Jones, R C Quantum Efficiency of Detectors for Visible and Infrared Radiation, in "Advances in Electronics and Electron Physics," (Vol II), Academic Press, 1959

4 Jamieson, J A , et al, Infrared Physics and Engineering McGraw-Hill, 1963

5 Kruse, Paul W , et al Elements of Infrared Technology Generation, Transmission, and Detection John Wiley and Sons, 1962

6 Fried, D L , "Noise in Photoemission currents " Applied Optics, 4 1, 1965

7 Noise in Multiplier Phototubes, IIT Industrial Laboratories, Application Note E-8, 1965

8 Schade, O H , Sr "An Evaluation of Photographic Image Quality and Resolving Power " Jour SMPTE, Vol 73, p 81 (1964)

9 Schade, O H , Sr "The Resolving - Power Functions and Quantum Processes of Television Cameras " RCA Review, 28 3 (1967)

10 Rose, A "Television Pick-up Tubes and the Problem of Vision," in Advances in Electronics, Vol 1 (1948)

11 Perkin-Elmer Corp Practical Application of Modulation Transfer Functions (1963)

12 Air Force Systems Command, Space Planners Guide (1965)

13 Fjeldbo, G and Eshelman, V R , "The Bistatic Radar-Occultation Method for the Study of Planetary Atmospheres " Jour. Geophys, Res , 70 15 (1965)

14 Fjeldbo, G et al , "The Two-Frequency Bistatic Radio Occultation Method for the Study of Planetary Ionospherics " Jour Geophys Res 70 15 (1965)

15 Fjeldbo, G and Eshelman, V R , "The Atmosphere of Mars Analyzed by Integral Inversion of Mariner IV Occultation Data." Space Sci , Vol 16 (1968)

16 McGillen, C D and Seling, T V , "Influence of System Parameters on Airborne Microwave Radiometer Design " IEEE Transactions on Military Electronics, (October 1963)

17 Jordon, P R Jr , "Design Nomographs for Microwave Radiometers " Microwaves, Feb , 1966